Bulletin of the University of Utah

Vol. 53 November 1964 No. 26

STORAGE AND FLOW OF SOLIDS

by

Andrew W. Jenike

Bulletin No. 123
of the
UTAH ENGINEERING EXPERIMENT STATION

Sixth Printing
(revised)
March 1970

University of Utah
Salt Lake City, Utah

DISCLAIMER

PREFACE

There hardly is an industry which does not store and handle solid materials in bulk form. When the volume of the solids is large, gravity is invariably relied upon to cause the solids to flow out of storage, through channels and reactors. Such materials as ore, coal, cement, flour, polypropylene, clay, soil, to which a general term of bulk solids is applied, flow by gravity or are expected to flow by gravity in thousands of installations and by the billions of tons annually. Mining relies on gravity flow in block-caving, in ore passes, as well as in storage and loading bins. Agriculture uses gravity flow in elevators, in feed plants, and in silos. The chemical and process industry depends on gravity flow of solids in process and out of storage.

This bulletin follows Bulletin No. 108 which was published in 1961. The present aim is to provide the engineer with enough information to enable him to design storage plants and flow channels for unobstructed flow. Only an outline of the theory of flow is given.

While the design procedure remains essentially unchanged, important refinements have been introduced in the past three years. These refinements have been based on both, further developments in the theory of flow, and an expanded background of industrial experience. In particular, the

calculations of the flow-factor for no-doming have been refined and the formula for the width of an outlet is more conservative. The interpretation of the tests of flow-functions has been modified, better to account for the effect of capillary forces. The evaluation of the angle of friction between a flowing solid and a wall material has also been altered and permits a less conservative design.

A simplified method of measuring the flow-function of a solid has been introduced. This method saves a great deal of time in separating free-flowing from non free-flowing solids, and in intricate testing problems.

The subject matter is organized in three chapters. Chapter I introduces the concepts of flowability of bulk solids and of channels, and the flow - no flow postulate. Chapter II describes the testing apparatus and procedure, and Chapter III contains applications to design. An outline of the derivation of channel flow-factors and flow - no flow formulas is given in an Appendix.

While the concepts of this theory were formulated by the author in 1953, most of the work was carried out at the Bulk Solids Flow Laboratory (1957-1962) of the Utah Engineering Experiment Station, University of Utah, where the author had the satisfaction of working with Dr. Jerry R. Johanson, who was then a graduate student. The author is grateful to Dr. P. J. Elsey, Assistant Director of the Station for his constant and sympathetic interest in the project, to Professor R. H. Woolley of the University of Utah for his assistance in setting up the Bulk Solids Flow Laboratory, and to Professor R. T. Shield of Brown University for the many long discussions of the topics of plasticity.

The cost of this project was substantial and the author gratefully acknowledges the initial support which he received from the American Institute of Mining Mineralogical and Petroleum Engineers, whose Mineral Beneficiation, Coal, and Research Committees were instrumental in providing AIME endorsement of the project in 1954. This was followed by a grant of money from Engineering Foundation and in 1956 by the support from research funds of the Utah Engineering Experiment Station. The AIME and the Engineering Foundation remained sponsors of the project to its completion in December, 1962.

Sincere thanks are due to Dr. S. S. Kistler, Dean of the College of Engineering, and to Dr. Carl J. Christensen, Director of the Utah Engineering Experiment Station, for their support in initiating the project and for keeping it alive through times of financial stress.

The main support for the applied part of the project, entitled "Bulk Solids Flow" came from the American Iron and Steel Institute, to whom the author is most grateful.

The mathematical concepts described in this report, as well as other work which has appeared elsewhere, were worked out under a 1959 grant from the National Science Foundation to a project entitled: "Flow of rigid-plastic solids in converging channels under the action of body forces."

Andrew W. Jenike
Winchester, Mass.
November, 1964

CONTENTS

NOTATIONS

A	area of a shear cell (1/13 sq ft)
B	width of a rectangular outlet, side of a square outlet, diameter of a circular outlet, ft
D	diameter of a pipe, major dimension of an outlet, diameter of a circular cylinder, ft
EYL	effective yield locus
$F = A \times f_c$	unconfined yield force, lb
FF	flow-function of a solid
H	moisture content, %
K	coefficient
L	length of a rectangular outlet, ft
Q	vertical force acting on a feeder, lb
$S = A \times \tau$	shearing force applied to a shear cell during consolidation, lb
$\overline{S}$	shearing force applied to a shear cell during shear, lb
T	temperature
TYL	time yield locus
$V = A \times \sigma$	normal force applied to a shear cell during consolidation, lb
$\overline{V}$	normal force applied to a shear cell during shear, lb
$V_1 = A \times \sigma_1$	major consolidating force, lb
$\overline{V}_1 = A \times \overline{\sigma}_1$	major force in a dome or a pipe, lb
V_t	vertical force applied to a shear cell during twisting, lb
WYL	wall yield locus
YL	yield locus
f_c	unconfined yield pressure of a solid, psf

ff	flow-factor of a channel
m	coefficient: m = 0 for plane flow, m = 1 for conical flow
q	feeder load coefficient
r,θ	plane radial coordinates
r,θ,α	spherical coordinates
s	stress function
t	time
x,y	plane cartesian coordinates
x,y,α	cylindrical coordinates
γ	bulk density of a solid, pcf
δ	effective angle of friction
θ'	hopper slope measured from the vertical
ϕ	kinematic angle of internal friction of a solid
ϕ',ϕ^{v}	kinematic angle of friction between a solid and a wall
ϕ_t	static angle of internal friction of a solid
σ	pressure, psf
σ_1	major consolidating pressure, psf
σ_2	minor consolidating pressure, psf
σ'	pressure on a wall in mass flow, psf
$\bar{\sigma}_1$	major pressure in a dome or a pipe, psf
$\bar{\sigma}_2$	minor pressure in a dome or a pipe, psf
σ_r	pressure in a radial direction, psf
σ_θ	pressure in a direction normal to radial, psf
τ	shearing stress, psf
τ'	shearing stress on a wall in mass flow, psf
$\tau_{r\theta}$	shearing stress in a coordinate direction, psf
ψ	angle between the direction of major pressure and a coordinate ray

CHAPTER I

FLOWABILITY OF BULK SOLIDS AND OF CHANNELS

Introduction

The first significant studies related to the storage of bulk solids were reported at the end of the nineteenth century. That work originated from the need to store large quantities of grain and was concerned mainly with wall pressures affecting the structural design of silos and bins. The Janssen formula [1], the work of Airy [2], Jamieson [3], and Ketchum [4] form the highlights of that period. Structural problems of bin and silo design have been the subject of texts written more recently by Caquot and Kerisel [5], M. and A. Reimbert [6] in France; Nowacki and Dabrowski [7], Sienicki, Domaszewski and Klos [8] in Poland, and of numerous articles [for example, 9 to 14]. Other related subjects which have been studied extensively, though mostly empirically, are the rate of flow of bulk solids through orifices [15 to 22], methods of preventing segregation, and patterns of flow [23 to 30]. Only representative articles are listed in the bibliography. Zenz and Othmer in their book [31] refer to most of the above topics even though their work is mainly concerned with fluidized materials. A bibliography on "Flow of Bulk Materials from Storage" has been published by the Research Department of the American Society of Mechanical Engineers.

One problem which is not resolved by the above literature and which is the subject of this publication is whether or not a given

solid will flow out of a given bin. It is well known that flow out of bins and hoppers is often unreliable, that time and money are spent - with or without success - on flow-promoting devices, that solids segregate in storage, feed erratically, flood, arch, pipe, and stick to the bin walls reducing the live capacity below specified values [32].

The theory of flow of bulk solids and the design of storage bins and channels for flow were the subject of studies by the author, first on his own (1952-1955) [33-36], then at the Utah Engineering Experiment Station, University of Utah (1956-1962). The work led to the postulation of a flow - no flow criterion and of flow properties of solids and of channels. The author has continued this work and the present bulletin contains an up-to-date report of the results. Since this bulletin is written for the design engineer, the theory is kept to a minimum. For a complete derivation of the formulas the reader is directed to references 37, 38, 39, 41 and 42.

It will be useful to consider the typical flow patterns of bulk solids in gravity flow and to define the terminology. Since relatively new concepts, such as "flowability of bulk solids" are used, it will be necessary not only to redefine some of the existing terms with greater precision but also to introduce new terms. However, first of all let us consider why some bulk solids do not flow by gravity but arch and pipe.

Obstructions to flow. While the number of obstructions to flow which may develop in a bin is infinite, two types will be analyzed here. They are: doming, Fig. 1; and piping, Fig. 2. It will be assumed that, if the design of the bin is such that these two obstructions cannot occur,

satisfactory flow will result.

When a stable arch or dome forms across the outlet of a hopper, it is apparent that the solid has enough strength to support its own weight. Yet, the same solid when fluffed up has no strength. Evidently, the strength of a solid varies, and depends on the degree of consolidation of the solid. While some exceptions are possible, in general, the strength of a solid increases with consolidating pressure.

Various solids develop various values of strength for the same consolidation. This is illustrated in Fig. 3 by the curves (a) and (b) which represent two different solids. Evidently, the stronger solid represented by line (b) will be less free-flowing than the weaker solid represented by line (a). Intuitively, one feels that for a given hopper there must exist a critical line - for instance as shown by the dashed line in the figure - such that, as long as the pressure-strength curve of the solid lies below the critical line, the strength of the solid is insufficient to support a dome, and the solid flows; whereas, when the pressure-strength line lies above the critical line, the solid domes.

The work which follows develops this concept: the pressure-strength curve of a solid is referred to as its flow-function, the dashed line is called the flow-factor of the channel. When these two lines intersect, the point of intersection usually determines the minimum size of the outlet required to assure unobstructed gravity flow. A similar reasoning is applied to piping.

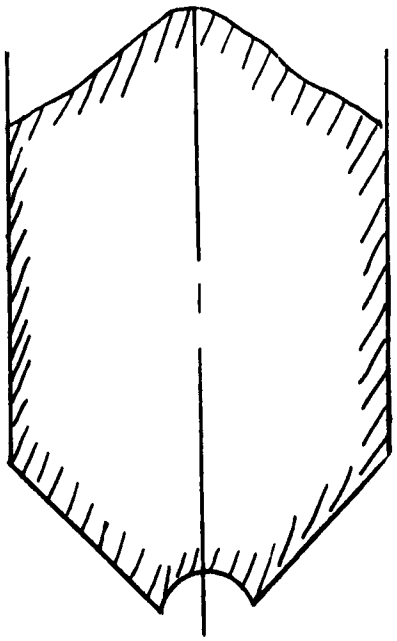

Fig. 1

Doming

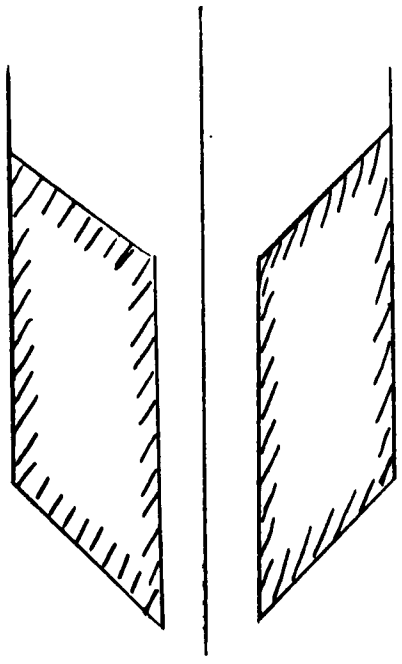

Fig. 2

Piping

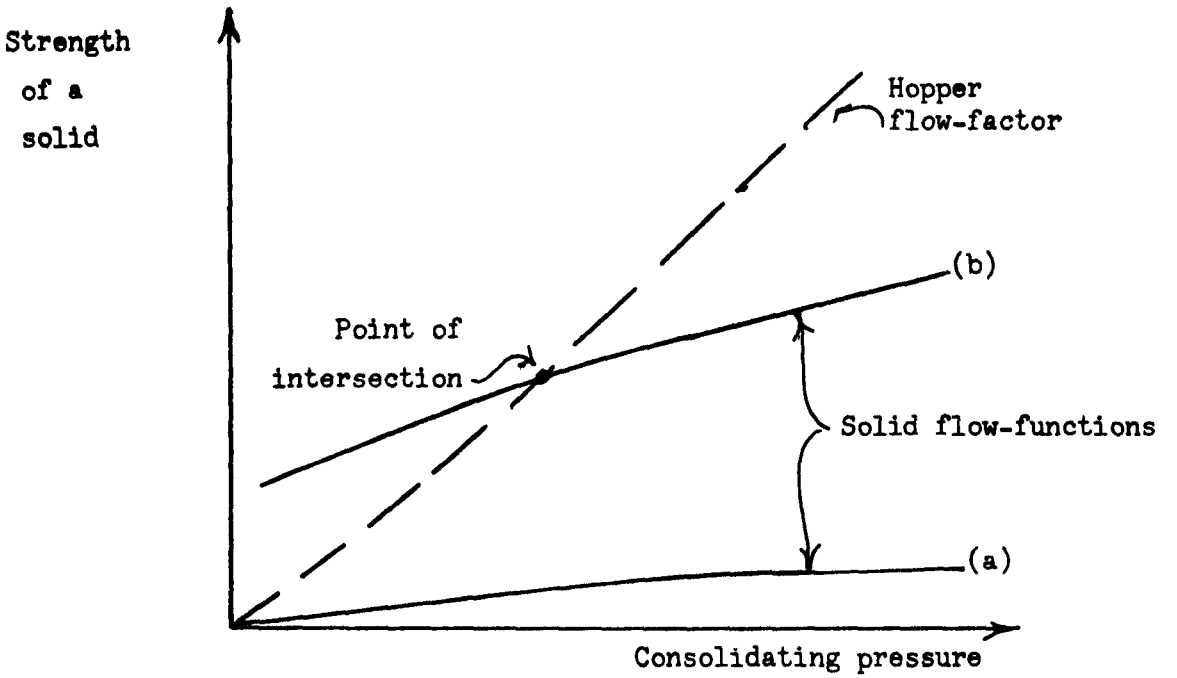

Fig. 3

Strength versus consolidating pressure

Angle of repose. When an unconsolidated (loose) bulk solid is deposited on a horizontal surface so as to form a pile, and the velocity of the stream onto the top of the pile is negligible, the particles of the solid roll down the pile and the slope of the pile forms an angle of repose with the horizontal. The angle of repose assumes values between 30° and 40° and is not a measure of the flowability of solids. In fact, it is only useful in the determination of the contour of a pile, and its popularity among engineers and investigators is due not to its usefulness but to the ease with which it is measured.

If a solid contains a wide range of particle sizes, it segregates; the fines collect along the trajectory of the charged solid while the coarse fraction rolls to the periphery of the pile. When the solid drops onto a pile from some height, the fines along the trajectory pack under the impact of the larger particles, gain strength, and form a slope angle steeper than the angle of repose, Fig. 4.

If a fine powder or a flaky solid drops from a height, it aerates and spreads at an angle smaller than the angle of repose.

Effective area of an outlet. It is necessary to differentiate between the physical size of an outlet of a pile, bin, or hopper, and its effective area because, in the development of a flow pattern of a solid within the pile or bin, it is the effective area which is significant. The effective area of an outlet is that part of the total area through which the solid actually flows when the feeder is in operation or the gate is open. It is important to realize that in many cases the effective area forms only a part, sometimes a small part, of the total

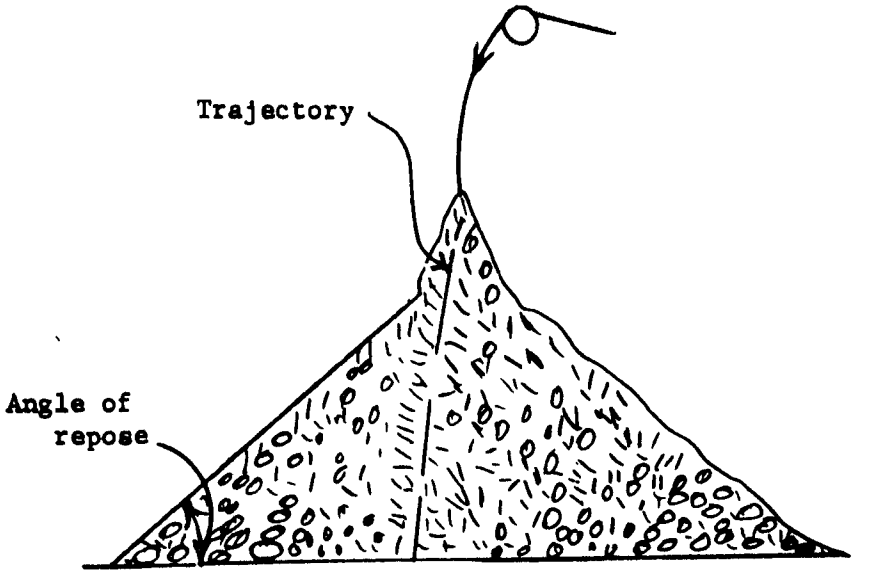

Fig. 4

Segregation and packing in a pile

outlet. Typical examples are provided by apron and belt feeders of constant width, Fig. 5, and by screw feeders of constant diameter and pitch, Fig. 6. If the length of the outlets exceeds, say, twice the width of the outlet at the apron or belt, or twice the diameter of the screw, it is a practical certainty that the solid will feed at one end of the feeder only. In an apron or belt feeder it is not possible to say, off-hand, which end it will be: it depends on the friction developed between the solid and the surface of the feeder. In a screw feeder the solid fills the screw at the end opposite the discharge (the back), the screw runs full over the remainder of its length and is unable to accept any more material. If the solid is at all cohesive it packs into a firm stable arch over the remainder of the screw. A similar situation occurs in a rotary table feeder when the skirts seal the solid around the table, Fig. 7: the solid then flows onto the table only through a channel over the plow; outside of that channel the solid remains stationary.

Stationary solid sliding over the feeder packs hard and creates large normal and frictional forces on the feeder contributing a major share to the power consumption and wear. This situation is therefore detrimental not only from the standpoint of flow but also from the standpoint of maintenance and consumption of power.

For a feeder to be effective along its full area, the capacity of the feeder must increase in the direction of flow of the solid within the feeder. Suitable feeder designs are described in Chapter III. In the discussion that follows it is assumed that the feeders are adequate and the outlets are fully active.

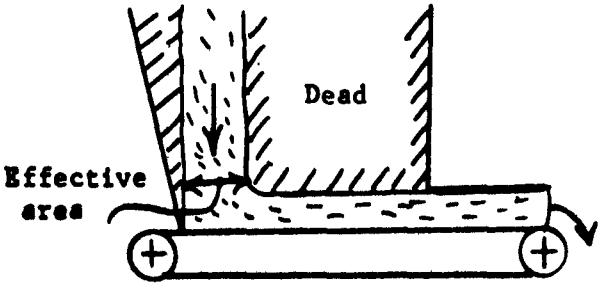

Fig. 5

Effective area of outlet in an apron feeder

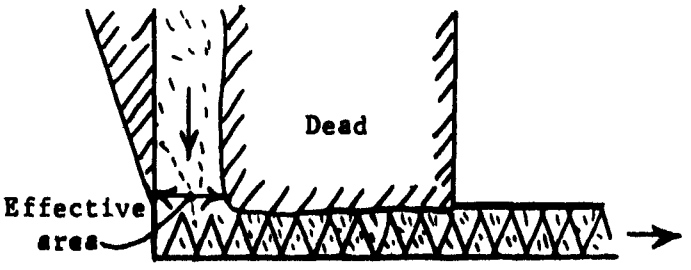

Fig. 6

Effective area of outlet in a screw feeder

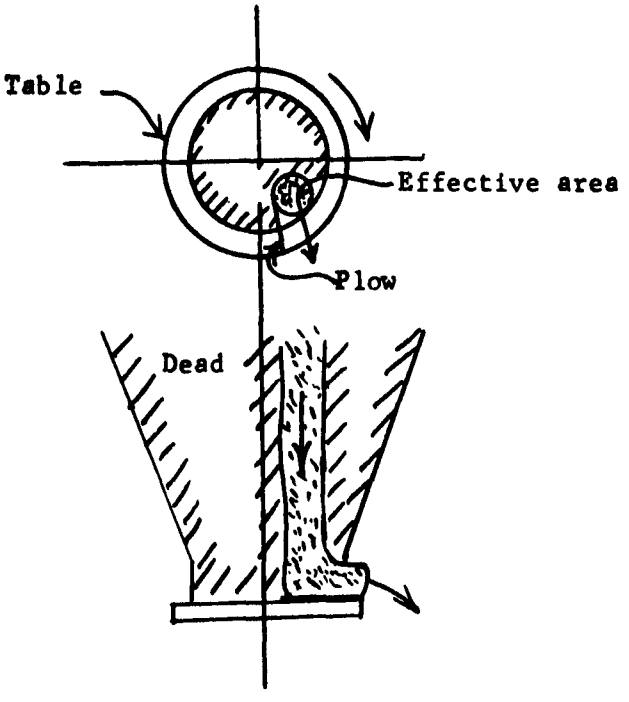

Fig. 7

Effective area of outlet in a rotary table feeder

Flow patterns. Two types of flow pattern will be considered: (1) Funnel-flow which occurs when a solid flows toward the outlet of the container in a channel formed within the solid itself. The solid outside of the channel is at rest and the shape of the walls of the container has no influence on either the shape of the channel or the velocity profile of the solid within the channel. (2) Mass-flow which occurs when the flowing channel coincides with the walls of the container. In perfect mass flow, all the solid in a bin is in motion whenever any of it is drawn out of the outlet. Mass flow hoppers are smooth and steep.

Flowability of solids

Comparison of solids and liquids. The word "flow" is more often associated with fluids than with solids, and when the "flow of solids" is mentioned, one is inclined to assume - by association - that the solid will behave much like a liquid. Such an assumption is incorrect. The properties of solids and of liquids differ so much that the mechanisms of flow of these phases are quite unlike. First of all, solids can transfer shearing stresses under static conditions - they have a static angle of friction greater than zero - whereas liquids do not. This is why solids form piles whereas liquids form level surfaces. Secondly, many solids, when consolidated - that is after pressure has been applied to them, possess cohesive strength and retain a shape under load. They can form a stable dome or a stable well; liquids cannot do that. Thirdly, the shearing stresses which occur in a slowly deforming (i.e. a flowing) bulk solid can usually be considered independent of the rate of shear and dependent on the mean pressure acting within the solid. In a liquid, the

situation is reversed, the shearing stresses are dependent on the rate of shear and independent of the mean pressure.

These fundamental differences are listed to explain why all attempts to derive flow - no flow criteria for solids from fluid flow concepts have been fruitless. A bulk solid has to be looked upon as a plastic and not a visco-elastic continuum.

Effective yield locus, EYL. Consider a solid flowing in a channel, Fig. 8, and, in particular, follow an element of the solid along its path through the channel. The particles of the element are assumed to be deposited at the top of the mass without impact. As the element flows down from the surface and is covered by new layers of the solid, pressures acting on the element increase, at first, then pass a maximum, and decrease toward the vertex of the channel [33-36,45]. Simultaneously, the shape of the element changes, causing the particles of the element to slide on one another. The particles are first brought closer together, as pressures increase, then farther apart, as pressures decrease.

During this process, which is called flow, the major pressure on the element is denoted by σ_1 and the minor pressure by σ_2. Since these pressures cause a change in the density of the solid - in fact, during flow, density is a function of the last set of pressures - they will be called consolidating pressures.

Experiments carried out on hundreds of bulk solids have demonstrated that the ratio σ_1/σ_2 varies but little as a solid of given moisture content H flows under a constant temperature T. This property of bulk solids is usefully expressed by the relation

$$\frac{\sigma_1}{\sigma_2} = \frac{1 + \sin \delta}{1 - \sin \delta}, \quad (H = \text{const.}, T = \text{const.}). \tag{1}$$

This relation is due to Jenike and Shield [37] and is referred to as the "effective yield function." Angle δ is called the "effective angle of friction," and for a given solid has been found to vary only within a few degrees for the range of pressures which occur in gravity channels.

Angle δ has been measured at between 30° and 70° for various solids. In general, fine and dry solids have low values of δ while coarse and wet solids have large values.

In the coordinates: pressure, σ, shearing stress, τ, Eq. (1) with a constant δ implies that, during flow, the Mohr stress circles* possess a straight envelope which passes through the origin. This envelope is called the "effective yield locus," EYL for short, and is inclined at an angle δ to the σ-axis, Fig. 9(a).

In the interpretation of tests, it is often more convenient to plot this and other relations in force coordinates. The corresponding plots are similar and differ only in units. For instance, it is convenient to replace the coordinates σ, τ by coordinates

$$V = A\sigma, \qquad S = A\tau, \tag{2a}$$

where A is the area of the cross-section of the shear cell used in the tests, Fig. 10. The forces applied to the shear cell can then be plotted directly.

*See any text on strength of materials.

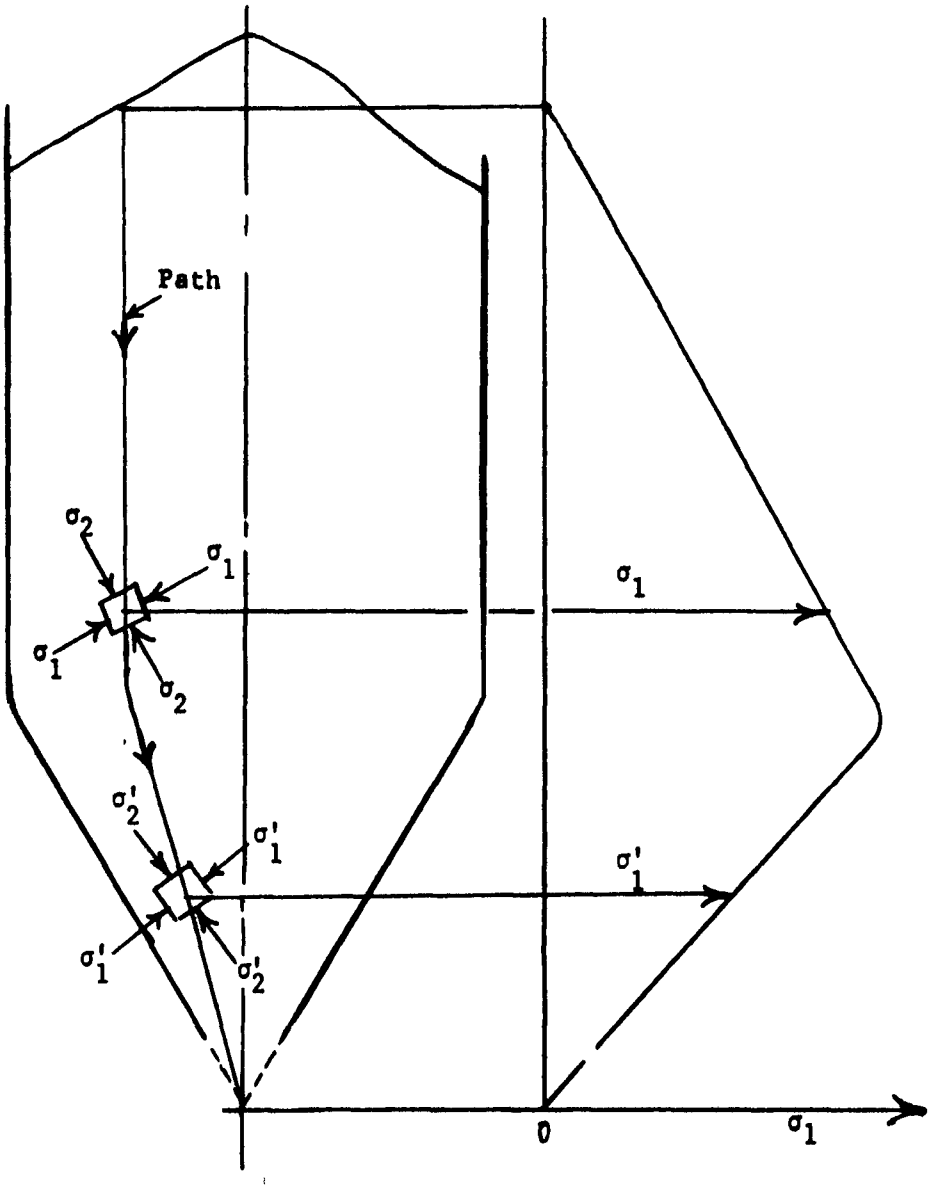

Fig. 8

Pressure acting on a flowing element

Relation (1) in principal consolidating forces

$$V_1 = A\sigma_1, \qquad V_2 = A\sigma_2 \tag{2b}$$

becomes

$$\frac{V_1}{V_2} = \frac{1 + \sin \delta}{1 - \sin \delta}, \quad (H = \text{const.}, T = \text{const.}). \tag{3}$$

This is shown in Fig. 9(b).

Yield locus, YL. In discussing the flow - no flow criteria of solids, it is necessary to consider the yield strength which a solid develops as it flows in a channel. An unconsolidated solid has no yield strength: in fact, an aerated solid may behave like a fluid. But, as the solid is placed in a channel, pressures arise under the weight of the superimposed mass, and - in the presence of a wetting liquid in the pores - also due to surface tension. Some air is forced out, the particles are brought closer together, and molecular forces develop: the solid consolidates and gains strength. The higher the pressure, the greater the consolidation and the strength of a given solid.

All solids do not gain the same strength under equal pressure. Gravel, dry sand are cohesionless; they gain practically no strength within the range of pressure which acts in storage plants. In order to cause such solids to shear, it is sufficient to overcome their angle of internal friction ϕ. If dry sand is placed in the shear cell, Fig. 10, loaded by a normal force V, and a shearing force S is applied, no continuous deformation occurs as long as $S < V \tan \phi$, and slip takes place for $S = V \tan \phi$. This is Coulomb friction. For values (V,S) lying below that line, Fig. 11, the solid can be considered to behave

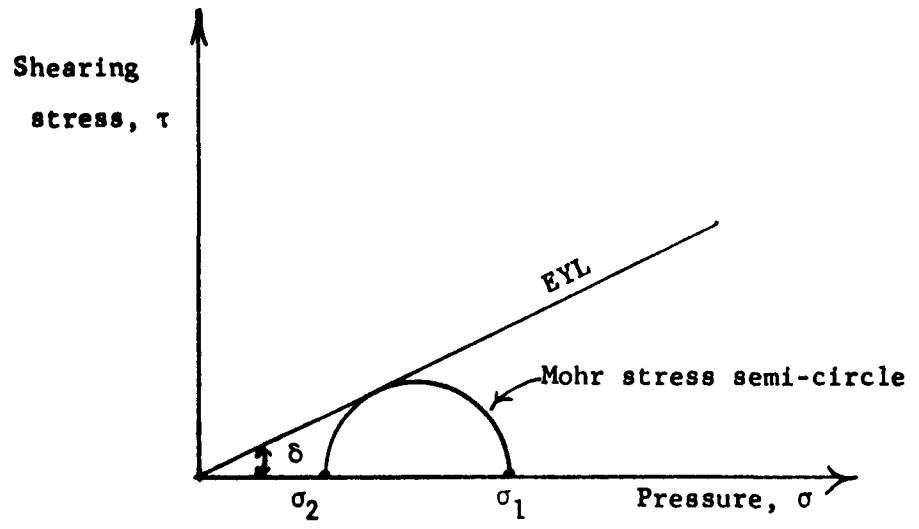

(a)

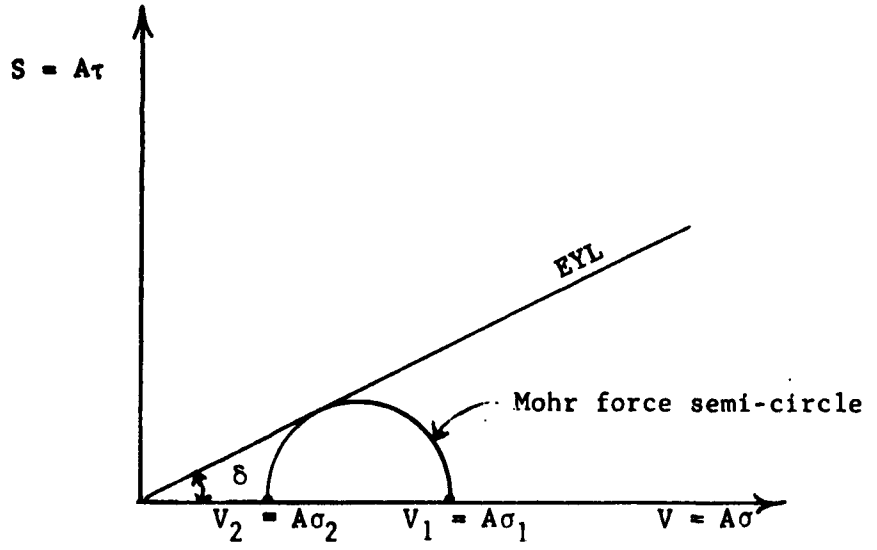

(b)

Fig. 9

Effective yield locus

rigidly (or elastically); for values lying on the line, slip or yield occurs. This line then is the locus of yield values of the normal and shearing forces and is therefore called the yield locus, YL for short. For free-flowing solids like gravel and dry sand, $\phi = \delta$, and the yield locus YL coincides with effective yield locus EYL.

Other solids are cohesive, they gain strength as pressure is applied to them. In V,S coordinates one such solid is now represented by a family of yield loci, each locus corresponds to a different consolidation. Consider a cohesive solid flowing in the channel, Fig. 8. If the flow of the element were stopped at the higher location, the element removed - undisturbed, placed in the shear cell, Fig. 10, sheared under a small normal load $\overline{V}$, and the shearing force $\overline{S}$ was measured, the point $(\overline{V},\overline{S})_1$ would define a point on the yield locus, YL, Fig. 12. If the experiment were repeated but with a somewhat larger normal load $\overline{V}$, a different shearing force $\overline{S}$ would be measured and point $(\overline{V},\overline{S})_2$ would also lie on the yield locus. Since, during flow, the element is continuously at yield, the Mohr force circle of flow defined by the principal consolidating forces $V_1 = A\sigma_1$ and $V_2 = A\sigma_2$ is also tangential to the yield locus.

If the above experiment were repeated from a different point of the path, where the principal consolidating pressures are smaller, say, σ_1' and σ_2', and the forces are V_1' and V_2', the solid would be less consolidated, and would possess a lower yield strength, as indicated by the yield locus YL' in Fig. 12. In each case, the yield locus terminates at a point E, or E', on the Mohr circles determined by the consolidating forces of flow. The effective yield locus EYL forms an envelope of these circles.

Kinematic angle of internal friction, ϕ. This is the angle between

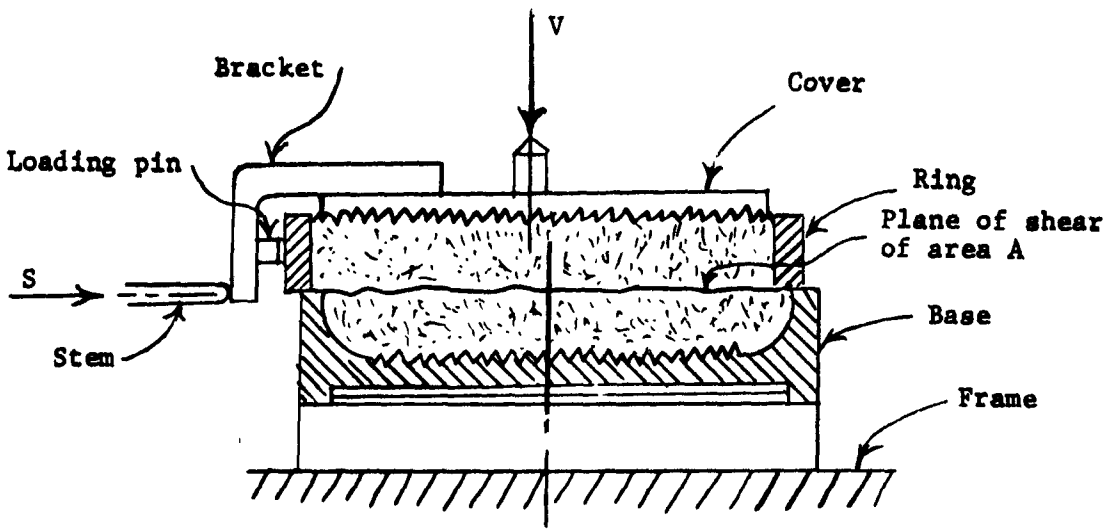

Fig. 10

A shear cell

the yield locus and the axis V, Fig. 12. In general, the yield loci form a family of convex-upward, curved lines and, therefore, the angle of friction of a solid varies with both, the particular yield locus and the normal force $\overline{V}$ under which shear is performed. The curvature of a yield locus is especially pronounced at low values of normal force. In fact, there are good reasons to suppose that angle ϕ increases all the way to 90° at the point of intersection of the locus with the V-axis [38,39]. Fortunately, the angle of friction ϕ does not appear in the analysis of flow.

Time yield locus, TYL. If the flow of a solid in a channel is interrupted for a period of time t, the forces V_1, V_2, which have acted on an element during flow, are assumed to remain essentially the same for that period of time, and tend to consolidate the element giving it greater yield strength. This is illustrated by a location of the time yield locus, TYL for short, above the YL, Fig. 13.

Unconfined yield forces, F and F_t. It is reasonable to assume that, when an obstruction to flow like a dome or a pipe is about to collapse, failure starts at an exposed surface of the obstruction and propagates from the surface into the mass. Therefore, the stress conditions which occur at an exposed surface during failure are of particular interest. They are also particularly simple because the stresses acting on an exposed surface are zero, the surface is a principal plane, and the major pressure within the solid is tangential to the surface. When this pressure causes yield, it is referred to as the unconfined yield pressure and denoted by the symbol f_c. The corresponding unconfined yield force is denoted by $F = Af_c$. At failure, a Mohr force circle is,

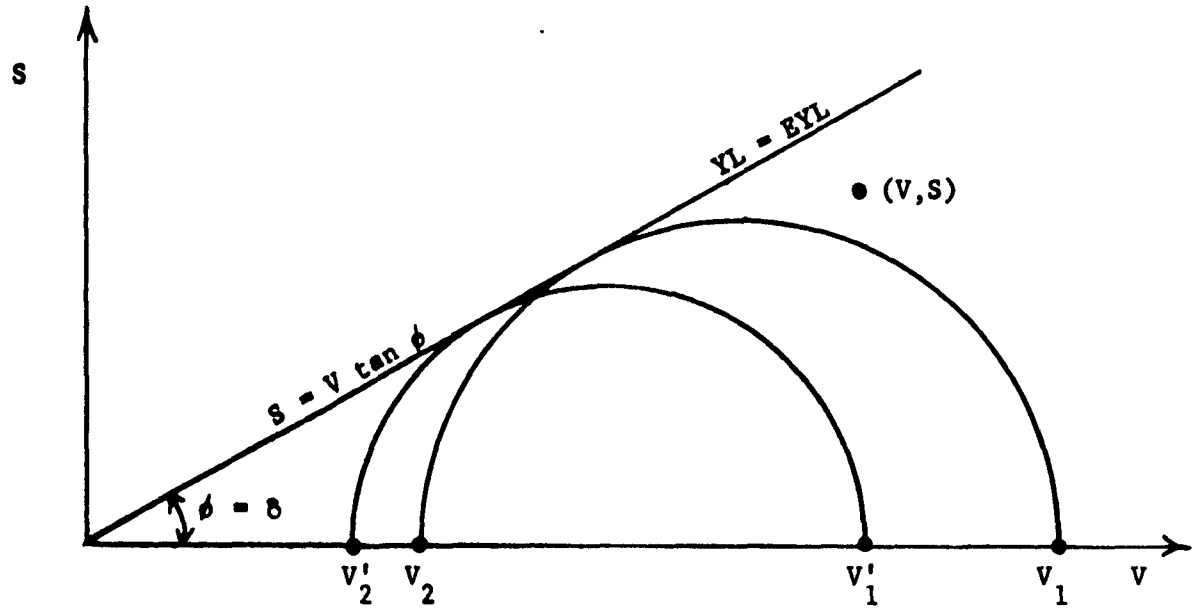

Fig. 11

Yield locus of dry sand

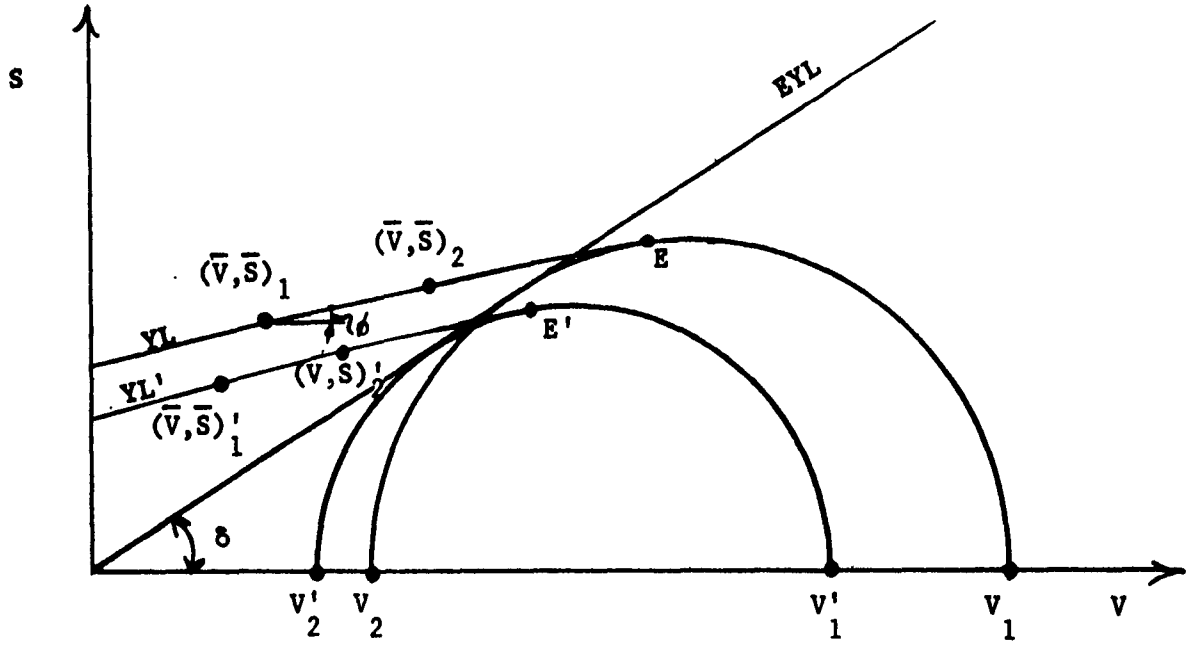

Fig. 12

Family of yield loci of a cohesive solid

of course, tangential to the yield locus. The value of F is therefore readily obtained, when the yield locus is known, by drawing a Mohr circle through the origin, V = S = 0, tangentially to the yield locus. The yield locus, YL, and the time yield locus, TYL, Fig. 13, define values of unconfined yield forces F and F_t, respectively. As a solid gains strength with time of consolidation at rest and its unconfined yield force F_t increases, the solid can support more extensive obstructions to flow; hence, it becomes less free-flowing.

Static angle of internal friction, ϕ_t. In the analysis of plug flow, it is also necessary to know the angle of internal friction which has developed within the solid at an exposed surface of a pipe. This angle is determined at the point of tangency of the TYL with the Mohr circle which determines the unconfined yield pressure F_t, Fig. 13.

Wall yield locus, WYL. In mass flow, a solid slides along the wall of the channel and the stress conditions along the wall enter the analysis of consolidating pressures. The normal and shearing forces at the wall during flow are denoted by V',S', respectively. They lie on the wall yield locus, WYL for short, Fig. 14. The WYL is another Coulomb friction line and is often in the form of a curved, convex-upward line.

Kinematic angle of friction between a solid and a channel wall, ϕ'. Since a wall yield locus is usually represented by a curved line, the kinematic angle of friction between a solid and a channel wall, ϕ', varies and is a function of the pressure at the wall. Yet the mathematical

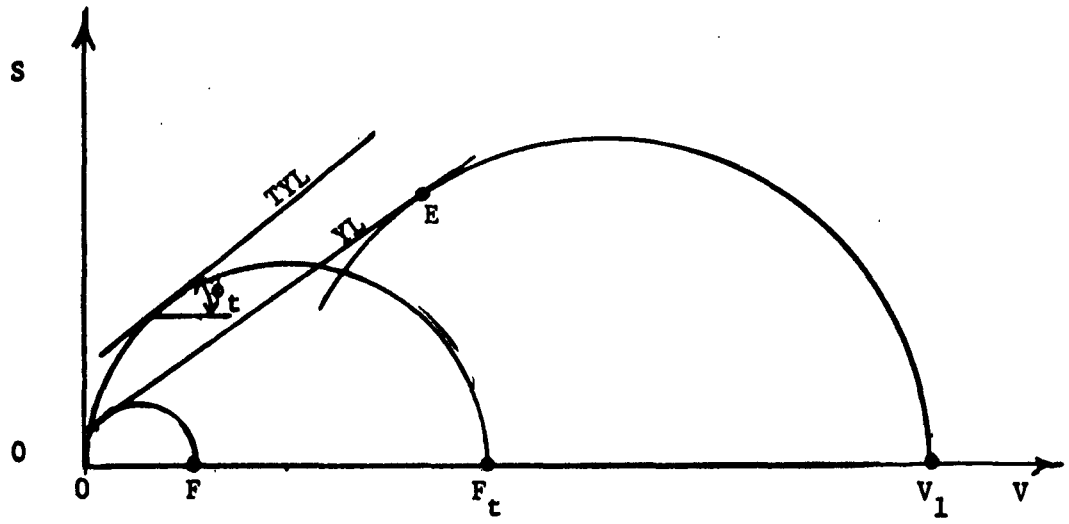

Fig. 13

Time yield locus

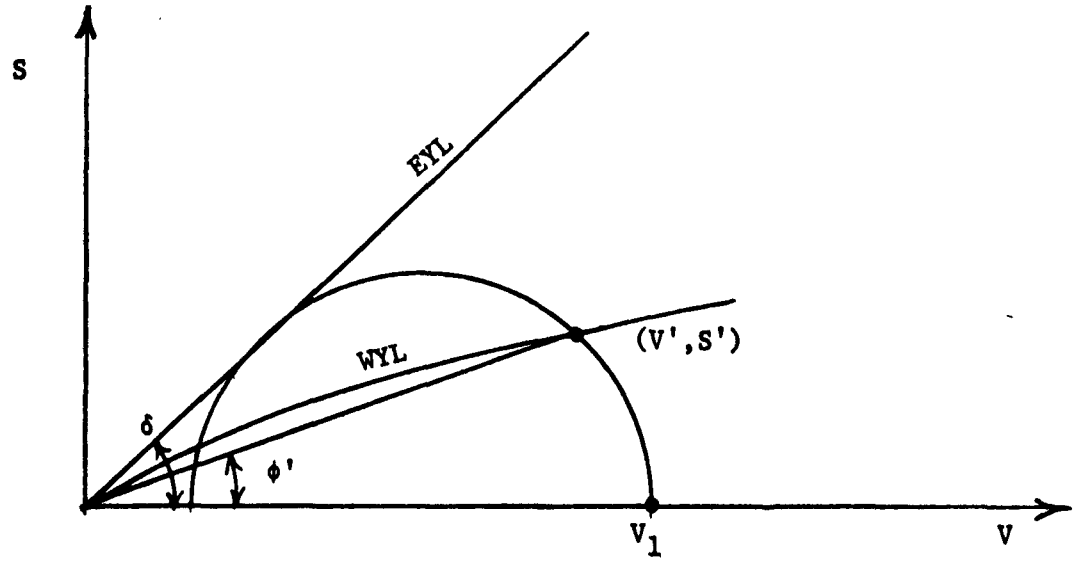

Fig. 14

Wall yield locus

analysis requires a constant value of ϕ'. It is therefore necessary to select a critical value of ϕ' for a safe design. In practice, the largest value of ϕ' is usually critical, and, for a convex-upward WYL, it occurs at the outlet of the hopper.

In the design process the values of the effective angle of friction δ and of the major consolidating force V_1 at the wall of the outlet are usually determined first. This permits the drawing of the EYL and the tangential Mohr semi-circle through V_1, as shown in Fig. 14. The point (V',S') is now determined, and the kinematic angle of friction ϕ' is found by drawing a straight line from the origin to point (V',S'). Then

$$\frac{S'}{V'} = \tan \phi'. \qquad (4)$$

While the Mohr circle provides two points of intersection with the WYL, the observed flow patterns require the point (V',S') shown in Fig. 14.

For asymmetric, plane-flow channels, it is simplest to assume that V_1 is the same at both walls. If the walls are made of the same material, then ϕ' is the same at both of them; if the materials are different, two WYL's are drawn in Fig. 14 and two angles ϕ' are determined.

Flow-function, FF. Consider again the solid flowing down the channel, Fig. 8. In general, moisture content H and temperature T affect the strength F of the solid. During continuous flow, T and H can usually be assumed constant, while the time of consolidation at rest t is, of course, equal to zero. Under these conditions, the yield

locus and the unconfined yield force F become a function of the consolidation of the solid which, in view of relation (3), and neglecting the effect of the third principal pressure, is fully determined by the major consolidating force V_1, thus

$$F = f(V_1), \quad (t = 0, \ H = \text{const.}, \ T = \text{const.}) \tag{5}$$

This relation is referred to as the instantaneous flow-function of a solid or, in brief, its flow-function.

Three typical flow-function curves are denoted in Fig. 15 by letters FF(a), FF(b) and FF(c). Evidently, the highest curve (c) marks a solid with most strength, greatest ability to support obstructions to flow and, hence, the least free-flowing one. On the other hand, dry, round sand, which develops no unconfined yield strength and is free-flowing has a flow-function curve coinciding with the V_1-axis. The curves in Fig. 15 could represent three different solids; they could also represent one and the same solid for three values of, say, moisture content.

When the flow of a solid is interrupted for a period of time t, the solid remains at rest under pressure and may gain additional strength. Flow-functions measured under these conditions are referred to as time flow-functions, they are of the type

$$F_t = f(V_1, t), \quad (H = \text{const.}, \ T = \text{const.}) \tag{6}$$

A further complication arises if, during the time of consolidation at rest, the moisture content or the temperature changes. This can be represented by the general relation

$$F_t = f(V_1, t, H(t), T(t)). \qquad (7)$$

The gain in strength at rest may be caused by any one or a combination of the following factors:

1. Escape of entrained air with corresponding increase of density.
2. Migration of water.
3. External vibrations due to operating machinery, railroads, or wind which cause a rearrangement of particles and an increase of density.
4. Evaporation of free water with concurrent precipitation of dissolved salts which cement the particles.
5. Break-up or softening of particles or crystals under pressure, causing an increase in the surface of contact and cohesion.
6. Changes in the surface of particles, e.g., crystallization, fermentation.

Experience indicates that functions of the type (6) are measured most frequently under ambient temperature for two to four moisture contents and one or two times of consolidation. Such tests apply to metallic ores and concentrates. Functions of the type (7) are usually measured for trace values of moisture, which is considered constant, and either for a constant temperature or for a decreasing temperature to reproduce cooling in storage. The latter condition usually leads to the critical design values for temperature-sensitive solids like plastics.

The flow-function curves are constructed from the yield functions. For instance, the values of F, F_t, and V_1 in Fig. 13 determine one point on each, the instantaneous ($t = 0$) and the time ($t > 0$) flow functions

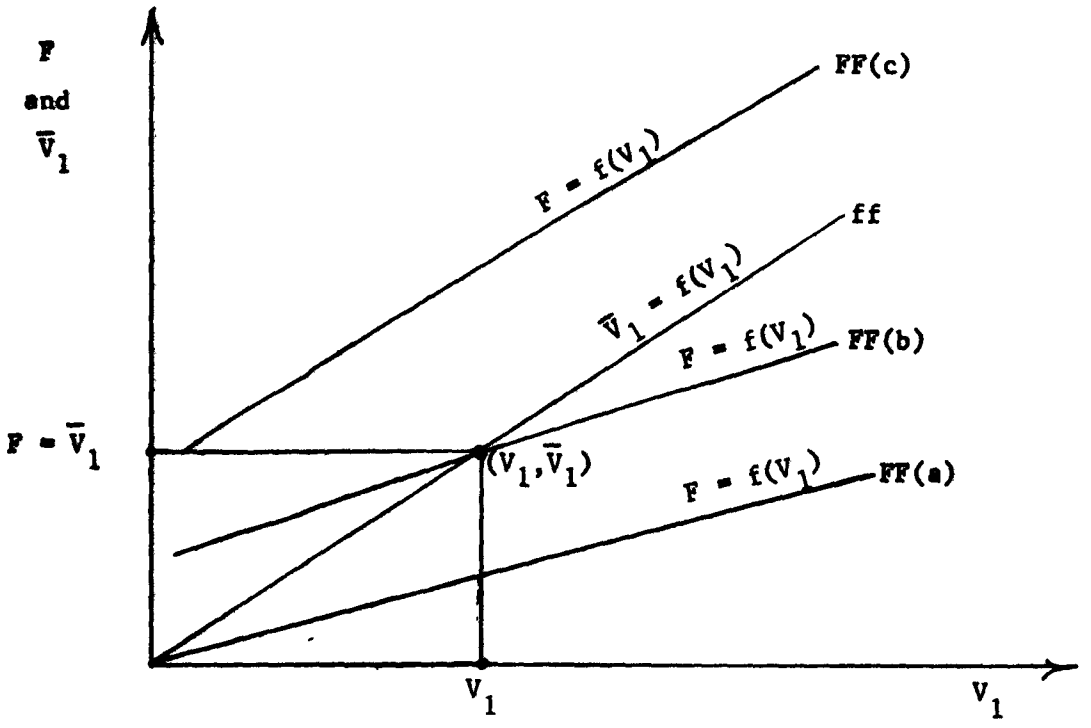

Fig. 15

Flow-functions

of Fig. 16(a). In the absence of a wetting liquid, a solid has no strength when unconsolidated; the flow-function curves pass through the origin, $V_1 = F = 0$ and the two points: (V_1F), (V_1,F_t) permit to draw two straight lines through the origin to approximate the flow-functions. When a wetting liquid is present, or its presence is suspected, the tests have to be repeated for a different value, say, V_1', and the straight lines through the two pairs of points now determine the approximate locations of the flow-functions, Fig. (16b). These lines are usually sufficient to expose the non-free-flowing solid and, in intricate cases, to show the direction in which the critical combination of parameters should be sought. Additional points are obtained later if it is necessary to define the flow-functions with greater precision.

Particle-size. As a general rule, solids which do not contain particles smaller than, say, 0.01 inch are free-flowing. There are exceptions to this rule. For instance, grain ferments under adverse moisture and atmospheric conditions and can develop sufficient strength to cease being free-flowing. Soybean meal contains oil which under conditions of high moisture and temperature binds the particles into a non-flowing mass. Flaky or stringy materials, like wood shavings, mica, asbestos, interlock and also form obstructions to flow. Most ores, coal etc. come under the general rule.

The flowability of a solid containing a range of sieve sizes, which include both fine and coarse particles, is invariably governed by the flow properties of the fine fraction. This is explained by the fact that during flow the shearing takes place across the fines. The coarse

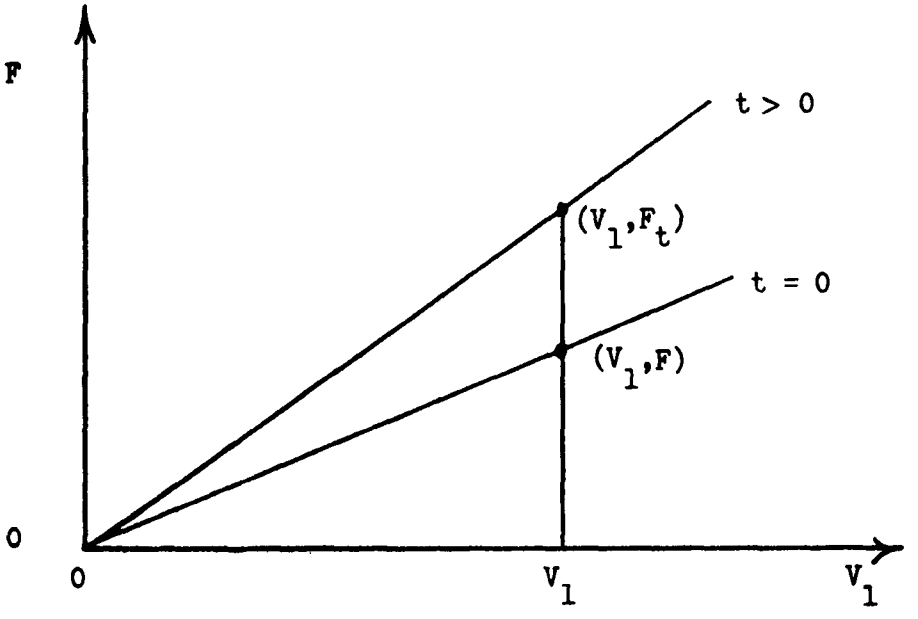

(a)

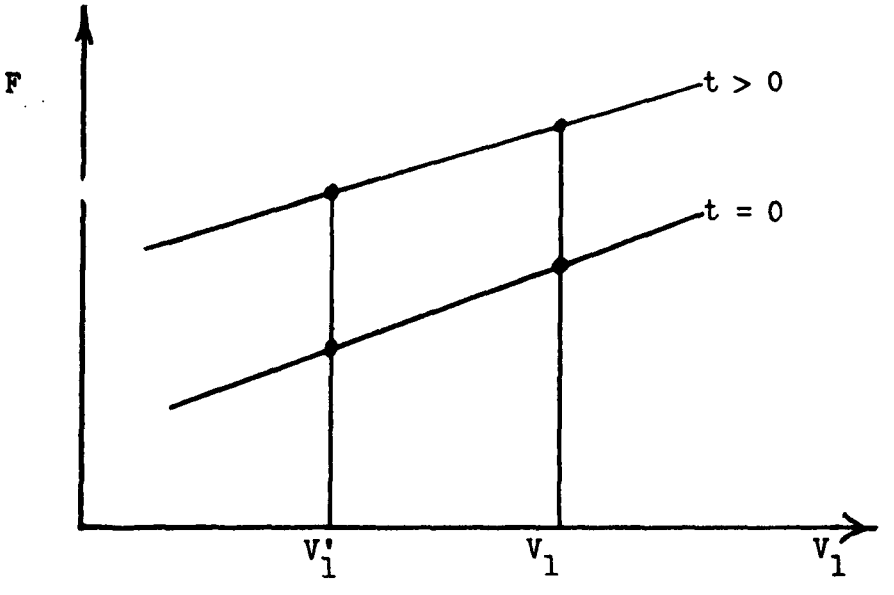

(b)

Fig. 16

Construction of flow-functions

particles are a passive agent in this process. However, the size of the coarse particles will affect the tendency to interlock at the outlet, and the impact of the heavy, coarse particles charged into a container may cause compaction of the solid along the trajectory of the falling stream.

Flowability of channels

Flow-factor, ff. While there is an infinite number of possible obstructions to flow, extensive observations point to the conclusion that a solid will flow if a dome does not develop across the channel. In mass-flow channels, this is sufficient. In plug-flow channels, it is also necessary to assure that the solid be unable to sustain an empty vertical pipe of excessive height. Fig. 2.

For an obstruction to occur in a channel, the solid has to be consolidated to such a degree that it develops sufficient strength to support the weight of the obstruction. Hence, the higher the consolidating pressures σ_1 in a channel, and the lower the pressures $\bar{\sigma}_1$ which act in an obstruction, the lower the flowability of the channel. This is expressed by the flow-factor,

$$ff = \sigma_1/\bar{\sigma}_1. \tag{8}$$

In corresponding force coordinates $V_1 = A\sigma_1$, $\bar{V}_1 = A\bar{\sigma}_1$, the flow-factor becomes

$$ff = V_1/\bar{V}_1. \tag{8a}$$

The smaller the value of ff, the better the channel.

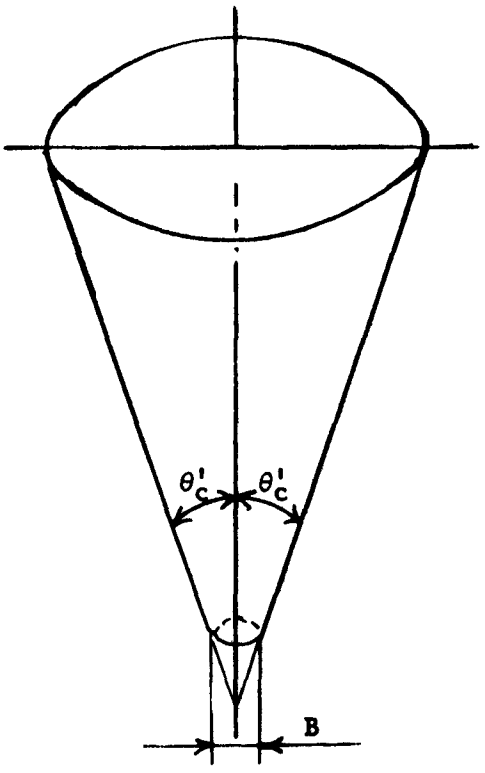

Fig. 17

Conical channel

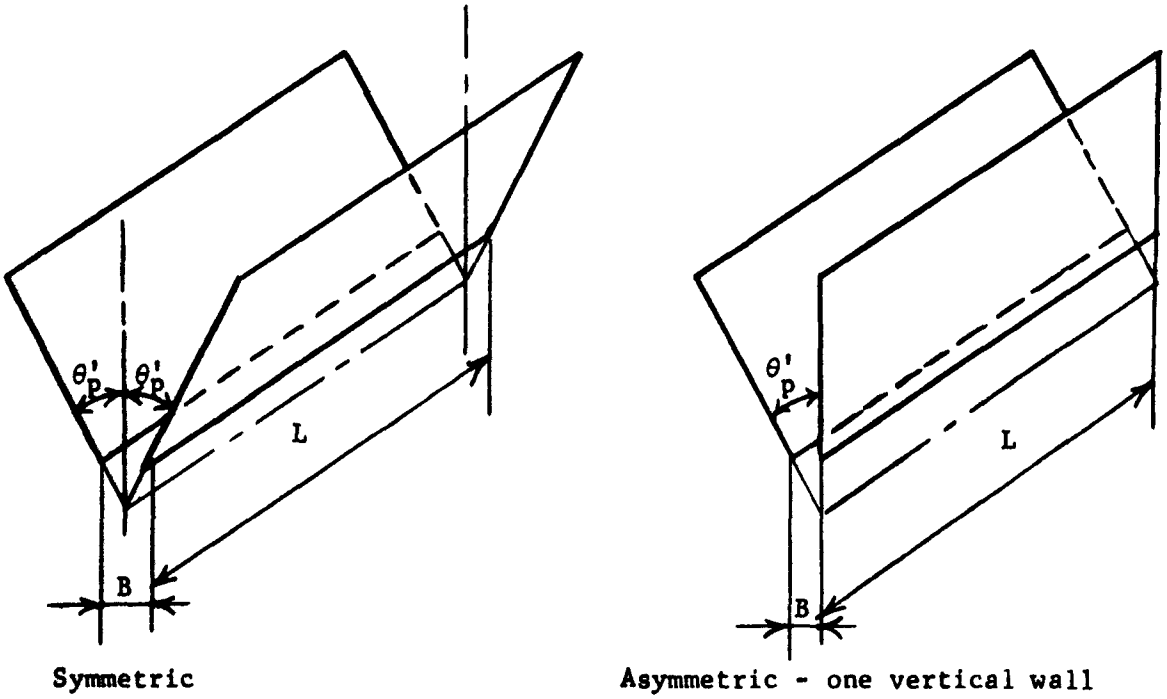

Symmetric

Asymmetric - one vertical wall

Fig. 18

Plane-flow channels

The no-doming flow-factors are computed for two horizontal shapes of channels: the conical channel, Fig. 17, and the plane flow channel, Fig. 18. It is evident that plane flow does not exist in reality; however, the results are useful because plane flow is closely approached at the sides of channels with rectangular (slot) outlets whose ratio of length L to width B exceeds 3. Such channels are of great practical importance.

In mass-flow, values of the flow-factor are plotted in Figs. 45 to 49 for conical channels; in Figs. 50 to 54 for symmetric, plane-flow channels; and in Figs. 55 to 57 for asymmetric, plane-flow channels. ff is a function of the slope angle of the channel θ', the kinematic angle of friction between the flowing solid and the wall ϕ', and the effective angle of friction δ. Contours of constant values of ff are drawn in θ', ϕ' coordinates for constant values of δ = 30°, 40°, 50°, 60° and 70° for the symmetric channels. This covers the useful range of parameters. For the asymmetric plane-flow channels, calculations have been carried out only for δ = 50°, and a kinematic angle of friction at a vertical wall ϕ^v = 20°, 30°, and 40°; θ'_p and ϕ' refer to the sloping wall. This is sufficient to provide a comparison of the flowability of symmetric and asymmetric plane-flow channels.

In plug-flow, the flow-factor depends on δ and the slope of the channel, Fig. A-7. For design purposes ff = 1.7 is recommended. Contours of the no-piping flow-factor are plotted in Fig. 35 as a function of the static angle of internal friction ϕ_t and the effective angle of friction δ.

Solids in a channel

Flow - no flow postulate. Gravity flow of a solid in a channel will take place provided the yield strength which the solid develops as a result of the action of the consolidating pressures is insufficient to support an obstruction to flow.

For an obstruction to fail, the stresses in an obstruction must exceed the yield strength of the solid at a critical location. It is assumed that the critical stress occurs at the exposed surface of an obstruction. The critical stress is then a major pressure and is denoted by $\bar{\sigma}_1$, while the corresponding major force is $\bar{V}_1 = A\bar{\sigma}_1$. The yield strength is clearly the unconfined yield pressure f_c. The flow postulate is expressed by

$$\bar{\sigma}_1 > f_c. \tag{9}$$

Dimensions of an outlet. The usefulness of the concepts of the flow-function and the flow-factor will now become apparent. $\bar{\sigma}_1$ is eliminated between expressions (8) and (9), leading to

$$\sigma_1/f_c > ff. \tag{10}$$

The pressures are replaced by the corresponding forces $V_1 = A\sigma_1$, $F = Af_c$, resulting in

$$V_1/F > ff. \tag{10a}$$

Now, in Fig. 15, coordinate $\bar{V}_1$ is plotted along the axis F. ff, Eq. (8a), plots as a straight line in the $V_1,\bar{V}_1$ coordinates and, for expression (10a) to be satisfied, the flow function FF of the solid must

lie below the ff-line. In the example, the solid represented by FF(a) will flow in the channel represented by the flow-factor ff; the solid represented by FF(c) will not flow in that channel, while the solid represented by FF(b) will flow in that part of the channel in which

$$F < \bar{V}_1 \tag{11}$$

Generally, the flow-function is convex-upward, as shown in the figure, and expression (11) determines a minimum dimension of the channel, i.e. the dimension of the outlet of the channel, B. This dimension is the minor dimension of an outlet, e.g. the side of a square outlet, the width of a rectangular outlet, the diameter of a round outlet, and is

$$B = H(\theta')\bar{V}_1/A\gamma, \tag{12}$$

where $H(\theta')$ is plotted in Fig. 43.

For no-piping in plug-flow, the analysis is similar. This time the no-piping flow-factor is drawn, and another point of intersection $(V_1,\bar{V}_1)$ is determined. For the solid at the surface of the pipe to fail, inequality (11) has again to be satisfied. The formula for the minimum diameter of the pipe is

$$D = G(\phi_t)\bar{V}_1/A\gamma, \tag{13}$$

where $G(\phi_t)$* is plotted in Fig. 36. Since the diameter of the pipe approaches the largest, i.e. major, dimension of the outlet, D determines this dimension. In a circular outlet, D is the diameter; in a square or rectangular outlet, D is the diagonal.

---

*In Bulletin 108, $G(\phi_t) = 4(d\omega/dn)_{n=1}$

CHAPTER II

TESTING THE FLOW PROPERTIES OF BULK SOLIDS

Apparatus

The field of soil mechanics was well developed at the time when this study originated (1952). Since soils are bulk solids, it was natural first to investigate the applicability of the available soil testing equipment to the measurement of the flow properties of bulk solids.

Direct shear apparatus and unconfined compression apparatus were tried. The results obtained with shear apparatus were not satisfactory, primarily, because the range of values of cohesion for which the soil test machines were designed was outside of the useful range for bulk solids. By the terminology of soil mechanics, bulk solids can be considered cohesionless, while soils under their usual degree of consolidation would not flow by gravity in any storage system. Unconfined compression apparatus was also found unsuitable because of the impossibility of applying a known, uniform consolidation and because the stresses due to the weight of the sample were in the range of the measured yield stresses. These samples often disintegrated during handling.

It was decided to develop a direct-shear tester especially for bulk solids. The direct shear method was selected in preference to other methods, and in particular to the triaxial method, because of several reasons: (1) Shear tests are easier and quicker to make than triaxial tests. In view of the large number of points which often need to be

obtained, the difference in the time required for testing is substantial. (2) All tests are made on loose solids which are consolidated under known pressures in the tester; hence uniform, easy and quick consolidation is important. The shape of the shear specimen lends itself better to uniform consolidation than the shape of the triaxial specimen, because it is easier to consolidate a shallow specimen than a deep one. The ratio of height to diameter of a shear specimen is below 1:2 as compared to 2:1, or more, required for a triaxial specimen. To simplify and speed up consolidation, the shear cells are made of circular cross-section. (3) The measured stresses are so low that the influence of the weight of the solid within a specimen must be taken into account. This is easily done in a shallow shear specimen whose plane of shear is horizontal but is practically impossible to do in a deep triaxial specimen with an oblique plane of shear. (4) The objectionable non-uniformity of stress distribution in a conventional shear cell has been overcome by a new design of the cell.

The shear cell, Fig. 10, is composed of a base located on the frame of the machine, a ring resting on top of the base, and a cover. The bottom of the cover and the inside of the base are roughened to increase adhesion of the tested solid. The base and the ring are filled with the tested solid. The vertical force V is applied to the cover. The horizontal shearing force S is applied by means of a stem which acts on a bracket attached to the cover. The stem acts in the plane of contact between the ring and the base. A part of the shearing force is transferred from the bracket to the ring through a loading pin. This ensures a sufficiently uniform distribution of the shearing force across the cell. The

standard shear cell is 3.75 inches inside diameter.

The tester which has been used since 1958 is shown in Fig. 19. It is equipped with a shear cell, a gravity vertical loading system, and an electro-pneumatic shearing force applicator. The applicator has a shearing rate of 0.106 in. per min. The shearing force S necessary to maintain the strain-rate is continuously recorded on a pneumatic recorder. This arrangement produces a permanent record of the stress-strain relations for each test.

The shear tester is used in conjunction with a six-cell consolidating bench in which the cells are placed for the time of consolidation at rest, Fig. 20, and covered to prevent moisture changes.

The bench shown in Fig. 21 is used for temperature sensitive solids. Here the consolidating bench is enclosed in a heating chamber which permits the control and recording of the temperature of the tested solid.

Purpose of tests

The purpose of the tests is to measure the effective angle of friction δ, the necessary flow-functions FF, the bulk density γ, and either the kinematic angle of friction ϕ' between the solid and a material of the wall - for mass-flow bins, or the static angle of internal friction ϕ_t of the solid - for the plug-flow bins.

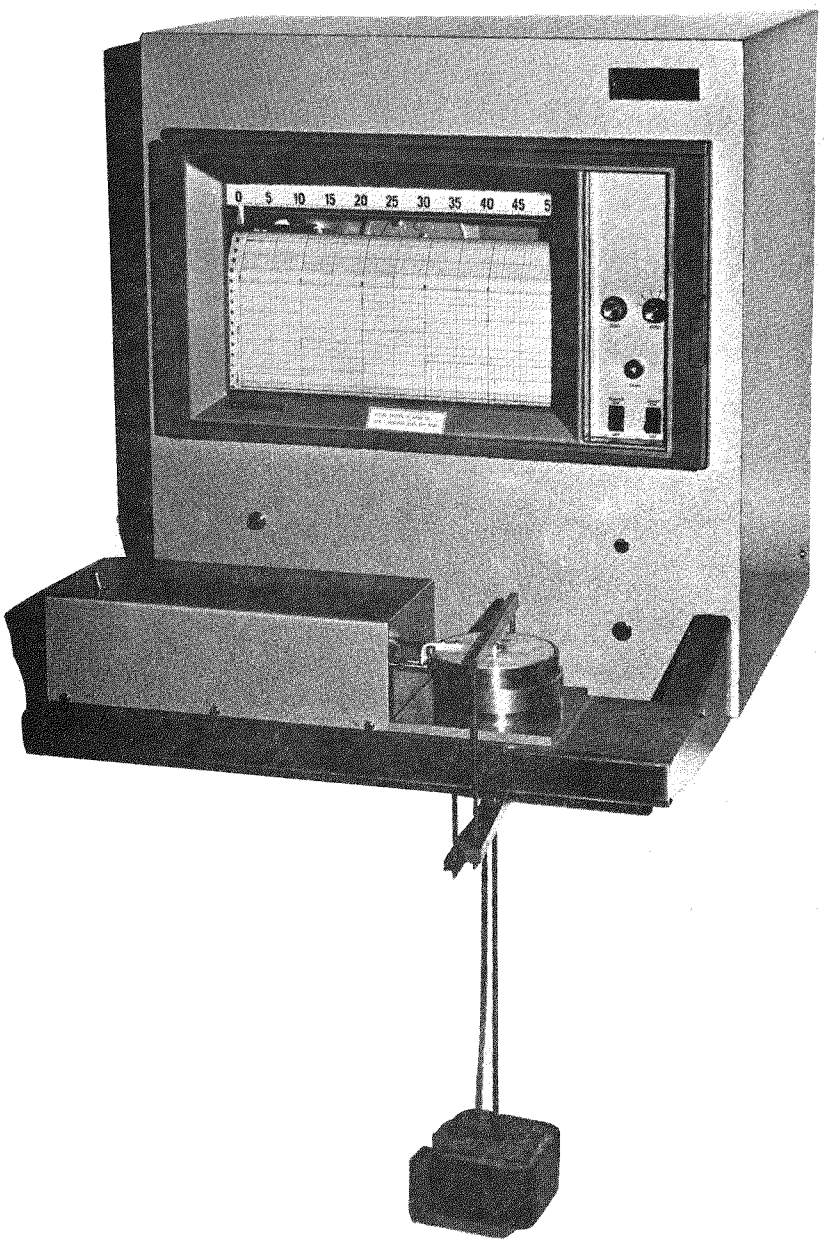

Fig. 19

Direct-shear tester

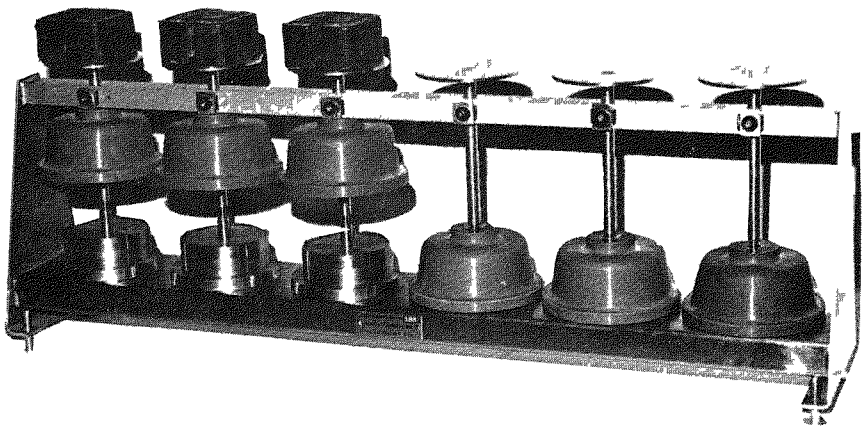

Fig. 20

Consolidating Bench

Test Specimens

In the execution of the tests it is necessary to ensure that the specimens of the tested solid and of the materials for the hopper walls are uniform and representative of the field conditions. In general, the yield locus of a solid for a given consolidating pressure and a given rate of shear is affected by the water content, temperature, and particle size distribution of the specimen. As a rule, the tests are conducted on solids containing water below the point of saturation. In view of the considerable influence which water content has on the yield loci of solids, it is necessary to reproduce the required content accurately, and to handle the samples and shear cells rapidly in order to minimize errors due to evaporation. When testing is done at a temperature other than ambient, handling of the cells should also be rapid.

The particle size distribution is not as perplexing as it might appear at first sight. In the flow of bulk solids, our interest lies in the conditions that lead to stoppages of flow. Stoppages occur when the solid reaches an excessive yield strength. Thus, the critical conditions to be considered are those of highest strength. During the flow of a mass of mixed particle sizes, the large particles move bodily while the material shears across the fines. Therefore, the yield strength of the mass depends on the properties of the fines. The coarse particles are a passive agent and, like aggregate in concrete, they do not develop yield strength without fines to bind them. Experience shows that screened out coarse solids are invariably free flowing; they do not develop any cohesion. To determine the yield loci of a mixed material, the fines are screened through an arbitrarily chosen No. 8 mesh (0.0937 in. aperture)

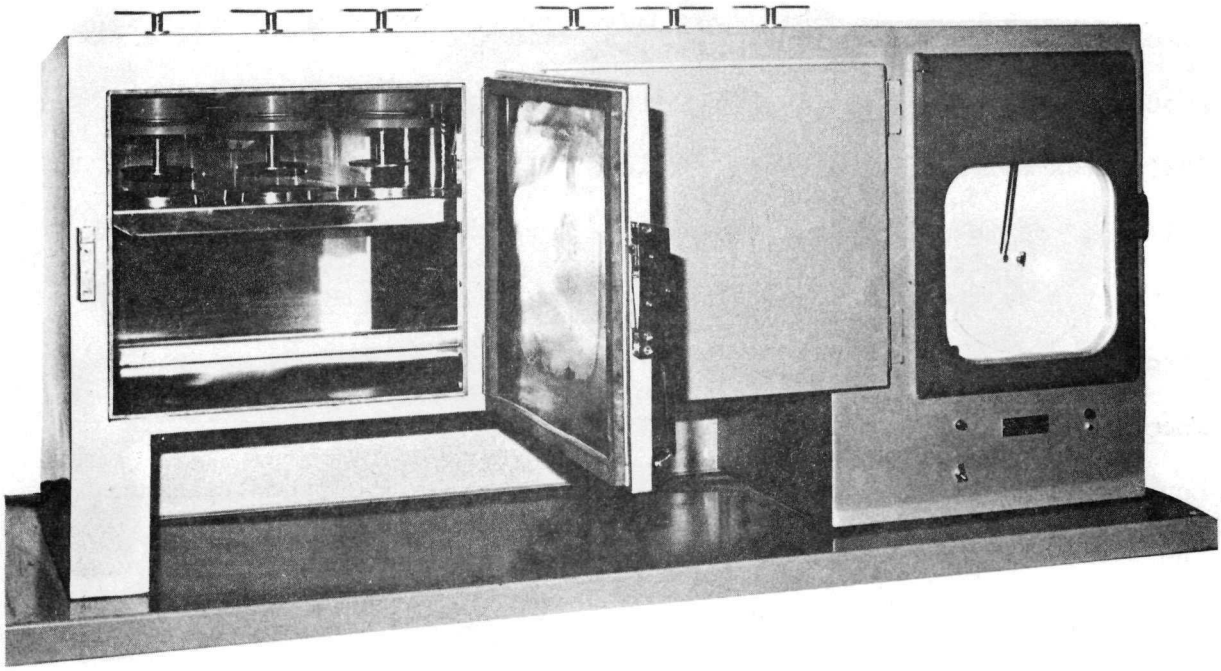

Fig. 21

Consolidating bench in a temperature controlled chamber

sieve, and tested.

Continuous flow

Consolidation. The consolidation of a sample is carried out in two stages. The first stage is called preconsolidation and its purpose is to prepare a uniform specimen. With the cover off the test cell, a packing mold is placed on top of the ring and both the mold and the ring are placed in an offset position on the base, as shown in Fig. 22. A sample of the tested solid is then placed in the cell. One layer after another is slightly packed with the fingers, up to the top of the mold. The excess material is scraped off level with the top of the mold. A twisting top is placed over the solid. A vertical force V_t is applied to the top by means of the system of lever and weight shown in Fig. 19. Force V_t causes a vertical pressure σ_t in the material. By means of a special wrench, a number of oscillating twists is now applied to the cover. This preconsolidates the solid and assures a uniform specimen. The value of V_t is discussed below in the example.

Consolidation is completed in the second stage by causing the specimen to flow under given stresses until a steady state is reached, or closely approached. This is attained in the following way: Load V_t is taken off, the twisting top and the mold are removed, the excess material is scraped off level with the top of the ring, and the test cover is placed on the material. A load V is now placed, and the stem of the shearing device is advanced against the bracket, Fig. 10.

The shearing force S divides between the cover and the ring. This method of applying the shearing force seems to assure a satisfactory distribution of stresses across the specimen. Prior to the adoption of

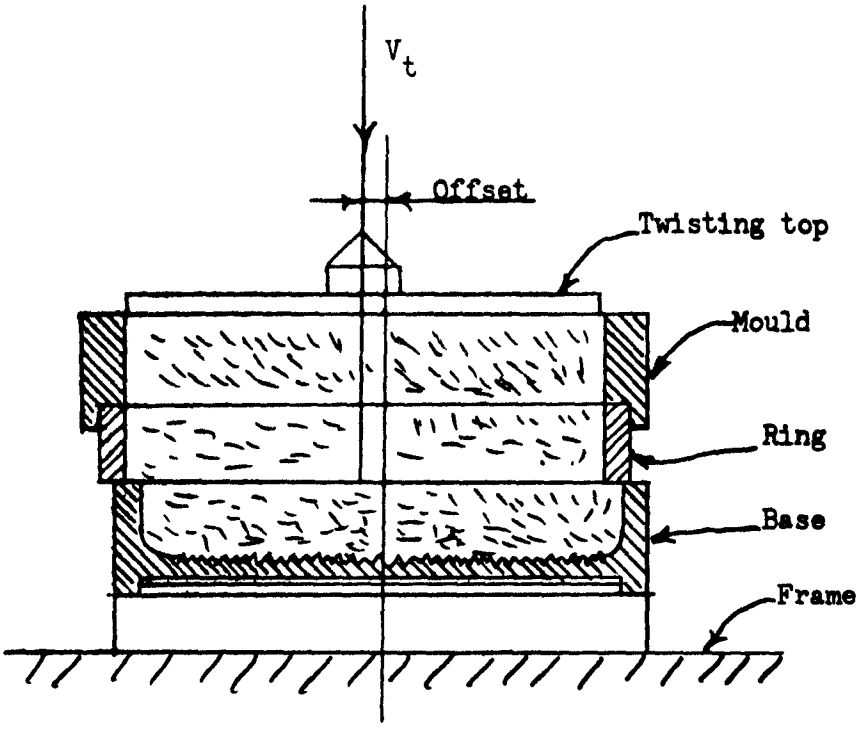

Fig. 22

Preconsolidation of a shear cell

this method, the shearing force used to be applied directly to the ring causing stress concentrations at the loaded edges of the ring and of the base and frequently leading to the shear of the solid within the ring rather than in the plane between the ring and the base. Furthermore, the unloaded side of the ring would often rise off the base, exposing the sheared specimen and weakening it significantly. It will be noted from Fig. 10 that the loading pin bears against the ring at its mid-height: this reduces the tendency of the ring to rise off the base. As an additional safeguard against the rising of the ring, it is sometimes pressed down with the fingers, at intervals, during the process of flow.

As shearing proceeds, a condition is reached when a layer of the solid across the whole specimen is caused to flow plastically: the recorded shearing force reaches a steady value S. The stresses which occur in the solid during this stage of consolidation have been described in references 38 and 39. Consolidation determines point (V,S), Fig. 23.

Shear. When consolidation is completed, the stem of the shearing force device is retracted. The vertical compacting load V is replaced by a smaller load $\overline{V}$ to locate a useful point $(\overline{V},\overline{S})$ of the yield locus, Fig. 23. The shearing force is now applied until a failure plane has developed. This fact is indicated on the recorder by the force $\overline{S}$ passing a maximum value. After shearing, the plane of failure of the specimen is checked. The plane of failure should roughly coincide with the plane of shear of the cell. If the planes deviate, it means that the measured point $(\overline{V},\overline{S})$ does not lie on the yield locus and the test is repeated.

The determination of one yield locus requires the measurement of two or three points of the locus $(\overline{V},\overline{S})_1$, $(\overline{V},\overline{S})_2$, and $(\overline{V},\overline{S})_3$, Fig. 23.

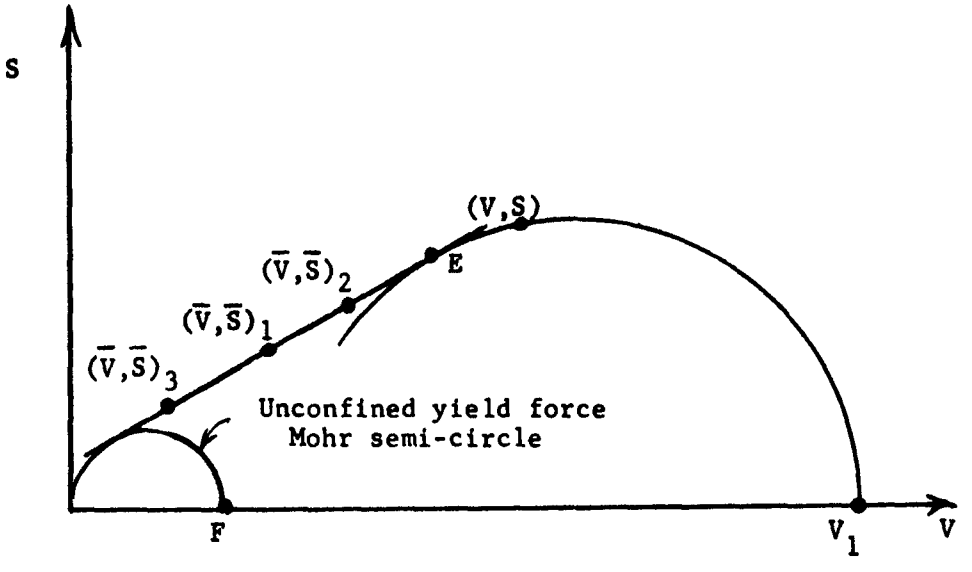

Fig. 23

Construction of a yield locus

For each point, the specimen is first consolidated and then sheared. The first specimen is sheared under an intermediate value of normal force $\overline{V}$; for the second specimen, force $\overline{V}$ is stepped up to about 2/3 of the force V. The location of the unconfined yield force Mohr semi-circle is estimated from the two $(\overline{V},\overline{S})$ points. This semi-circle is drawn through the origin tangentially to the yield locus. A third value of $\overline{V}$ is selected so as to lie somewhat to the right of the point of tangency between the yield locus and the semi-circle. Any point $(\overline{V},\overline{S})$ lying to the left of the point of tangency should be rejected, because it implies tensile stresses within the shear cell, to which the cell is obviously not adapted. It is necessary to obtain the values of these points for the same steady consolidating shear each time. This is accomplished by running a sufficient number of tests to permit interpolation* to a suitably selected value of S.

The yield locus is now drawn and extrapolated toward the higher values of V and a Mohr semi-circle is drawn through point (V,S) tangentially to the yield locus. The point of tangency E locates the terminus of the yield locus. The point of intersection of the semi-circle with the V-axis determines the value of the major consolidating force V_1. The Mohr semi-circle for the unconfined yield force F is now drawn. The force F is determined by the point of intersection of the circle with the axis V, as shown in the figure.

---

*The reader will notice the difference from the earlier procedure published in references 38 and 39, which recommended interruption of consolidation at 95% of a value of S obtained in a preliminary test.

Example: A typical recorder chart is shown in Fig. 24. The curves are numbered and represent the following steps:

1. Preconsolidation under load V_t = 8.9 lb.
2. Consolidation of the first specimen under a vertical load V = 8.9 lb.
3. Shearing of the first specimen under a vertical load $\overline{V}$ = 3.9 lb.
4. Consolidation of the second specimen under the same vertical load V.
5. Same as 2. Test 2 is repeated because of the scatter in the values of S.
6. Consolidation of the third specimen under the same vertical load V.
7. Shearing of the third specimen under a vertical load $\overline{V}$ = 5.9 lb = approx. 2/3 x 8.9.
8. Consolidation of the fourth specimen under the same vertical load V.
9. Shearing of the fourth specimen under a vertical load $\overline{V}$ = 2.9 lbs.

The measured and prorated values are shown below:

	Measured				Prorated		
V	8.9	8.9	8.9	8.9	8.9	8.9	8.9
S	8.9	8.5	8.7	8.8	8.7	8.7	8.7
$\overline{V}$	3.9	3.9	5.9	2.9	3.9	5.9	2.9
$\overline{S}$	5.5	5.3	6.8	4.6	5.4	6.8	4.55

The prorated values are those shown in Fig. 25. In drawing the yield locus, it should be born in mind that, on theoretical grounds of convexity of yield surfaces (46), the yield locus cannot be concave upwards. In this case the locus defines V_1 = 22.4 lb and F = 9.3 lb. These values determine a point of the flow-function in Fig. 25.

A tangent to the V_1-circle is also drawn through the origin in Fig. 25. The slope of this tangent determines the effective angle of

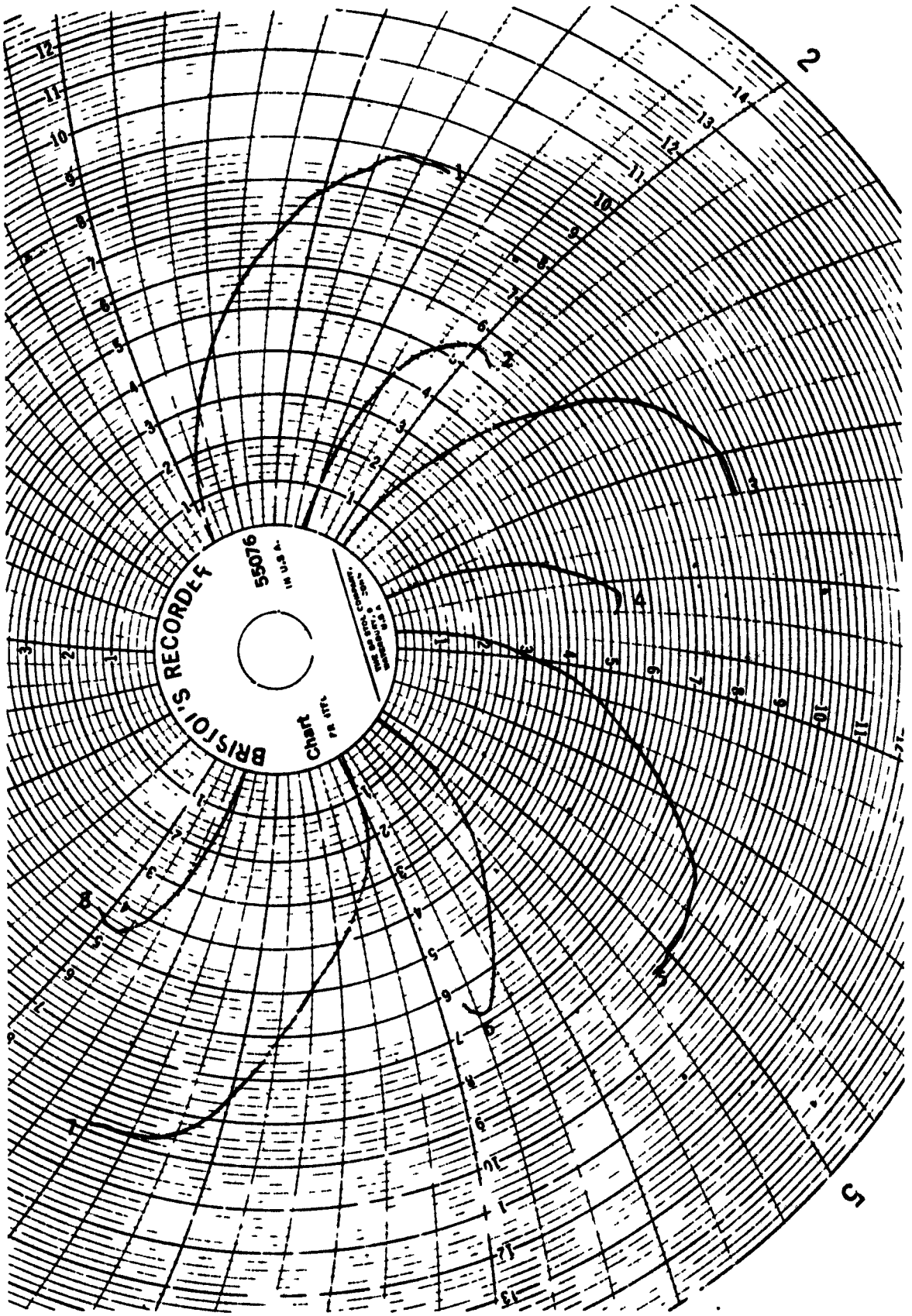

Fig. 24

A typical recorder chart - measurement of flowability

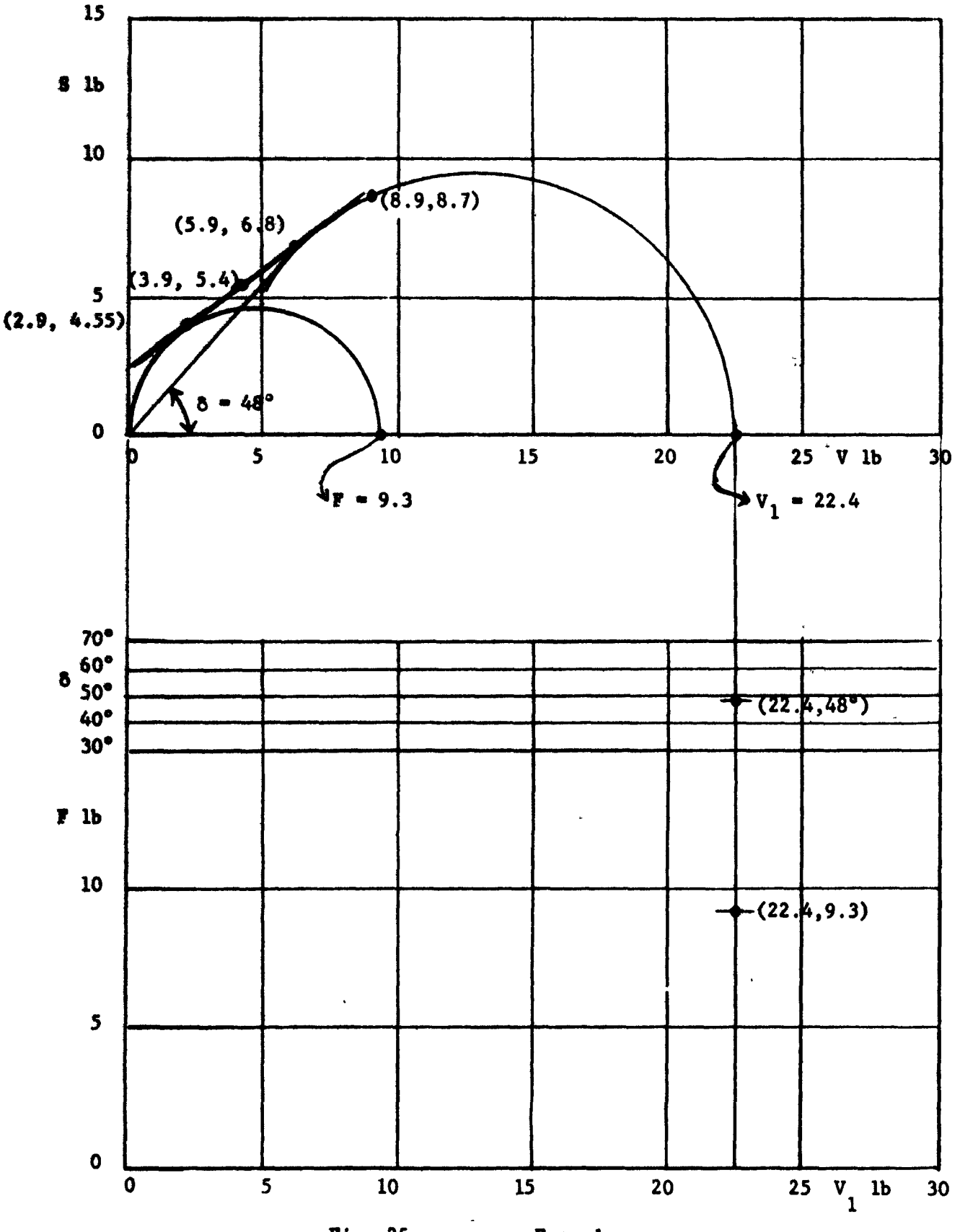

Fig. 25 Example

friction $\delta = 48°$ for $V_1 = 22.4$ lb.

In preconsolidation, a vertical force $V_t = V$ is used at first. V_t is increased above V if the force S during consolidation keeps rising and does not reach a steady value within $\pm$ 1/16 inch of the central position of the ring on the base. V_t should not be so large as to cause force S to go over a maximum, since this indicates over-consolidation in the preconsolidation stage, and the development of a weak plane across the specimen.

Time effect

When the flow of a solid in a channel is stopped for an interval of time, the solid remains under the action of static pressure and consolidates with time. Since consolidation at rest significantly increases the strength of some solids and, thus, reduces their flowability, it is necessary to measure the time effect in order to know whether or not the flow of a solid can be restored after storage at rest.

In these tests, the solid is first consolidated in the shear cells under conditions described above for continuous flow, and then the cells are placed in the consolidating bench under a static load for the prescribed interval of time. No shearing force is applied in the consolidating bench and the vertical force is V_1. The load V_1 is selected on the assumption that the static pressures in the channel during storage at rest are the same as the pressures which prevailed during flow. Experience indicates that the results of tests are not sensitive to an error of 5 to 10% in the value of V_1.

After the lapse of the prescribed interval of time, the cells are placed in the shear tester, one at a time, and sheared as described

above for continuous flow. The yield locus is plotted through the points $(\overline{V},\overline{S})$ and the value of the unconfined yield force F_t is obtained in the same way as F was obtained for continuous flow. The value of V_1 measured for continuous flow applies here in plotting the time flow-function.

During the static consolidations it is necessary to preserve the moisture content of the specimen. This is done by covering the shear cells with the plastic cups shown in Fig. 20. The bottoms of the cups are immerged in baths of a sealing liquid.

Density

Since the analysis shows that the influence of the compressibility of a solid (change of density with consolidating pressure) on the process of flow is negligible [39], it is not necessary to obtain a function of density versus pressure. However, the density γ of a solid at the outlet of a channel, or within a pipe, enters the flow formulas and, hence, needs to be obtained.

The easiest way to measure the density is to weigh the whole cell after it has been sheared to failure, subtract the weight of the cell itself and divide the net weight by the volume of the cell.

Kinematic angle of friction between a solid and a wall material, ϕ'.

The angle of friction ϕ' between a solid and a material of the wall is measured on the same apparatus. The arrangement of the cell is shown in Fig. 26. In this case, a sample of the wall material is placed on a filler so that the top surface of the sample is level with the center of

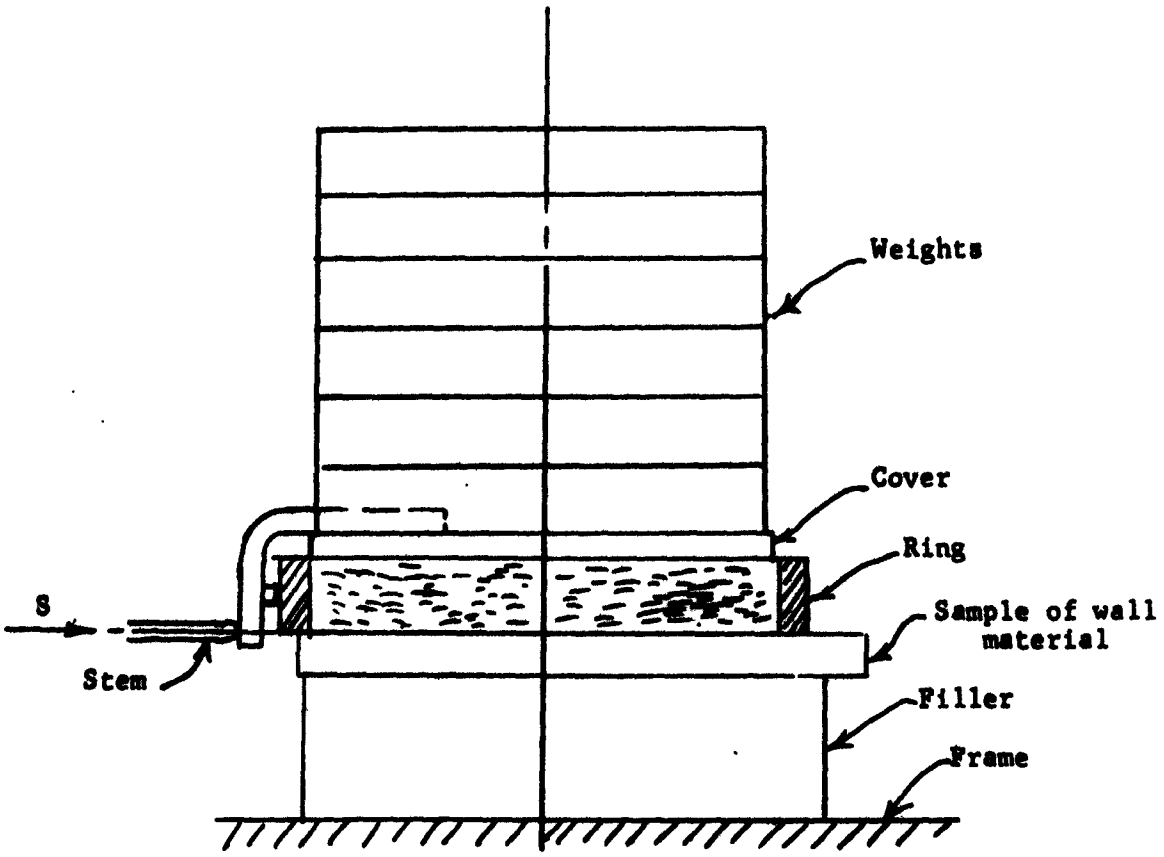

Fig. 26

Measurement of the kinematic angle of friction between a solid and a wall material

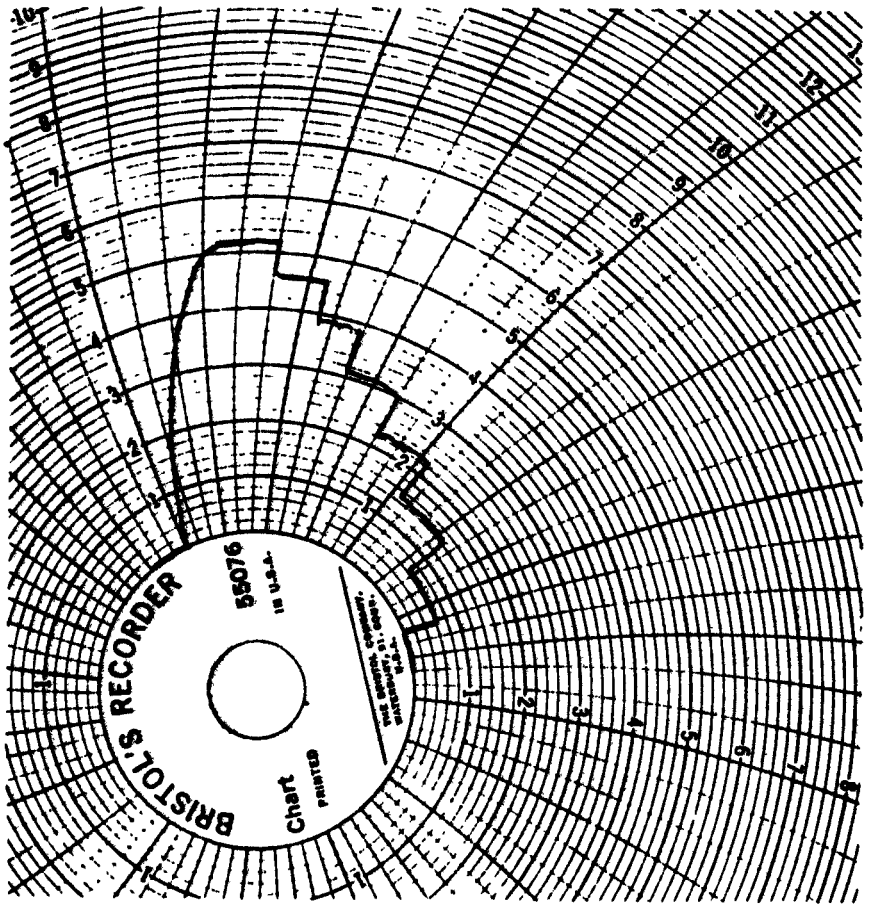

Fig. 27

A typical recorder chart - measurement of ϕ'

the stem. The ring is placed over the sample, filled with the solid, compacted slightly, and enclosed with the cover. All the tests necessary to determine angle ϕ' are now run without replacing the solid.

Several (say, six) one or two-pound weights are placed directly on top of the cover of the shear cell to give the largest required load V. The stem is advanced. As the force S levels off, the ring is twisted slightly with the fingers in order to assure that it does not transfer any significant vertical force directly to the wall material. When S has levelled off, one weight is removed, after a while S again levels off, another weight is removed and so on, till all the weights have been removed. The cover, ring and the enclosed solid are then weighed. Their weight plus the superimposed weights determine the vertical loads V.

A typical recorder chart is shown in Fig. 27. The points (V,S) are plotted in Fig. 28. A smooth line is drawn through these points and this is the wall yield locus, WYL. Typically, the WYL is convex-upward.

Simplified testing procedure

On the assumption that: (1) the yield locus is straight, and (2) point E, Fig. 23, coincides with the measured point (V,S) an approximate yield locus, Fig. 29, and one approximate point of the flow-function (V_1,F) can be obtained from one consolidation/shear test. The relations are

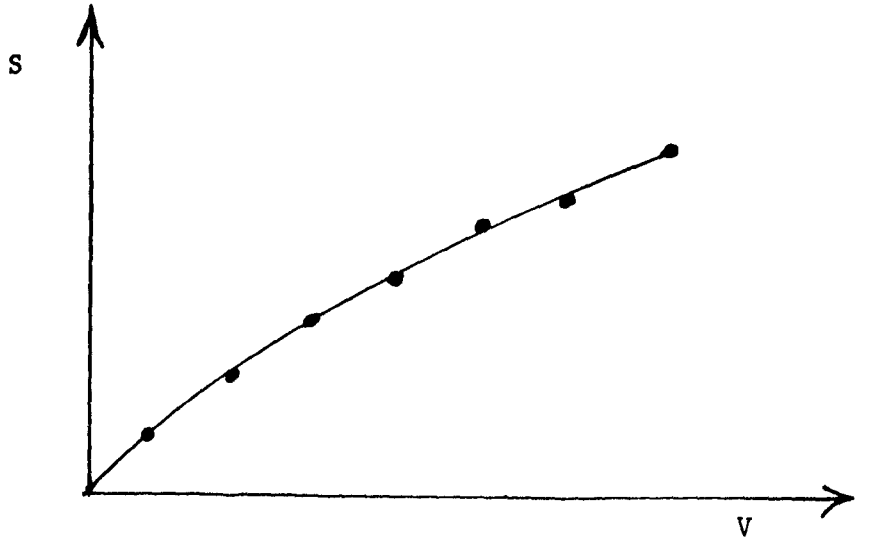

Fig. 28

Plotting the WYL

$$V_1 = V + KS, \tag{14}$$

$$F = 2K(S - V\frac{S - \bar{S}}{V - \bar{V}}), \tag{14a}$$

$$\sin \delta = \frac{(K^2 + 1)S}{2KV + (K^2 - 1)S} \tag{15}$$

$$\tan \phi = \frac{S - \bar{S}}{V - \bar{V}} \tag{15a}$$

where

$$K = \frac{S - \bar{S}}{V - \bar{V}} + \sqrt{1 + (\frac{S - \bar{S}}{V - \bar{V}})^2}. \tag{16}$$

A repetition of this test for a different value of V produces a second point (V_1,F) and a straight line through the two points is an approximate flow-function, Fig. 16(b)

The time flow-function can be obtained similarly, with the additional assumption that: (3) TYL is parallel to YL. The unconfined yield force F_t is computed from the formula

$$F_t = 2K(\bar{S}_t - \bar{V}_t\frac{S - \bar{S}}{V - \bar{V}}). \tag{17}$$

By this method the free-flowing solids are readily identified and no additional time is wasted on them. This method is also useful when a range of two or more parameters (moisture content, temperature, time of consolidation at rest) needs to be examined. It permits a rapid narrowing down on the range to those values for which a solid is not free-flowing. If the solid is to be handled for these values of the parameters, then complete tests are carried out and minimum outlet dimensions are established.

Slip-stick solids

Some fine powders exhibit slip-stick properties which may appear during consolidation and/or during the frictional tests. The shearing force does not level off but oscillates.

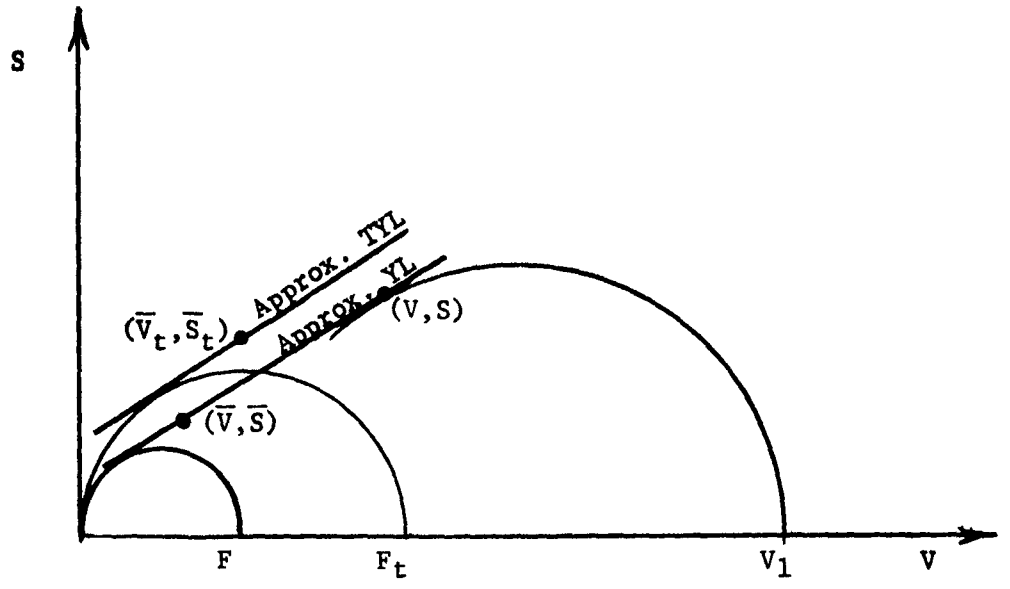

Fig. 29

Simplified testing procedure

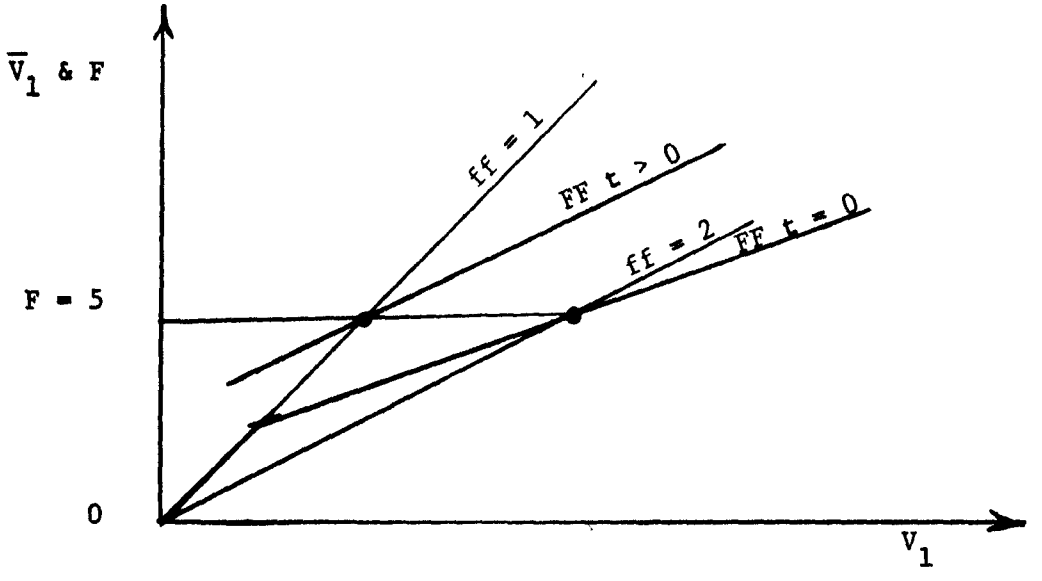

Fig. 30

General classification of flowability of solids

In order to consolidate such a solid, a normally-closed, spring-loaded button-switch is placed in the electric supply cord of the tester. Consolidation proceeds until the peak value of the shearing force S has been reached, say, three times; then, on the next approach, the stem is "inched" toward the peak value by depressing and releasing the switch. When the peak has been reached, the stem is retracted manually so as not to disturb the cell.

A safety factor is imposed on the flow-factor in the design for these solids. This is discussed in the next chapter.

General classification of flowability of solids

Several numbers and curves are required for a precise definition of the flowability of a solid. At times it is convenient to forgo some precision for a gain in brevity of definition. For instance, it is evident from Fig. 30 that for $F > 5$, the instantaneous flow-function lies below the line $ff = 2$, and the time flow-function lies below $ff = 1$. The flowability of this solid can thus be written briefly as: $FF > 2$, $FF_t > 1$ for $F > 5$.

The flowability of solids can be classified according to the limiting FF-values thus:

$FF < 2$	very cohesive and non-flowing
$2 < FF < 4$	cohesive
$4 < FF < 10$	easy-flowing
$10 < FF$	free-flowing

CHAPTER III

DESIGN

Funnel flow bins

A solid drawn through an outlet of a flat bottom bin forms a channel within the stored mass and flows toward the outlet within that channel while the mass around it remains stationary. This flow pattern is referred to as funnel-flow. The channel tends to assume the shape of a vertical, circular cone. At the bottom, the diameter of the cone may approach the largest dimension of the outlet. Thus, with a rectangular outlet, that diameter may approach the diagonal dimension of the outlet. As the solid is discharged and its level within the channel drops, solid at the outside sloughs off the top of the stationary mass and slips into the channel, Fig. 31(a). As more and more material is withdrawn, flow finally ceases and a crater is exposed within the remaining, stable mass. When the solid is completely cohesionless, the slope angle of the crater is equal to the angle of repose (b). For all other solids, the crater (c) is composed of three regions: From the outlet - whatever its shape - the channel expands upward to a circular cross-section; when the outlet is rectangular, the walls are steeper at the ends than at the sides; in fact, at the ends the walls may overhang the outlet. In the middle region the circular cone extends over some height. At the top, the crater expands along a cone of slip.

The included angle $2\theta'$ of the middle cone is always quite small

and frequently zero; the middle part is then a vertical cylinder, or a pipe. The height of the vertical cylinder varies. In extreme cases it can extend tens of feet and through the whole height of a bin (d). This condition is referred to as piping, or rat-holing, and severely reduces the live capacity of a storage plant. As long as the height H of the vertical cylinder or middle cone is less than its diameter D, the operation of the bin should be considered satisfactory. In estimating the live capacity of a funnel-flow bin it is unreasonable to expect a more complete discharge unless either the stored solid is free-flowing, or final discharge is enforced by means of vibration or some other flow-promoting device.

A pyramidal hopper, Fig. 32, has in-flowing valleys which provide firm support to the solid and tend to hold it stable. As a result, in the vicinity of a valley, the solid is forced to form a channel across itself and that leads to funnel-flow unless the solid is sufficiently free-flowing and the hopper sufficiently steep and smooth. Mass flow in a pyramidal hopper is discussed later.

When an empty funnel-flow bin is filled, the solid which first falls into the bin rolls to the periphery and remains there until the bin is again completely emptied out. This is a serious drawback in the storage of solids which deteriorate with time; it also leads to obstructions to flow of solids which pack and gain strength when left undisturbed under pressure.

Like all bins, funnel-flow bins are subject to arching or doming of solids with complete cessation of flow, Fig. 32(a). In this respect, funnel-flow bins are erratic because a solid does not flow uniformly in a

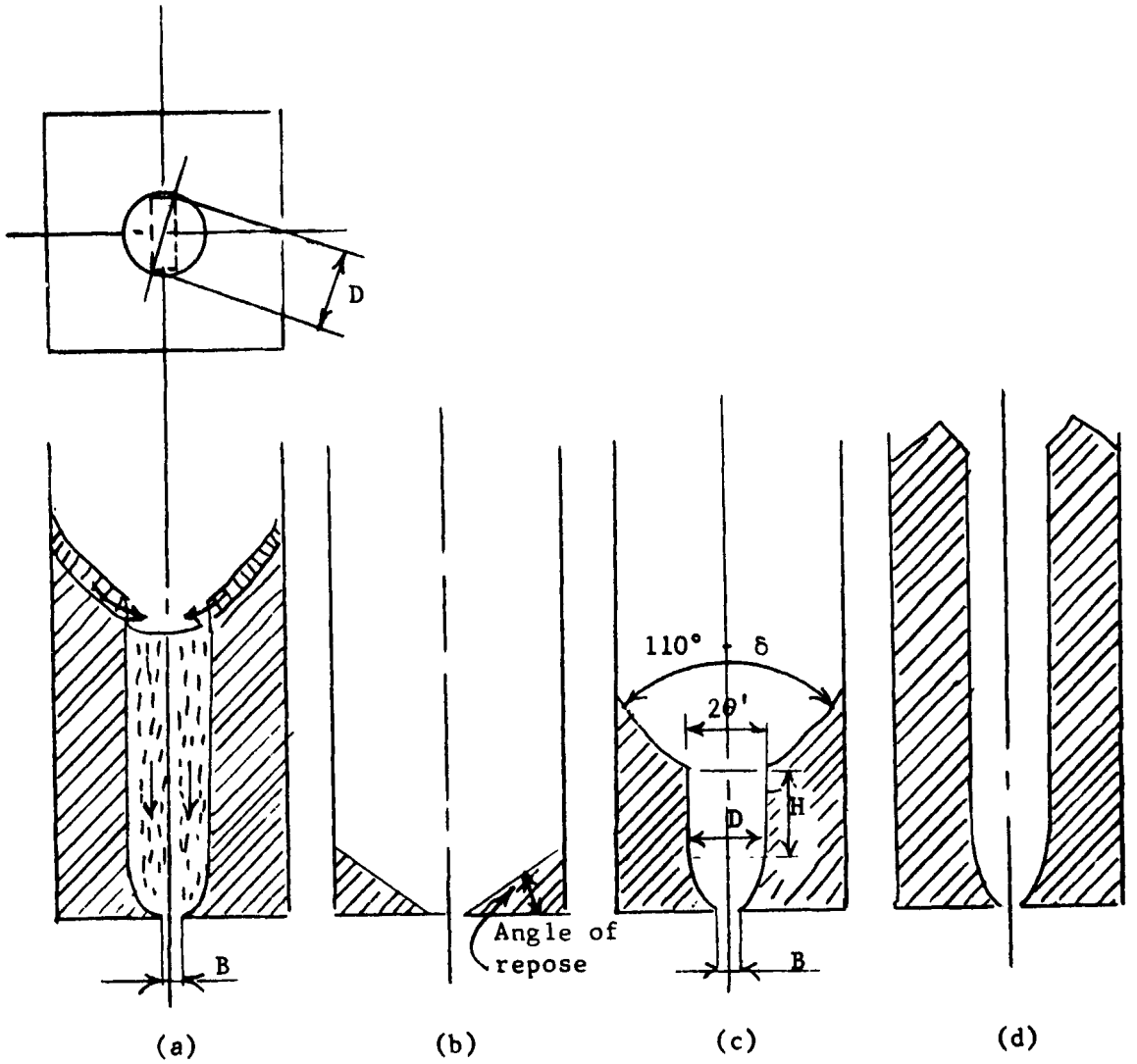

Fig. 31

Flat bottom bin

vertical or very steep channel. A solid flowing down such a channel tends to form voids topped with domes, (b). As a dome breaks, the solid falls into the void; under the impact, the solid tends to pack and dome again. Surging flow is the rule in funnel-flow bins. In the storage of powders, surging results in flooding which occurs when the void under a dome momentarily extends all the way to the feeder, (c). The falling mass of solid aerates and acquires fluid-properties as it impacts the feeder. A falling mass may also act as a piston, and develop high air pressure in the region of the hopper, causing a break through a hopper wall, or a detachment of the hopper from the bin structure. These accidents have been serious and have led to the loss of life.

A bin or hopper is often required to act as a gas seal. Funnel-flow with its irregularities is quite unsuitable for this purpose.

The flow pattern which obtains in funnel-flow bins is also detrimental when storing materials which segregate during charging into a bin because there is very little remixing as the solid flows down the vertical channel. When the trajectory of the charged material is located over the outlet, fines congregate within the region of the flow channel, while coarse material rolls to the sides, Fig. 33. The bin draws a preponderance of fines when the level of the solid in the bin is rising (a), and of coarse - when the level is falling (b). When the rate of draw is the same as the rate of charge, the level remains steady and a last-in first-out flow pattern obtains; in effect, the bin acts as a spout (c).

When a solid domes in a funnel-flow channel, it is difficult to break up the dome because there is no direct way of reaching the

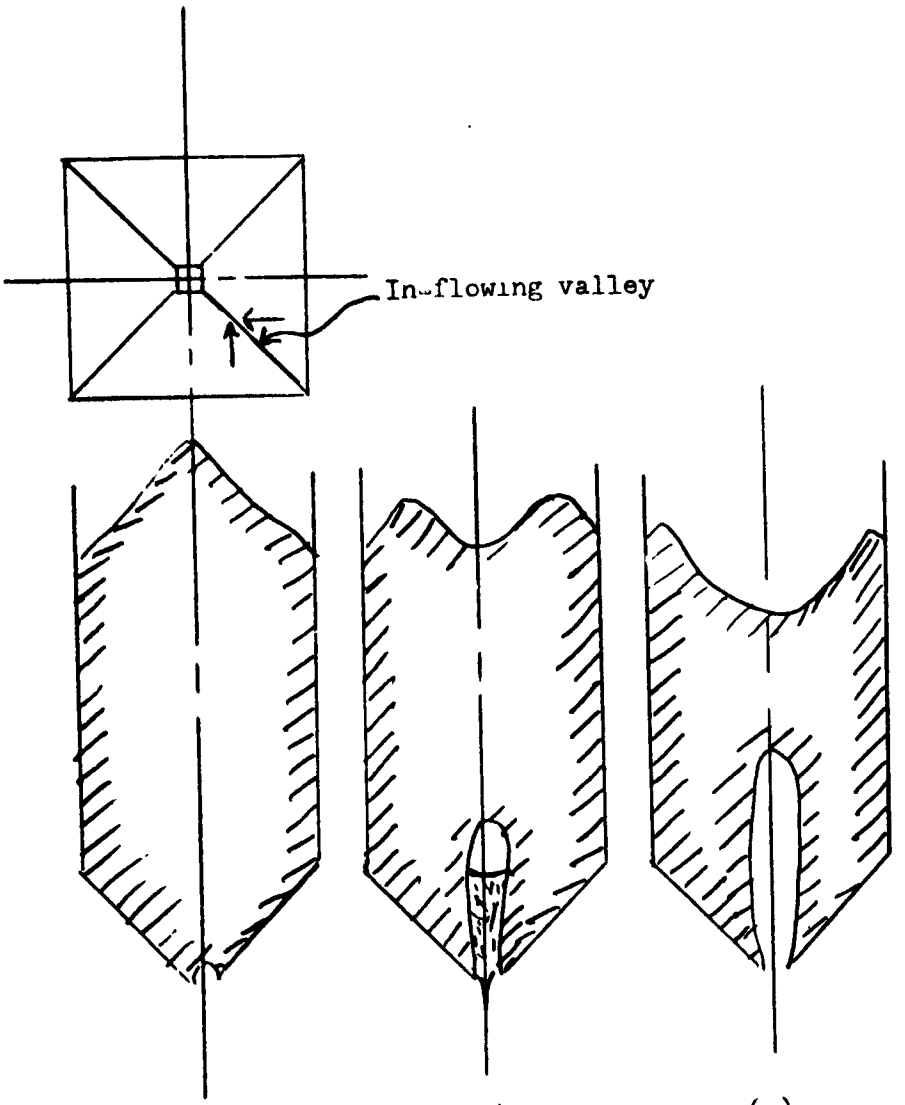

Fig. 32

Funnel flow

obstruction. Vibrators or inflatable panels applied at the walls must first disturb the stable, compacted solid around the channel. This calls for a substantial input of energy which carries the danger of additional consolidation in other parts of the bin and, subsequently, more flow problems. Since it is seldom possible to observe the conditions inside a hopper, it is easy to continue operating a vibrator or an inflatable panel after the initial dome has collapsed and the void in the bin has been filled. This leads to serious obstructions to flow requiring manual prodding to dislodge the severely packed solid.

From the aforesaid it follows that funnel flow is acceptable only under certain conditions:

(1) Segregation has to be unimportant either because it is insignificant, as is the case with solids of uniform particle size and density, like sand or gravel, or because it is slight and can be tolerated, as is the case in small bins, like weigh hoppers.

(2) Deterioration does not occur during the scheduled time of storage.

(3) The outlet is sufficiently large so that the solid flows without flow-promoting devices.

Funnel-flow bins are useful for the storage of hard, abrasive, lumpy solids because in funnel flow there is little wear of the hopper walls. However, it should be remembered that in mass-flow hoppers the wall pressures are relatively low and the wear is seldom unreasonable. If the solid is very cohesive after it has been stored at rest and requires very large feeders in funnel flow, it may be more economical to use mass-flow bins, save on feeders and build heavier hoppers to provide for wear.

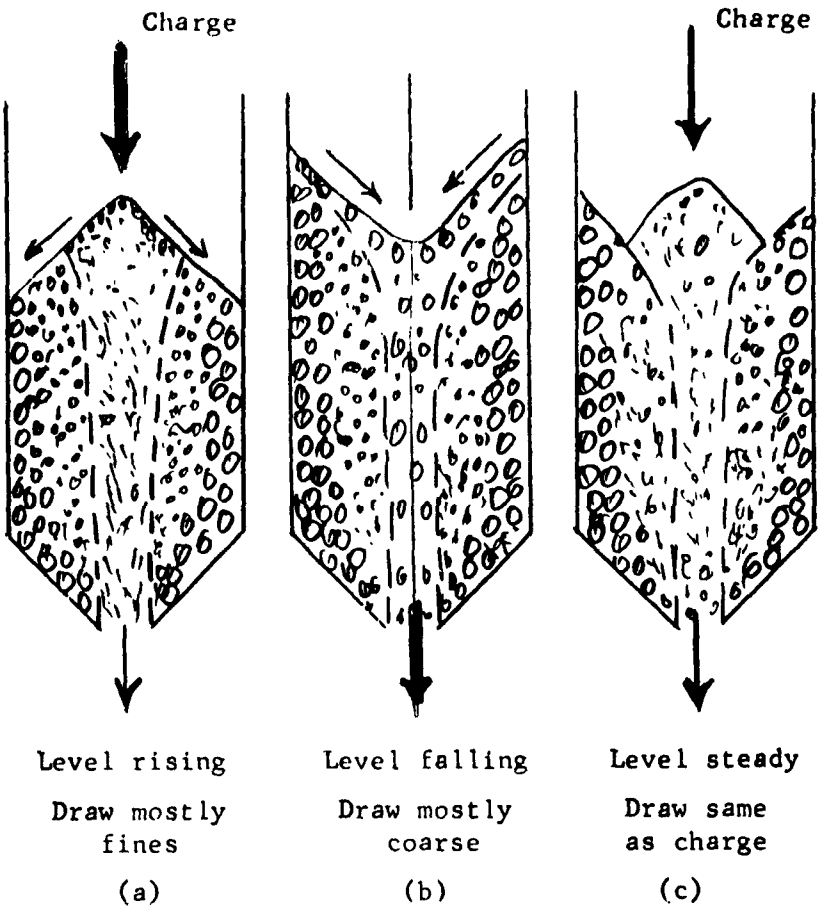

Fig 33

Flow pattern in funnel-flow bins

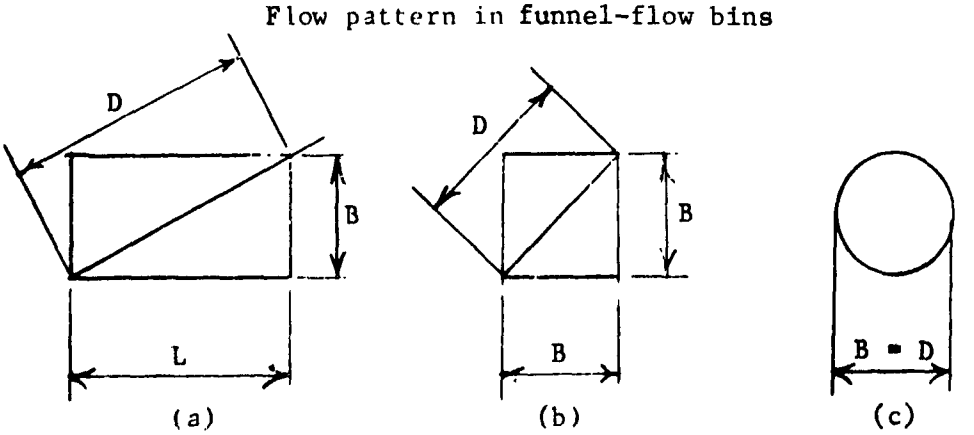

Fig 34

Dimensions of an outlet

Funnel-flow bins are also useful for the storage of mine-run ores which contain large rock. Here the argument against the mass-flow bins is that large rock falling from a considerable height tends to pack the ore in a steep hopper and to cause doming. Coarse ore storage is discussed in another place in the chapter.

However, the main reasons why funnel-flow bins are so commonly used today are: the general lack of knowledge of the existence and the advantages of mass-flow bins, and the notion that funnel-flow bins are cheaper per unit volume. That "economy" is more apparent than real: it often becomes quite expensive in terms of excessive startup time, disrupted production schedules, additional shifts, lowered product quality, unrealized storage, redesigns, modifications, flow-promoting devices, and time spent by operating and supervisory personnel in keeping the solids flowing.

Dimensions of the outlet.* In order to assure satisfactory flow in a funnel-flow bin, it is necessary that the outlet be large enough so that piping and doming do not occur. Flow should not rely on flow-promoting devices. Typical shapes of outlets are shown in Fig. 34. The major dimension of the outlets is D, and the pipe which tend to form will have that diameter. To make this pipe unstable, D must be selected at least equal to the value computed in the following way:

(1) Using the height, h, and hydraulic radius, R ($= \frac{\text{cross-sectional area}}{\text{length of perimeter}}$) of the bin, estimate the effective consolidating head:

$$h_e = \frac{2.5R}{\tan \phi'}(1 - e^{-0.4 \frac{h}{R} \tan \phi'}) \qquad (17A)$$

(1A) Compute major consolidating load V_1

$$V_1 = \frac{\gamma h_e}{13} \qquad (17B)$$

(2) Using this value of V_1, find $\overline{V}_1$ and ϕ_t from the time flow-function.

*For more details, see J. R. Johanson, "Effect of Initial Pressures on Flowability of Bins," ASME J. Engr. Ind., V. 91, Ser. B, No. 2, May 1969, p. 395-400.

(3) Compute D from Eq. (13). For a shearing cell with an area A = 1/13 sq. ft, this equation becomes

$$D = 13\bar{V}_1 G(\phi_t)/\gamma \tag{18}$$

Function $G(\phi_t)$ is plotted in Fig. 36.

In a square or circular outlet computed for no-piping, doming cannot occur. In a rectangular outlet of diagonal D, the minor dimension of the outlet, which is the width of the outlet B, Fig. 34(a), must also be computed so that doming does not occur. A flow-factor ff = 1.7 is used here. This assures a slope angle θ' not less than 30°, Fig. A-7, at the sides of the rectangle. Such an angle is necessary to expand the crater from a width B to a diameter D, Fig. 31(c), otherwise a stable pipe of a smaller diameter will form. B is calculated as follows:

(1) Draw the flow-factor ff = 1.7 over the time flow-function of the solid and determine the value of $\bar{V}_1$ at the point of intersection, Fig. 15.

(2) Compute B from Eq. (12). For A = 1/13 sq. ft, and H(30°) = 1.15, this equation becomes

$$B = 15\bar{V}_1/\gamma. \tag{19}$$

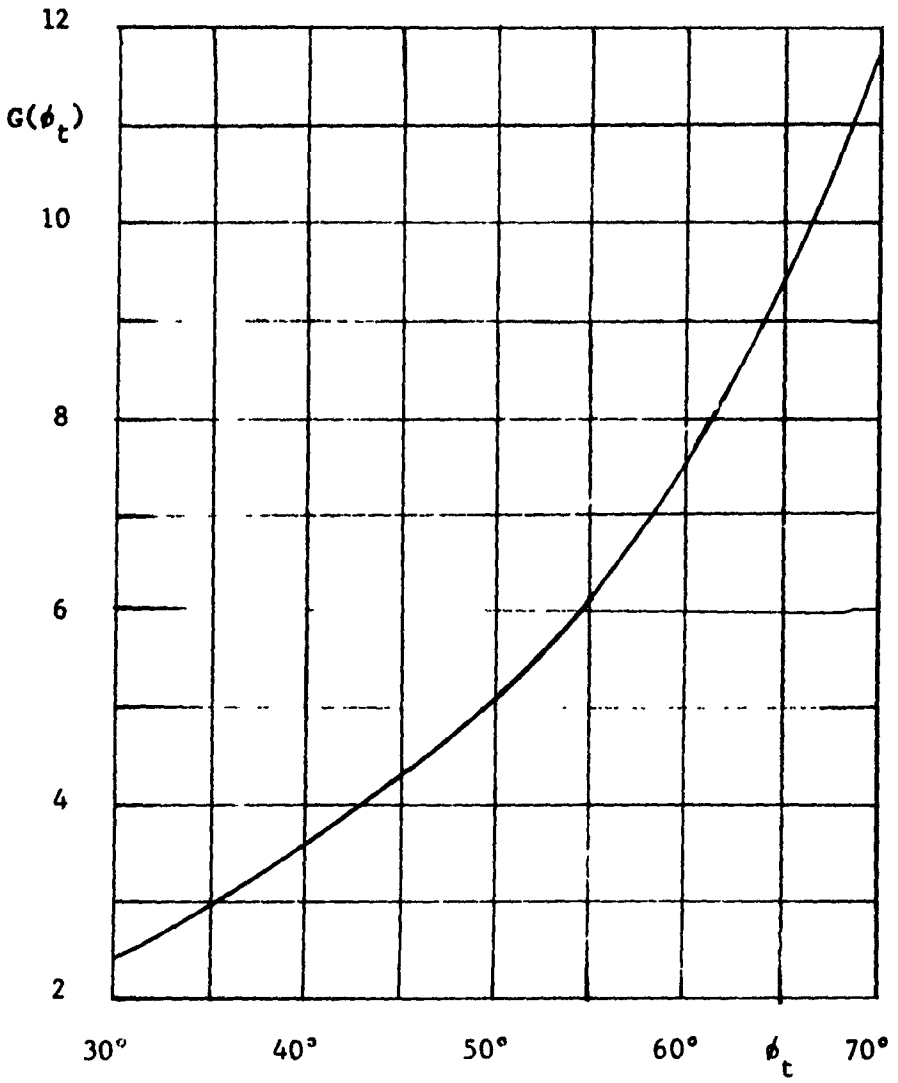

Fig. 36

Function $G(\phi_t)$

Live capacity. A funnel-flow bin with a sufficiently steep pyramidal or conical hopper can be cleared completely of the stored solid by means of vibration, aeration, or manual rodding and air-lancing.

If the walls of the hopper are sufficiently smooth as well as steep, a funnel-flow bin will clear by gravity. To attain gravity clearance, it is essential that the material of the hopper does not corrode and retains smoothness during storage. Stainless steel, ceramic tile, resin coatings seem to provide satisfactory hopper materials. Unless the stored solid is quite free-flowing, the hopper slope θ' should provide a margin of safety, for instance,

$$\theta' \leq 65^\circ - \phi'. \tag{20}$$

The total storage capacity of these bins is easy to determine from the geometry of the bin.

It is more difficult to estimate the capacity of a pile or of a funnelflow bin without flow promoting devices, and without a smooth hopper. A safe estimate results from the shape of the stable crater shown in Fig. 31(c), provided the outlet has been designed for no-piping and no-doming, and H is taken equal to D.

Mass-flow bins

When a bin has a sufficiently steep and smooth hopper then, whenever the feeder is set in motion, all the solid in the bin flows; there are no inactive or dead regions. Under these conditions, mass-flow is said to occur. Mass-flow bins can have a variety of shapes, as shown in Fig. 37, but they are all characterized by steep hoppers and,

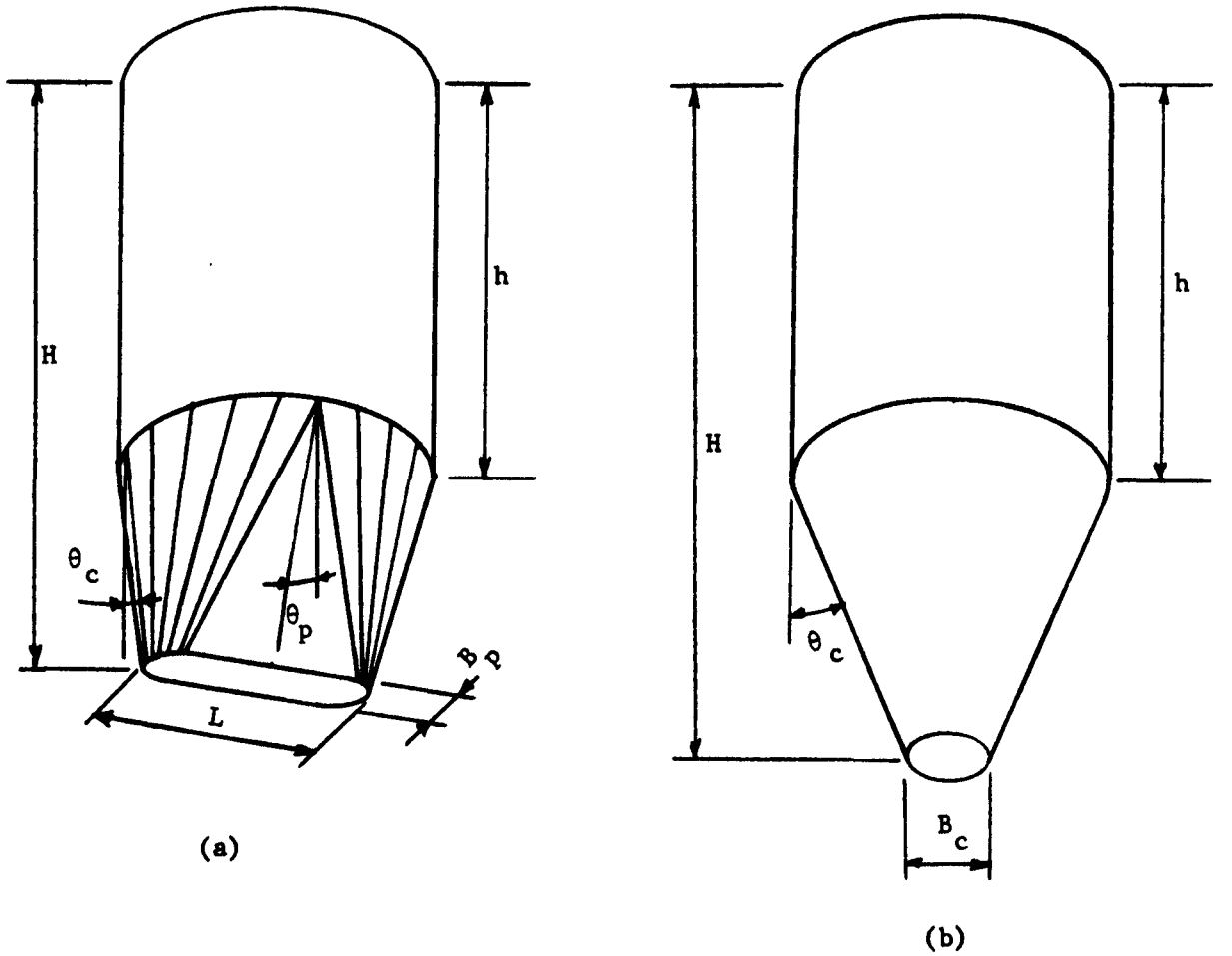

MASS-FLOW BINS

Fig. 37

usually, also by the absence of in-flowing valleys and sharp transitions.

Mass flow has the following properties:

(1) Channeling, hang-ups, surging and flooding are absent.

(2) Flow is uniform, and steady state flow can be closely approached. As a result, analysis based on steady flow can be applied to design with a high degree of confidence.

(3) The bulk density of the drawn solid is constant, and practically independent of the head of the stored solid. This is very advantageous in all cases of controlled flow rate, and essential when the rate is controlled volumetrically. It should be noted here that highly aerated powders should have a sufficient residence time to deaerate and form a contact bed.

(4) Pressures throughout the mass and at the walls are relatively low, with resultant low consolidation and attrition of the solid and wear of the walls.

(5) Pressures are relatively uniform across any horizontal cross-section of the hopper, causing uniform consolidation and uniform permeability, which is important in gas seals and gas-solids reactors.

(6) There are no dead regions within the bin, hence, there is a minimum of consolidation at rest, degradation and spoilage.

(7) A first-in first-out flow pattern can be obtained, if desired. This is useful in the storage of solids which deteriorate with time.

(8) Non-segregating storage is obtained in a first-in first-out bin because, while segregation takes place during the charging of a solid into such a bin, re-mixing occurs within the hopper.

(9) By circulating a mixture around a suitable mass-flow bin, blending may be obtained.

Conical and plane-flow hoppers. Hopper slope angles θ' which lead to mass flow have been computed for conical channels, Fig. 17, and for plane-flow channels, Fig. 18. For both shapes of channels the slope angle θ' depends on the effective angle of friction of the solid δ, and the kinematic angle of friction between the solid and the wall ϕ'. The regions within which mass flow can prevail are those covered by the flow-factor contours in Figures 45 to 57. Each figure is drawn for a constant value of δ. It will be observed that, for conical channels, Figures 45 to 49, the regions of mass flow are quite restricted. For instance, Fig. 38 shows the cross-sections of three conical channels from Johanson's work [44]. For the steepest channel, $\theta_c' = 15°$, mass flow obtained; for $\theta_c' = 21°$, flow at the walls was observed at first but then plug flow developed; for $\theta_c' = 30°$, plug flow developed from the beginning. In this case, δ was measured at 50° and ϕ' at 24°. In Fig. 47, the corresponding points (15°,24°), (21°,24°), and (30°,24°) are marked with crosses. The first point lies within the mass-flow region, the second at the boundary between mass and plug flow, and the third in the plug-flow region.

In designing a conical hopper, Fig. 37(b), for mass flow, it is necessary to stay within the boundary line by some 3 to 5 degrees in the value of θ'_c in order to allow for deviations which may occur between the laboratory value of the angle ϕ' and the real value which obtains in the hopper.

In designing plane-flow hoppers, Fig. 37(a), the regions of mass-flow are much wider, Figs. 50 to 57. However, it is recommended that the slope angle θ'_p be selected to the left of the dashed lines in order to prevent the development of excessive non-flowing regions on the sides and at the top of a bin. Such regions take place and extend upward to the surface of the solid when the head of the solid in the vertical portion of a bin is low and the transition from the vertical portion to the hopper is sharp. If the transition is smooth with a radius of curvature $R \geq D/3$, Fig. 39, then θ'_p may be increased by, say, 5°.

These limits on the angle θ'_p are not rigid like those on θ'_c. It is not necessary to stay 3° to 5° to the left of the dashed lines for θ'_p. In fact, the actual value of ϕ' in plane flow will often be smaller in the bin than was measured in the laboratory because the plane walls will tend to polish as the solid flows on them during the periods when the head of solid in the bin is high. In a conical channel, flow will never start if ϕ' is too large and point (θ'_c, ϕ') is outside of the region of flow and the walls will never have a chance to become polished.

The end slopes θ'_c of the transition hopper, Fig. 37(a), are selected from the charts for conical hoppers, Figures 45 to 49.

(J. R. Johanson)

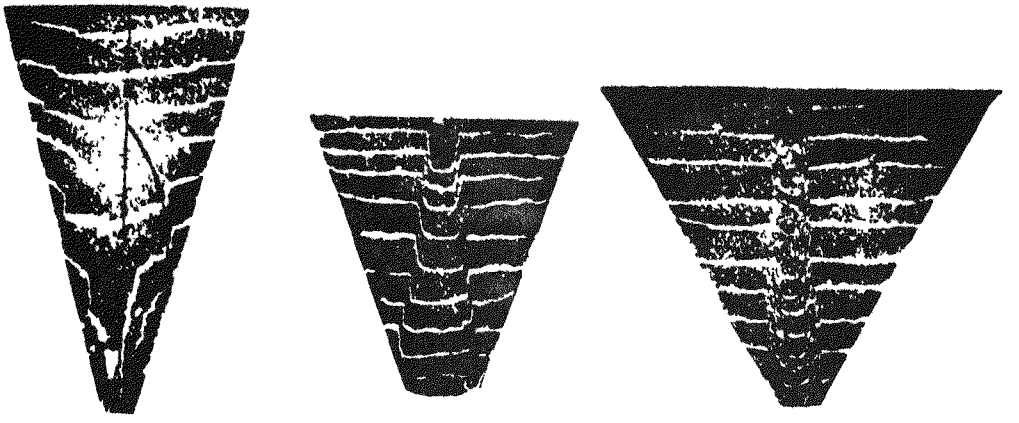

$\theta_c' = 15°$ $\theta_c' = 21°$ $\theta_c' = 30°$

Fig. 38

Flow in conical channels, $\delta = 50°$, $\phi' = 24°$

Within the mass-flow regions, the flow-factor contours indicate the flowability of the hoppers; the lower the value of ff, the better the hopper. It will be observed that for all shapes and values of angle δ there is a trough of low ff-values. Thus, for a given value of friction at the walls ϕ', there is an optimum slope angle θ'. Making the slope steeper, as well as less steep, decreases the flowability of the hopper. The decrease of flowability toward the steeper slope is computed conservatively; the analysis is based on the assumption that the domes which might form across the channel would fail across the solid and not along the walls. This assumption is justified by the fact that the angle of friction at the wall after storage at rest, i.e. the static angle of friction, is usually greater than the kinematic angle ϕ', and that even a slight increase in ϕ' is sufficient to eliminate the weakness at the wall and to require failure across the solid [33].

Hoppers should be built of materials which do not corrode or scar and permanently increase the angle of friction ϕ' during operation. A temporary increase of ϕ' may occur during storage at rest. This is not harmful as long as ϕ' reverts to its original value when flow is restored.

Hoppers with a vertical wall made of a smooth material seem to have a slight advantage over symmetric hoppers in starting the flow of a solid after storage at rest. This is probably due to the fact that flow tends to start in a vertical plug along the smooth wall. Such plug flow develops more readily than either plug flow within the solid in a symmetric hopper, or mass flow. The advantage in the flow-factor due to the vertical wall is probably in the range of .1 to .3. The drawback of

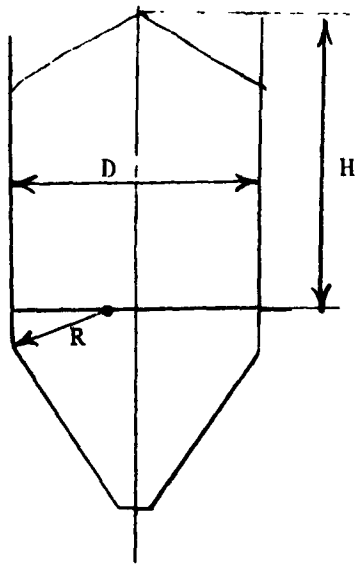

Fig 39

Bin with a smooth transition to a wedge hopper

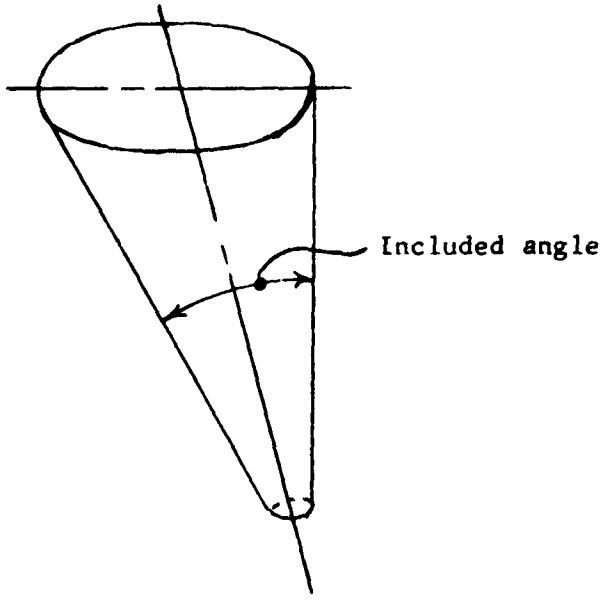

Fig. 40

Conical hopper with one vertical side

the asymmetric design is that, once plug flow has developed, it may persist and may fail to transform into mass flow.

Flow-factors for mass, plane-flow hoppers with one vertical wall have been computed and are shown in Figures 55, 56, 57 for $\delta = 50°$ and for angles of friction along the vertical wall respectively, $\phi^v = 20°$, 30° and 40°. θ'_p and ϕ' in the figures refer to the sloping wall.

To date, only the axi-symmetric, conical and the straight, plane-flow channels have been analyzed. For other shapes, the theory becomes less certain and the computational difficulties increase out of proportion to the likely practical benefits. This does not imply that no other mass-flow hoppers are possible.

A conical hopper with its axis tilted from the vertical, e.g. with one side vertical, Fig. 40, will lead to mass flow but its included angle should be only 1.25 θ'_c, where θ'_c is the slope angle of a symmetric cone for mass flow. If the included angle is too large plug-flow will develop along the vertical wall.

Rectangular, full-slot hopper. Such a hopper can lead to mass flow provided its valleys are filled or rounded to prevent material from adhering. It is advisable to design the outlet length greater than six times the width in order to guard against the possibility of funnel flow higher within the hopper.

(DELETED)

Pyramidal hoppers. A pyramidal hopper, Fig. 32(a), may lead to mass flow in spite of the in-flowing valleys; however, observations indicate that the flow-factor of this hopper is more than 4 for mass flow, and the valley angles should be within the mass-flow region for conical hoppers. Since the flow-factor of a plug-flow channel is less than 1.3, Fig. A-7, plug flow will tend to develop in a pyramidal hopper unless the solid is sufficiently free-flowing and the walls of the hopper sufficiently steep and smooth.

(DELETED)

Dimensions of the outlet. The proper selection of the shape and slope of a hopper leads to mass flow - if flow develops. To that effect it is necessary to assure that doming does not occur by making the outlet sufficiently large.

In mass-flow hoppers only one dimension of the outlet, Fig. 34, is determined. That dimension, B, is either the width of a rectangular outlet, or the side of a square outlet, or the diameter of a circular outlet. In the design of a rectangular outlet, it is assumed that plane flow occurs at the sides of the outlet. For this assumption to

be valid, the ratio of length L to width B of the outlet should be not less than 3.

The procedure is outlined below, step by step. It is also illustrated in Figures 42(a) to (e). Figures (a) to (d) are drawn in V_1, F & $\overline{V}_1$ coordinates, while Fig. (e) is drawn in V,S coordinates.

(1) Estimate δ, ϕ' and γ at the outlet.

(2) Select θ'. For circular and square outlets, use the conical-flow charts, Figures 45 to 49. For rectangular outlets, use the plane-flow charts, Figures 50 to 57.

(3) Read ff from the appropriate chart.

(4) Plot δ, FF and ff. There are four possibilities:

(a) There is no intersection, and FF lies below ff.

The analysis does not determine a minimum dimension B. Select B from considerations of rate of flow, particle size to avoid interlocking, standard designs and, using Eq. (12) with A = 1/13 sq. ft, compute

$$\overline{V}_1 = B\gamma/13H(\theta'). \tag{22}$$

The function $H(\theta')$ is given in Fig. 43 for circular, square and rectangular outlets. Locate point $\overline{V}_1$ on the ff-line to determine the value of V_1 at the outlet.

(b) There is an intersection at point $(V_1, \overline{V}_1 = F)$. This analysis determines a minimum dimension B from formula (22), thus

$$B = 13\overline{V}_1 H(\theta')/\gamma. \tag{23}$$

(c) There is no intersection and FF lies above ff. The solid will not flow. If lower values of ff are available, select θ' and, possibly, ϕ' by using a smoother wall material to reduce ff, and start again from step (1). If lower values of ff are not available, and if FF is an instantaneous flow-function, either solids conditioning or non-gravity storage is required.

(d) The time flow-function FF_t lies entirely above ff but the instantaneous flow-function FF lies below ff. External vibrators are specified to start flow after storage at rest, and the outlet is designed with a safety factor to allow for the unfavorable effects of vibration. This is accomplished by selecting V_1 so that, at the outlet,

$$\bar{V}_1 = 1.5F. \tag{24}$$

The construction is shown in the figure. The width B is then computed from Eq. (23).

(5) Now check ϕ' at the outlet. This is shown in Fig. 42(e) in the following order:

- draw WYL,
- read δ from the appropriate Fig. (a) to (d) for the selected value of V_1, and draw EYL,
- mark point $(V_1,0)$,
- draw the indicated Mohr semi-circle through $(V_1,0)$ tangentially to the EYL,
- the indicated point of intersection of the semi-circle with

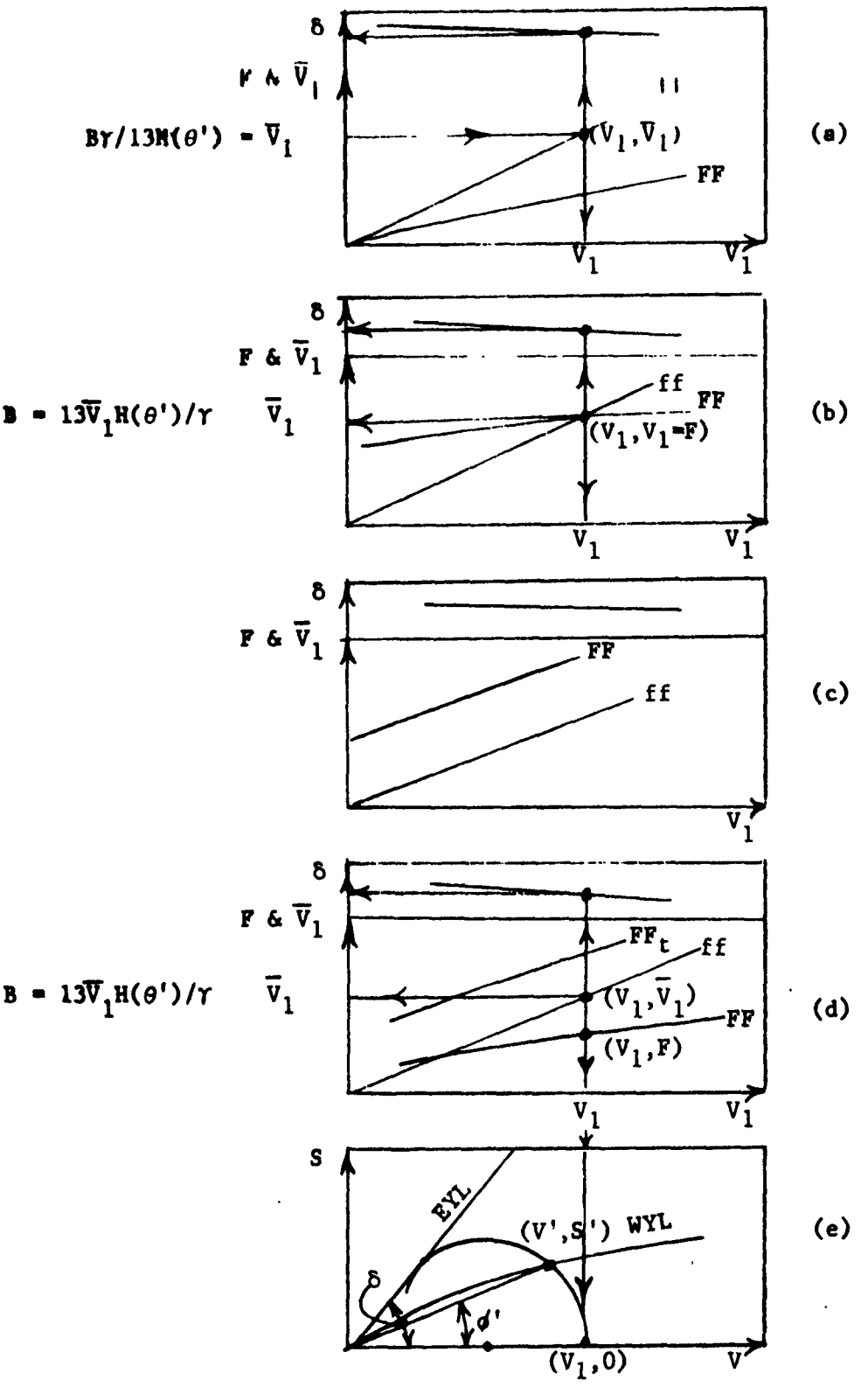

Fig. 42

Calculation of outlet dimensions in mass flow

the WYL is (V',S'),

- draw a straight line through (V',S') and the origin; the angle between this line and the V-axis is ϕ'.

The above procedure assumes:

- A straight or convex-upward FF. In the exceptional case of a concave-upward FF, the point of intersection (V_1,$\overline{V}_1$ = F), would determine the largest width, side, or diameter of the hopper.
- A straight or convex-upward WYL. In the exceptional case of a concave-upward WYL, it may be necessary to check the dimension B at a few elevations within the hopper, as well as at the outlet. At each level, the procedure would be the same as described above for the outlet.

Since the values of ff are insensitive to small changes in the angle δ, it is not necessary to define this angle with great precision.

Stresses on walls. The pressure σ' which a flowing solid of bulk weight γ exerts on the wall of a channel of width B, Fig. 44, is computed directly from the plots presented in Figures 58 to 67. For example, in a conical hopper of $\theta' = 15°$, $\phi' = 22°$, for $\delta = 40°$, $\gamma = 100$ pcf, and B = 2 feet, $\sigma'/\gamma B$ is read from Fig. 59 at .50. Hence $\sigma' = .50 \times 100 \times 2 = 100$ psf. Similarly, for a plane-flow channel for the same values of θ', ϕ', δ, γ and B, from Fig. 64, $\sigma'/\gamma B = 1.04$, and $\sigma' = 1.04 \times 100 \times 2 = 208$ psf.

It will be observed that these pressures are quite low and that they increase upwards from the outlet as the width B of the hopper increases.

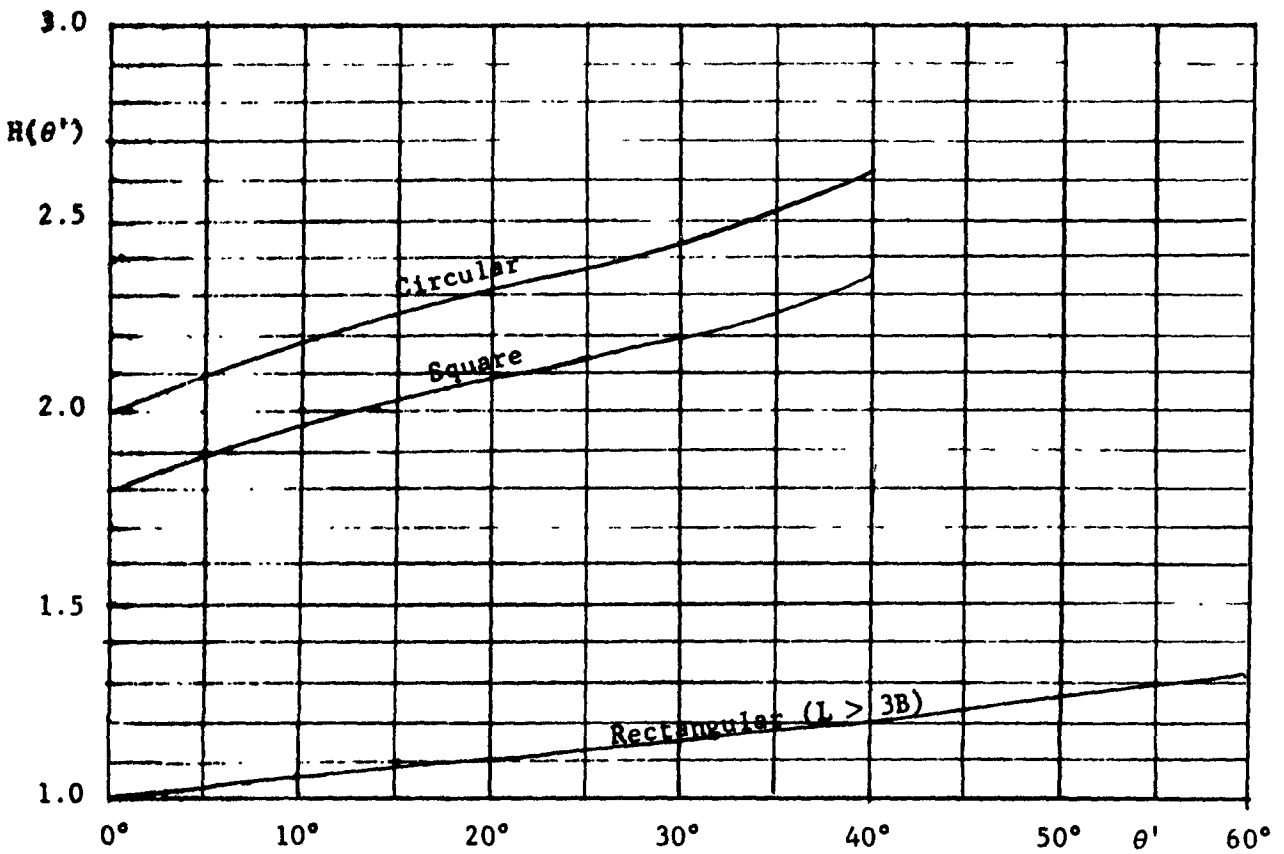

Fig. 43

Function H(θ')

The shearing stress τ' which acts at the wall under the same conditions can be computed from Eq. (4), with the substitution $V' = A\sigma'$, $S' = A\tau'$, thus

$$\tau' = \sigma' \tan \phi'. \qquad (25)$$

The above stresses occur in contact beds in mass flow. If an aerated solid is charged into a bin, the pressures are hydrostatic until a contact bed has developed. In plug-flow bins, within the flowing channel, stresses are non-steady. Around the channel, within the non-flowing mass, they are statically indeterminate, hence, highly dependent on the method of charging and draw, time in storage, and the relative deformation of the stored solid and the containing structure. Thus, in plug-flow bins, the wall stresses cannot be computed with any precision. This situation is reflected in the large number of publications on pressures in silos and bins and in the general lack of agreement among the authors.

Slip-stick solids

Solids which exhibit slip-stick properties during the shear tests are evidently incapable of steady flow, and the consolidating pressures during flow are likely to be higher than those computed on the assumption of steady state flow. To account for the over-pressures, the flow-factor used in design should be increased in accordance with the amplitude of the oscillations of the pen, as shown in the following table:

Oscil-	2S/3 and S	Design	1.2ff
lations	S/3 and S	flow-	1.4ff
between	0 and S	factor	1.6ff

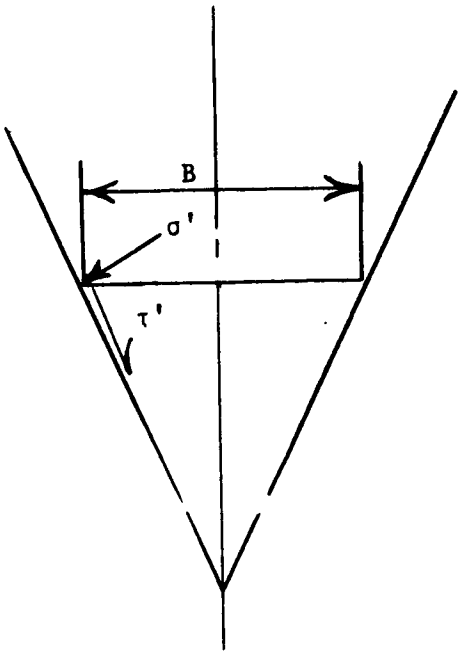

Fig. 44

Stresses on hopper walls

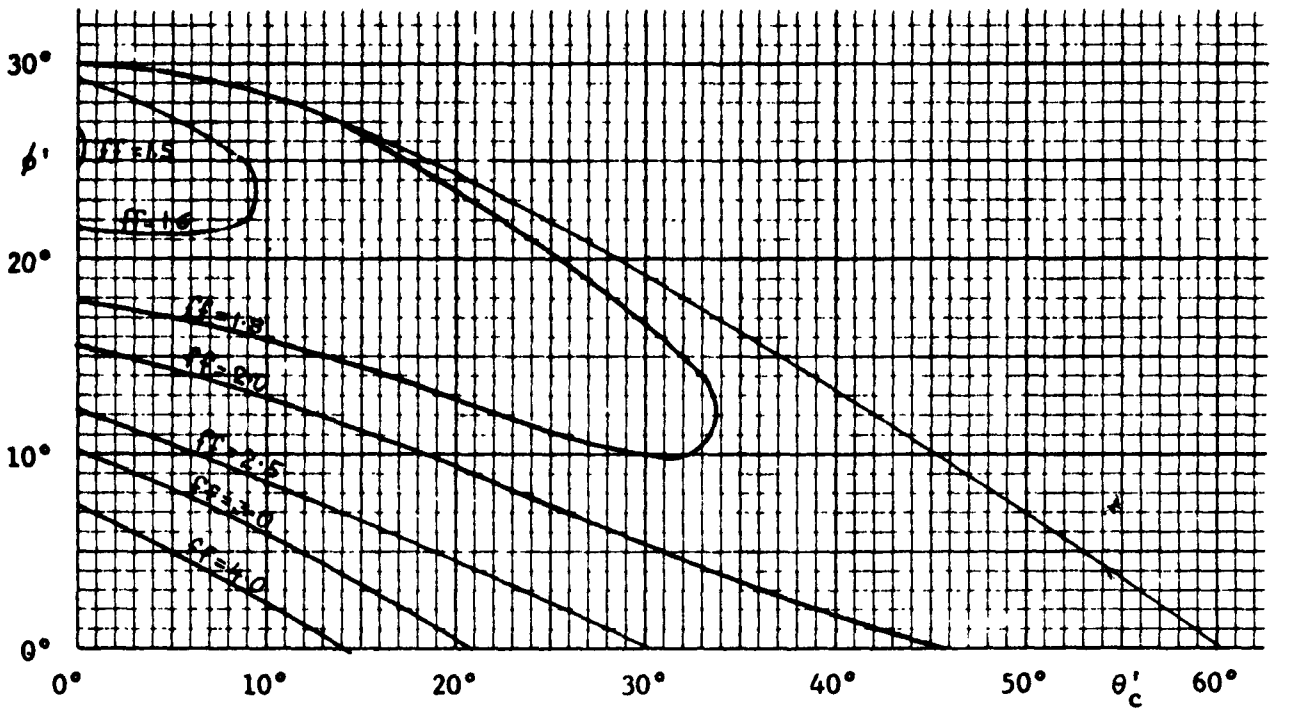

Fig. 45

ff contours for conical channels, δ = 30°

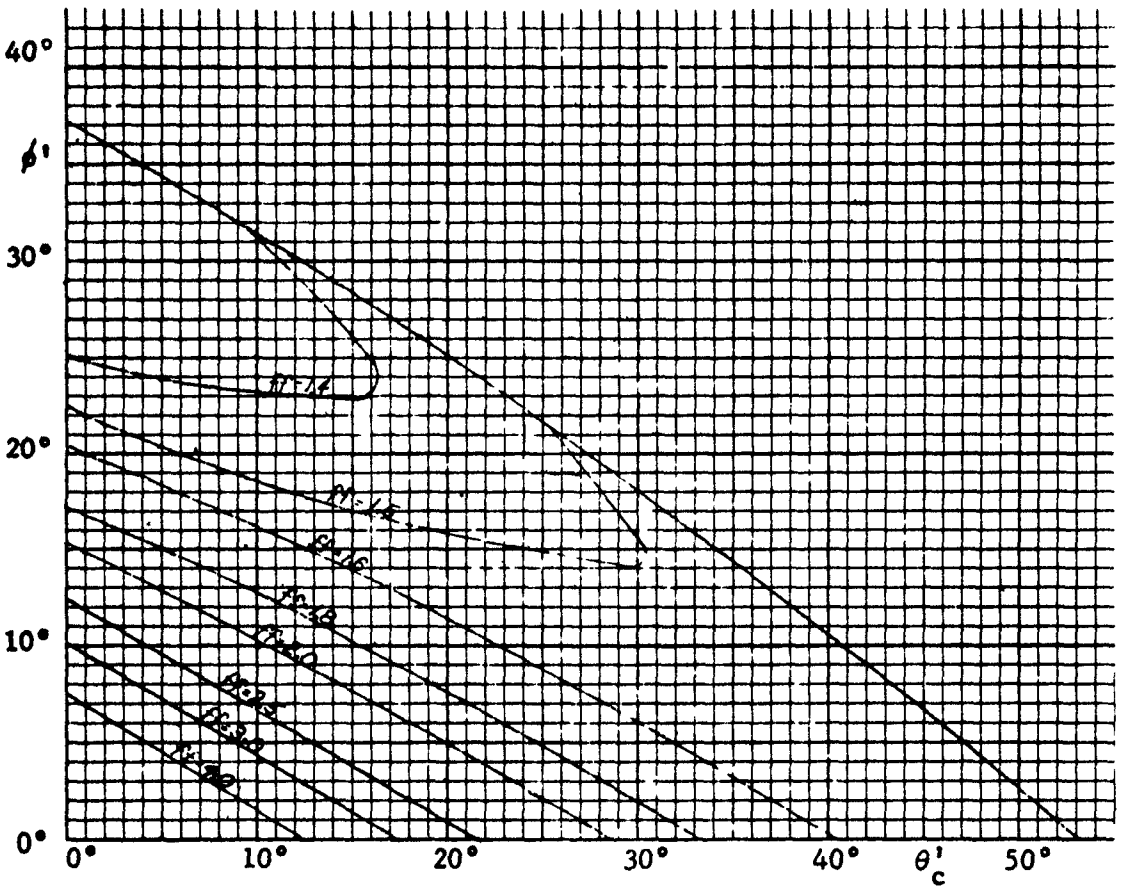

Fig. 46

ff contours for conical channels, $\delta = 40°$

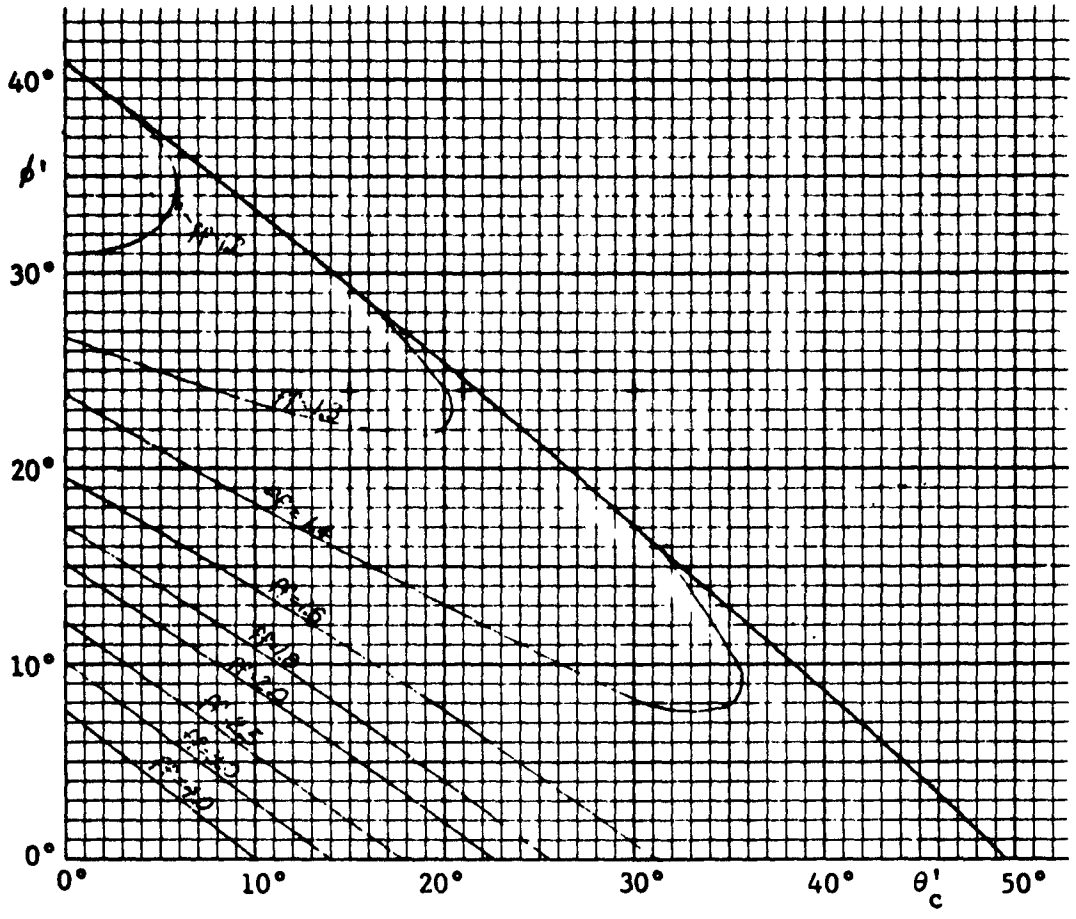

Fig. 47

ff contours for conical channels, δ = 50°

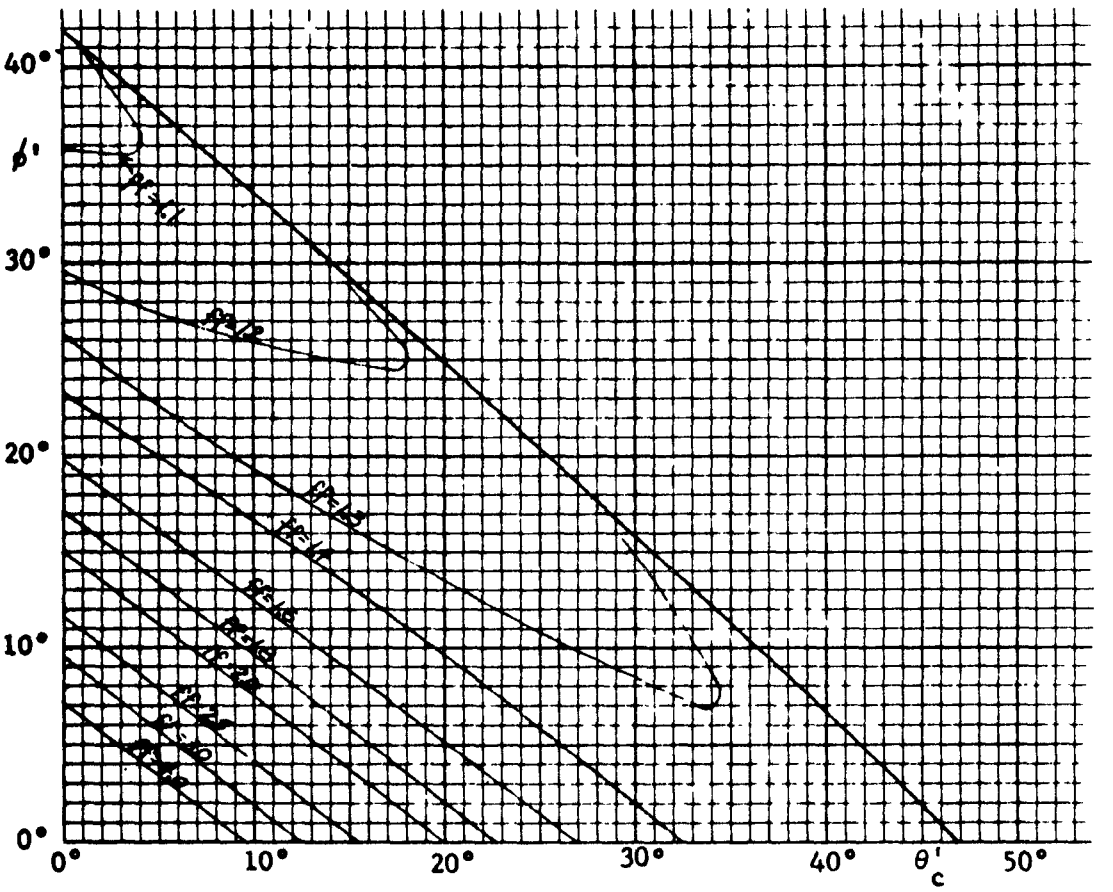

Fig. 48

ff contours for conical channels, $\delta = 60°$

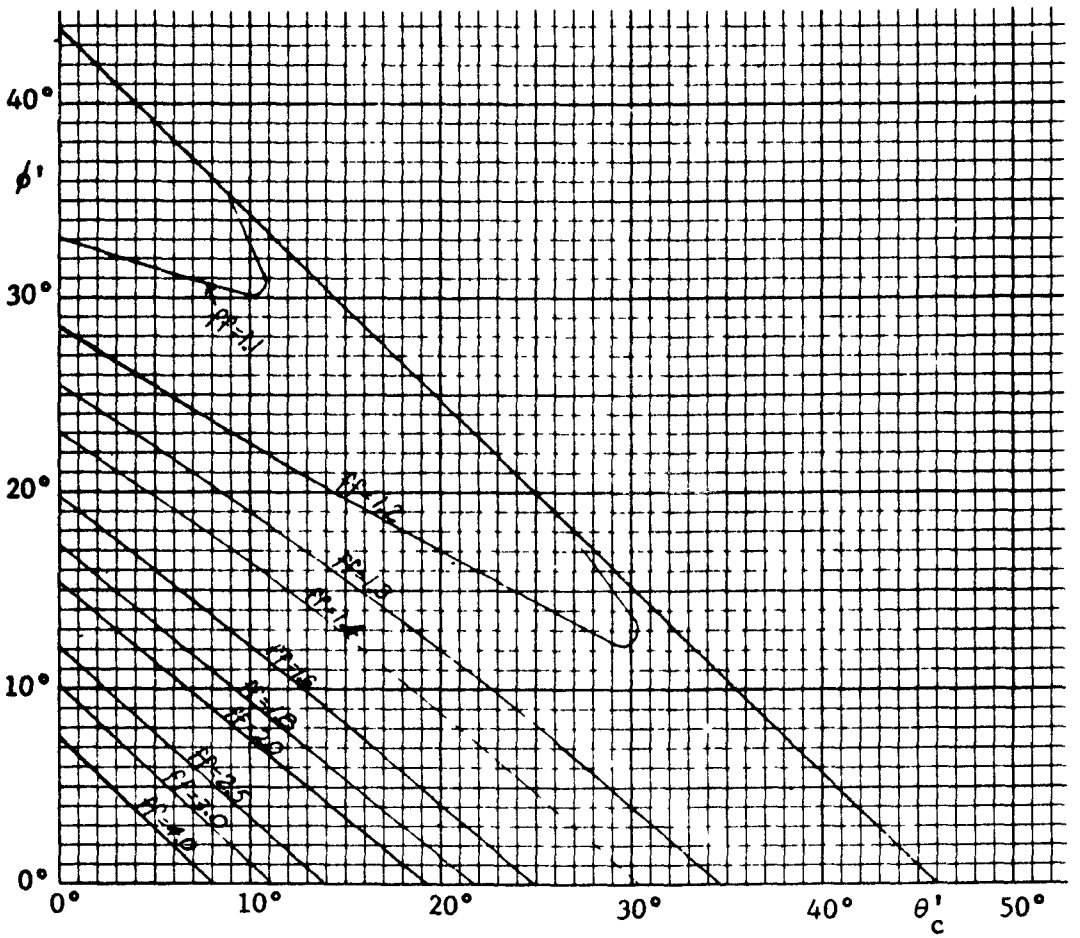

Fig. 49

ff contours for conical channels, $\delta = 70°$

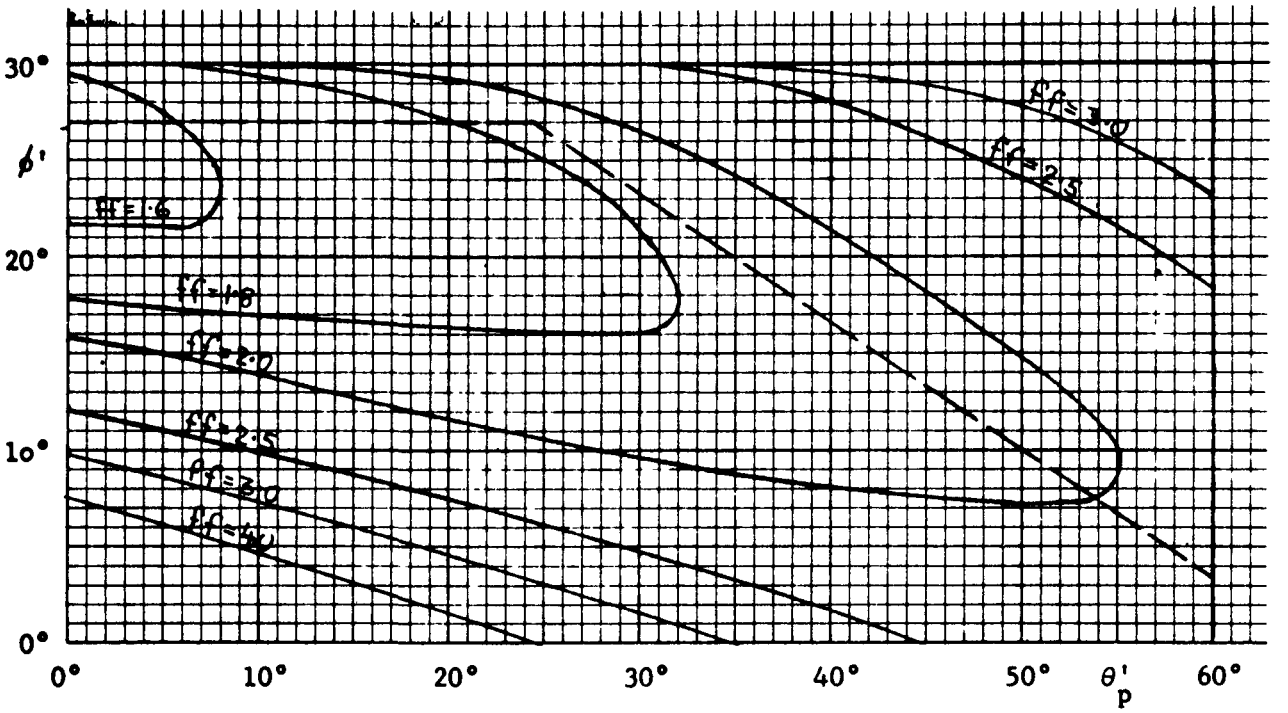

Fig. 50

ff contours for symmetric plane-flow channels, $\delta = 30°$

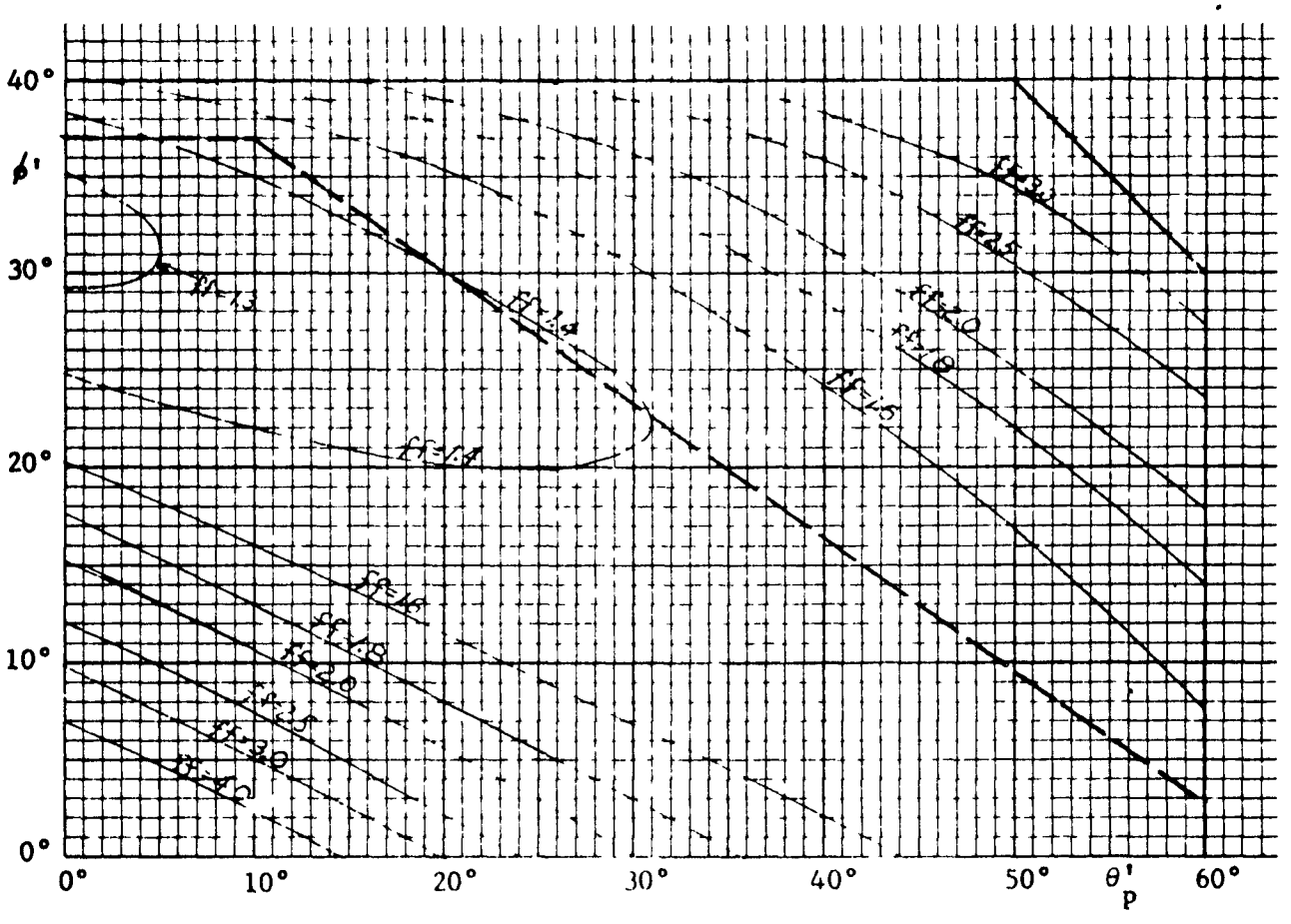

Fig. 51

ff contours for symmetric plane-flow channels, $\delta = 40°$

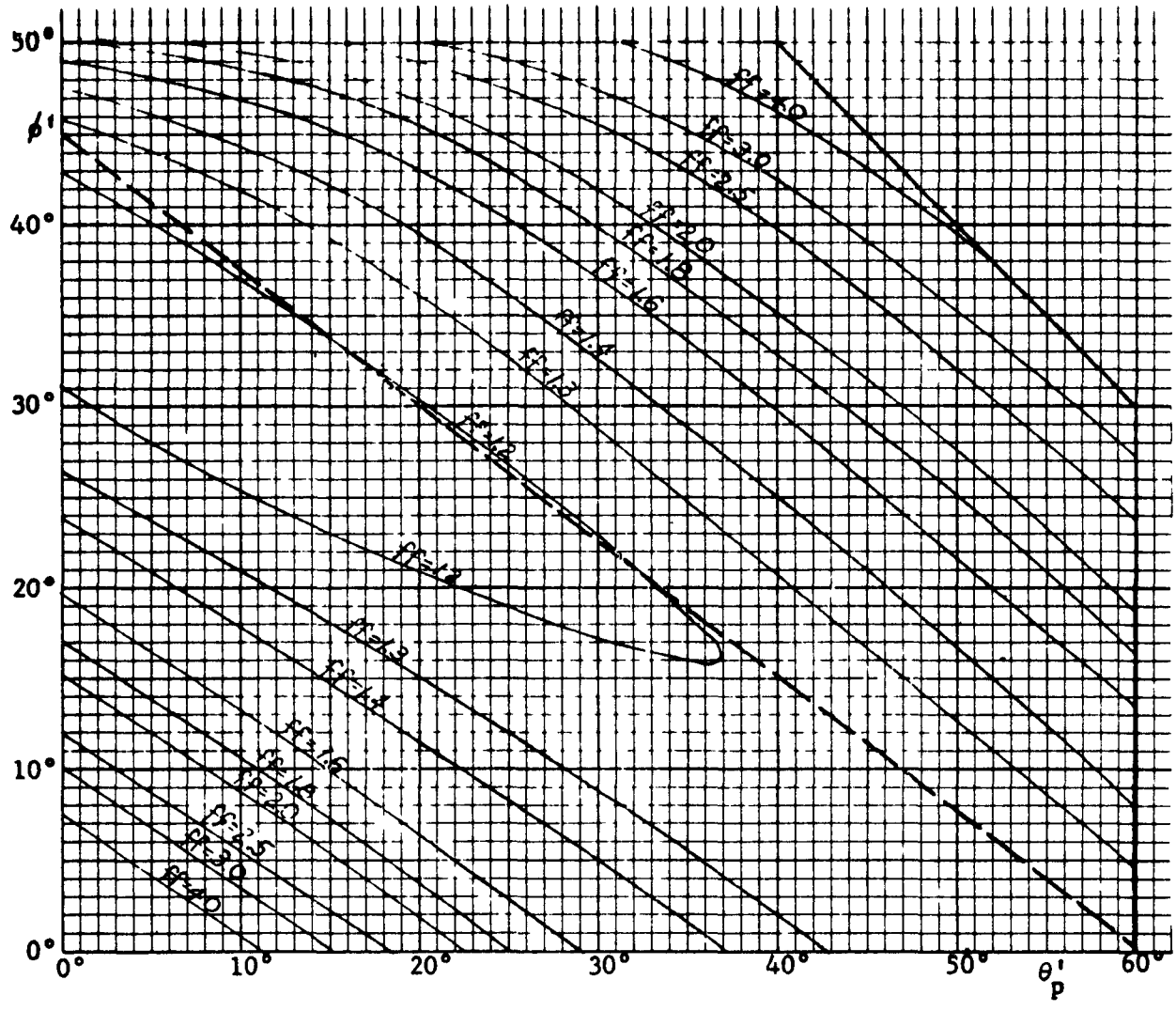

Fig. 52

ff contours for symmetric plane-flow channels, $\delta = 50°$

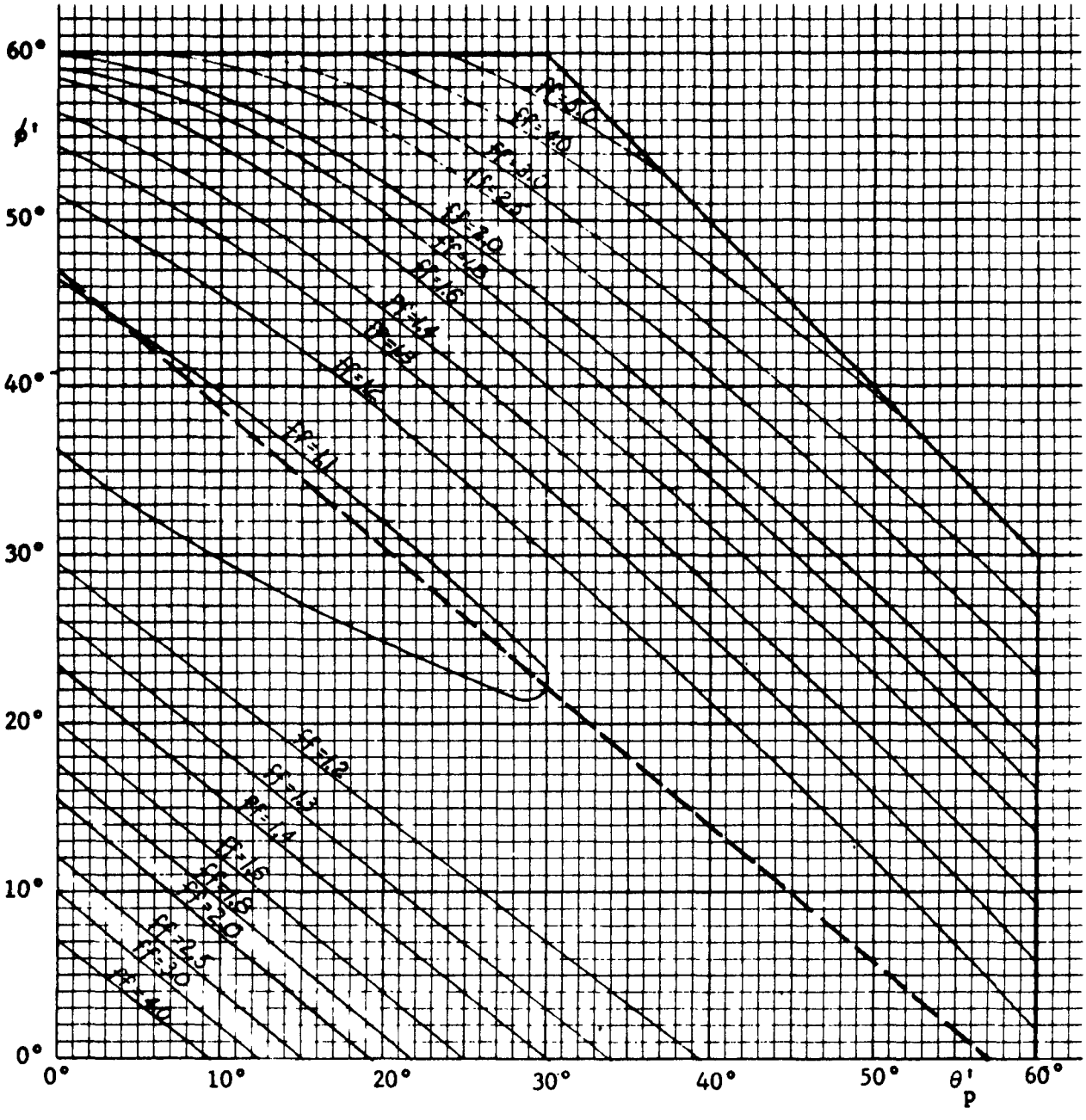

Fig. 53

ff contours for symmetric plane-flow channels, $\delta = 60°$

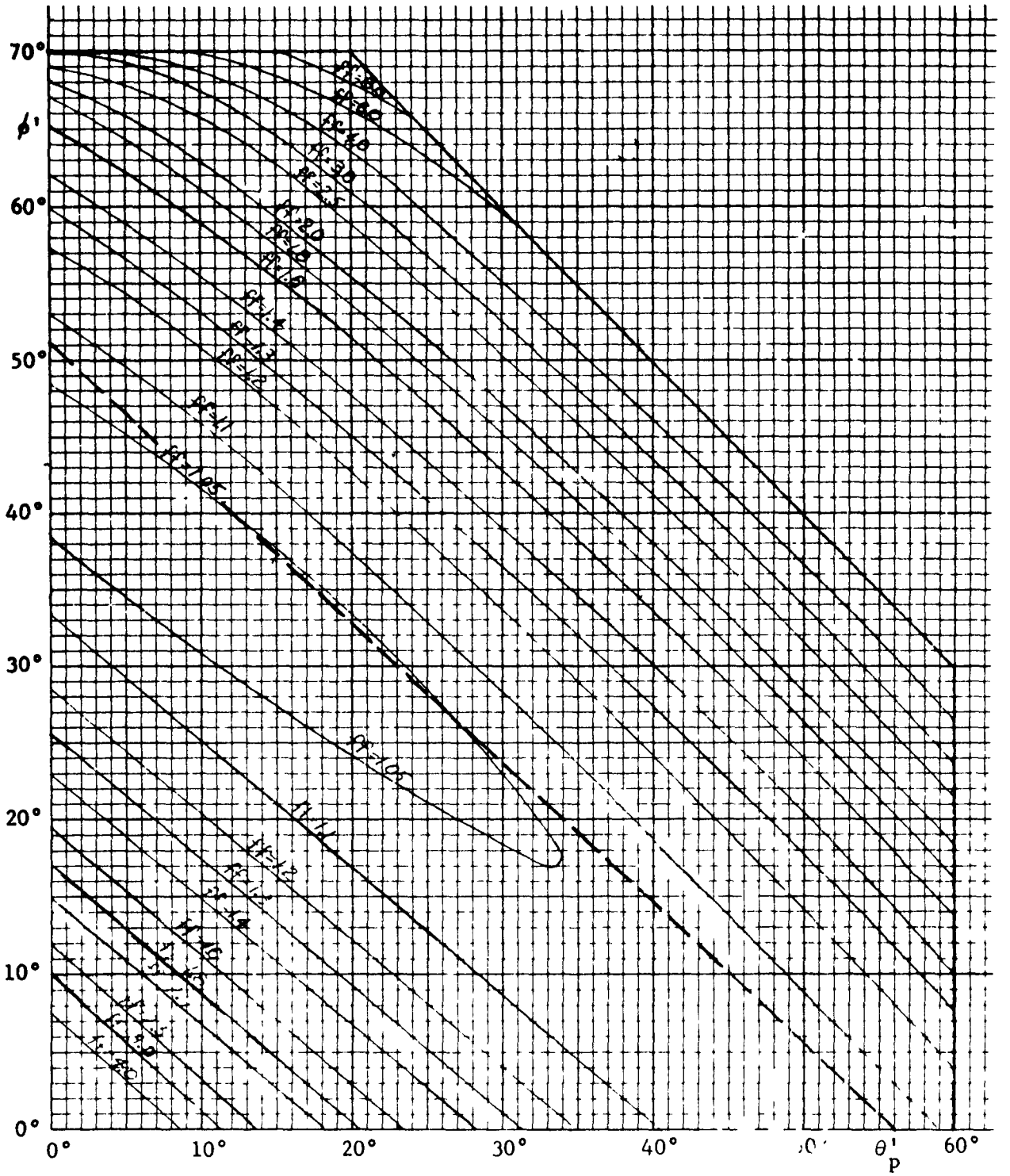

Fig. 54

ff contours for symmetric plane-flow channels, $\delta = 70°$

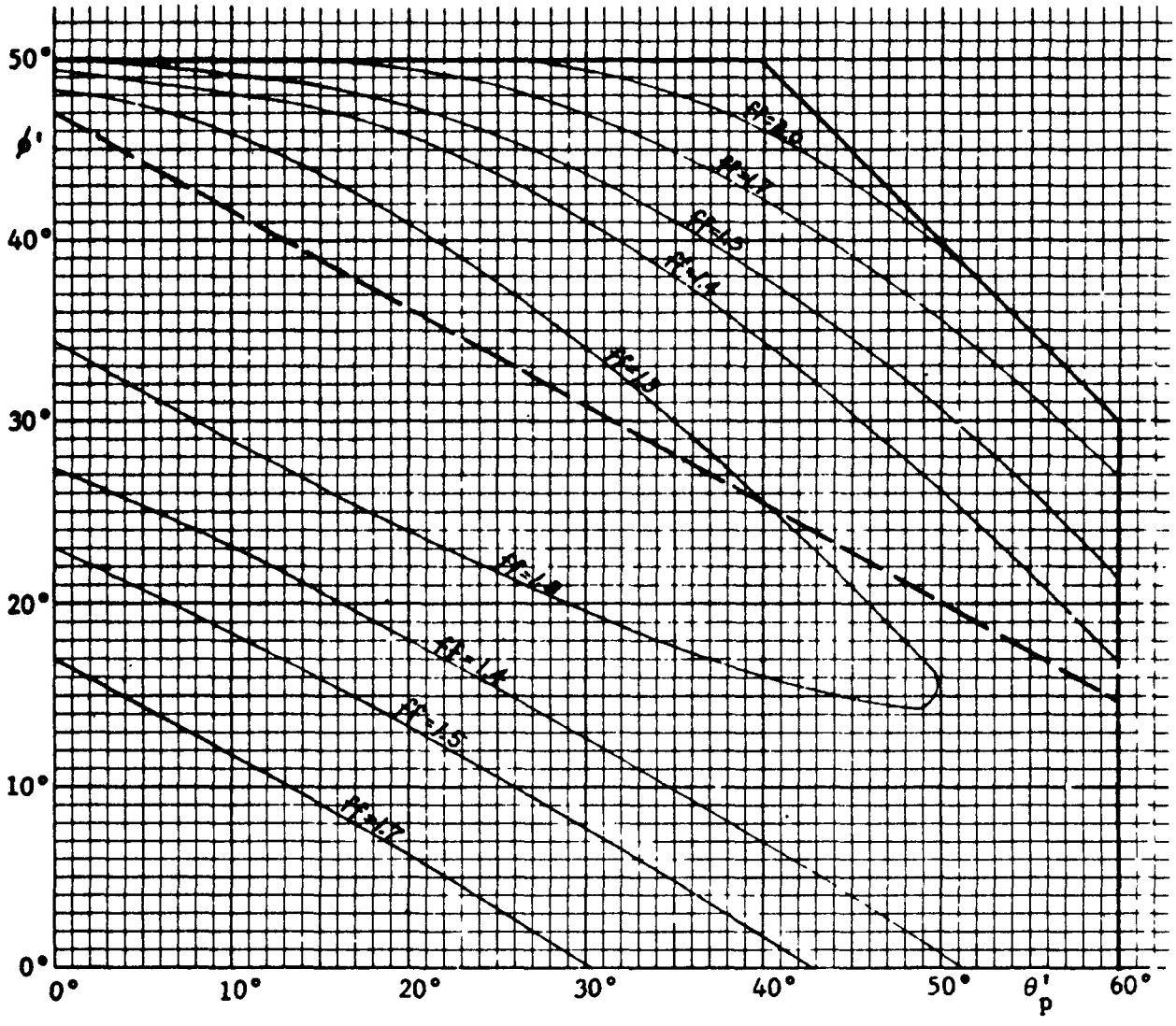

Fig. 55

ff contours for asymmetric plane-flow channels with one vertical wall, $\delta = 50°$, $\phi^V = 20°$

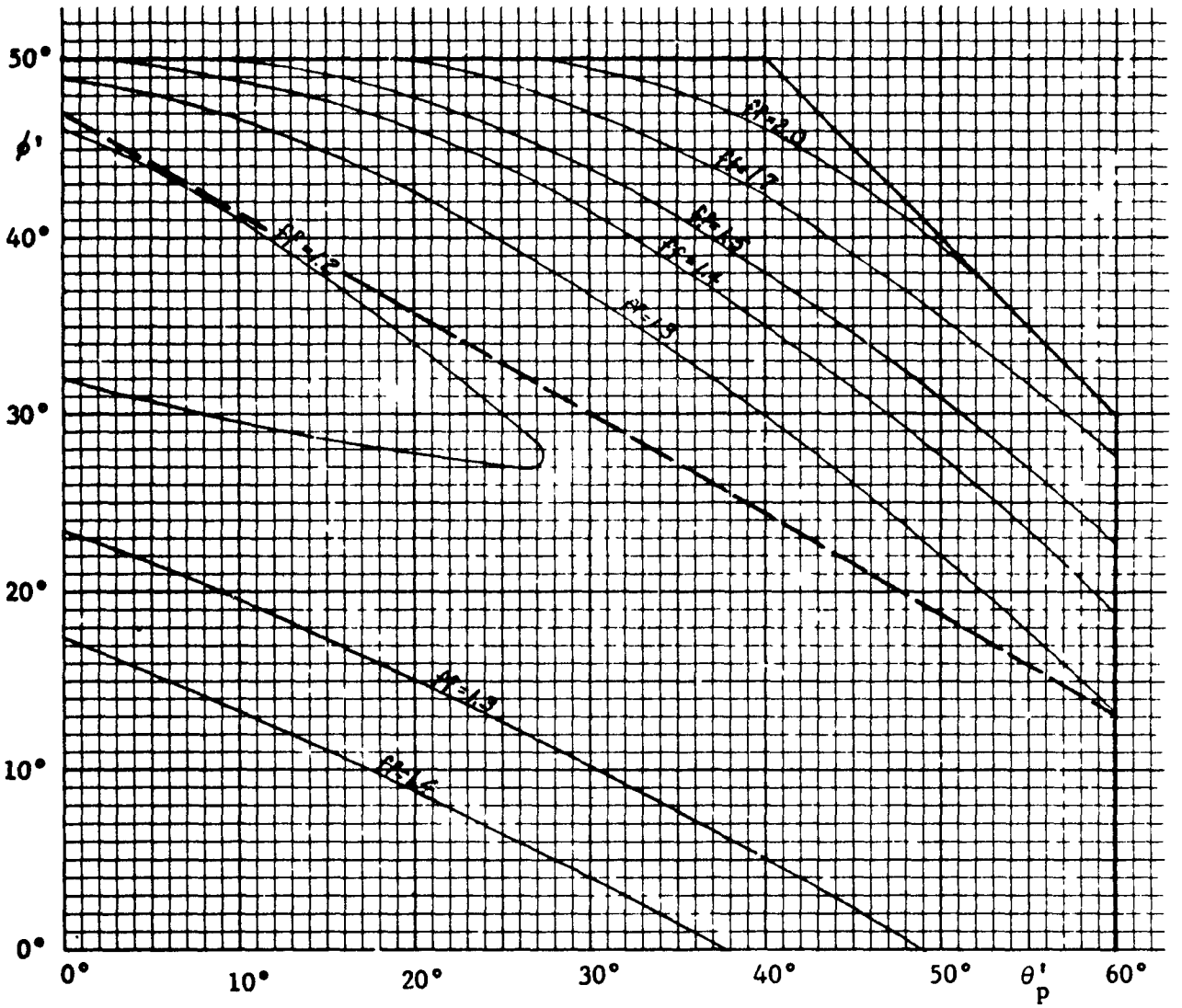

Fig. 56

ff contours for asymmetric plane-flow channels with one vertical wall, $\delta = 50°$, $\phi' = 30°$

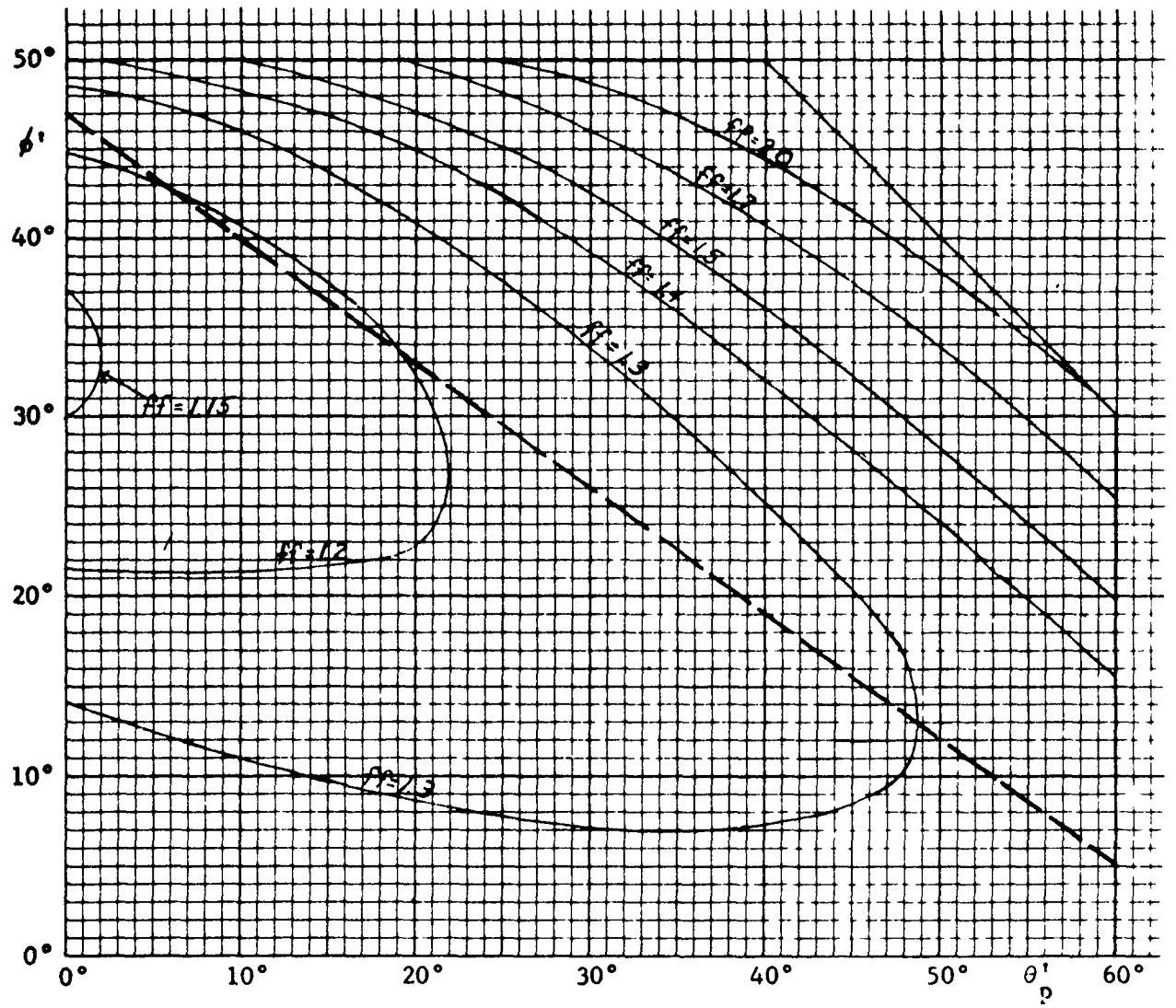

Fig. 57

ff contours for asymmetric plane-flow channels with one vertical wall, $\delta = 50°$, $\phi^v = 40°$

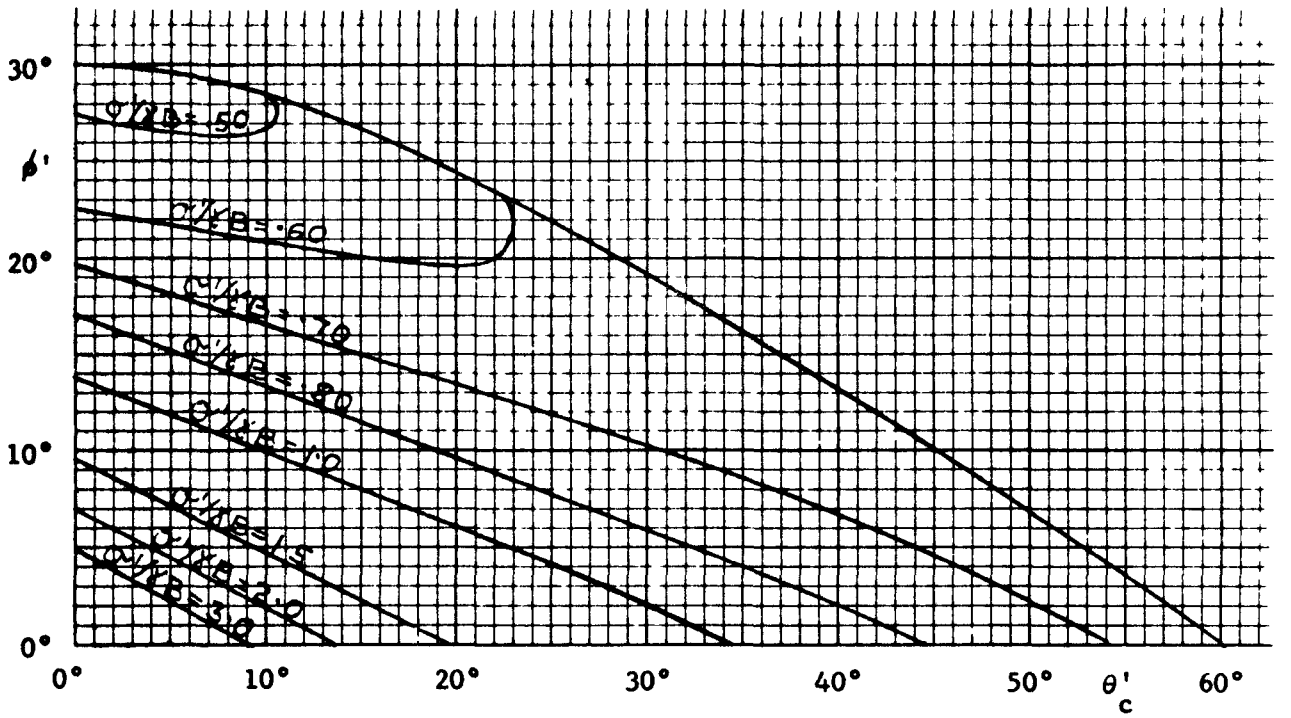

Fig. 58

$\sigma'/\gamma B$ contours for conical channels, $\delta = 30°$

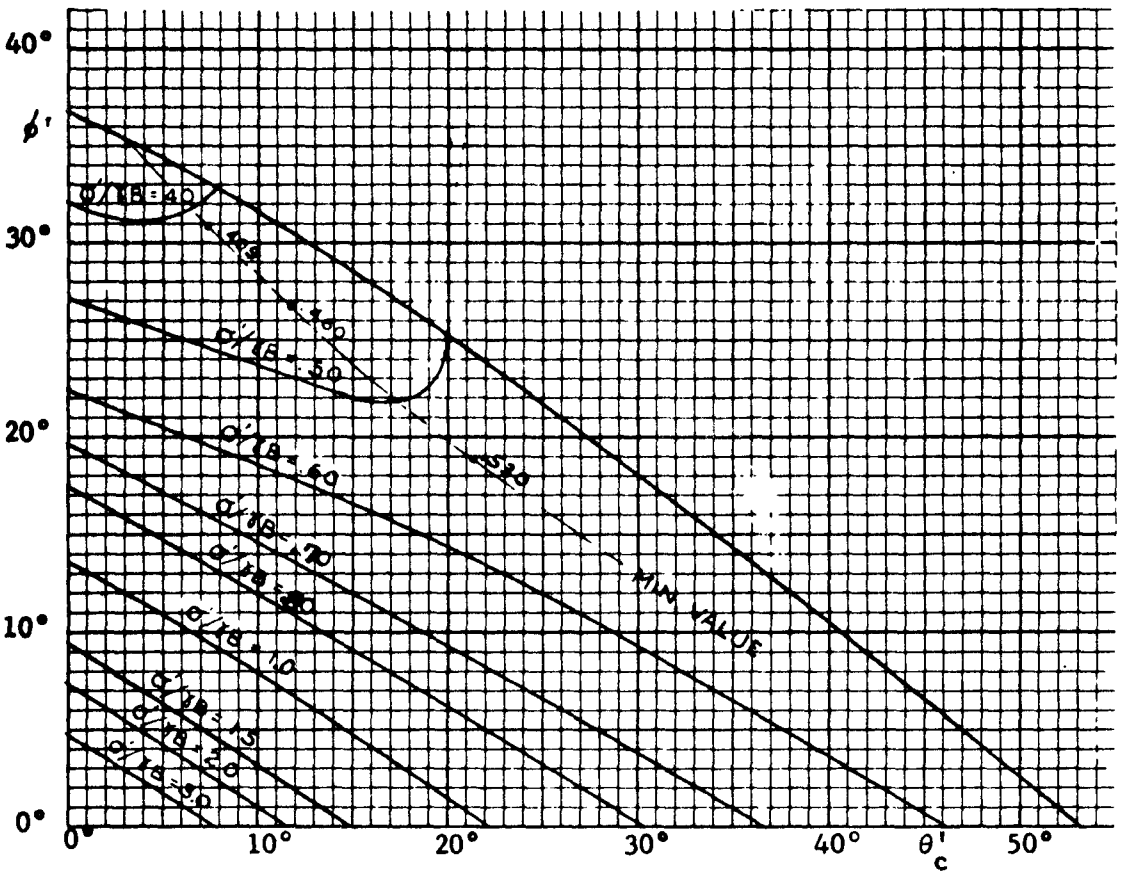

Fig. 59

$\sigma'/\gamma B$ contours for conical channels $\delta = 40°$

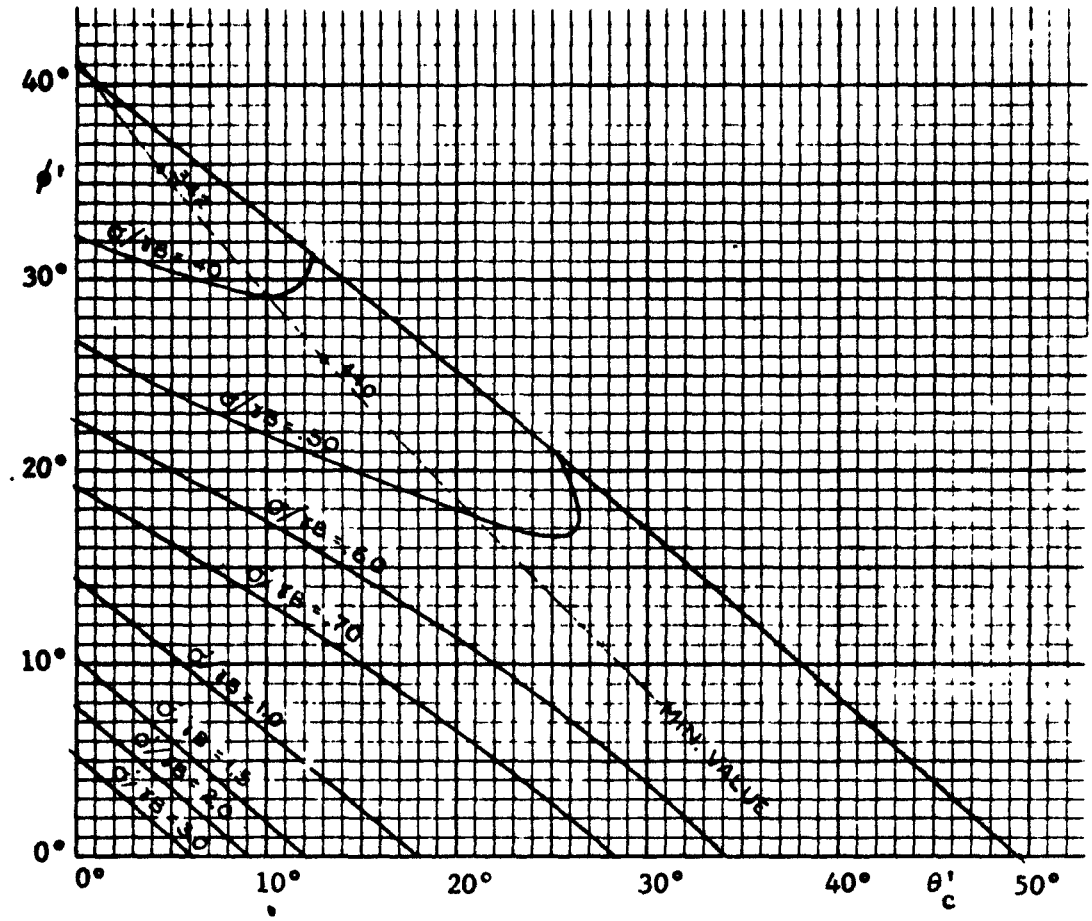

Fig. 60

$\sigma'/\gamma B$ contours for conical channels, $\delta = 50°$

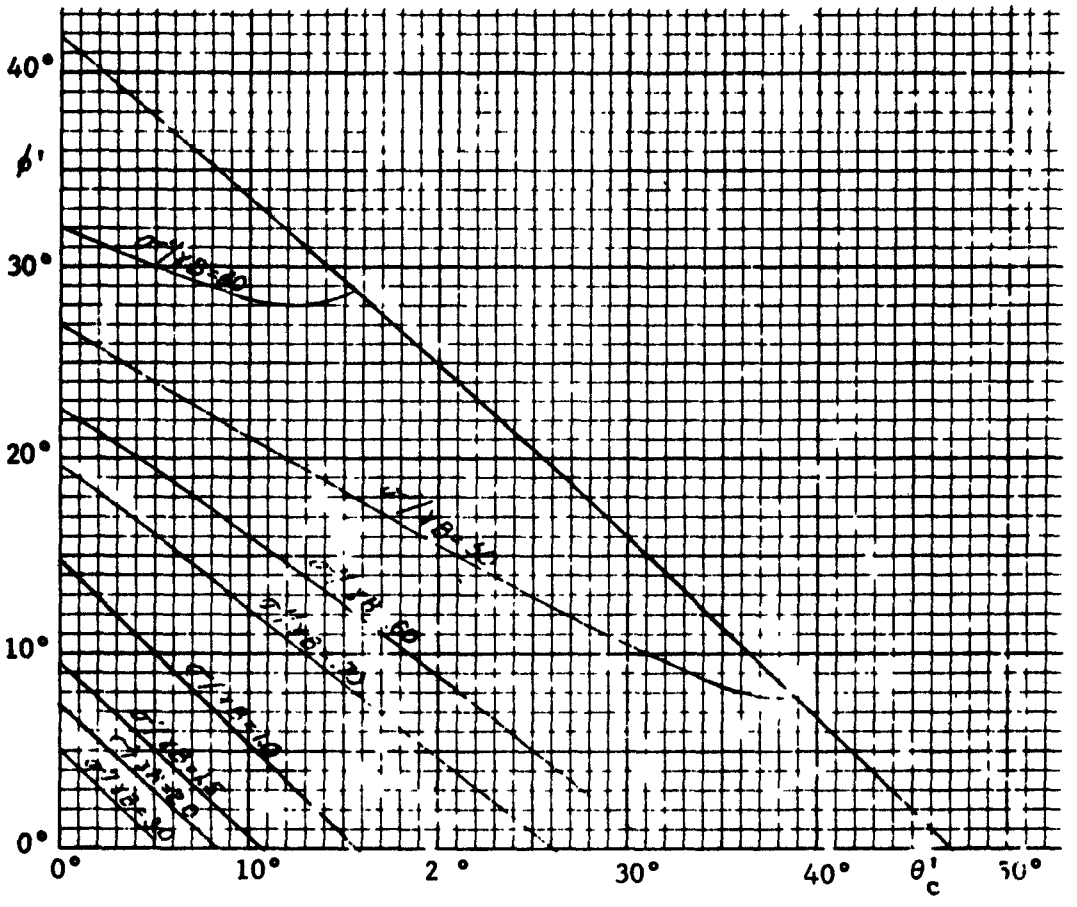

Fig 6'

σ'/γB contours for conical channels, ϑ = 60°

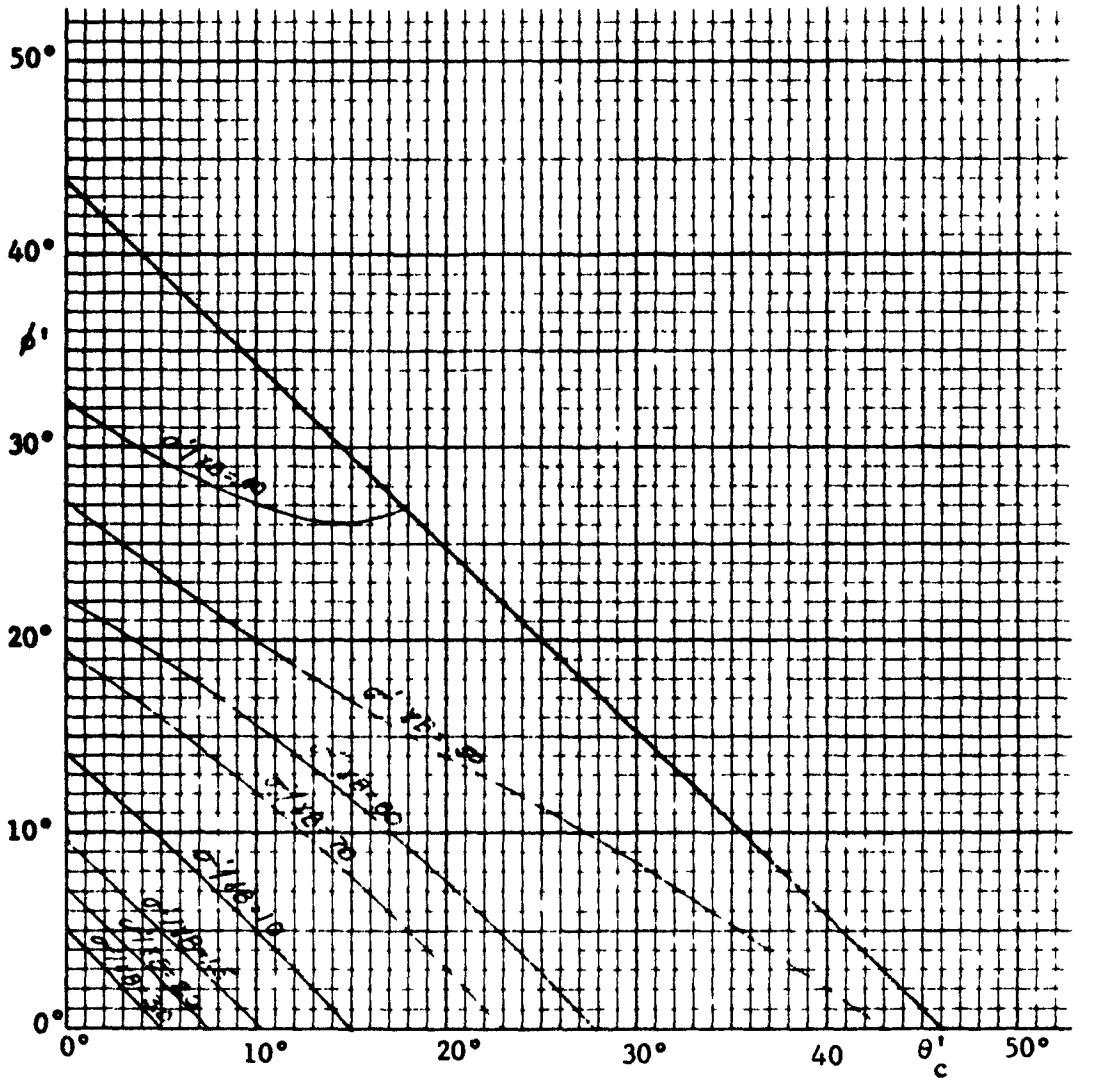

Fig. 62

σ'/rB contours for conical channels, δ = 70°

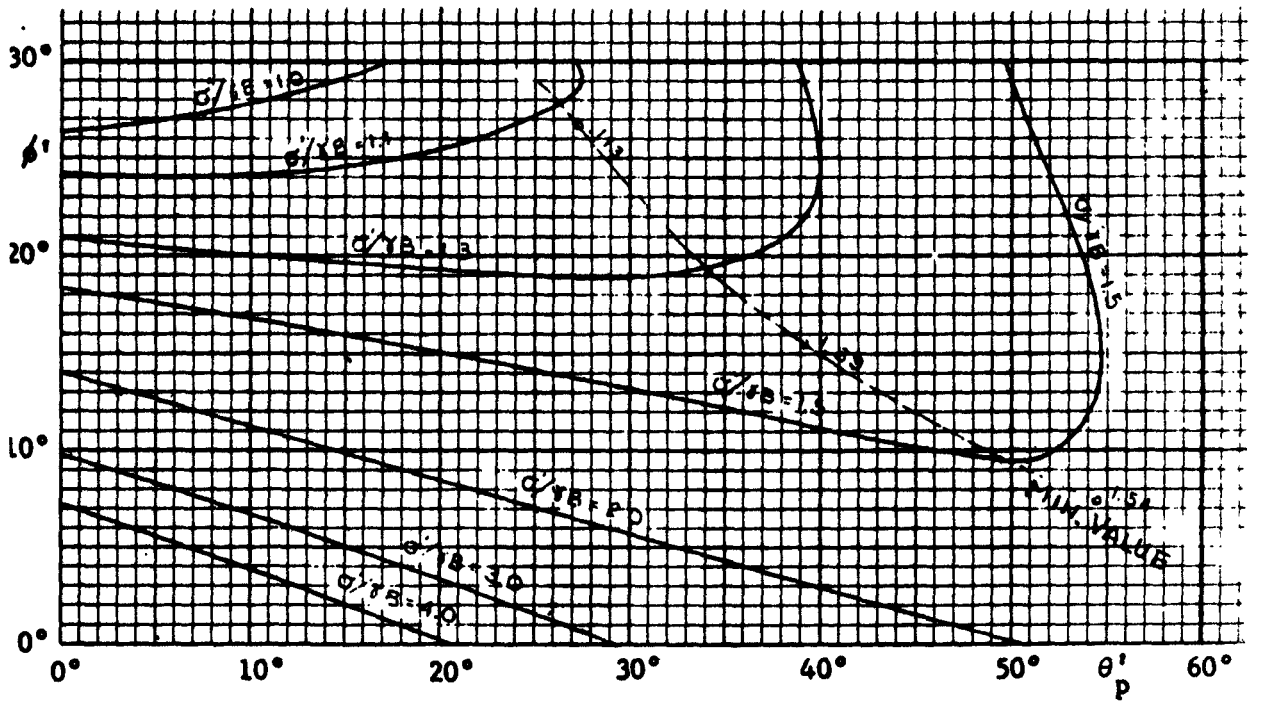

Fig. 63

$\sigma'/\gamma B$ contours for symmetric plane-flow channels, $\delta = 30°$

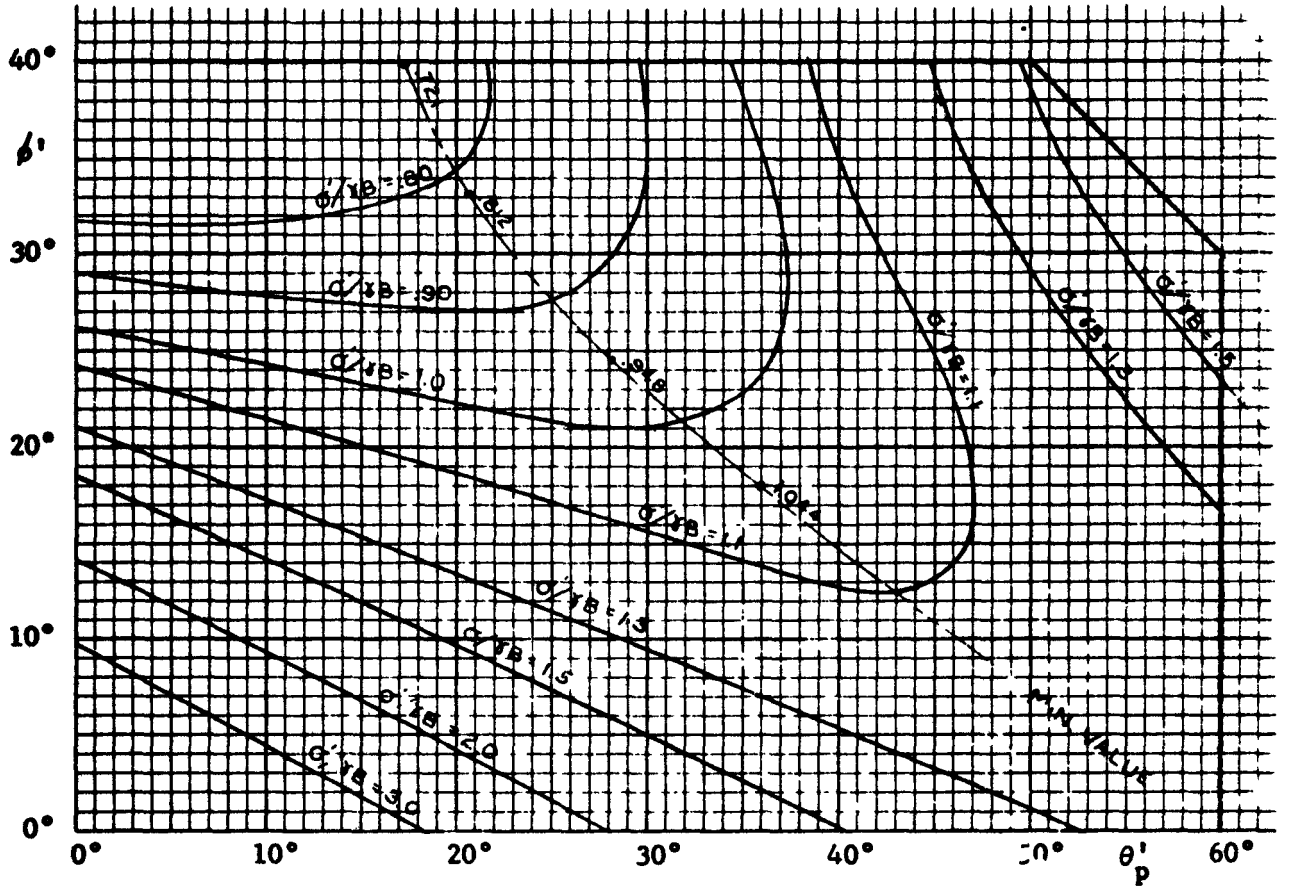

Fig. 64

$\sigma'/\gamma B$ contours for symmetric plane flow channels $\delta = 40°$

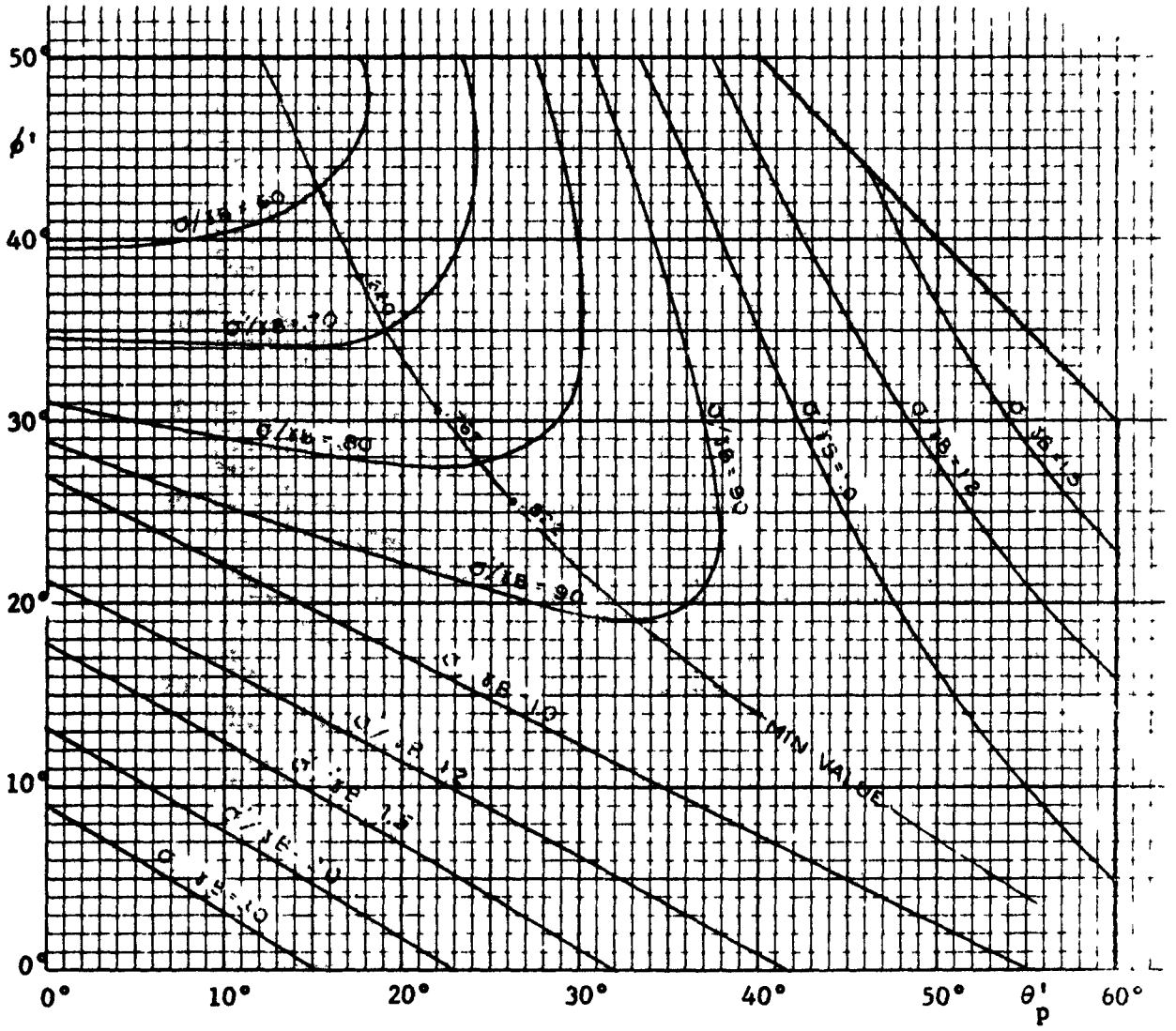

Fig. 65

σ'/γB contours for symmetric plane-flow channels, δ = 50°

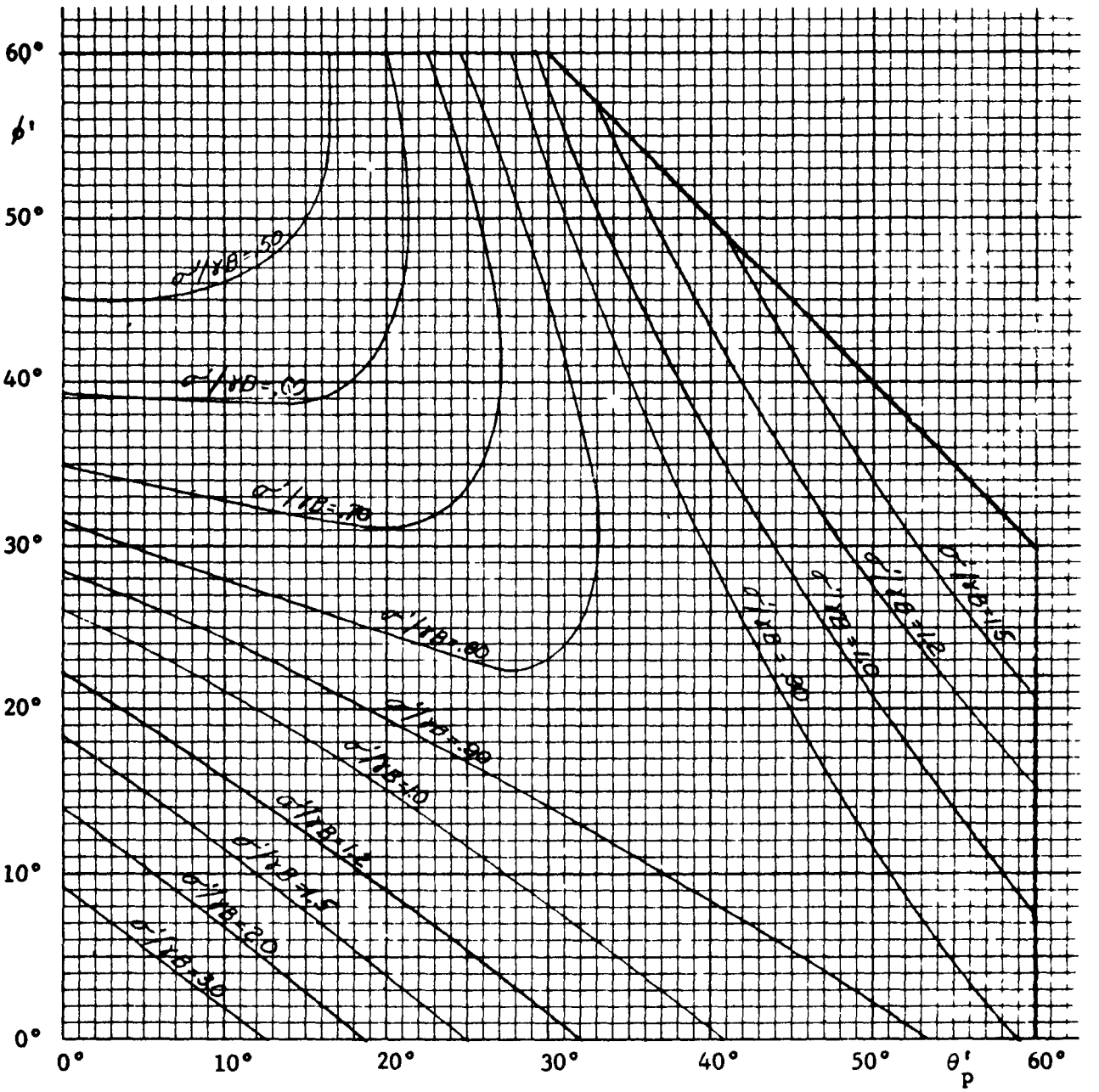

Fig. 66

$\sigma'/\gamma B$ contours for symmetric plane-flow channels, $\delta = 60°$

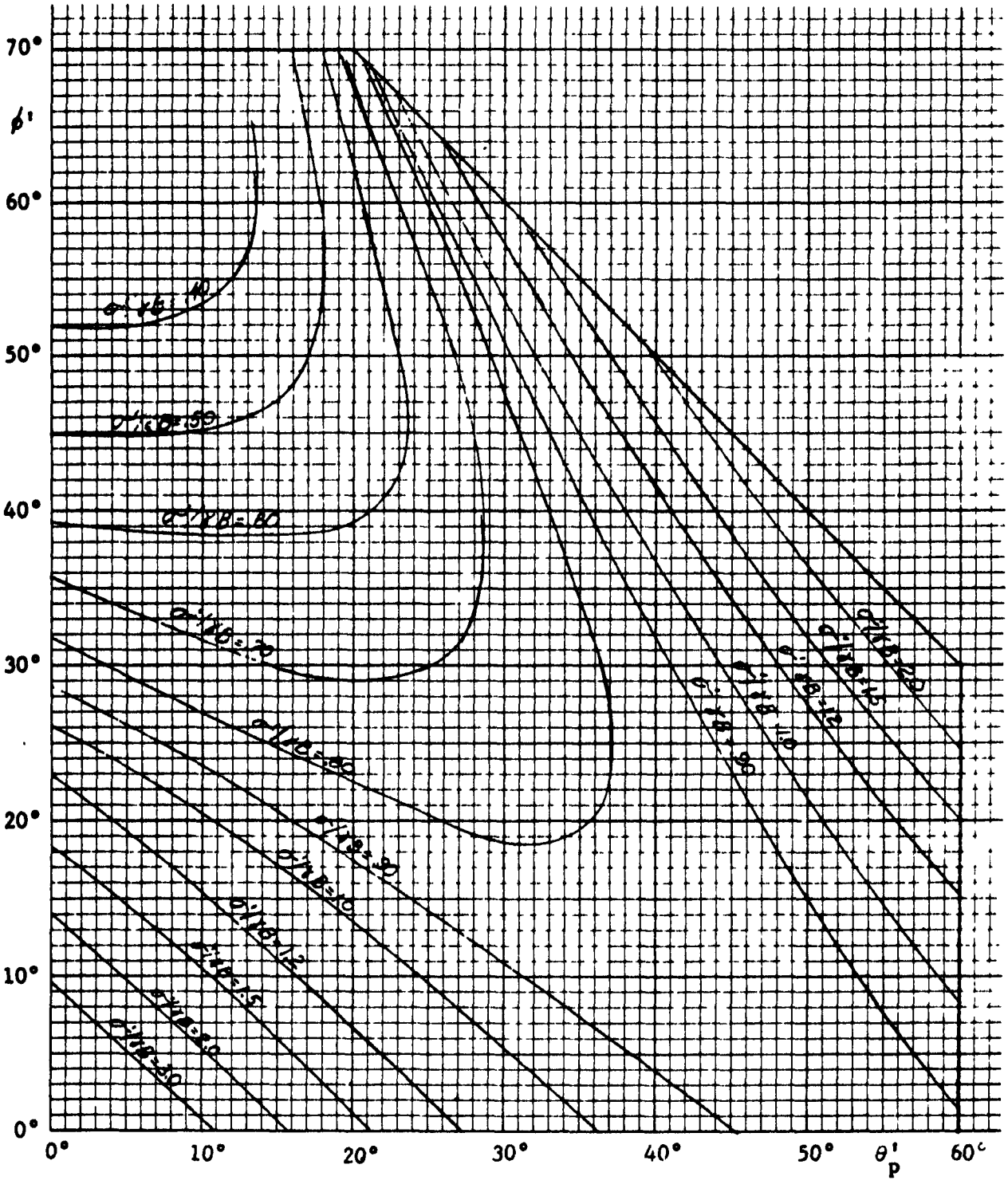

Fig. 67

σ'/γB contours for symmetric plane-flow channels, δ = 70°

Dischargers and feeders

The outlet computed in the previous sections must be effective, i.e. the solid must flow through the whole area of the outlet. A discharger or a feeder should draw the solid across the whole area of the outlet to make it fully effective. It is not necessary to provide a constant velocity of the solid across the whole area of the outlet. As long as all the solid above the outlet is in motion, the outlet is effective.

The size of the outlet is determined by the flow criteria. Frequently, the computed dimensions of the outlet are many times greater than might be required either by the rate of flow or by the largest particle size. When this occurs, the use of a discharger should be considered to loosen up the solid in the region of the outlet and to cause the solid to flow through a smaller outlet into a smaller feeder, valve, or gate. Such a combination may be cheaper than a large feeder.

Dischargers. A discharger is a device which permits the stored solid to flow out of a hopper but does not meter the rate of flow.

A vibrating hopper, Fig. 68, is a discharger with a circular pan, a central outlet, and a baffle fixed to the pan above the outlet. The pan is suspended from the hopper and is flexibly connected to the hopper. Torsional oscillation is applied to the pan about its vertical axis. This motion loosens up the solid above the pan and causes it to flow around the baffle and into the outlet. Like all vibrating devices, the vibrating hopper is applicable to solids whose instantaneous flow-function satisfied the safety factor expressed by Eq. (24).

An air-hopper, Fig. 69, is a discharger which uses air panels to reduce the angle of friction ϕ' at the hopper walls close to zero, and to aerate the solid in a small region above the outlet. It will be noticed from Figures 45 to 54 that for $\phi' \simeq 0$ the troughs of low values of the flow-factor occur for slope angles $\theta'_c = 40°$ to $50°$ for conical hoppers, and $\theta'_p = 50°$ to $55°$ for symmetric plane hoppers. The air-hopper works best at these slope angles. The whole area of the air-hopper should be lined with air panels.

It should be stressed that the air-hopper does not rely on an expanded bed for operation, the aerated region is limited to the vicinity of the outlet and air flows out of the hopper through the outlet. In an expanded bed, air flows upward through the bin. It also follows from the figures that a reduction of ϕ' to zero along steeper hopper walls, say, $\theta'_c = 12°$, or $\theta'_p = 20°$ would lead to flow-factor values of 2 to 4, hence, to a reduced flowability of the hopper. Therefore, air panels should not be placed on steep hopper walls. An air-hopper is particularly well suited for discharging into an air conveyor.

Both the vibrating hopper and the air-hopper have the advantage of requiring little headroom.

Other dischargers like stirrers, vibrating panels are effective in small hoppers. In large bins it is advisable not to have any devices inside the stored solid as they are likely to lead to major maintenance problems. When a device is located in the central channel over the outlet, its efficacy is limited because it cannot break up a piping solid.

Internal dischargers are undesirable in mass-flow hoppers because they usually prevent mass-flow from developing.

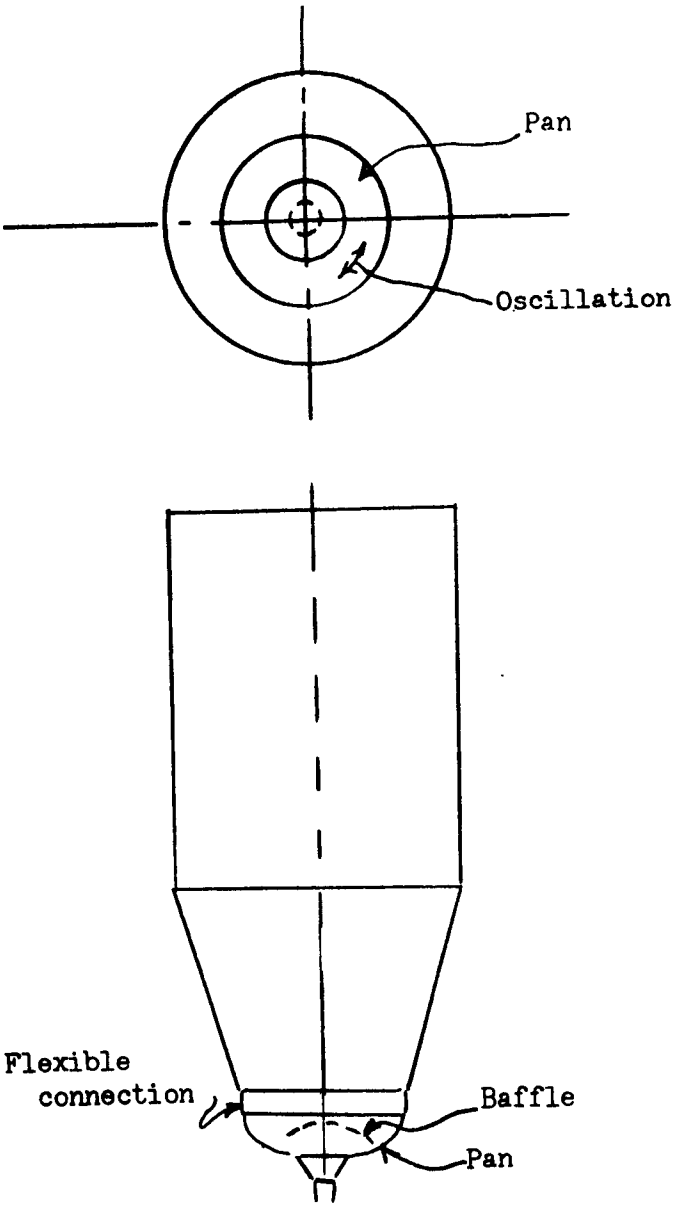

Fig. 68

Vibrating hopper

Feeders. A feeder is a discharger which permits the regulation of the rate of flow of the solid out of a bin.

A screw feeder of screw diameter B and length L substantially greater than B should have a rate of flow of the solid increasing in the direction of flow. This is attained either with a tapered screw, Fig. 70, which widens the stream in the direction of flow, or by an increasing-pitch screw, Fig. 71, which speeds up a stream of constant cross-section in the direction of flow. A stepped up screw, Fig. 72, with steps of 1/4 pitch and 1.5B length, will generally work as well as a screw with a continuously increasing pitch. Two or more screws can be placed side by side to widen the outlet.

For mass-flow hoppers, the clearance between the screw and the trough should be small. In particular, for tapered screws, the trough should also be tapered. Otherwise plug flow may develop.

A belt feeder can also be used with a tapered outlet. However, here the height of the flowing bed within the hopper is uncertain and, therefore, the ratio of the widths of the outlet B_2/B_1, Fig. 73, should be as large as possible and preferably greater than 2. It should be born in mind that in a tapered outlet the smaller width of the taper B_1 should be equal to the computed value of B so that doming does not occur. For greater uniformity of flow, the front of a hopper with a tapered outlet should be vertical, as shown in the figure.

If the hopper outlet is raised above the belt so that a gap of height a = 1/4 to 1-1/2 inches is formed, Fig. 74, the outlet becomes fully effective without a taper. The gap is of constant height and the solid flows through it into the side pockets as well as through the

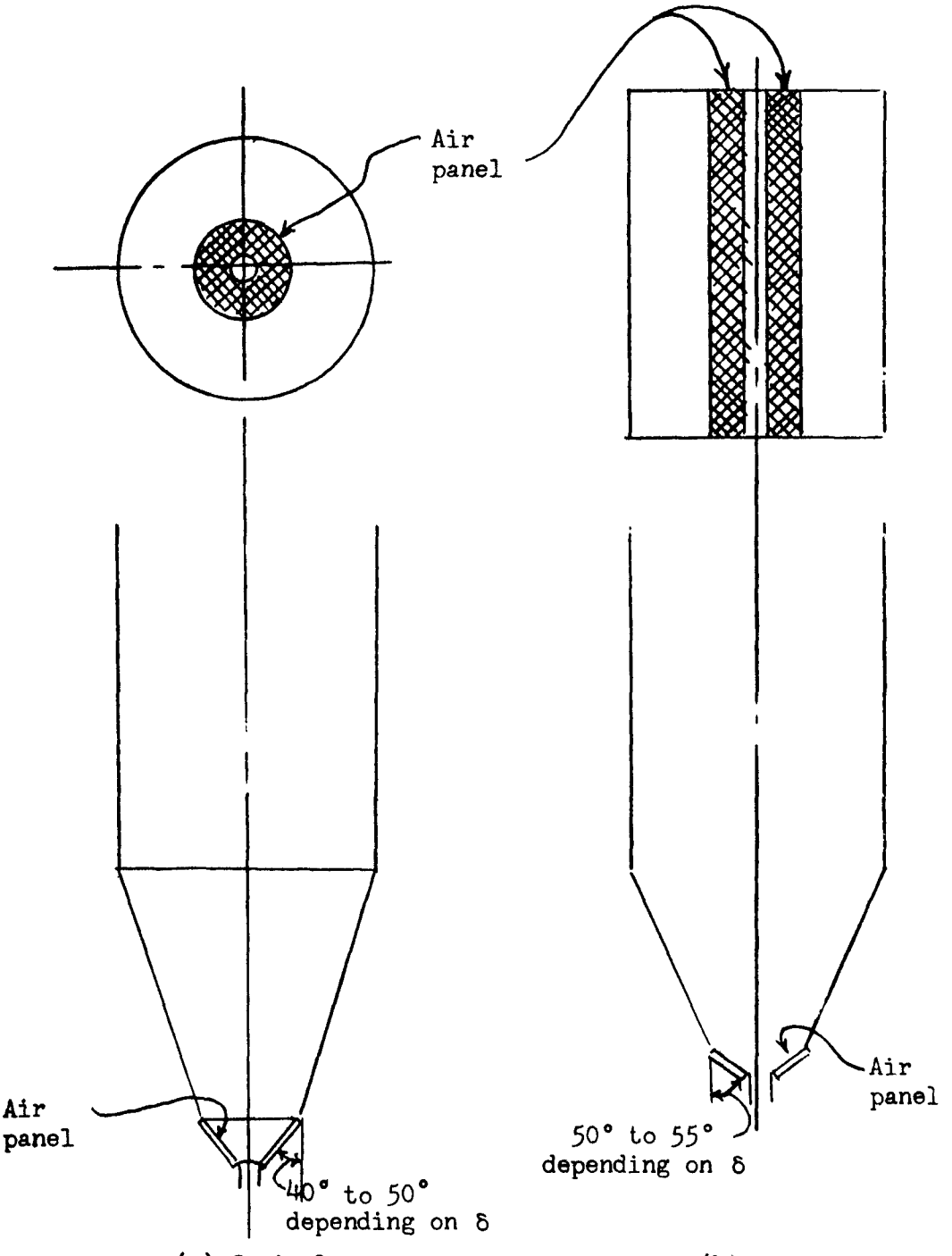

Fig. 69

Air hopper

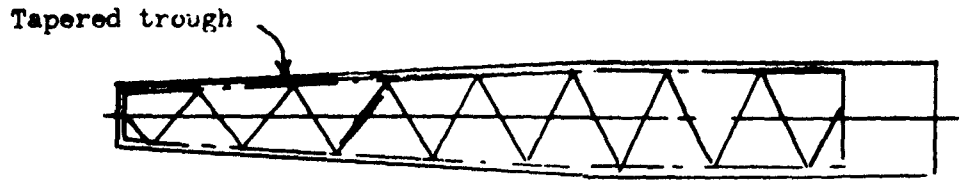

Plan

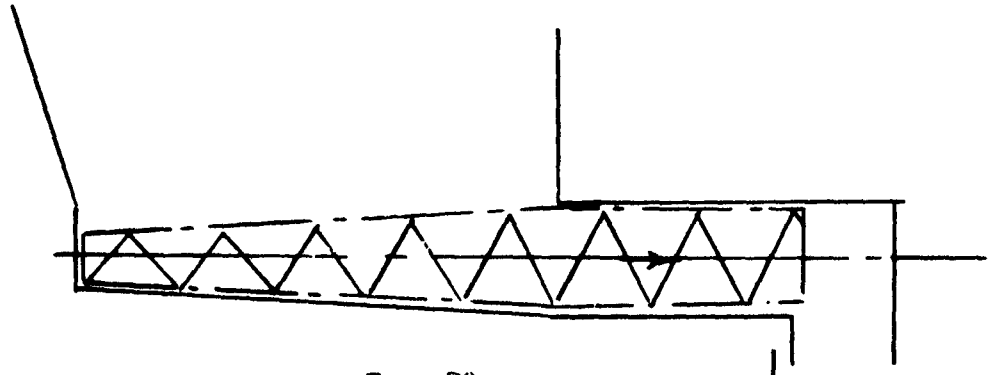

Fig. 70

Tapered screw feeder

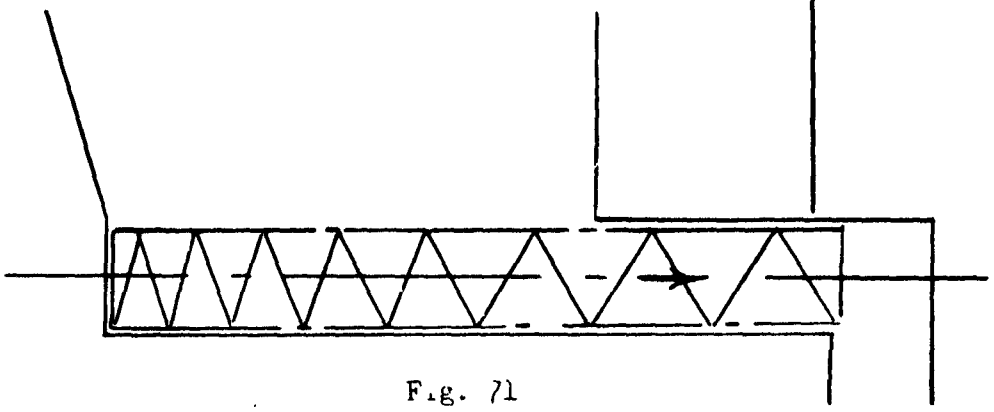

Fig. 71

Increasing pitch screw feeder

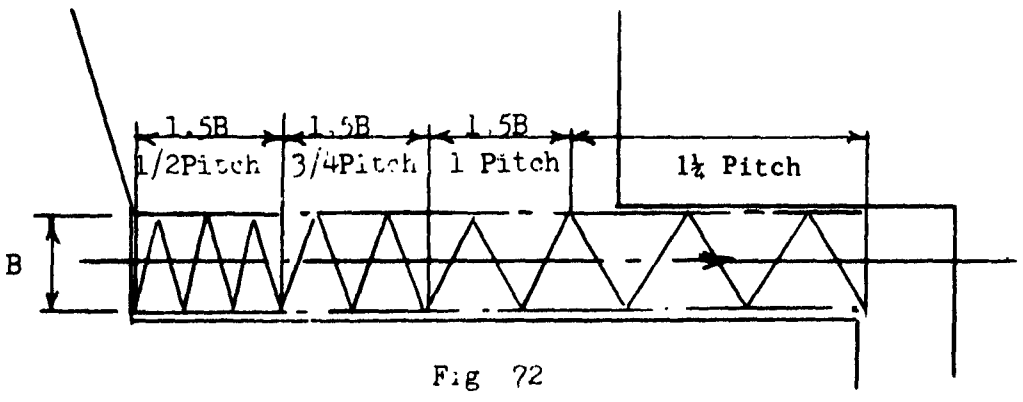

Fig 72

Stepped pitch screw feeder

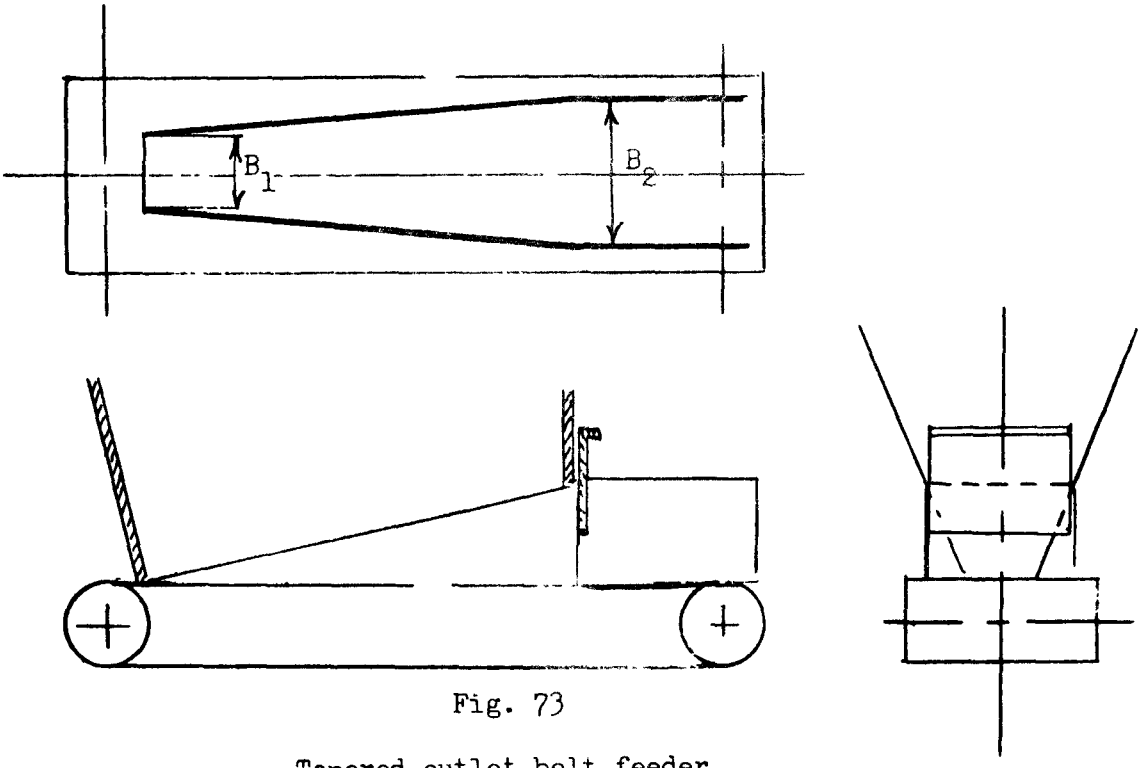

Fig. 73

Tapered-outlet belt feeder

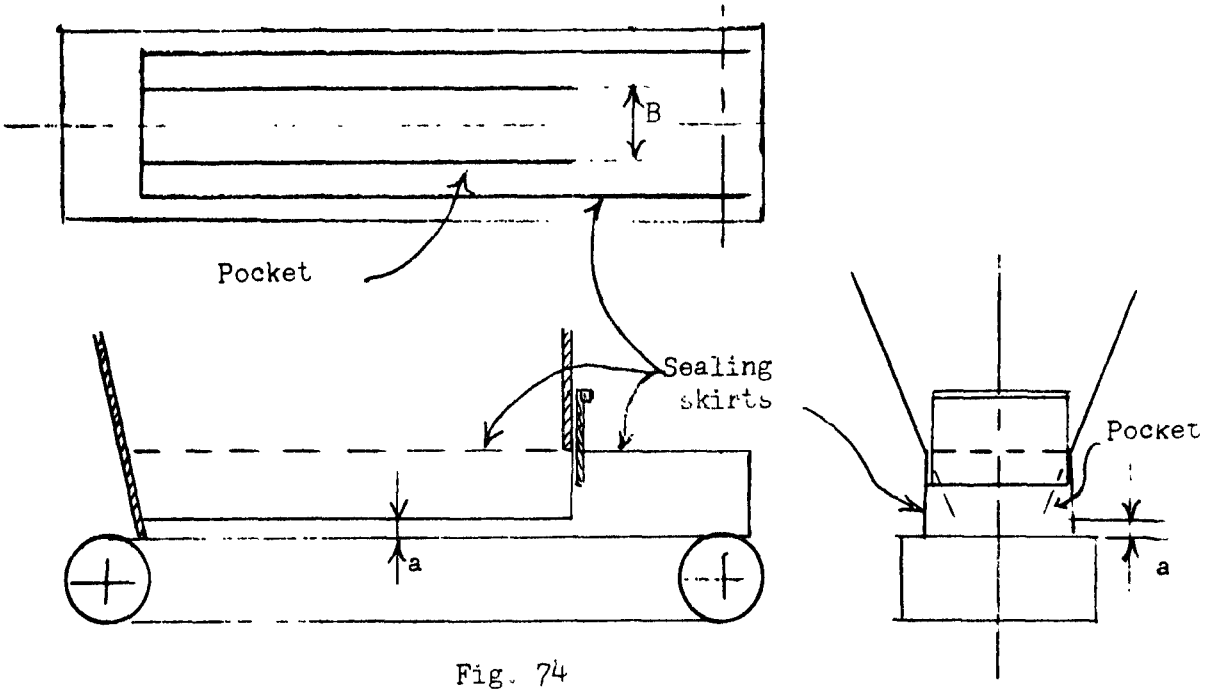

Fig. 74

Raised-hopper belt feeder

front opening of the hopper. This is a very efficient design for solids which do not contain material over 1 inch size because, obviously, the size of the particles must be smaller than the height of the gap for this design to work. If the gap is too large, flow becomes difficult to control. Sealing skirts can be provided on the outside of the hopper. The rate of feed is controlled by a variable speed drive. The front gate should be adjusted to provide uniform flow into the slot and the support of the feeder should permit initial adjustment of the height of the gap. Since the pressure on the sealing skirts is small, this feeder, when properly supported, leads to feeder loads which are close to the theoretical values (see below); the horsepower and wear are also at a minimum. A raised hopper can be placed directly over a belt conveyor, dispensing with the feeder and sealing skirts altogether. An example is given in the section on Fine Ores.

A slide-belt, that is a belt supported by a continuous, smooth plate - either troughed or flat - is preferable from the standpoint of flow to idler support. It is also cheaper and simpler.

An apron feeder is normally used for large size solids, e.g. mine-run and primary crusher ores, and its dimensions are usually governed by the largest rock size. Whenever the length of a rectangular outlet over the feeder is greater than the width, this feeder does not provide an effective outlet and mass-flow is unlikely to develop. The outlet can be made effective by either tapering out the feeding area of the outlet or by feeding across the side of the rectangle. The latter arrangement, Fig. 75, has not been used so far - to the knowledge of the writer - probably because it is more expensive and its advantages

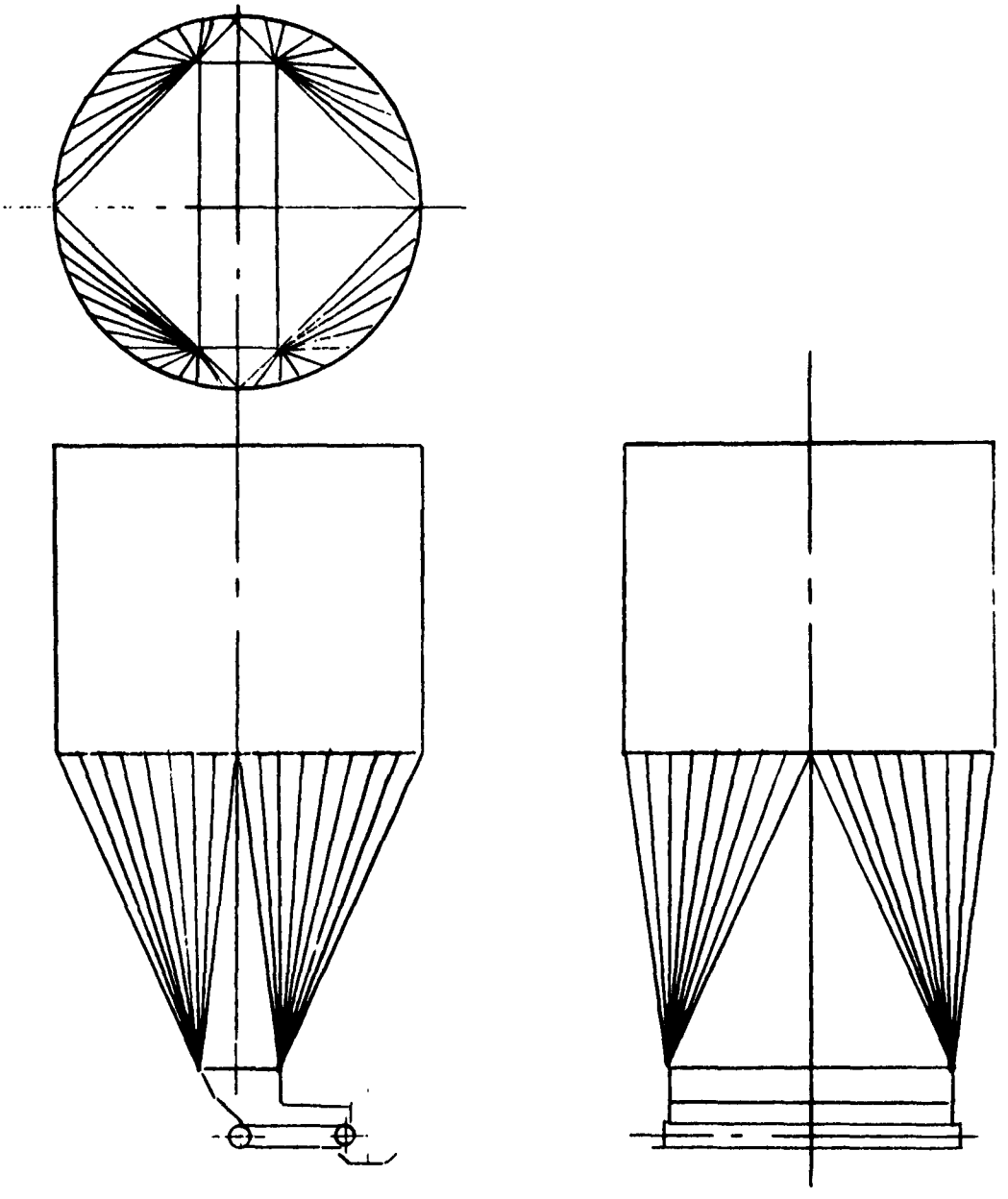

Fig. 75

Side discharge apron feeder

are not known to industry.

A side-wise reciprocating pan feeder is shown in Fig. 76. This feeder [39] seems to be particularly well suited to provide an active outlet for large size solids like mine-run and primary crusher ore. It differs from the orthodox reciprocating feeder in its direction of oscillation. The orthodox feeder oscillates length-wise with respect to the rectangular outlet and its stream does not increase in the direction of flow. The side-wise reciprocating feeder is capable of drawing along the full length of the outlet. If necessary, such feeders can be placed side by side to activate an outlet of any desired length. The feeders discharge onto a parallel belt conveyor as shown in the figure.

A star feeder, Fig. 77, provides positively uniform draw along the length of a slot-outlet. This feeder is particularly useful for solids which require but a narrow outlet, say, B = 4 to 8 inches, to assure flow, The feeder discharges into a chute or gathering conveyor as shown in the figure. The space between the feeder and the conveyor should never be full of solid.

A rotary table feeder, Fig. 78, has a tendency to feed above the plow with the rest of the solid sliding on the table. In order to make the outlet fully effective, it is necessary to provide a gap between the hopper outlet and the table, as shown in the figure. This permits the solid to flow out of the hopper along the whole circumference; the plow then need not enter the hopper. Outside skirt can

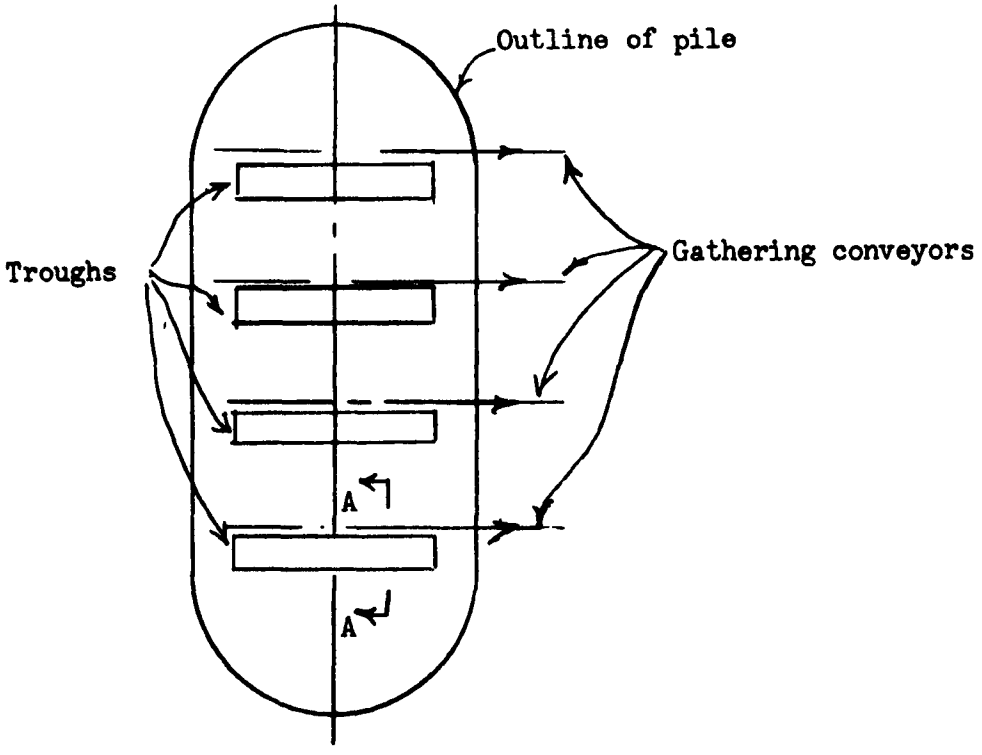

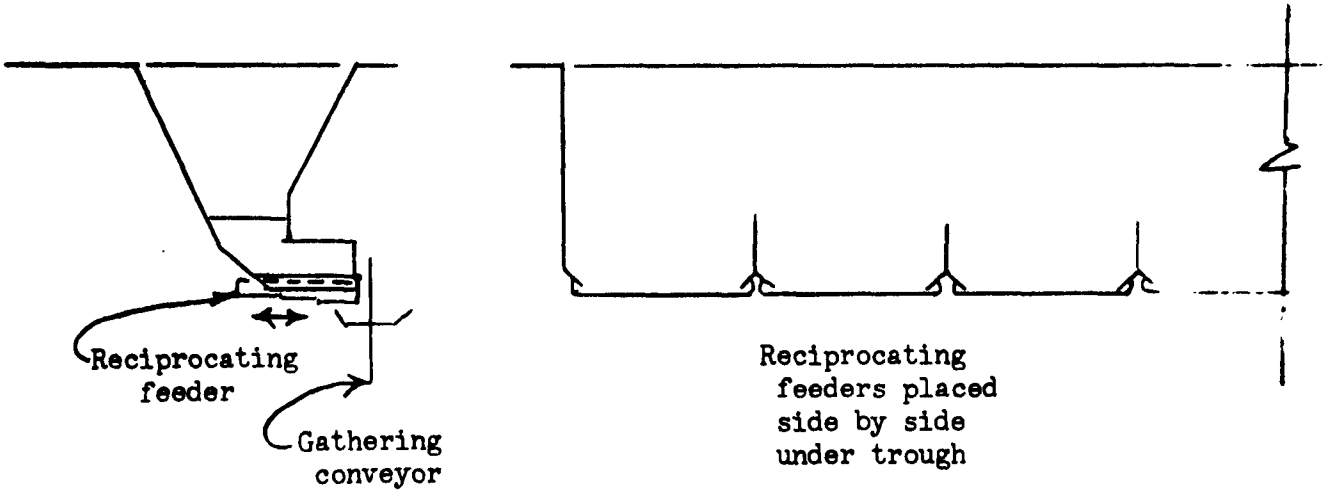

Section A - A

Fig. 76

Side-wise reciprocating feeder

be provided for sealing purposes. This feeder has much similarity to the raised hopper belt feeder.

An air-slide feeder is shown in Fig. 79. The air in introduced into the bottom chamber, flows through a porous diaphragm, aerates the solid above the diaphragm and conveys the solid out of the hopper into the air conveyor. The bottom chamber is divided into separate compartments of length equal to 2 to 3 times the width, and air in-flow into each compartment is controlled independently in order to assure that the feeder is effective along its full length.

An air-slide feeder is particularly well suited to operate with a slot-outlet air-hopper. In this combination, the solid flowing into the feeder is already aerated and it is not necessary to divide the bottom chamber.

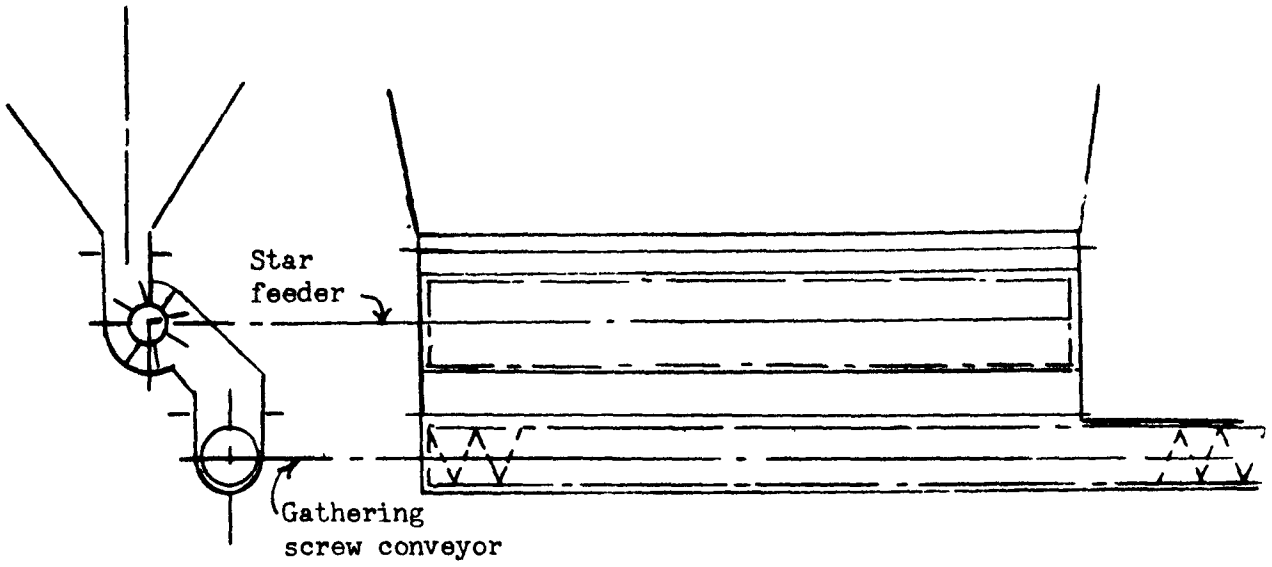

Fig. 77

Star feeder

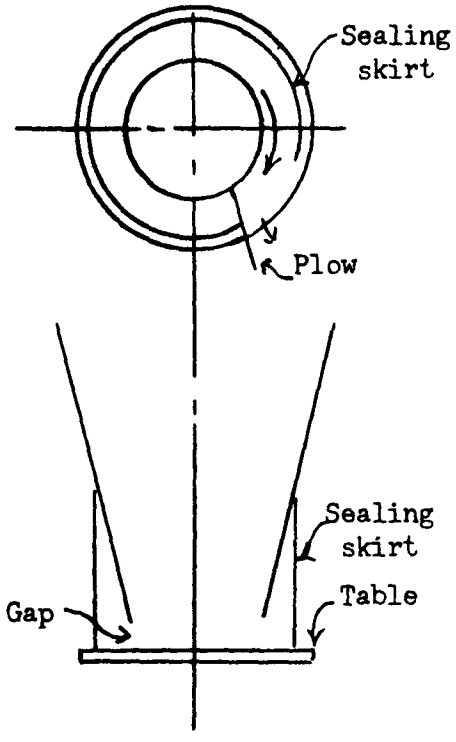

Fig. 78

Rotary table feeder

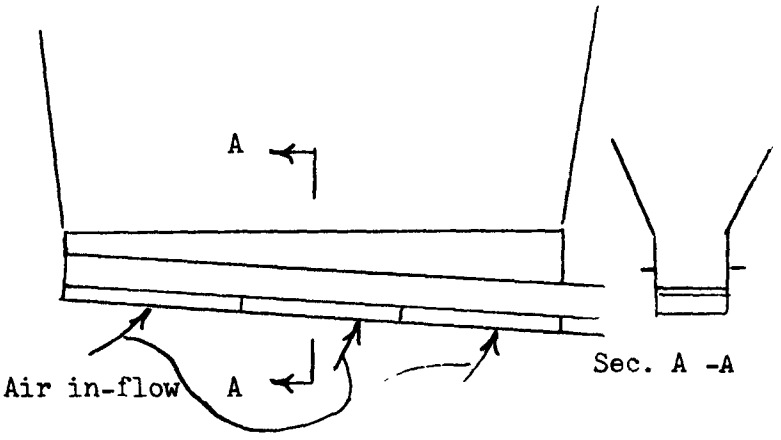

Fig. 79

Air-slide feeder

Summary of dischargers and feeders. The applicability of the above feeders is summarized in the following table:

Type of Discharger of Feeder		Shape of outlet			Maximum particle size		
		○	□	▭	< 1"	1" to 8"	> 8"
Vibrating hopper		x			x		
Air-hopper		x	x	x	x		
Screw feeder	Single screw	x	x	x	x	x[1]	
	Multiple screw	x	x	x	x	x[1]	
Belt feeder	Orthodox	x	x		x	x	
	Tapered outlet		x	x	x	x	
	Raised hopper	x	x	x	x		
Apron feeder	Length-wise		x	x[2]		x	x
	Side-wise			x		x	x
Reciprocating feeder	Length-wise		x	x[2]	x	x	x
	Side-wise			x	x	x	x
Star feeder		x	x	x	x		
Rotary table feeder		x			x	x	
Air-slide feeder			x	x	x		

Notes: [1] Largest particle size must be less than the smallest pitch.

[2] Not effective for L > B unless outlet is tapered.

Feeder loads. The ideal vertical force Q which a flowing solid exerts on a feeder can be computed from the formula

$$Q = q\gamma B^3, \tag{26}$$

for circular outlets; and

$$Q = q\gamma LB^2, \tag{27}$$

for rectangular outlets. Both these formulas are derived from Eq. (A-53).

Contours of the parameter q are plotted in Figures 80 to 85 for conical and plane mass-flow hoppers, for $\delta = 30°$, $40°$ and $50°$. For solids of δ larger than $50°$, the $\delta = 50°$ charts can be used. For oblong outlets, the plane flow formula gives conservative results.

As an example: assume a hopper with conical walls inclined at an angle $\theta' = 12°$, angles $\phi' = 28°$, $\delta = 44°$, $\gamma = 80$ pcf, and an outlet of diameter B = 1.5 feet. It is safe to use the chart for the lower value of $\delta = 40°$, Fig. 81; the point $(12°,28°)$ specifies $q = 0.20$, and Eq. (26) yields $Q = 0.20 \times 80 \times 1.5^3 = 54$ lb.

And another example: a hopper with a rectangular outlet 1 ft x 3 ft., side hopper slopes $\theta' = 25°$, angles $\phi' = 30°$, $\delta = 60°$, and $\gamma = 110$ pcf. From Fig. 85, $q = 0.35$ and from Eq. (27) $Q = 0.35 \times 110 \times 3 \times 1^2 = 116$ lb.

One conclusion is apparent: these ideal forces are small. They have been computed on the assumption that the feeder is perfectly efficient, and that no sliding of packed solid occurs. These forces do not allow for the weight of the solid which would collect in the

pockets outside the hopper (see Fig. 74), for the confining pressures from skirts, and for starting loads.

The starting loads in particular may be several times (a factor of ten has been measured [50] as much as the running loads. The reasons are as follows: the low pressure which a solid exerts on a feeder during flow is due to the arching stress pattern which develops within the flowing solid and which causes most of its weight to be transferred directly to the hopper walls. This occurs whenever the feeder is in motion and the solid is flowing. When a solid - especially a coarse solid - is charged into an empty bin, while the feeder is at rest, the impact of the falling stream produces pressures which may be many times those which obtain during flow. This situation is often aggravated by the fact that, as the solid is charged into a bin, its total weight increases, and the bin structure deflects. If the feeder supports are rigid and the feeder does not deflect in unison with the bin, the feeder may take up a considerable part of the weight of the bin and of the stored solid. Of course, as soon as the feeder has started and flow in the bin has developed, the vertical force drops, but the initial force on the feeder may be very large.

The peak loads are particularly detrimental to belt feeders which rely on pre-tension for traction. In order to assure traction during the peak loads, the pre-tension must be high - much higher than is required during normal flow. This high tension contributes to the loss of horsepower and to the wear of the feeder.

These starting peaks can be eliminated by running the feeder, however slowly, whenever the bin is being filled or, more positively,

by providing flexible support to the feeder, for instance, a spring support. Feeders or dischargers, which are suspended from the hopper, lend themselves particularly well to such relief because springs can be incorporated in the supporting rods. The reciprocating feeder and the vibrating hopper provide examples. In floor-supported feeders, it may be necessary to build springs into the support of the feeder. The springs should be so designed that they do not deflect until a load 2Q has been reached. A total spring constant of 1/4 inch deflection per load Q will be found satisfactory.

Laboratory tests [50] have shown that a very small deflection: in the range of a few hundredths of an inch is sufficient to relieve the peak loads.

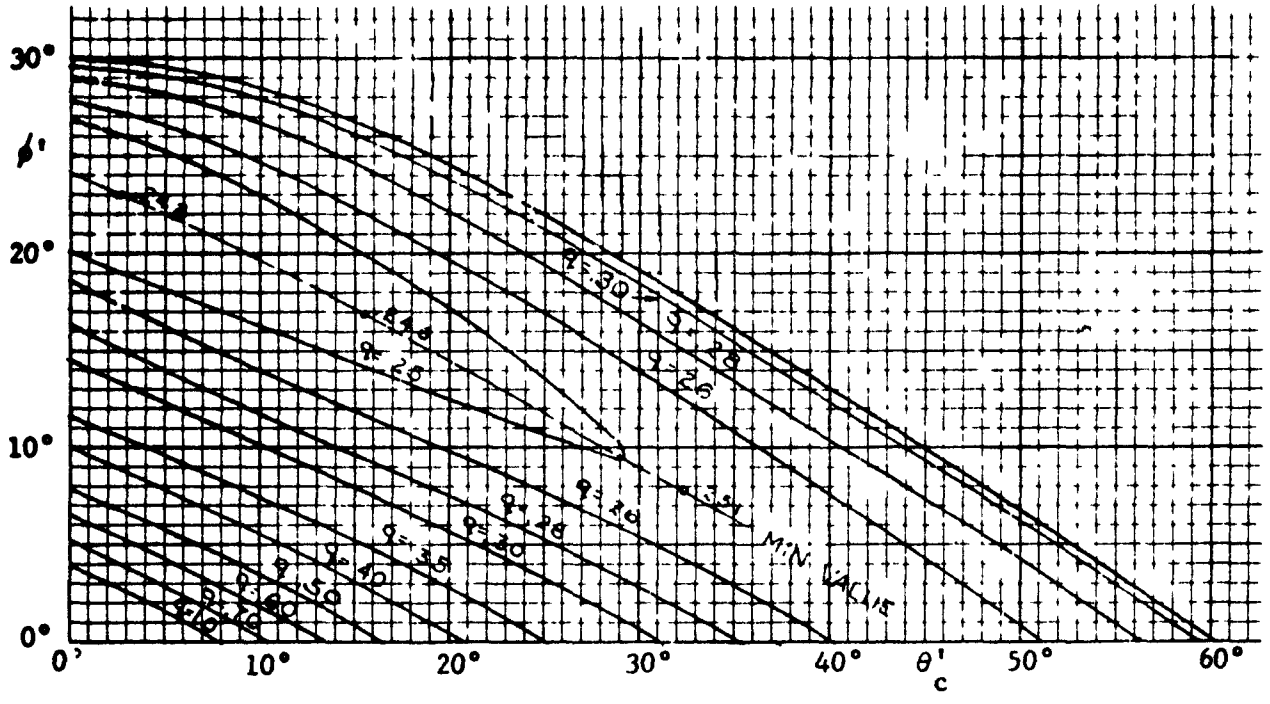

Fig. 80

q contours for conical channels, $\delta = 30°$

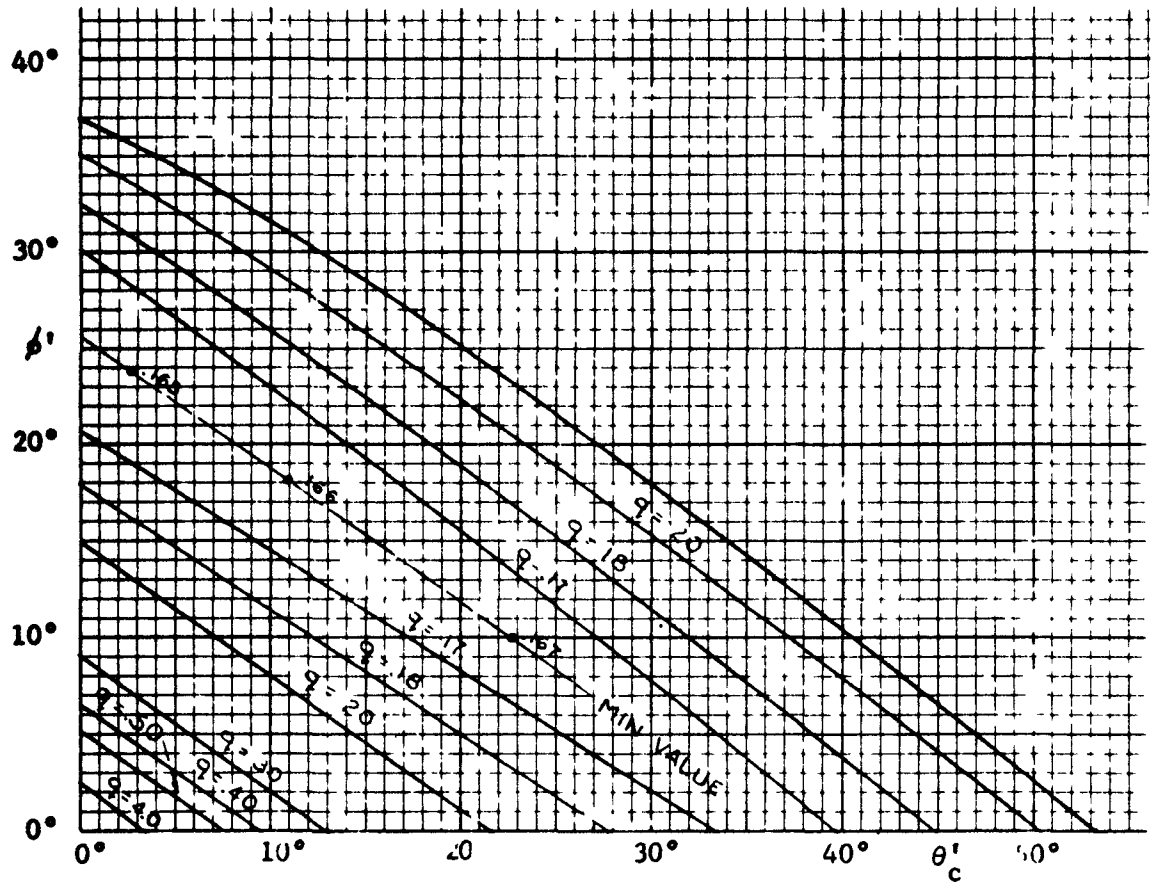

Fig. 81

q contours for conical channels, $\delta = 40°$

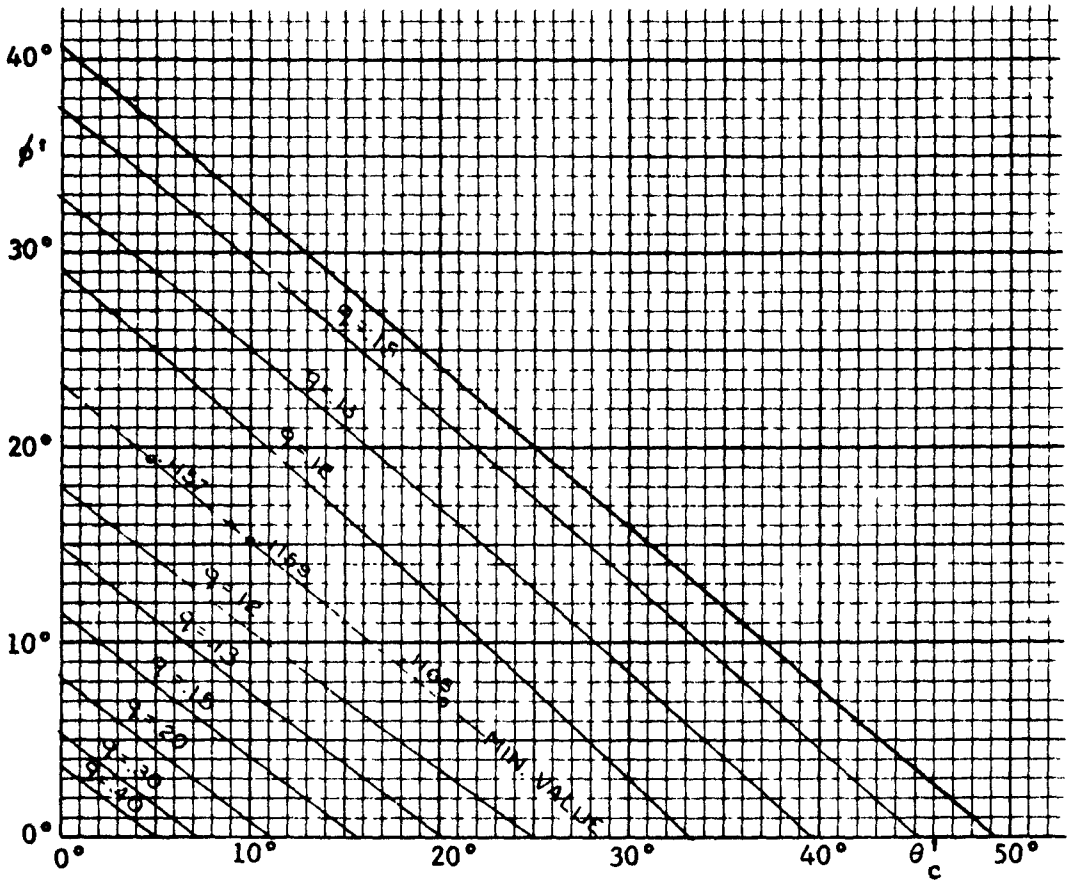

Fig. 82

q contours for conical channels, $\delta = 50°$

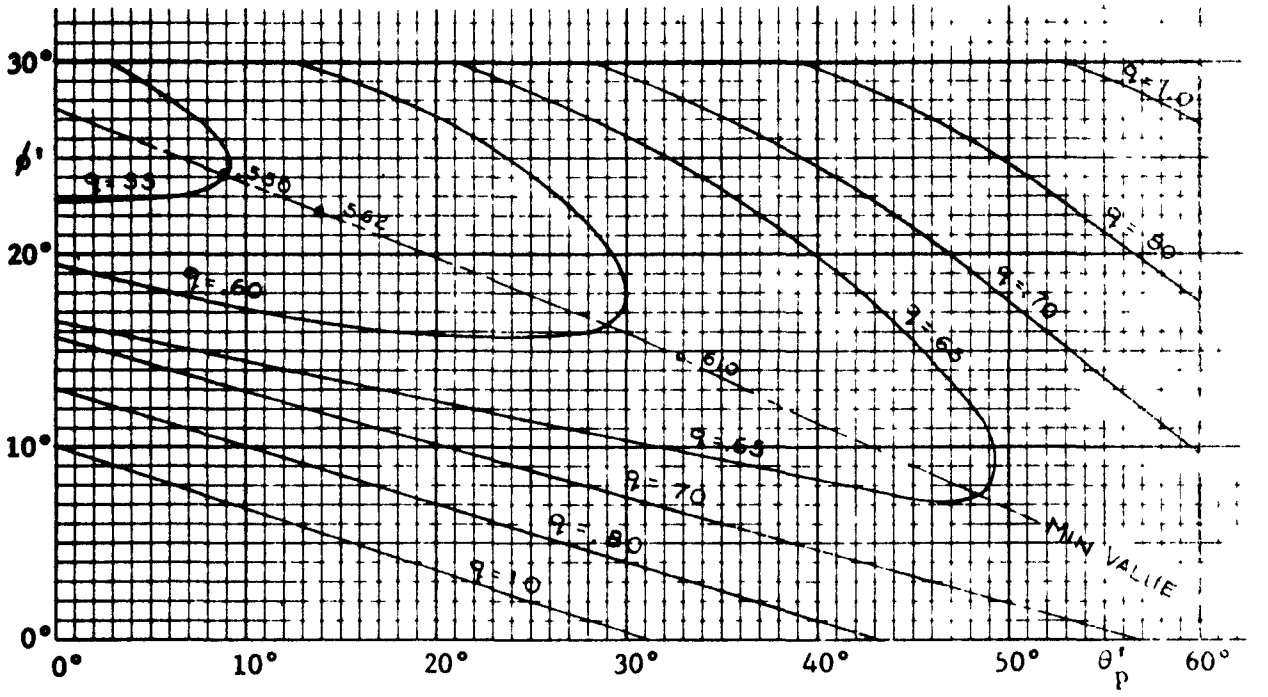

Fig. 83

q contours for symmetric plane-flow channels, $\delta = 30°$

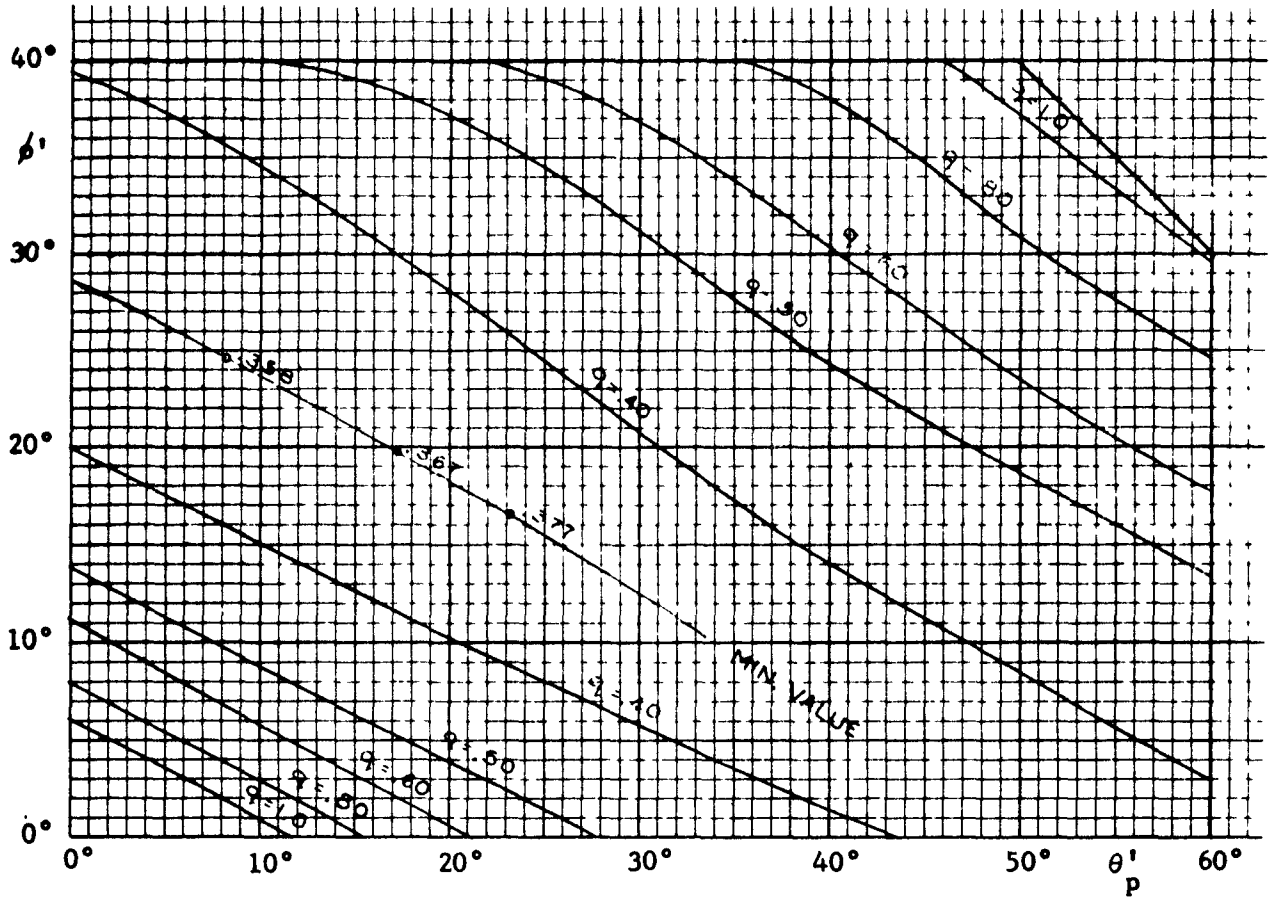

Fig. 84

q contours for symmetric plane-flow channels, $\delta = 40°$

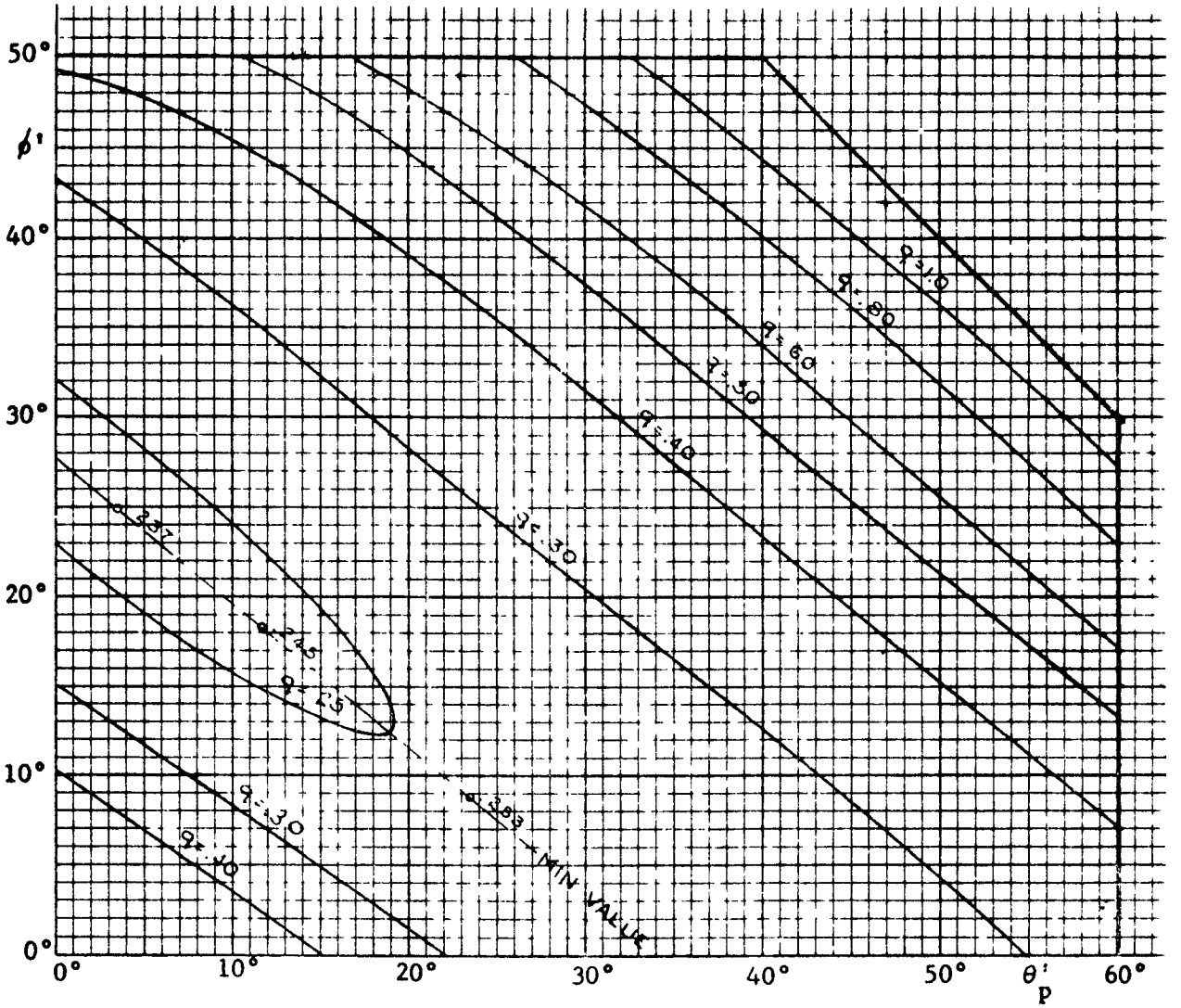

Fig. 85

q contours for symmetric plane-flow channels, $\delta = 50°$

Promotion of flow

Impact pressures. The pressures which consolidate a solid as it flows in a hopper are roughtly proportional to the width of the hopper and are practically independent of the head of the solid in the bin. That means that the consolidating pressures in the region of the outlet of a hopper are quite low during flow.

On the other hand, when a solid is charged into a bin, the pressures at the point of impact increase with the height of fall, and in a tall bin may be much higher than the consolidating pressures of flow. The impact pressures may be sufficient to cause doming. This condition is common in the storage of solids which contain both coarse and fine particles, because the large particles produce high impact pressure while the fines develop the strength to sustain the dome.

When a solid is carried into a bin by a high-velocity air stream, there is also the likelihood of high impact pressure with possible doming.

Impact pressures can usually be kept below a dangerous level by: (a) Maintaining a minimum level of solid in the hopper, so that the sensitive part of the hopper is not exposed to impact. (b) Increasing the impact area. A baffle or impact breaker placed in the stream spreads the particles over a large area of the bin. (c) Directing the stream at the wall of the hopper and not at the hopper outlet. (d) Expanding the air stream of an air conveyor to reduce its velocity prior to discharge into the bin.

Circulation. There are many solids which flow as long as the particles are in relative motion with respect to each other but cake when left in storage at rest. Some freshly produced solids behave like this for a period of hours until the surface conditions of the particles have reached equilibrium.

In those cases, circulation of the solid around the bin can be considered. Circulation causes the particles to move with respect to one another and break up the bonds before they can gain full strength. Evidently, circulation is effective only in mass-flow bins. There is usually no need to keep the solid in motion all the time; 10 seconds of flow every, say, 30 minutes may be sufficient.

Solids conditioning. Good mass-flow hoppers have a flow-factor of 1.1 to 1.6 and can accommodate a vast majority of the solids handled by industry. However, there are solids whose instantaneous flow-functions are high and which require impractically large outlets for gravity flow. The choice then lies only between a non-gravity form of recovery from storage, and solids conditioning.

Solids conditioning means changing some property of a solid in order to improve its flowability.

It is, of course, much easier to specify the proper conditions of a solid during the design stage and to design the process accordingly, than it is to alter the conditions in a completed plant. Flowability tests carried out at the design stage will point out such factors as the maximum acceptable moisture content and, hence, the required filter or dryer capacity; the permissible range of temperatures and, hence, the needed cooling capacity; the preferred crystalline structure of the

solid; the need to screen out the coarse particles from the fines.

The two most important parameters are moisture content and temperature. As the moisture content of a solid is increased, its flowability decreases reaching a minimum at 85 to 95 percent of saturation. If a saturated solid is stored in a bin for any length of time, water drains out, and the solid tends to reach the moisture content of minimum flowability. It is always desirable to store solids at a moisture below 85 percent of saturation. If a solid is allowed to lose moisture through evaporation, while in storage at rest, the particles may become cemented by the salts precipitated out of solution, causing a marked decrease in flowability.

Temperature has a significant effect on the flowability of many solids. As temperature increases, the particles tend to develop greater adhesion and the solid becomes less free-flowing. Some solids will flow at a certain temperature, provided it is kept constant, but gain strength and lose flowability if the temperature is allowed to drop during storage at rest.

Flow promoting devices. For mass-flow bins, the recommended device is an externally mounted vibrator to start flow after consolidation at rest. However, the safety margin prescribed by Eq. (24) should be satisfied. It is sound practice to have mounting pads for vibrators on all hoppers likely to carry solids which cake during consolidation at rest. It is then easy to mount vibrators, should that become necessary. In a mass-flow bin the energy from a vibrator is applied right at the abutments of the doming solid and, therefore,

the vibrator is very effective.

In funnel-flow bins designed for no piping, devices are used for the final clearance of the solid from the hopper, Fig. 32(a). Either vibrators or air panels can be used. A simple air panel can be formed from filter cloth attached to the hopper walls with air inlets spaced under the cloth.

There is, of course, a large number of other flow-promoting devices such as: inflatable panels, internal vibrating panels and frames, arch breakers, flexible rubber cones, etc. These devices are not required in bins designed for flow, though they find numerous applications in existing installations which were not so designed.

When an existing bin does not perform adequately, the operating engineer often finds it easier to add a flow-promoting device - sometimes several of them - than to replace the existing hopper with a new one. The new hopper, as likely as not, would have to be of the mass-flow type and would provide less theoretical capacity. This is looked upon as wasteful of plant space. However, an analysis of the gains in product uniformity, quality, reliability, savings in maintenance, and total availability of the stored solid will usually show that a hopper redesign provides the more economical and certain solution.

Small hoppers. In small hoppers, used to feed small quantities of reagents and additives, the feeders have to be small and it is often not practical to use gravity alone to cause flow into and through a feeder. Here, dischargers and flow-promoting devices are indeed most

useful. Vibration of the whole hopper assembly, tilting hoppers, vibrating panels, aeration are used to fluidize the solid and cause it to flow.

Segregation and blending

During the storage and handling operations, a bulk solid tends to segregate (separate) according to the particle size, shape and density. Since segregation is usually detrimental in the processing and merchandising of a solid, the conditions leading to segregation, means of minimizing segregation, and methods of remixing during flow will now be discussed.

Most of the segregation takes place in the following two situations: (1) In a freely falling stream which has a horizontal component of velocity. In free fall, each particle is acted upon by two forces: its weight, and air resistance to motion. The former is equal to the product of the volume and density of the particle, and acts vertically down; the latter is a function of the size and shape of the particle and of its velocity, and acts in the direction opposite to the velocity. In vertical free fall, both these forces are vertical and, while the terminal velocities of the various particles may vary, their trajectories do not, hence there is no significant segregation. When a solid is discharged over a conveyor pulley or spouted through an inclined chute, an initial horizontal component of velocity is introduced, the two forces are not aligned any longer and, as their ratios differ for the various particles, so do the trajectories of the particles, which then segregate.

(2) When a stream hits a sloping surface. Whenever a stream hits a sloping surface, the particles roll down the slope: the large, heavy, and more nearly spherical particles tend to roll farther than the fine, light, and flaky particles which tend to remain at the point of impact of the stream. As a pile of the solid builds up, the fines congregate in a column which has the shape of the trajectory; the size of the particles gradually increases with the distance from the column toward the periphery of the pile or the walls of the container. If the outlet of a pile or of a plug-flow bin is located directly beneath the trajectory, the draw will be heavily segregated: an excess of fines will be drawn every time the feeder is started after charging the solid while the feeder was at rest. When the container has several outlets, the outlet located under the trajectory will consistently draw an excess of fines. This phenomenon can be exploited when some size separation is desired, otherwise the outlets should be located away from the trajectory.

The aforesaid indicates that segregation is a dynamic effect and occurs inevitably when the solid is in free fall. It also indicates methods of minimizing segregation, which are: reducing the velocity of the particles by shortening the height of free fall, reducing the horizontal component of velocity, and limiting the area of the slopes over which the particles roll. The last method calls either for narrow bins or for means to spread the stream over the top surface of the container. Spreading can be accomplished either by placing a shelf in the stream or by moving the point of discharge. A combination of the two can be very effective in minimizing segregation.

When segregation in storage is to be avoided, a mass-flow bin with a high vertical portion should be used, Fig. 86, and the range of operation should be as shown in the figure. This causes the solid to flow like a rigid plug in the vertical portion of the bin. A first-in, first-out flow pattern is enforced and, while the solid segregates in charging, it automatically remixes within the hopper.

In slot-outlet bins charged by means of a tripper-conveyor, segregation is much smaller if the slots are perpendicular to the conveyor, Fig. 87(a), than if they are parallel, (b), because in the former case the slot draws a cross-section of the segregated solid which is remixed in the feeder.

In a multiple-outlet bin, segregation is reduced by drawing simultaneously through all the outlets and blending the draw.

A series of bins can be used to even out the grade of a run-of-mine ore, Fig. 88, by charging the bins in sequence and drawing them simultaneously.

A bin can be used for the blending of a solid by recirculating the solid in a closed circuit about the bin, Fig. 89, provided the following conditions are satisfied: (a) The solid is non-segregating, e.g. it is composed of uniform size, shape and density particles, or of very small size particles; (b) a mass flow bin is used, so that there are no dead regions of the solid within the bin; (c) there is a substantial velocity gradient in every horizontal cross-section of the channel, so that first-in, first-out flow does <u>not</u> occur.

The points (b) and (c) imply a steep, smooth bin with a short vertical portion, whose height does not exceed one-half the diameter

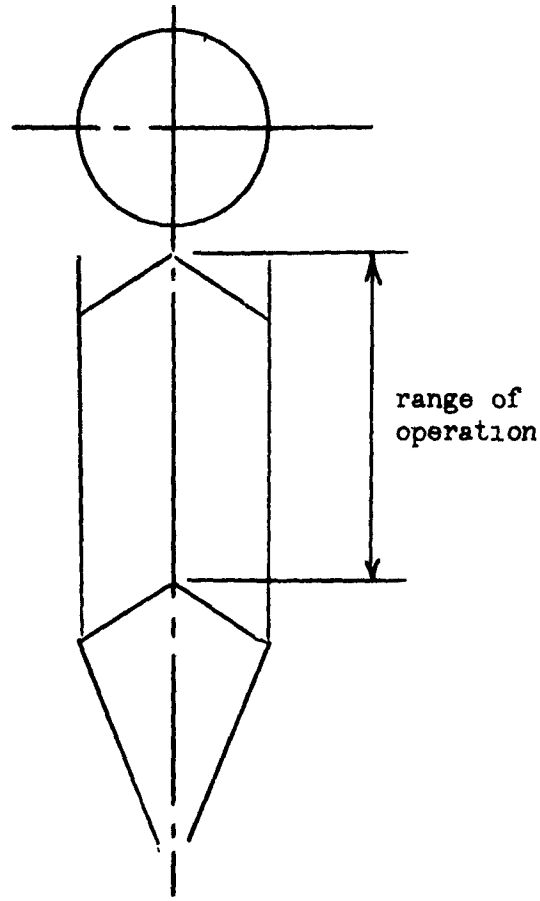

Fig. 86

Non-segregating bin

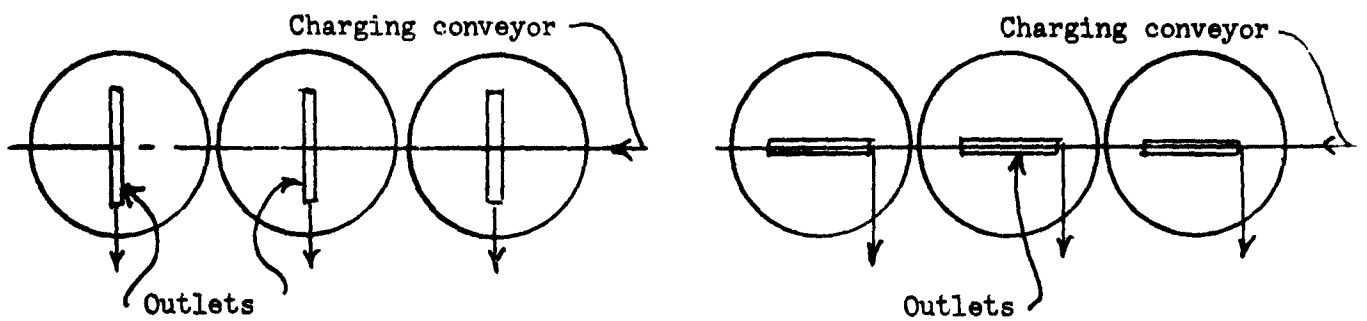

(a) Perpendicular layout

(b) Parallel layout

Fig. 87

Layout of slot-outlet bins

of the cylinder or no vertical portion at all. A higher vertical portion would induce first-in, first-out flow, like the non-segregating bin. An insufficiently steep hopper would cause dead-regions to develop at the transition.

Flooding

Fine solids which aerate readily should be stored in mass-flow bins in order to prevent flooding. In a funnel-flow bin, flow is non-steady, momentary voids form within the flow channel. As the domes over the void fail, the solid falls, and aerates. Unless the feeder is completely air-tight, flooding occurs.

Gas counterflow

A contact bed is assumed. In channels which serve as chemical reactors, the solid flows down by gravity, while a gas flows upward under the action of a gas pressure gradient. This gradient opposes the forces of gravity and buoys the solid. In a converging channel, the gas pressure gradient is greatest in the narrowest part of the channel, i.e. at the outlet. The maximum pressure gradient which can be applied without disturbing the gravity flow of the solid is about 70% of the bulk weight of the solid, γ.

It is important that the gas pressure at the outlet be maintained at a uniform level without sudden changes, either up or down. When the process is steady, the consolidating pressures in the solid are reduced by the gas pressure gradient in the same ratio as the pressures of failure, and gravity flow is not affected. If gas pressure fluctuates, the solid may consolidate under the pressures of gravity unrelieved by

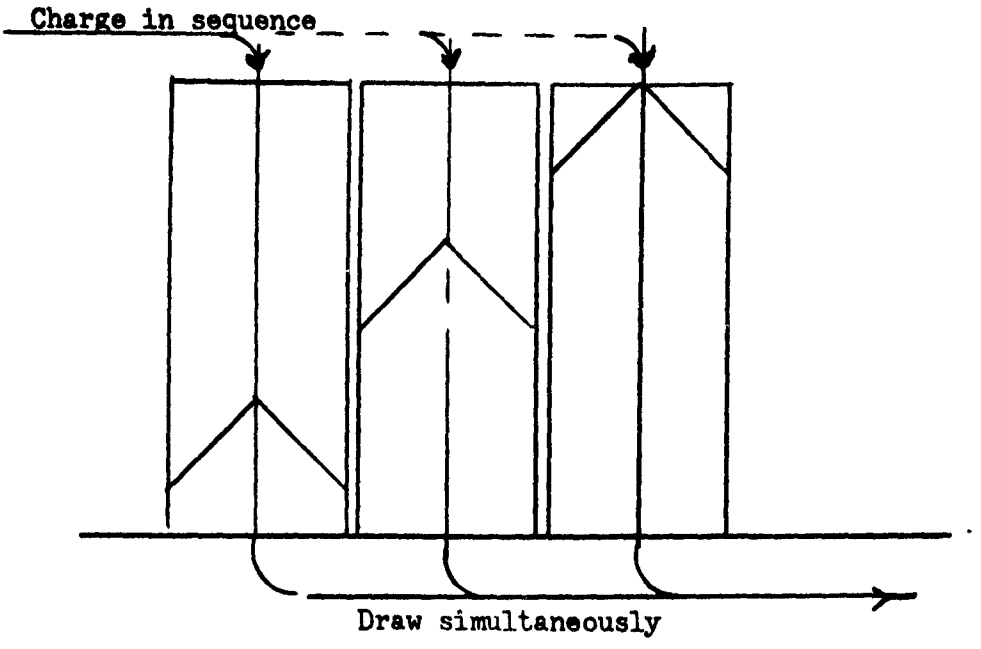

Fig. 88

Blending of mine-run ores in bins

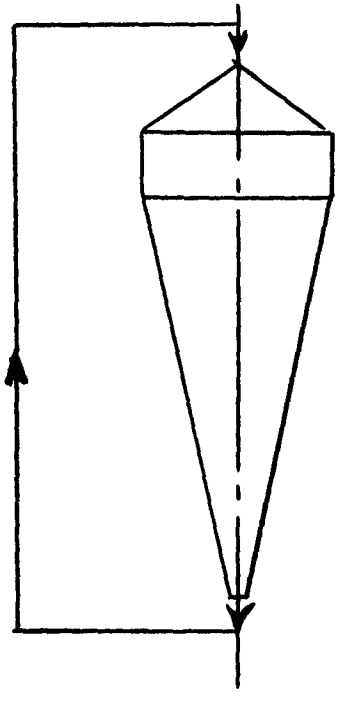

Fig. 89

Blending by recirculation

the gas pressure gradient, and dome when the pressures of failure are decreased as the gas gradient becomes high. If the process is intermittent, then, during the stoppages of flow of the gas, the pressure gradient vanishes and the solid consolidates under the full pressures of gravity. If the gas gradient is then applied prior to the re-establishment of gravity flow, the gas gradient supports the solid, reduces the pressures of failure, and flow may not start. It is better to start gravity flow first, and then gradually apply the gas pressure.

Since the gravity flow of a solid in a vertical channel tends to be unsteady and erratic, narrow vertical channels should not be used as reactors. Vertical spouts connecting sections of a reactor, as shown in Fig. 90, should have by-pass pipes for the gas, otherwise doming in the spouts may occur.

Only mass-flow channels should be used in conjunction with gas counterflow. Funnel-flow channels lead to piping and uncontrolled flow.

Bin failures

Failures of bin structures can be divided into two categories. In the first category belong those failures which are due to recognized structural causes, such as: foundation failure, uneven settlement of footings of a multi-column bin, wind loads, earthquakes. In the second category are the failures caused by irregularities in the flow pattern of the stored solid. The latter are of particular interest in this work.

The most dangerous failures occur when a stored solid domes at or above the transition between the vertical portion of a bin and the

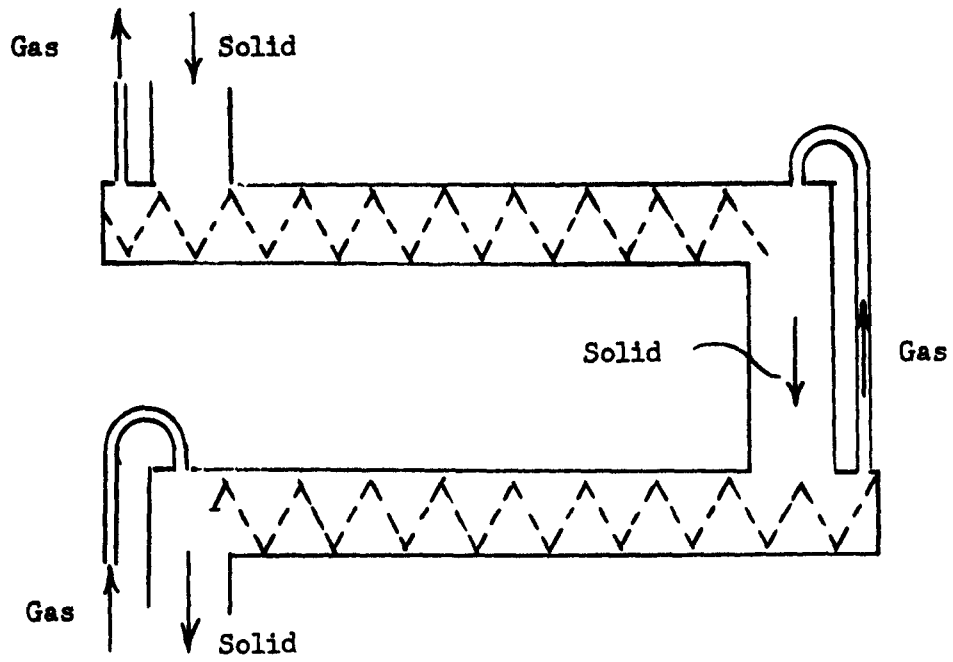

Fig. 90

Gas by-passes of spouts

hopper, while the hopper empties out. A large void then forms under the doming solid. If the whole mass happens to break away simultaneously, it acts like a piston, impacts the hopper, compresses the air in the hopper, and either splits the bin open or tears the hopper off its suspension. Solids whose time flow-functions approach a straight line, are most likely to dome at or above the transition. Bins for such solids (many agricultural products belong here) should be built with rounded, smooth transitions and with rough vertical walls to reduce the consolidation at the transition.

While a break-away of a large doming mass develops a high pressure in the hopper, it also develops a vacuum at the top of an enclosed bin and, unless the top is vented, the roof of the bin may be sucked in. A vent may be closed by a diaphragm to keep the dust in; the diaphragm being designed to fail if the pressure differential exceeds a safe value. Such vents are also recommended to safeguard against minor dust explosions [51].

Less dangerous failures occur typically in asymmetrically loaded bins of circular horizontal cross-section. In a circular cross-section, the hoop stresses are tensile and the walls require no bending reinforcement, provided the stresses acting on the walls from the solid are uniform all-around. This condition is satisfied if the solid is charged and drawn at the center of the bin. Therefore, the hopper, if any, must be circular and symmetric with respect to the vertical axis: only one outlet is permitted. If the hopper is offset to one side, Fig. 40, the pressures from the solid on the vertical side are decreased and the hoop stresses in the hopper may pull that side in. Bending reinforcement is

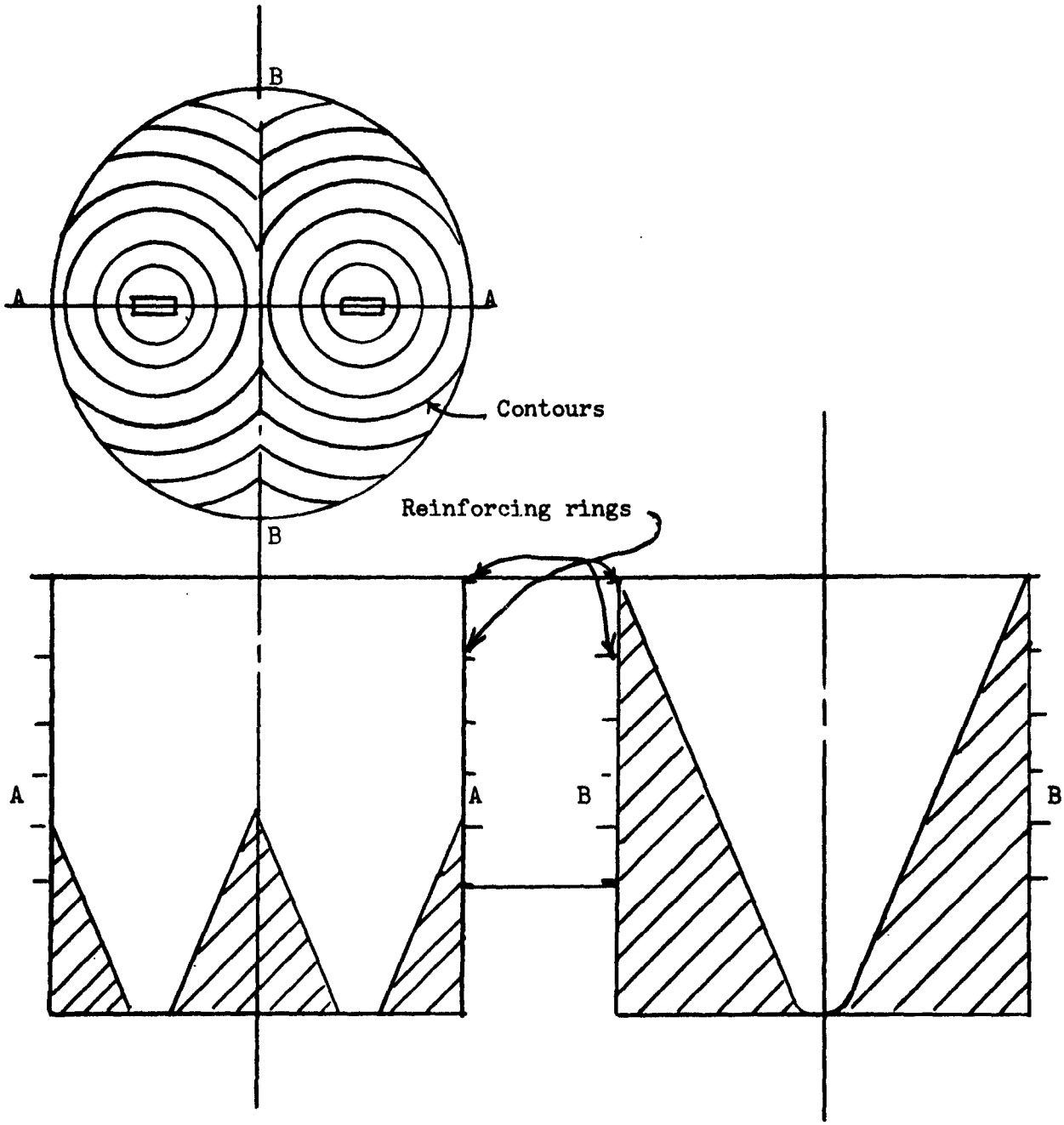

Fig. 91

Uneven draw in a cylindrical bin with

two outlets

required to retain the shape of this hopper.

In a cylindrical, flat-bottom bin with two (or more) outlets, Fig. 91, the solid empties out of two craters centered at the outlets and the pressures on the walls at points A fall to zero while, simultaneously, at B the solid presses against the walls. As a result, the walls at A are pulled in. To counteract this effect, the cylinder should be reinforced by rings between the A and B levels.

Ore storage

Coarse ore (-8 inch). Flat bottom storage, Fig. 31, is generally preferred for coarse ore because of the possibility of wedging of the solid in a steep hopper under the impact of the falling rock, and also because of the wear of hopper walls. However, if a layer of ore is always retained over the feeder to cushion the impact and reduce consolidation, a short mass-flow hopper can be used to advantage in expanding the channel beyond the dimension D required for no-piping. The design of such a hopper is described in Example 8. The layout shown in Fig. 76 is well suited for the storage of cohesive coarse ore, but this layout is expensive. It may be cheaper to screen out the -1 inch fraction. The coarse fraction then becomes free-flowing and will flow through outlets just sufficiently large to prevent interlocking, say, 30 x 30 inches, while the fine fraction can be handled as a fine ore.

Fine ore (-1 inch). Fine ore is usually stored as a mill feed, and size segregation has to be minimized. To achieve almost perfect non-segregation, the bin shown in Fig. 86 should be used. However, the layout of Fig. 87(a) is usually satisfactory provided the outlet is

fully effective. This can be accomplished quite economically by using raised-hopper feeders in troughed belts without skirts, Fig. 92.

Tests of fine ores frequently show that a width B of 6 to 12 inches is sufficient to assure flow. Slot lengths of 12 to 20 feet can then be used on belts 18 to 42 inches. The long slots can be broken at intervals by structural members tying the sides of the outlet.

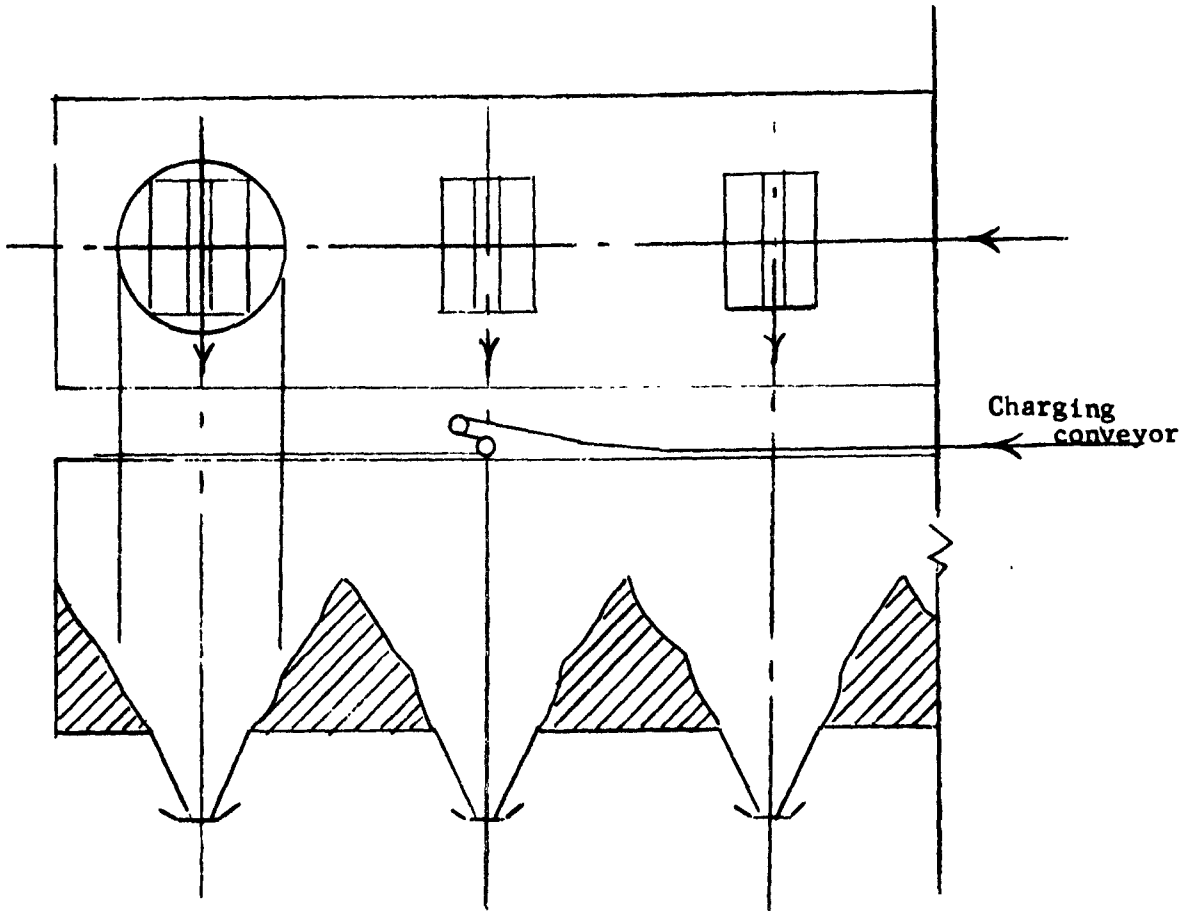

Fig. 92

Fine ore bin

Examples of design for flow

1. Provide storage capacity for a dry sand. The bin will be emptied out completely at regular intervals. The sand is free-flowing (FF and FF_t > 10) for F > 0. Segregation is not a problem because the range of particle size is narrow. The material of the hopper should be black steel. The angle of friction ϕ' = 30° to 32° on black steel.

The funnel-flow bin, Fig. 93, is selected with a hopper of slope θ' = 45°. A flatter hopper, say, θ' = 60° can be used with vibrators for final clearance. The outlet dimensions are not determined from this analysis; they should be sufficient to assure the required rate of discharge.

2. Design a square storage bin for a granulated solid. The bin is charged at intervals during five days of the week and drawn continuously 24 hours a day, 7 days a week. The solid contains about 3% dust, which should not be allowed to segregate out. The granulated solid is free-flowing for F > 0, but the dust is not. The angle of friction ϕ' = 20° on epoxy-coated steel. The effective angle of friction δ is between 40° and 50°.

The mass-flow bin, Fig. 94, is selected. Mass-flow is required to minimize segregation. The valley slope angle is determined from Figures 46 and 47 at 23°, which gives a wall slope angle

$$\tan \theta' = \frac{\tan 23°}{\sqrt{2}}, \text{ or } \theta' = 17°$$

As in Example 1, the outlet dimensions are determined by the required rate of discharge.

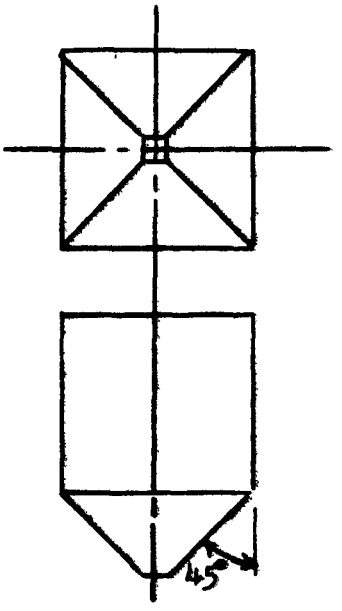

Fig. 93

Funnel-flow bin for dry sand

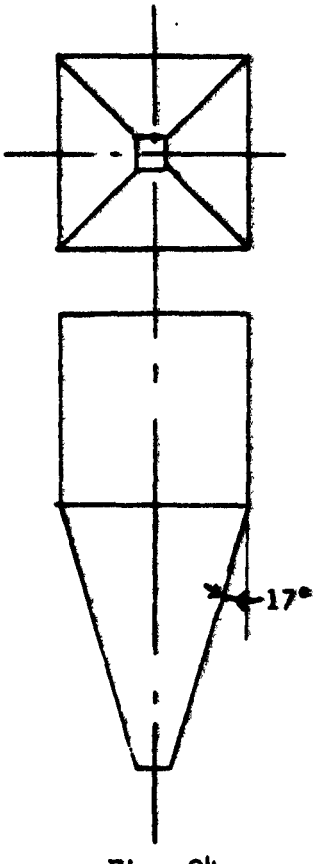

Fig. 94

Mass-flow bin for a free-flowing granulated solid for continuous draw

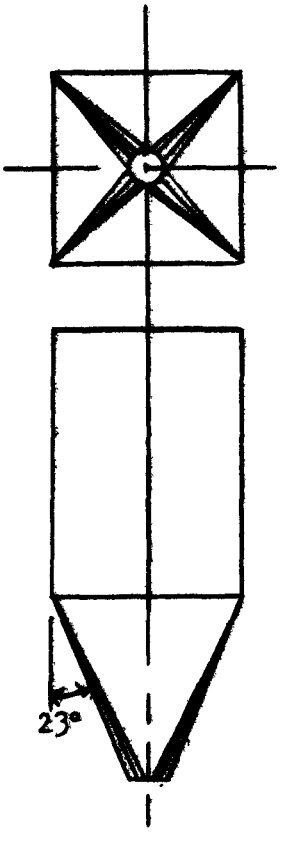

Fig. 95

Mass-flow bin for a free-flowing granulated solid for continuous charge and a 5-day a week draw

3. Design a square bin for the granulated solid of Example 2 to supply a bagging machine. The bin will be charged continuously and drawn only during the day shift, five days a week.

As the solid is charged during the weekend without being drawn out, some dust will percolate through the granules to fill the voids in the region of the hopper, and the solid may cease to be free-flowing. If the hopper is made of steel, the type shown in Fig. 94 can be used with vibrators mounted on the hopper to initiate flow on Monday morning. If the hopper is made of concrete, it should be built without valleys in order to have an adequately low flow-factor. A square-to-round transition is recommended as shown in Fig. 95. The flow-factor of this transition hopper in its lower region is likely to be equivalent to that of a conical hopper. Hence, the slope angle of the hopper walls needs to be $\theta' = 23°$.

If headroom is at a premium, a discharger can be used, as shown in Fig. 68. The rate of flow out of the discharger should not exceed the demand of the bagging machine by too large a margin as this may cause disintegration of the granules.

4. Design a mass-flow bin for the solid whose δ, FF, FF_t and WYL on the selected wall material are given in Fig. 96. The bulk density $\gamma = 50$ pcf.

There are several possibilities:

(a) Unassisted gravity flow. This requires that the hopper outlet be designed for the point of intersection of FF_t with the hopper flow-factor. Assume ff = 1.3 as shown in Fig. 96. At the point of intersection, $V_1 = 4.7$, and for this value $\delta = 50°$. The

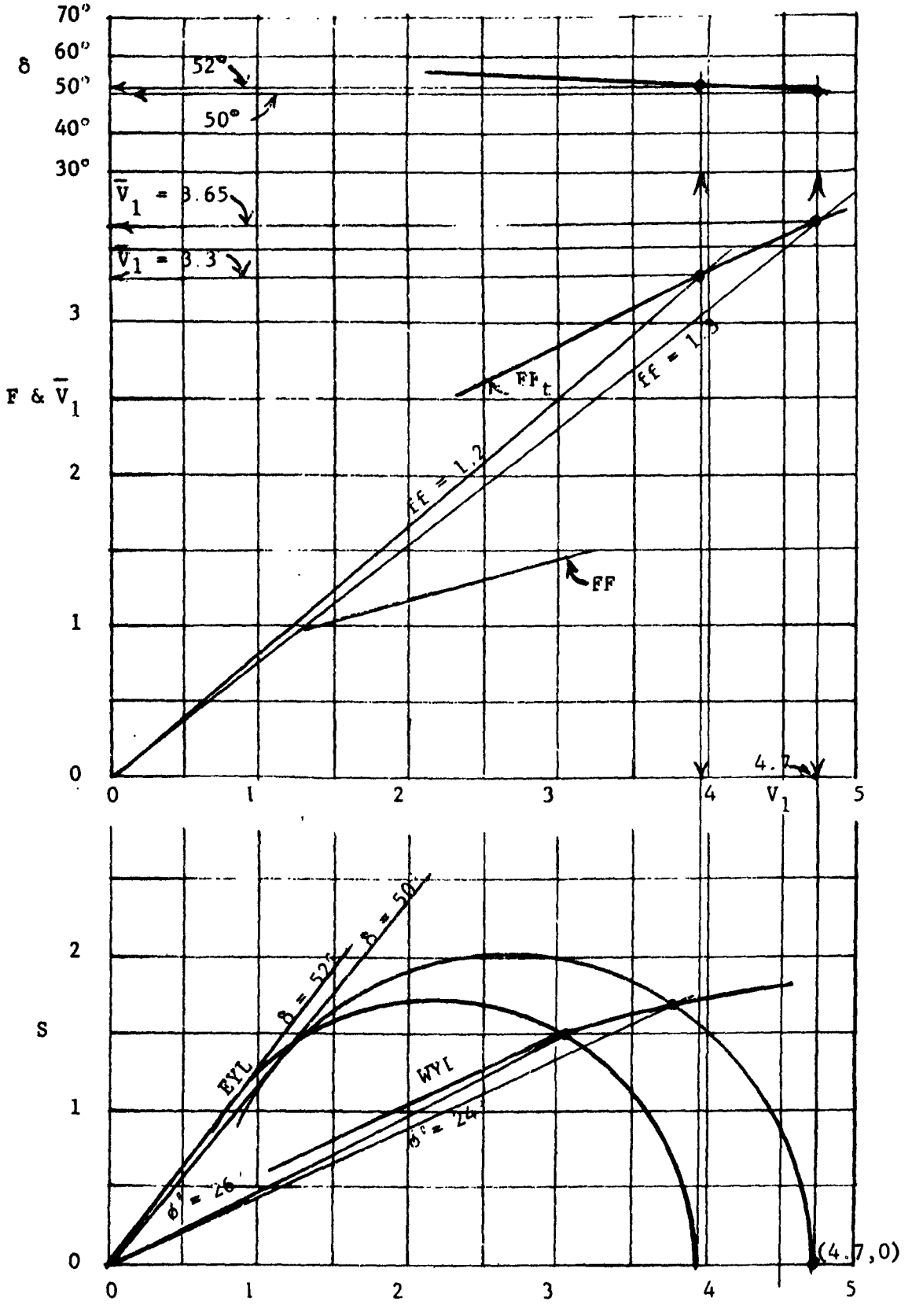

Fig 96

Flow properties, Example 4(a)

corresponding EYL is drawn over the WYL and a Mohr semi-circle is drawn through point (4.7,0) tangentially to the EYL. $\phi' = 24°$ is now found as the angle between axis V and the line connecting the origin with the appropriate point of intersection between the semi-circle and the WYL, as shown in the figure.

For these values of δ and ϕ', the largest acceptable values of θ' are selected from Figures 47 and 52, for conical and plane-flow channels, respectively. The corresponding values of ff are also read from these figures. $H(\theta')$ is obtained from Fig. 43, and B is computed from Eq. (23). The values are tabulated:

Channel	δ	ϕ'	$\bar{V}_1$	θ'	ff	$H(\theta')$	B
Conical	50°	24°	3.65	17°	1.28	2.27	2.16
Plane-flow				28°	1.20		

For conical flow, the obtained ff-value of 1.28 is slightly on the safe side from the assumed 1.3 and no further analysis is necessary. For plane flow, ff = 1.2 differs by a larger margin and a new trial is made: ff = 1.2 is drawn in Fig. 96, a new point of intersection is found, and the corresponding values of δ and ϕ' are again obtained. The corresponding value of ff is interpolated between ff = 1.19 for $\delta = 50°$, Fig. 52, and ff = 1.09 for $\delta = 60°$, Fig. 53. These values as well as $H(\theta')$ are tabulated. B is computed and also tabulated:

Channel	δ	ϕ'	$\bar{V}_1$	θ'	ff	$H(\theta')$	B
Plane-flow	52°	26°	3.3	25°	1.17	1.13	.97

For the plane-flow outlet, the length L should be at least 3 feet. In a transition hopper, the end slopes are selected at $\theta'_c = 17°$.

Possible bins are shown in Fig. 37. The diameter, or width, and height of the bins are determined from the required capacity.

(b) A vibrator is to be used to start flow after consolidation at rest. δ, FF, FF_t, WYL, and ff = 1.2 are redrawn in Fig. 97. In accordance with Eq. (24), a value $V_1 = 2.25$ is selected for which $\overline{V}_1 = 1.9 \simeq 1.5F$, where F = 1.25. Proceeding as before, δ and ϕ' are obtained, and θ' and ff are interpolated for $\delta = 55°$ between Figures 47 and 48 for the conical hopper, and between Figures 52 and 53 for the plane-flow hopper. The following table shows the results.

Channel	δ	ϕ'	$\overline{V}_1$	θ'	ff	H(θ')	B
Conical	55°	28°	1.9	12°	1.21	2.20	1.09
Plane-flow				23°	1.14	1.12	.55

In view of the safety factor in Eq. (24), there is no point in refining this analysis further. The possible bins are the same as computed at (a), except for smaller outlets.

It should be noted that, as the outlet dimensions are reduced, the analysis calls for a steeper hopper. This is due to the convex-upward shape of the WYL and hence an increasing angle of friction ϕ' as the forces $\overline{V}_1$ and V_1 decrease. When ϕ' is constant, the slope angle θ' is independent of pressure and, therefore, of the width of the hopper. In the example, the optimum hopper would have a slope angle θ' increasing upward from the outlet as shown in Fig. 98(a). While such a hopper is, generally, impractical, a hopper made up of

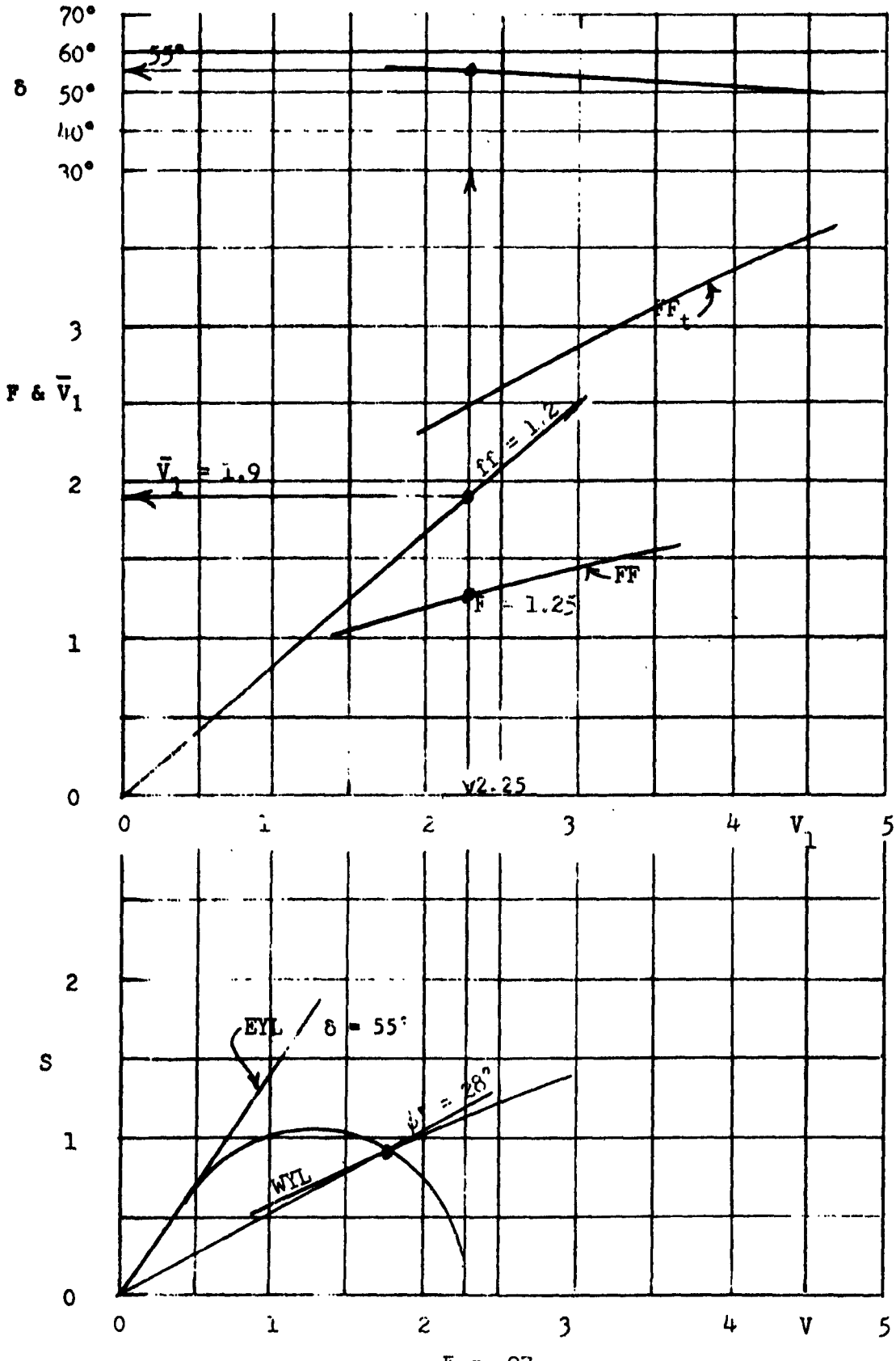

Fig. 97

Flow properties. Example 4(b)

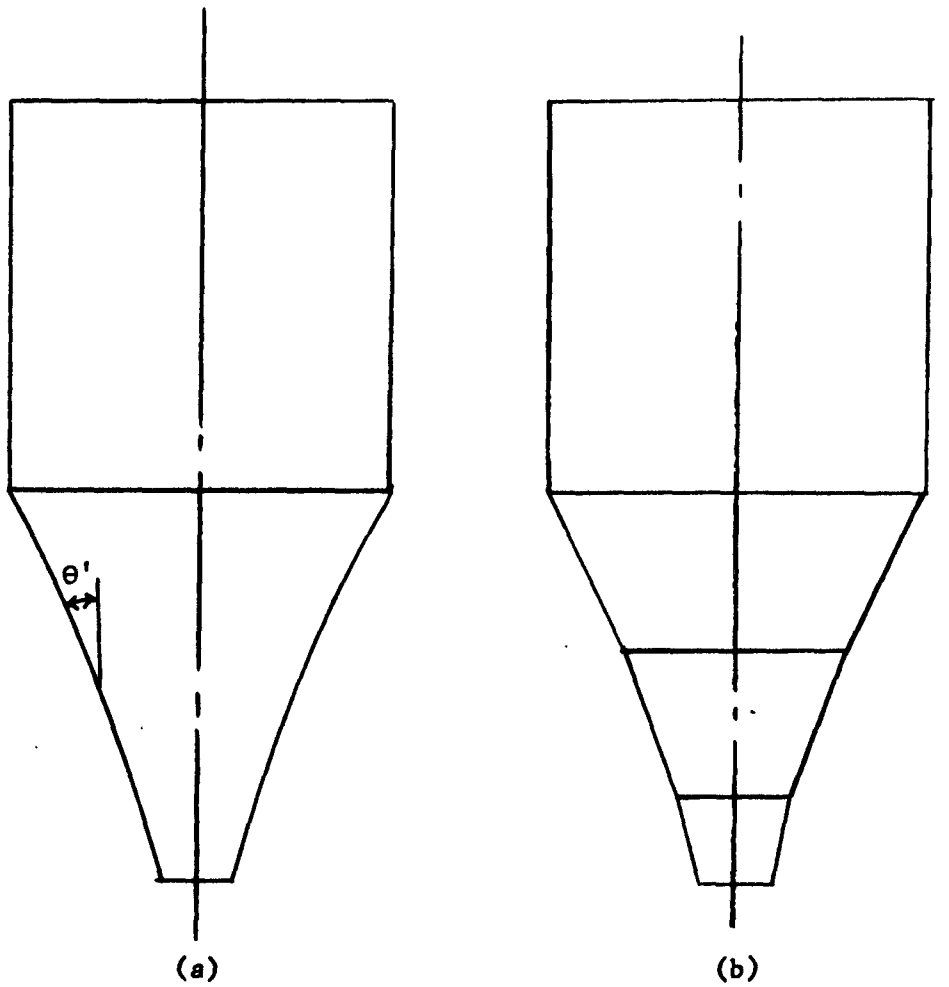

Fig. 98

"Hyperbolic" hopper

sections, Fig. 98(b) may save some headroom, especially where the curvature in the WYL is substantial. In fact, hoppers of that type have been recommended by some investigators [28,52,53,54], who arrived at the same conclusion by different and several lines of thought, which this writer does not follow.

5. Some solids will discharge out of the hopper but dome at the transition from the hopper to the vertical part. This case is important because it may lead to a structural failure of the bin when the doming mass collapses.

Consider the solid whose δ, FF, FF_t and WYL are shown in Fig. 99, γ = 20 pcf; and design a circular mass-flow bin with a vibrating hopper (discharger), Fig. 100. Assume ff = 1.3. In accordance with Eq. (24), V_1 is found equal to 3.3. For this value, $\overline{V}_1 = 2.5 \div 1.5F$, where F = 1.65. This determines $\delta = 50°$ and $\phi' = 23°$. From Fig. 47, there is $\theta'_c = 18°$ and ff = 1.29 -- close enough to the assumed value. From Fig. 43, $H(\theta') = 2.29$, B is then computed from Eq. (23). The values are tabulated:

Channel	δ	ϕ'	$\overline{V}_1$	θ'_c	ff	$H(\theta')$	B
Conical	50°	23°	2.5	18°	1.29	2.29	3.7

A 4-foot diameter vibrating hopper is adequate to start flow.

Consider now the conditions in the vertical part of the bin where $\theta' = 0$, and $H(\theta') = 2$. From Eq. (22), with B = D = 12, there is $\overline{V}_1 = 12 \times 20/13 \times 2 = 9.2$. Assume ff = 2.0. This determines $V_1 = 18.4$, $\delta = 40°$ and $\phi' = 15°$. From Fig. 46 for $\theta'_c = 0$, $\phi' = 15°$, ff checks out at about 2.0. It is evident that the FF_t lies above

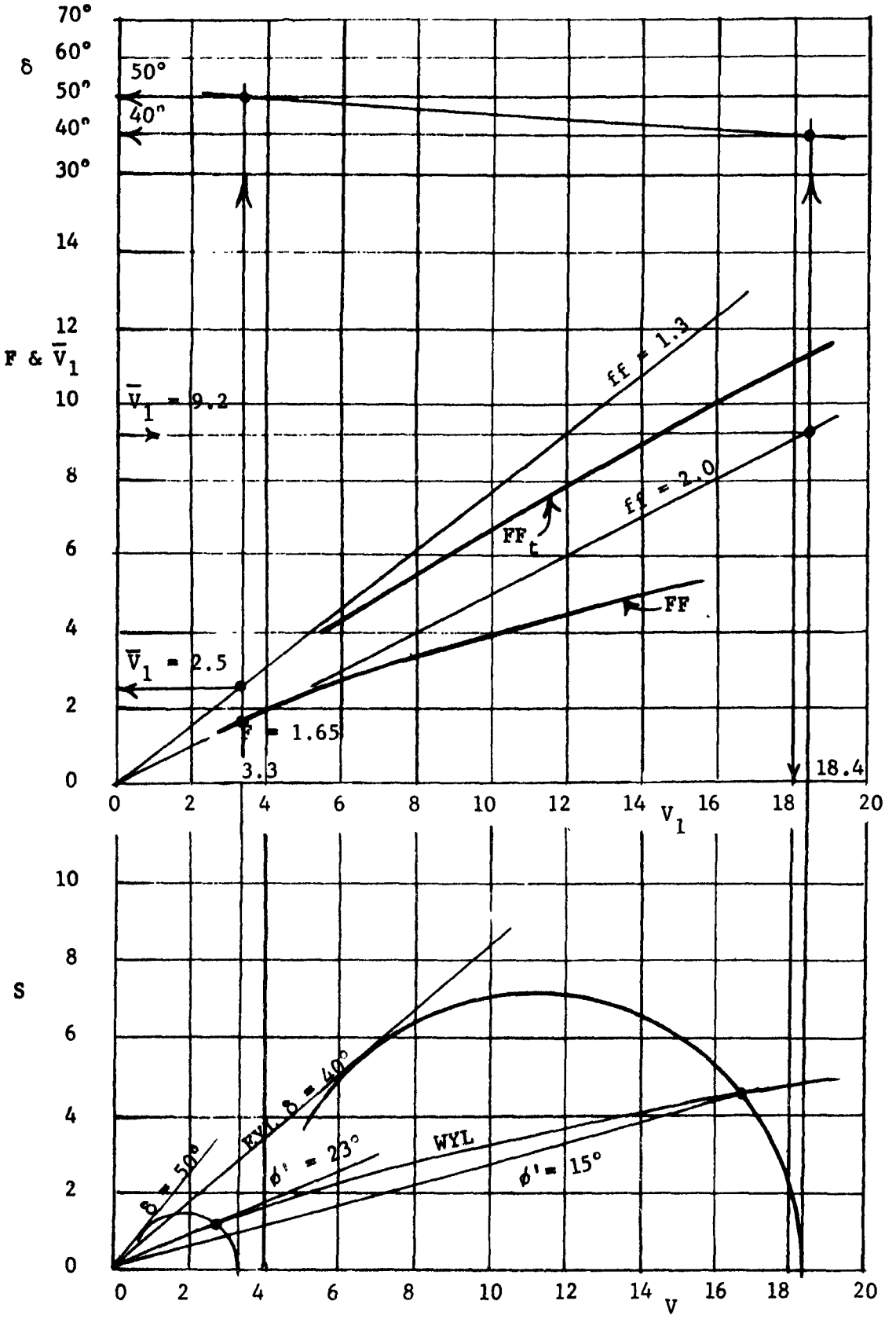

Fig. 99

Flow properties, Example 5

the ff in the vertical part of the bin, and that doming will occur.

To correct this situation it is necessary to roughen the vertical wall so as to increase its angle of friction ϕ' toward, say, 30°, and bring the point (θ'_c, ϕ') into the trough of low ff-values, Fig. 46. It is also advisable to fill in the corner between the vertical part and the hopper.

These conditions prevail whenever the critical FF < 2 for $F = AD\gamma/2$, where D is the diameter of the cylindrical bin, or for $F = AB\gamma$, where B is the width of the vertical portion of a rectangular bin.

6. An iron concentrate is to be stored. The question is: what should be the moisture content of the concentrate?

Assume a mass-flow, slot-outlet hopper. A function will be developed between the moisture content and the width of the slot needed for gravity flow. The price of the feeders can then be balanced against that of the filters needed to extract the water for a minimum overall cost.

Iron concentrate at high moisture develops full strength immediately upon consolidation: $FF_t = FF$. Hence the time effect need not be considered. Vibration is not recommended for these materials.

Three sets of δ, FF, and WYL curves are drawn in Fig. 101, $\gamma = 150$ pcf. The sets are marked by letters (a), (b), and (c), respectively. The ff-values are estimated at 1.2, 1.075, and 1.05 for the sets (a), (b), and (c), respectively, and the $\bar{V}_1$, δ and ϕ' values are obtained. The largest acceptable values of θ'_p and the corresponding ff-values are read and interpolated from Figures 52 to 54.

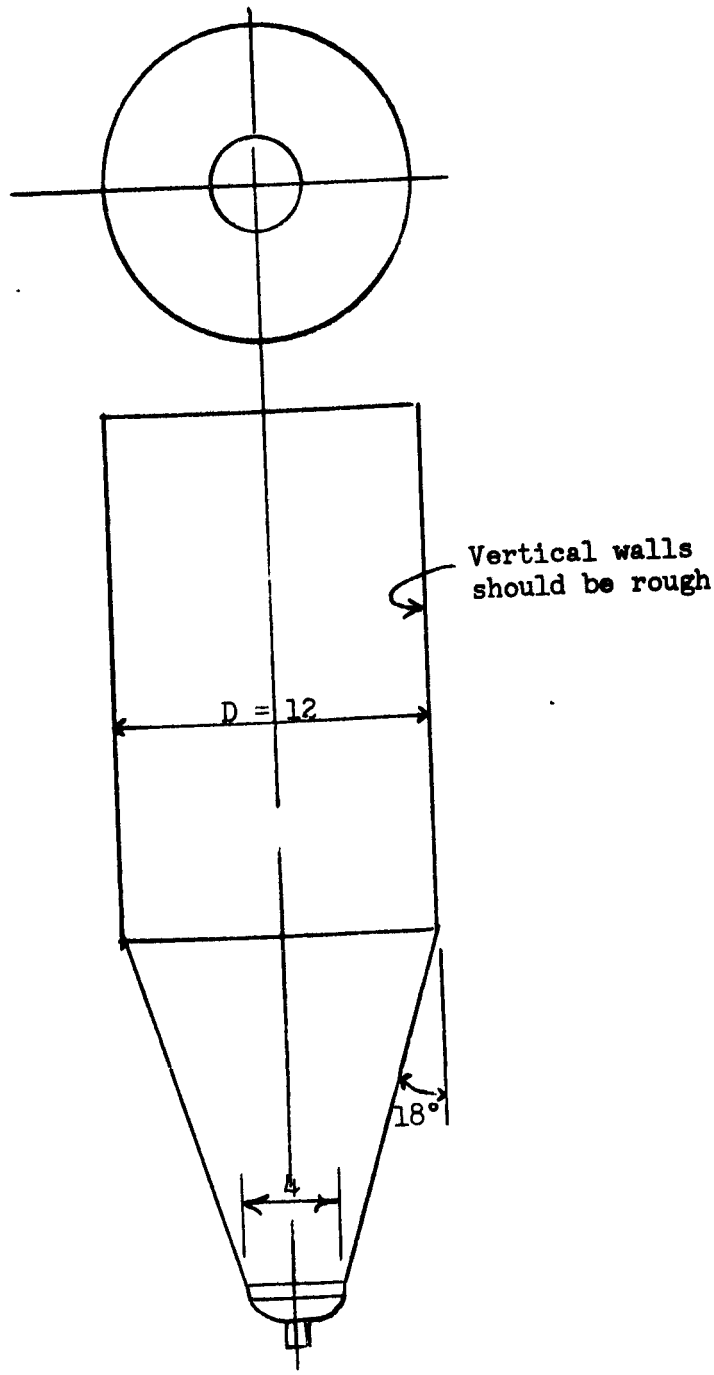

Fig. 100

Bin, Example 5

Parameter $H(\theta')$ is read from Fig. 43 and B is computed from Eq. (23). θ'_c angles are read and interpolated from Figures 47 to 49. All the values are tabulated:

Set	H_2O	δ	ϕ'	$\bar{V}_1$	θ'_p	ff	$H(\theta')$	B	θ'_c
(a)	5.3%	50°	29°	14.4	22°	1.2	1.12	1.4	11°
(b)	7.6%	65°	32°	32.3	20°	1.07	1.11	3.1	7°
(c)	8.7%	70°	35°	52.2	18°	1.05	1.10	5.0	5°

B is now plotted versus the moisture content H_2O in Fig. 102. Any one of the slot-outlet, mass-flow bins shown in Fig. 37 can be used for storage. Depending on the selected width B, a raised hopper slide belt or an idler-supported belt feeder can be used.

7. A solid whose flow properties are shown in Fig. 103 and whose bulk density $\gamma = 80$ is to be stored in a square bin. Segregation is not a problem and the bin will be emptied periodically. From required volume and available space considerations, it has been determined that, at the bottom of the bin, the effective consolidating head $h_e = 20'$. Two alternatives are considered:

(a) A funnel-flow bin with a vibrating hopper (discharger) and a small screw feeder, Fig. 104(a). The outlet diameter D of the static hopper is designed for no-piping. From Eq. (17B), $V_1 = 80 \times 20/13 = 123$ lb. From Fig. 103, we read $\bar{V}_1 = 14$ lb and $\phi_t = 45^\circ$. A value of $G(\phi_t) = 4.3$ is read from Fig. 36 and D is computed from Eq. (18). This results in $D = 9.8'$.

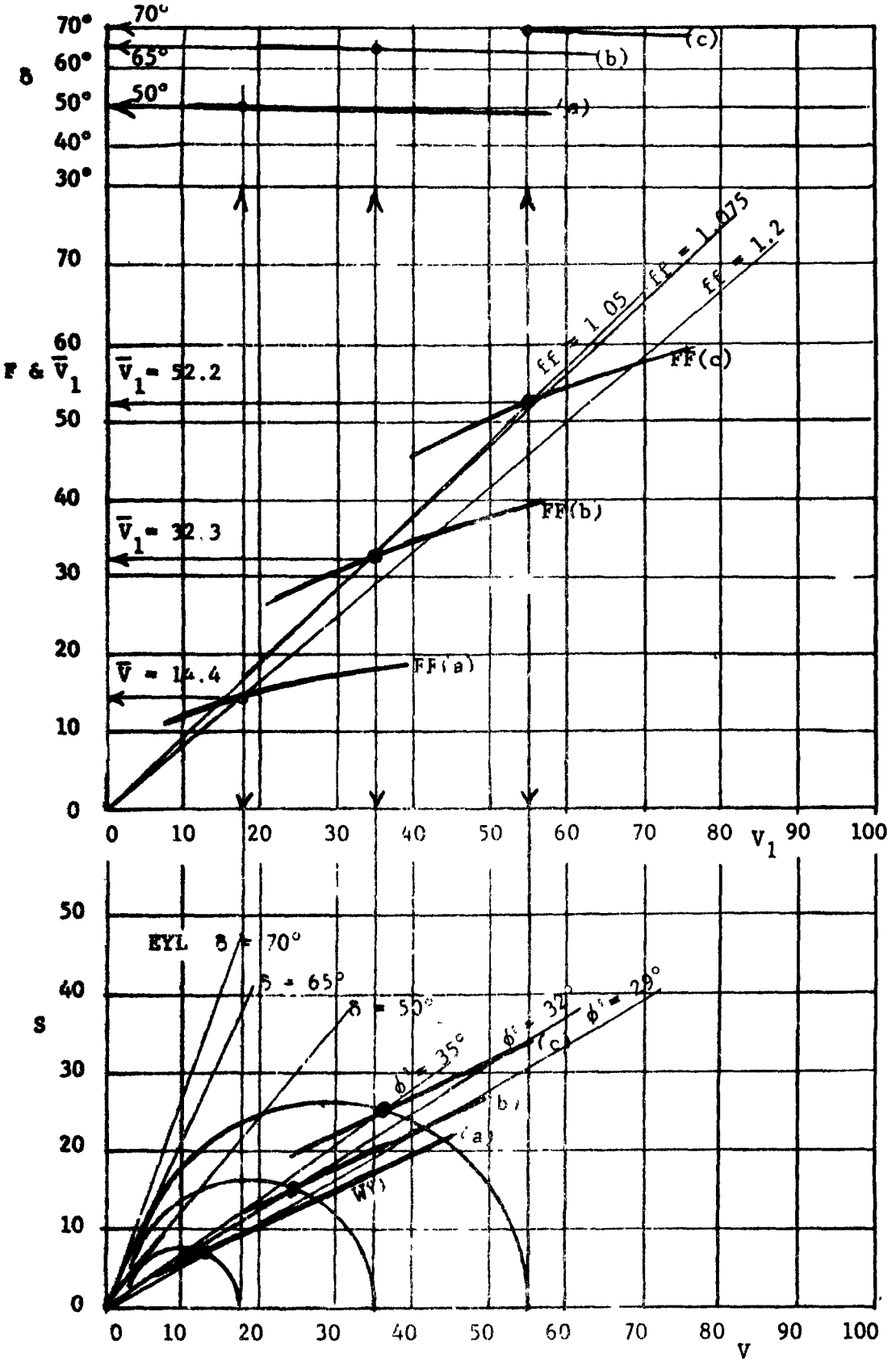

Fig. 101

Flow properties, Example 6

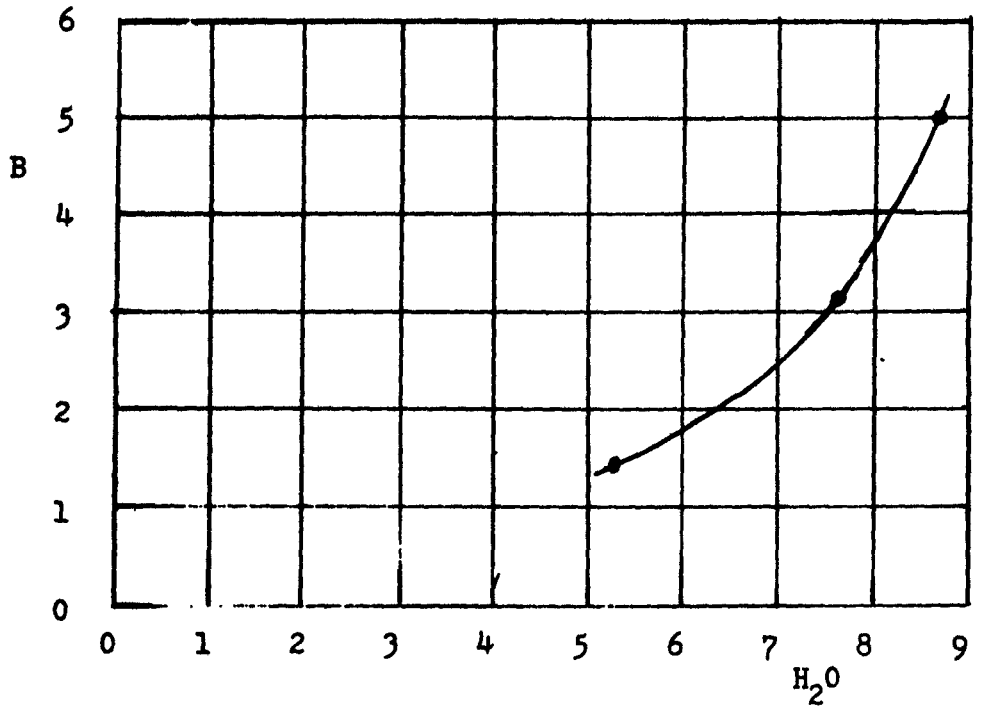

Fig. 102

Example 6: width B of slot outlet as a function of H_2O

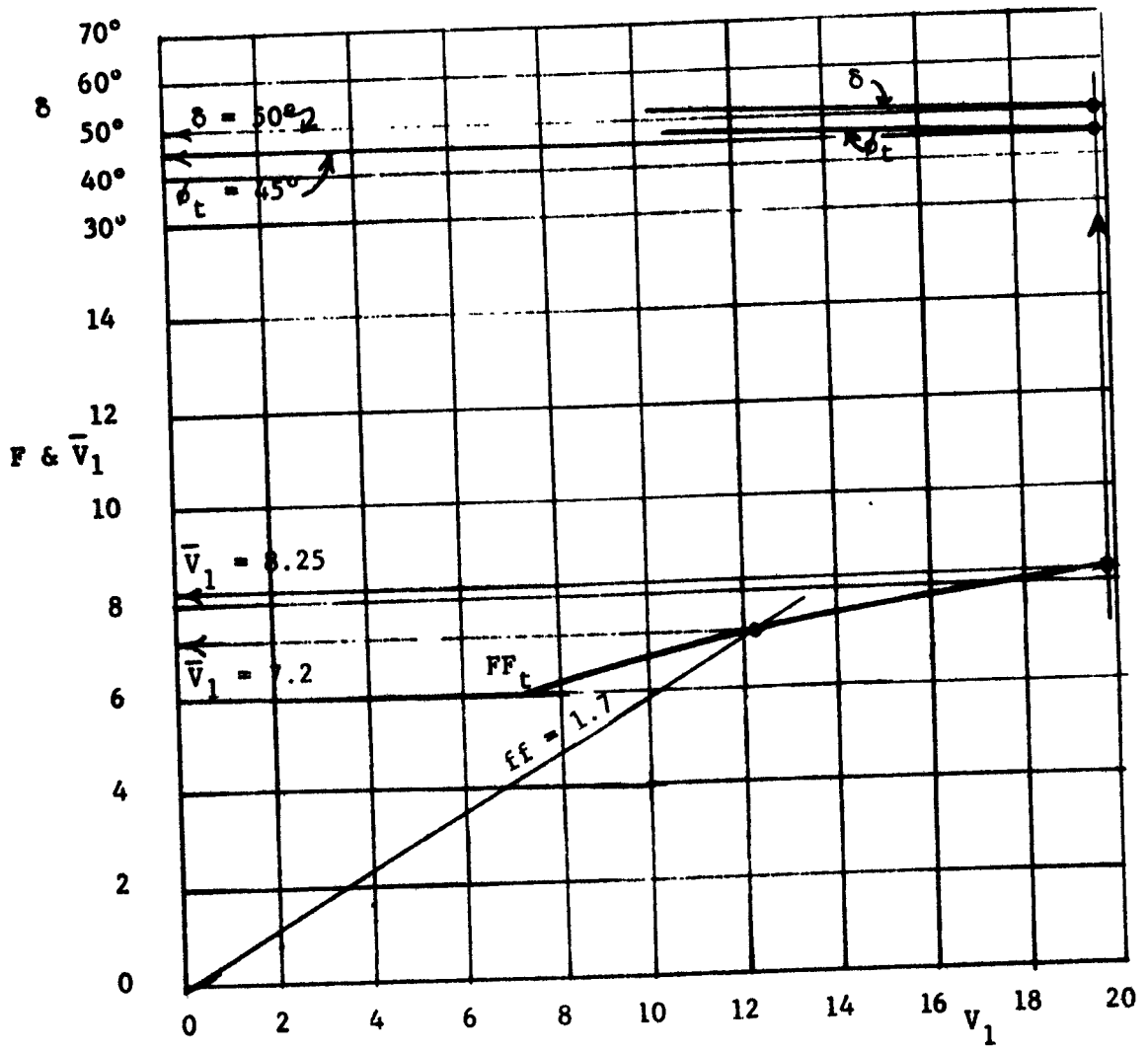

(a)

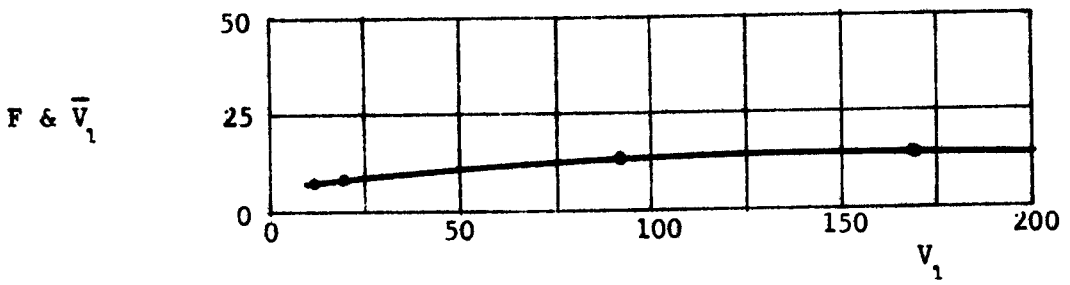

(b)

Fig. 103 Flow properties, Example 7

A 10-foot vibrating hopper is required. If the walls of the square-to-round transition hopper are sufficiently smooth and made of a non-corroding material, it is likely that with the assistance of the vibration from the discharger, the bin will be self-cleaning. A wall slope of 35° is recommended, Fig. 104(a).

(b) A funnel-flow bin with a screw feeder, Fig. 104(b). The intersection of ff - 1.7 with FF_t, Fig. 103, determines $\overline{V}_1 = 7.2$. The width of the outlet is computed from Eq. (19) at B = 15 x 7.2/80 = 1.35. A 24" stepped-pitch (1/2, 3/4, 1 and 1-1/4) screw is selected for a total length L = 10.0'

The diagonal D is in excess of 9.8 found above to be sufficient to prevent piping. Two wall vibrators are located on the side walls for final clearance only.

8. Design a storage pile, Fig. 76, for coarse ore weighing 130 pcf. The flow properties are given in Fig. 105, the layout around the outlet is shown in Fig. 106. The hopper is of the mass-flow type; the height of the hopper is designed so that the diagonal D at the top of the hopper be sufficient to prevent piping from developing within the flat-bottom part of the bin. During operation the hopper will always be kept full of ore to minimize the effect of impact. The hopper is designed for the time-flow-function and, hence will give unassisted gravity flow, and vibrators are not required.

At the outlet ff = 1.1 is assumed, the point of intersection

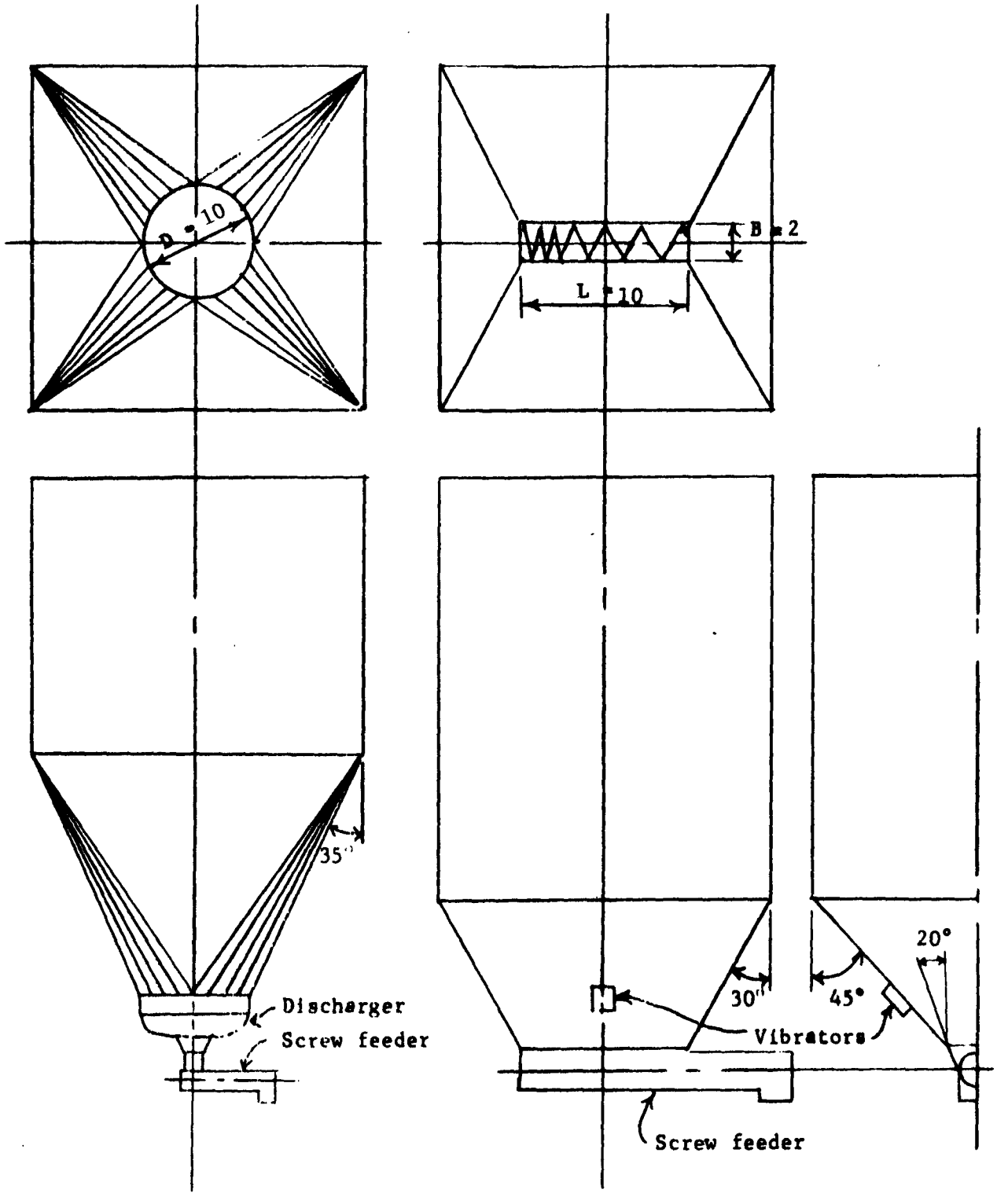

(a)

Bin with a discharger and a small screw feeder

(b)

Bin with a screw feeder and wall vibrators for final clearance only

Fig 104

Bin, Example 7

with FF_t determines $\bar{V}_1$ = 27.3, δ = 60° and ϕ' = 32°. From Fig. 53, θ' = 20° is assumed. This checks out the assumed value of ff. $H(\theta')$ is read off Fig. 43 and B is computed from Eq. (23). The values are tabulated below.

δ	ϕ'	$\bar{V}_1$	θ'_p	ff	$H(\theta')$	B
60°	32°	27.3	20°	1.1	1.1	3.0

Above the hopper, funnel-flow analysis applies. An effective consolidating head h_e = 25' is assumed. From Eq. (17B), V_1 = 130 x 25/13 = 250 lb. From Fig. 105, we obtain $\bar{V}_1$ = 45 lb and $\phi_t = 40^o$. A value of $G(\phi_t)$ = 3.6 is read from Fig. 36 and D is computed from Eq. (18). This results in D = 16.2'.

A hopper with straight ends is used, as shown in Fig. 106. This widens the hopper width to 15 feet at the top and produces a diagonal $D = \sqrt{9^2 + 15^2}$ = 17.5 feet.

The side-wise reciprocating feeder is recommended for this installation.

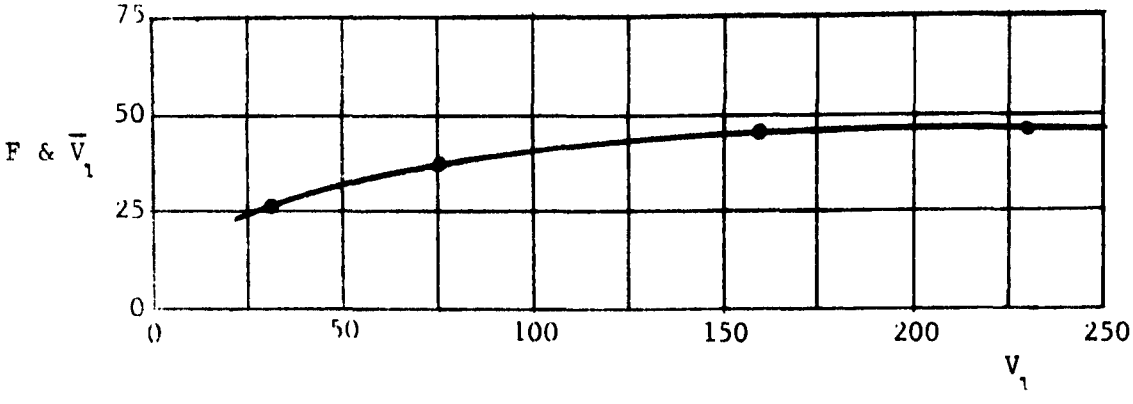

Fig. 105(a) Flow properties, Example 8

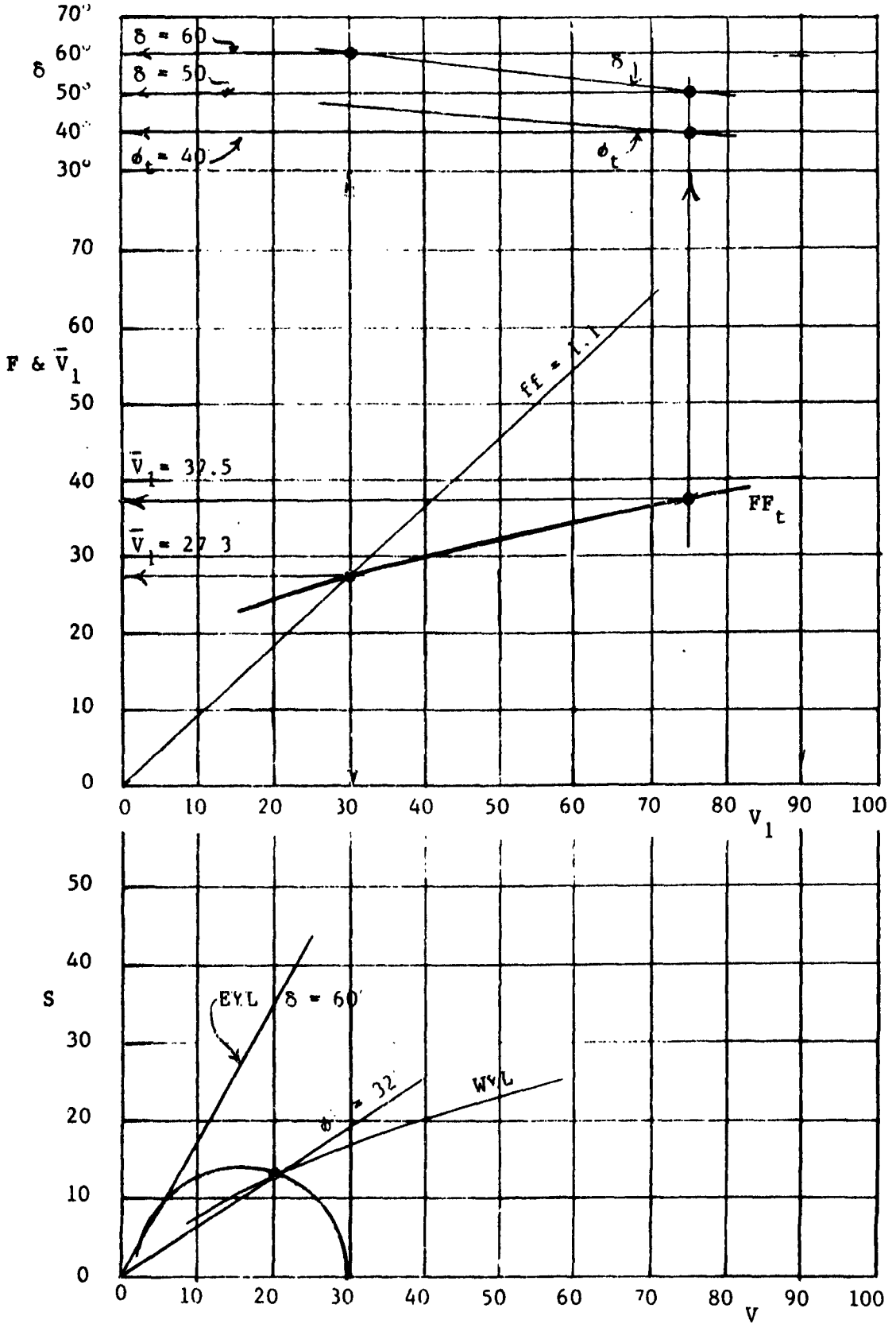

Fig 105 (b)

Flow properties, Example 8

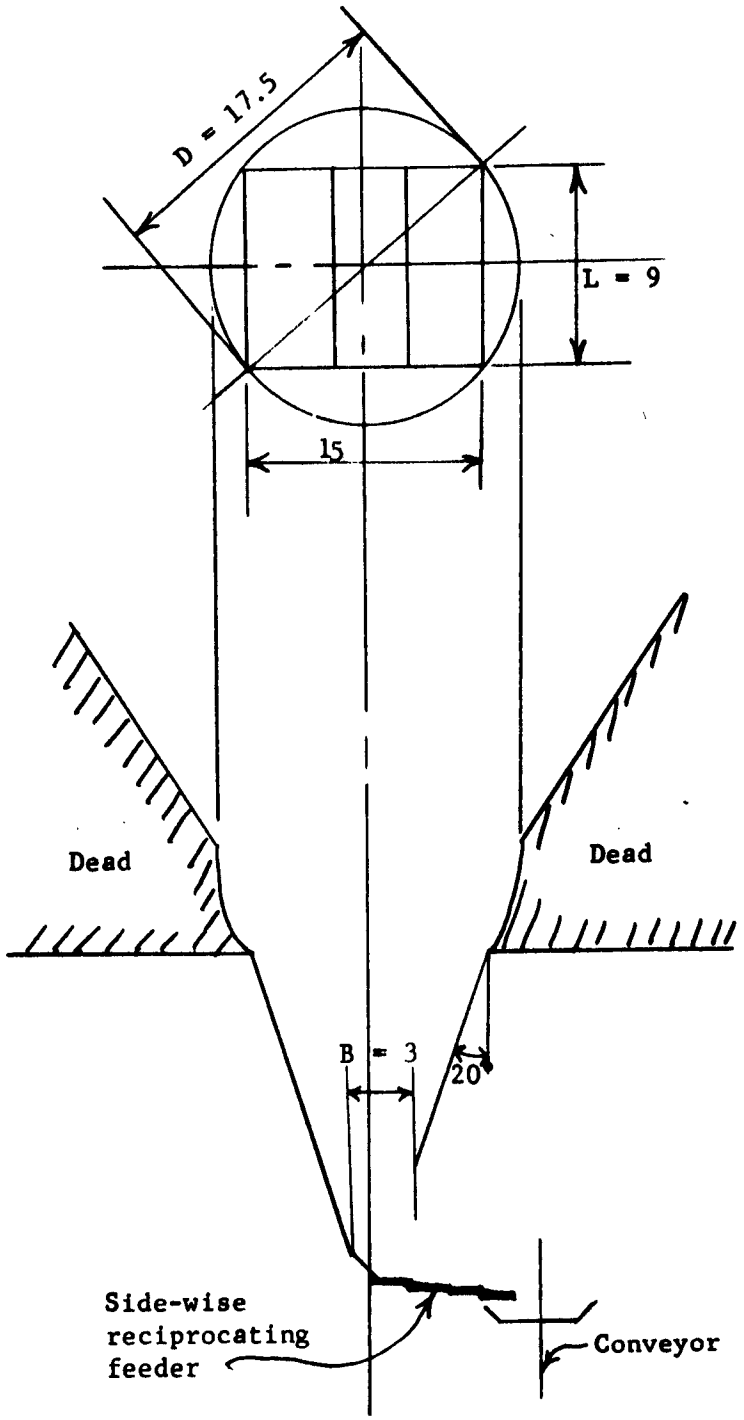

Fig. 106

Layout around the outlet, Example 8

APPENDIX

Introduction

The solids which are considered in this work are rigid-plastic. In the plastic regions, the solids are assumed isotropic, frictional, cohesive and compressible. During incipient failure an element of a solid expands, while during flow, the element either expands or contracts as does the pressure along the streamline. Steady flow is assumed.

The determination of the flow-factors for no-doming and no-piping requires the solution of steady state flow stress fields in converging and vertical channels. The fields are solved in plane flow (plane strain) and in conical flow (axial symmetry). These fields are statically determinate and are solved without reference to velocity fields. Since the prevailing stresses are compressive, pressures are considered positive and tensions negative. Plane-polar and spherical coordinates are used in converging plane and conical flow, respectively. In order to handle both types of fields with one set of equations, coefficient m is introduced and assigned the values:

$$\left.\begin{aligned} m &= 0, \text{ in plane flow,} \\ m &= 1, \text{ in conical flow.} \end{aligned}\right\} \qquad \text{(A-1)}$$

Doming

Consolidating pressure in converging channels, σ_1. A solid consolidates under the pressures which occur during flow. The analysis of these pressures is based on the following equations:

(a) Two equations of equilibrium

$$\frac{\partial \sigma_r}{\partial r} + \frac{1}{r}\frac{\partial \tau_{r\theta}}{\partial \theta} + \frac{1}{r}\left[\sigma_r - \sigma_\theta + m(\sigma_r - \sigma_\alpha) + m\tau_{r\theta}\cot\theta\right] + \gamma\cos\theta = 0. \qquad \text{(A-2)}$$

$$\frac{\partial \tau_{r\theta}}{\partial r} + \frac{1}{r}\frac{\partial \sigma_\theta}{\partial \theta} + \frac{1}{r}\left[m(\sigma_\theta - \sigma_\alpha)\cot\theta + (2+m)\tau_{r\theta}\right] - \gamma\sin\theta = 0. \qquad \text{(A-3)}$$

The coordinates and the stresses are defined in Fig. A-1.

(b) The equation of state, Eq. (1), written in the above component stresses

$$(\sigma_r + \sigma_\theta)\sin\delta - \sqrt{(\sigma_r - \sigma_\theta)^2 + 4\,\tau_{r\theta}^2} = 0. \qquad \text{(A-4)}$$

(c) In axial symmetry, the Haar and von Karman hypothesis [47] which, in converging flow sets the value of the circumferential pressure σ_α equal to the major pressure σ_1 of the meridian plane r,θ.

$$\sigma_\alpha = \sigma_1. \qquad \text{(A-5)}$$

In plane flow, pressure σ_α does not appear.

(d) A one-to-one relation between mean pressure,

$$\sigma = 1/2(\sigma_r + \sigma_\theta). \qquad \text{(A-6)}$$

and density, γ

$$\gamma = \gamma(\sigma). \qquad \text{(A-7)}$$

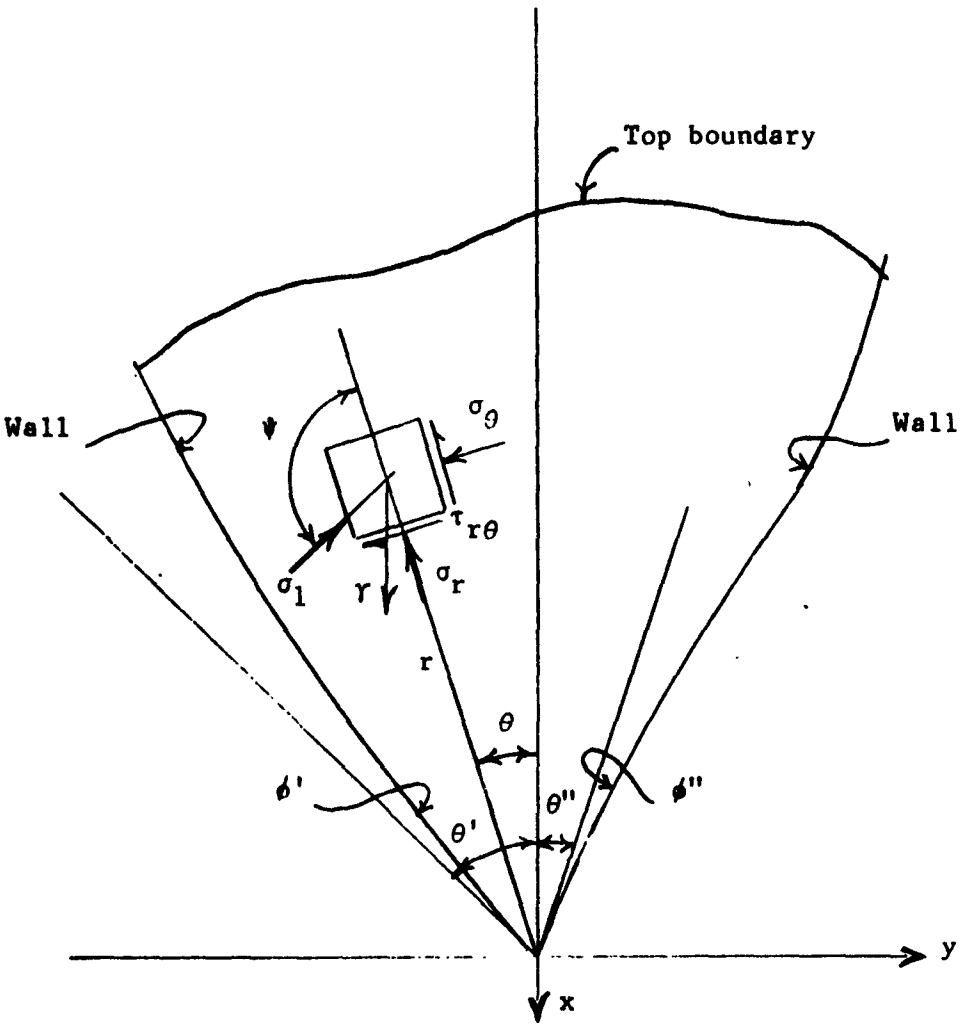

Fig. A-1

A general channel

These equations together with appropriate stress boundary conditions define a general stress field.

Radial stress fields. First of all, particular stress fields, called "radial stress fields" are obtained. The radial fields satisfy the functions

$$\sigma = \gamma\, r\, s(\theta), \tag{A-8}$$

$$\psi = \psi(\theta), \tag{A-9}$$

in which $s(\theta)$ is a stress function and ψ is the angle between the direction of the major pressure σ_1 and the coordinate ray, Fig. A-1. Density

$$\gamma = \gamma_o \tag{A-10}$$

is constant, i.e. the solid is incompressible.

In accordance with Fig. A-2, the component pressures are expressed as follows:

$$\sigma_r = \sigma(1 + \sin\delta \cos 2\psi), \tag{A-11}$$

$$\sigma_\theta = \sigma(1 - \sin\delta \cos 2\psi), \tag{A-12}$$

$$\tau_{r\theta} = \sigma \sin\delta \sin 2\psi, \tag{A-13}$$

$$\sigma_1 = \sigma(1 + \sin\delta). \tag{A-14}$$

The substitution of the above expressions and their derivatives for the component stresses in Equations (A-2) and (A-3) yields after transformations.

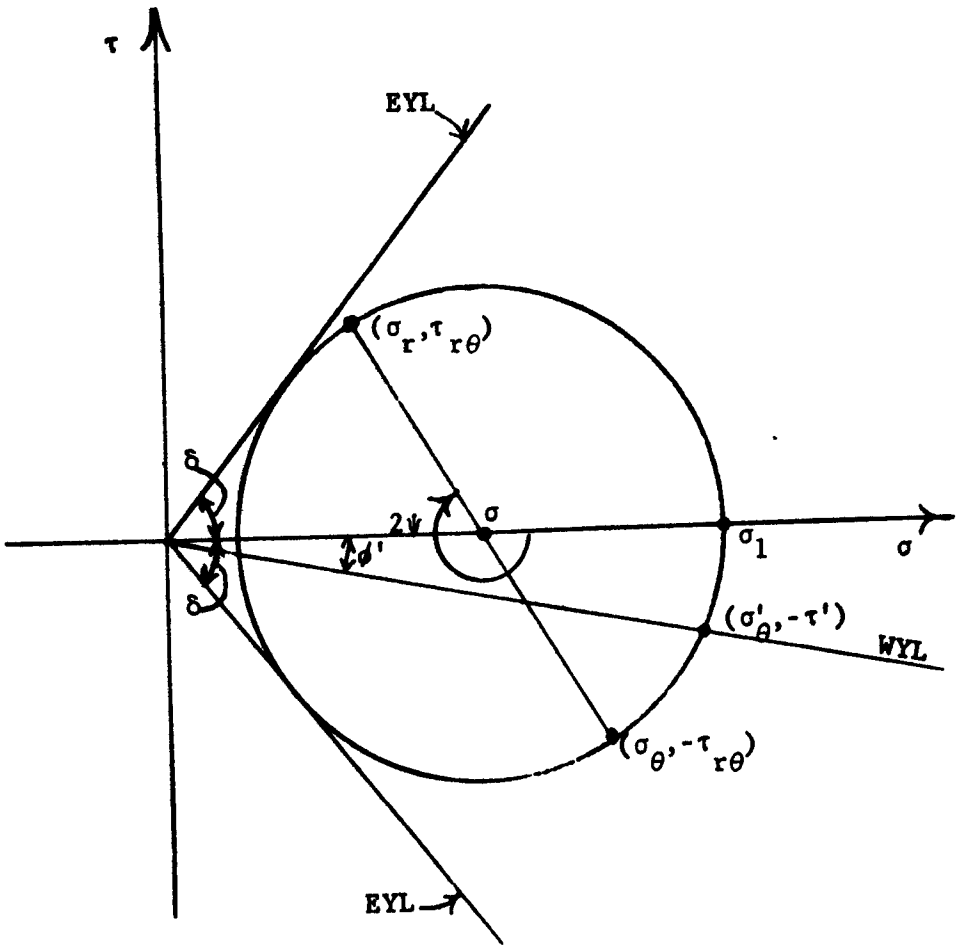

Fig. A-2

Mohr stress circle

$$\frac{d\psi}{d\theta} = F(\theta,\psi,s) =$$

$$= -1 - [m\, s \sin\delta(1 + \sin\delta)(\cot\theta \sin 2\psi \cos 2\psi - 1) + \cos\theta -$$

$$- \sin\delta \cos(\theta + 2\psi) + s \cos^2\delta]/2\, s \sin\delta(\cos 2\psi - \sin\delta), \qquad \text{(A-15)}$$

$$\frac{ds}{d\theta} = G(\theta,\psi,s) =$$

$$= \frac{s \sin 2\psi + \sin(\theta + 2\psi) + m\, s \sin\delta[\cot\theta(1 + \cos 2\psi) - \sin 2\psi]}{\cos 2\psi - \sin\delta}. \qquad \text{(A-16)}$$

It will be noticed that r has cancelled out and does not appear in the equations. These equations are equivalent to the integral equations

$$\psi(\theta) = \psi(\theta^\circ) + \int_{\theta^\circ}^{\theta} F[t,\psi(t),s(t)]dt, \qquad \text{(A-17)}$$

$$s(\theta) = s(\theta^\circ) + \int_{\theta^\circ}^{\theta} G[t,\psi(t),s(t)]dt, \qquad \text{(A-18)}$$

which have been solved numerically from initial conditions ($\theta^\circ = 0, \psi(\theta^\circ) = \pi/2, s(\theta^\circ) = s^\circ$) for a range of useful wall conditions (θ', ψ'), for symmetric channels, Fig. A-3(a); and from initial conditions ($\theta^\circ = 0, \psi(\theta^\circ) = \psi^v, s(\theta^\circ) = s^\circ$) for wall conditions ($\theta', \psi', \psi^v$), for asymmetric plane flow channels, Fig. A-3(b). The results are plotted in θ', ϕ' coordinates. This requires a change of variables from ψ' to ϕ' and from ψ^v to ϕ^v. Since

$$\tau'_{r\theta}/\sigma'_\theta = -\tan\phi', \text{ and } \tau^v_{r\theta}/\sigma^v_\theta = \tan\phi^v, \qquad \text{(A-19)}$$

it follows from Equations (A-12) and (A-13) that

$$\left.\begin{aligned} \psi' &= \frac{\pi}{2} + \frac{1}{2}(\phi' + \text{Arc sin}\frac{\sin\phi'}{\sin\delta}), \\ \psi^v &= \frac{\pi}{2} - \frac{1}{2}(\phi^v + \text{Arc sin}\frac{\sin\phi^v}{\sin\delta}). \end{aligned}\right\} \qquad \text{(A-20)}$$

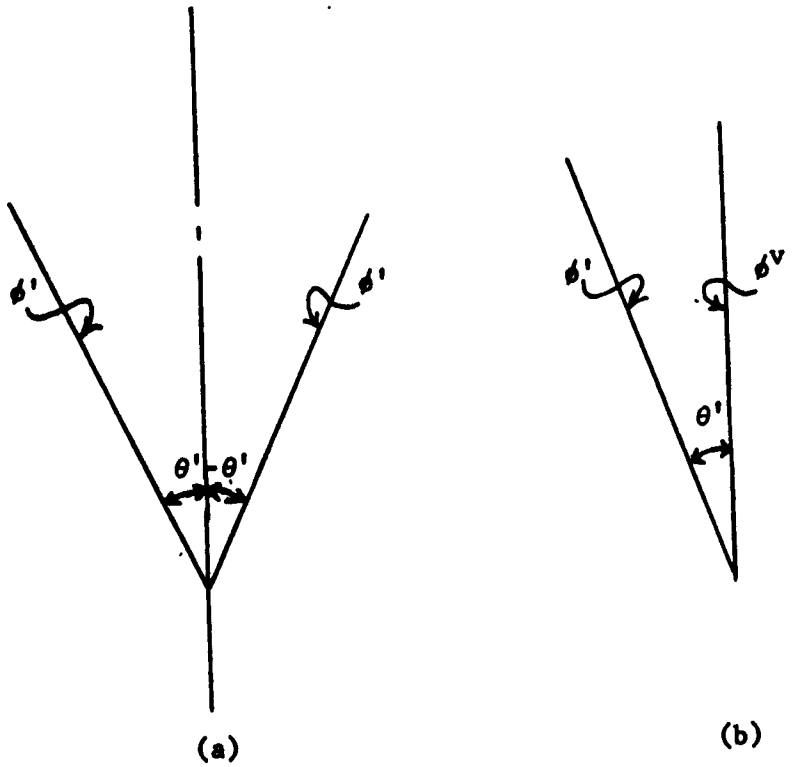

Fig. A-3

Channels

Equations (A-17) and (A-18) are then in the form

$$\psi = \psi(m,\delta,\theta',\phi'), \tag{A-21}$$

$$s = s(m,\delta,\theta',\phi'), \tag{A-22}$$

in symmetric channels, and

$$\psi = \psi(m,\delta,\theta',\phi',\phi^{v}), \tag{A-23}$$

$$s = s(m,\delta,\theta',\phi',\phi^{v}), \tag{A-24}$$

in plane asymmetric channels with one vertical wall. The component pressures are now readily obtained from Equations (A-11) to (A-14). For details of the analysis the reader is directed to references 39 and 43.

Convergence of general stress fields to radial stress fields.

The significance of the radial stress fields lies in the fact that real stress fields in plane strain and in axial symmetry converge to the radial stress fields as the vertex of the channel is approached, i.e. for $r \to 0$. This convergence is of fundamental importance in the derivation of flow-no flow criteria because most obstructions to flow originate at the outlets of channels, i.e. in the vicinity of the vertex. Since in real channels, convergence to a radial stress field is very rapid [44], the stresses in the region of an outlet are usually sufficiently well represented by the radial stress field for design purposes. Therefore, the stresses in the region of the outlet can be predicted on the basis of the slope and angle (or angles) of friction of the walls at the outlet without reference to the top boundary conditions, such as the head

of the solid over the outlet, the shape of the top, traction-free boundary, and the shape of the walls away from the outlet.

This independence of the head and boundaries away from the vertex has been observed by investigators and engineers for a long time [1, 20, 48]. An analysis of the equations shows how this convergence takes place.

It is compatible with experience and with the equation of state (A-4) to assume that density is represented by the function

$$\gamma = \gamma_o + \gamma(\sigma). \tag{A-25}$$

where $\gamma(0) = 0$, and the function is continuous. In general fields, the functions (A-8) and (A-9) do not hold but can be written in the form

$$\sigma = r[\gamma_o + \gamma(\sigma)]s(r,\theta). \tag{A-26}$$

$$\psi = \psi(r,\theta). \tag{A-27}$$

Expression (A-26) is substituted for σ in the expressions (A-11) to (A-14) which are, in turn, substituted for the component stresses and their derivatives in the equations of equilibrium (A-2) and (A-3) leading, after transformations, to

$$\frac{\partial s}{\partial \theta} + s\, f(r,\theta) + g(r,\theta) = 0, \tag{A-28}$$

$$r\,\frac{\partial s}{\partial r} + s\, h(r,\theta) + j(r,\theta) = 0, \tag{A-29}$$

where

$$f(r,\theta) = 2\left(\frac{\partial\psi}{\partial\theta} + 1\right)\frac{\sin\delta}{\cos^2\delta}\sin 2\psi + 2r\,\frac{\partial\psi}{\partial r}\,\frac{\sin\delta}{\cos^2\delta}\,(\sin\delta + \cos 2\psi) +$$

$$+ \frac{1}{\gamma}\,\frac{\partial\gamma}{\partial\theta} + m\,\frac{\sin\delta}{\cos^2\delta}\,(1 + \sin\delta)[\sin 2\psi - \cot\theta(1 + \cos 2\psi)], \qquad \text{(A-30)}$$

$$g(r,\theta) = -\,\frac{\sin\delta}{\cos^2\delta}\sin(\theta + 2\psi) - \frac{\sin\theta}{\cos^2\delta}, \qquad \text{(A-31)}$$

$$h(r,\theta) = 1 + 2\left(\frac{\partial\psi}{\partial\theta} + 1\right)\frac{\sin\delta}{\cos^2\delta}\,(\cos 2\psi - \sin\delta) - 2r\,\frac{\partial\psi}{\partial r}\,\frac{\sin\delta}{\cos^2\delta}\sin 2\psi +$$

$$+ \frac{r}{\gamma}\,\frac{\partial\gamma}{\partial r} + m\,\frac{\sin\delta}{\cos^2\delta}\,(1 + \sin\delta)(\cot\theta\sin 2\psi + \cos 2\psi - 1), \qquad \text{(A-32)}$$

$$j(r,\theta) = -\,\frac{\sin\delta}{\cos^2\delta}\cos(\theta + 2\psi) + \frac{\cos\theta}{\cos^2\delta}\,. \qquad \text{(A-33)}$$

Equations (A-28) and (A-29) have real characteristics whose directions are

$$\frac{dr}{d\theta} = r\cot\left[\psi \pm \left(\frac{\pi}{4} - \frac{\delta}{2}\right)\right]. \qquad \text{(A-34)}$$

The equations are hyperbolic for $r \neq 0$, but parabolic for $r = 0$ ($\psi = \pi/4 - \delta/2$ and $\psi = 3\pi/4 + \delta/2$ lie outside of real channels, because ϕ' and $\phi^v < \delta$). A typical field of characteristics for the general channel of Fig. A-1 is shown in Fig. A-4 in orthogonal axes θ,r. It is apparent that the effect of the variable r decreases as $r \to 0$. At $r = 0$, the parabolic solution is independent of the derivatives with respect to r and, in fact, is the same as the radial stress field. Hence, barring discontinuities, the general stress field converges to the radial stress field at the vertex.

The concepts of plasticity permit stress discontinuities. In

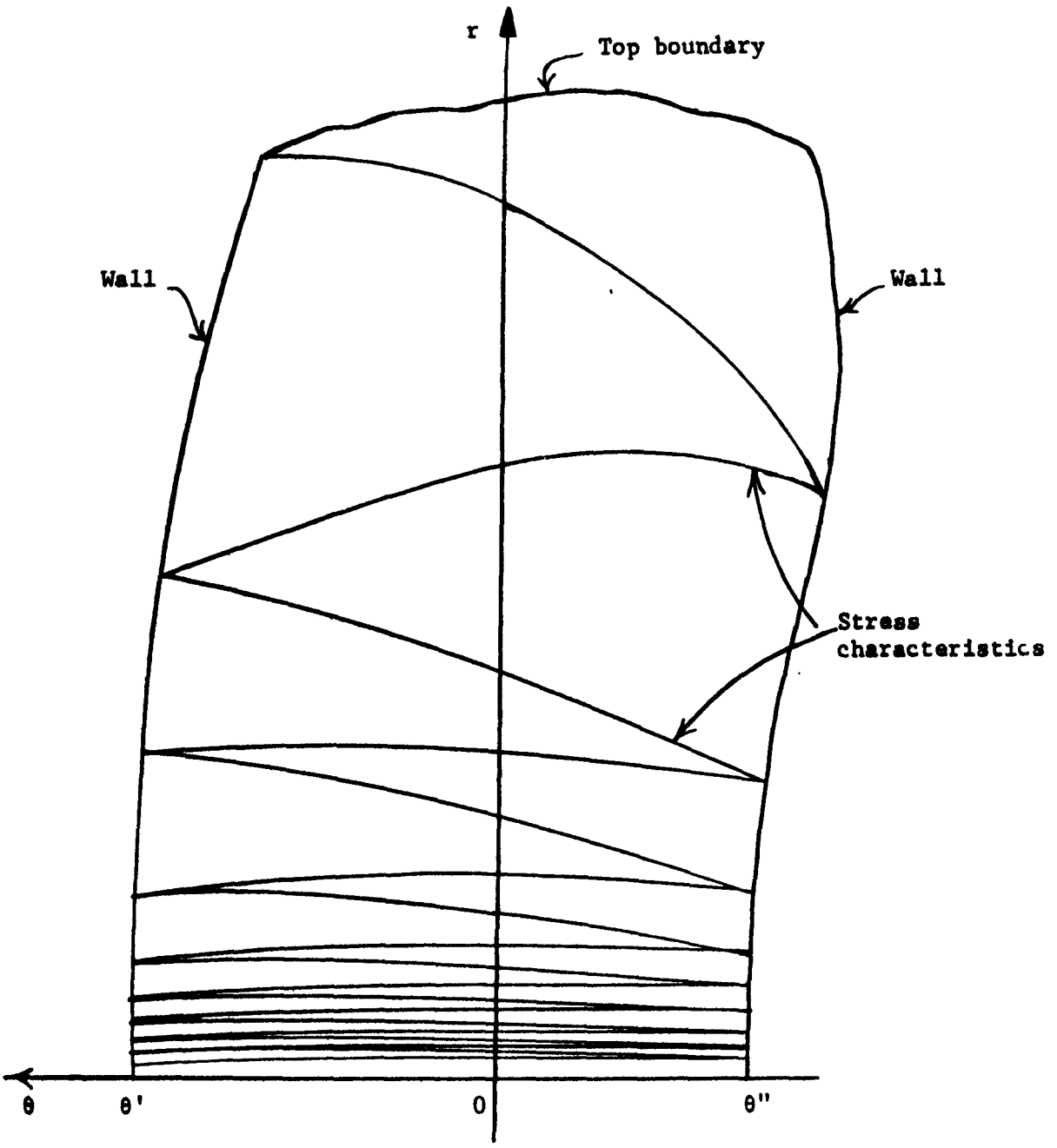

Fig. A-4

Field of characteristics

particular, a discontinuity can follow a streamline. This type of discontinuity does not affect the present discussion because such a discontinuity can be looked upon as a wall and the regions on each side of the discontinuity can be considered as separate channels. Any other discontinuity would reach a wall, reflect from it, and continue reflecting from wall to wall since the field is hyperbolic. A solid flowing across these lines of stress discontinuity would undergo successive, discontinuous expansions and contractions. It is unlikely that these conditions can satisfy the second law of thermodynamics.

In physical channels, discontinuities do not seem to appear in flowing solids. If a discontinuity is introduced at the wall of a channel, the solid either does not flow at all, or remains rigid (elastic) in a part of the channel, and forms new walls across itself. Surface discontinuities along a top boundary are invariably contained within rigid regions.

Results of numerical solutions of general fields have been presented by Johanson [44] and an example from his paper is shown in Fig. A-5. Mean pressures, Eq. (A-6), are plotted: σ° is the value along the axis of symmetry and σ'' along the wall. The dashed lines represent radial stress values. The wavy lines represent the values of the general field which arises from a high vertical head of the solid above the conical part. The convergence is very rapid.

Critical pressure in a dome, $\bar{\sigma}_1$. While the stress field in a doming mass of a solid may not be uniquely determined, it appears possible to establish a lower bound $\bar{\sigma}_1$ for use in formulas (8) and (9) to assure the yielding of the dome. The reasoning is as follows:

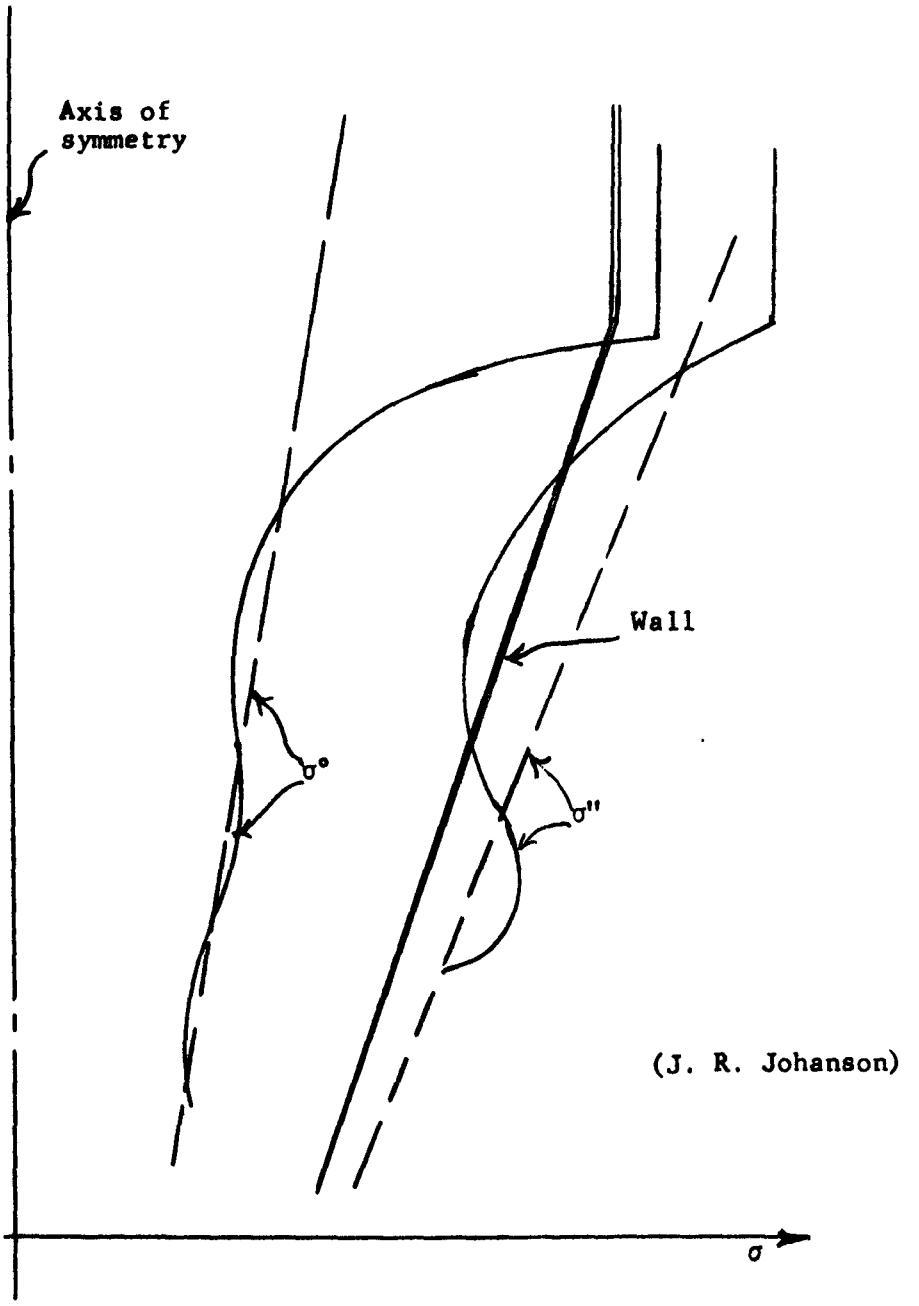

Fig. A-5

Example of convergence

(a) Consider a mass of a solid forming a stable dome across the channel, Fig. A-6. The traction-free, bottom surface of the dome has assumed some shape expressed by the function

$$r = a\, f(\theta). \tag{A-35}$$

Assume that the shape of the dome is such that the critical pressure is at a minimum. Evidently, such a shape will be smooth. The critical pressure is assumed to occur at the abutments of the dome. Take $f(0) = 1$ and the parameter a constant along the surface of the dome.

(b) Consider the mass of the solid as being made up of superimposed layers, each bounded by surfaces similar to that of the traction-free, bottom surface, i.e. given by Eq. (A-35) with parameter a different but constant on each surface.

(c) Assume that each layer is self-supporting, i.e. no stresses act between adjacent layers. The pressures $\bar{\sigma}_1$ at the abutment of each layer are then directly proportional to r', the distance from the vertex.

(d) The above conditions lead to a lower bound on the pressure in the bottom layer of the dome because, in fact, pressures do act between adjacent layers and, in particular, on the bottom layer from the mass above.

The pressures between adjacent layers arise because, if pressure $\bar{\sigma}_1 = f_c$ in the bottom layer, then $\bar{\sigma}_1 > f_c$ in the higher layers which therefore cannot be self-supporting. $\bar{\sigma}_1 > f_c$ in the higher layers because, while $\bar{\sigma}_1$ is proportional to r', f_c increases with r' at a

smaller rate due to two reasons:

(1) In the region of radial stress, consolidating pressure σ_1 increases linearly with r'. But flow-function curves are, generally, convex-upward and/or have a positive intercept on the f_c axis. Hence, f_c increases at a rate smaller than linear with σ_1.

(2) At some height of the channel, the real consolidating pressure σ_1 falls below the radial consolidating pressure. Above that height, the strength f_c falls still further below the value required for self-support, in fact, f_c may fall to zero at the top, traction-free surface of the solid.

The problem of the lower bound thus resolves to finding the shape of a layer bounded by surfaces a $f(\theta)$ and $(a + da)\, f(\theta)$, such that, for a solid of given bulk density γ spanning a distance B, the non-dimensional ratio

$$H(\theta') = B\gamma/\bar{\sigma}_1 \qquad \text{(A-36)}$$

is at a maximum. Density γ is assumed constant in this analysis which is described in detail in reference [42]. Function $H(\theta')$ has been computed and is plotted in Fig. 43 for conical and plane-flow channels. The value of $H(\theta')$ for square channels is estimated at 0.9 of $H(\theta')$ for conical channels.

Replacing $\bar{\sigma}_1$ by $\bar{V}_1 = A\bar{\sigma}_1$, the critical width B of a dome is obtained from Eq. (A-36), thus

$$B = H(\theta')\bar{V}_1/A\gamma. \qquad \text{(A-37)}$$

This is Eq. (12) in Chapter I.

In vertical channels, i.e. for $\theta' = 0$, $H(\theta') = 2$ in conical channels, and $H(\theta') = 1$ in plane-flow channels. These particular results were published in reference 33.

No-doming flow-factor. It is evident from Fig. A-6 that

$$B = 2r' \sin \theta'. \tag{A-38}$$

From Equations (A-36) and (A-38), the critical pressure at the abutment of a dome is

$$\bar{\sigma}_1 = 2\gamma\, r' \sin \theta'/H(\theta'), \tag{A-39}$$

while the major consolidating pressure is found from Equations (A-8), (A-14) and (A-22) for $\theta = \theta'$ to be

$$\sigma_1 = \gamma\, r'(1 + \sin \delta)s(m,\delta,\theta',\phi') \tag{A-40}$$

for symmetric channels.

The flow-factor is now obtained in accordance with the definition (8)

$$ff = H(\theta') \frac{(1 + \sin \delta)s(m,\delta,\theta',\phi')}{2 \sin \theta'} . \tag{A-41}$$

For asymmetric channels in plane flow with one vertical wall, the function $s'(\delta,\theta',\phi',\phi^V)$, Eq. (A-24), has been computed [39] but the function $H(\theta')$, Eq. (A-36) is not available. Therefore, the same value of the latter function is used as for symmetric channels. This yields the following safe expression for asymmetric channels

$$ff = H(\theta') \frac{(1 + \sin \delta)s(m,\delta,\theta',\phi',\phi^V)}{2 \sin \theta'} \tag{A-42}$$

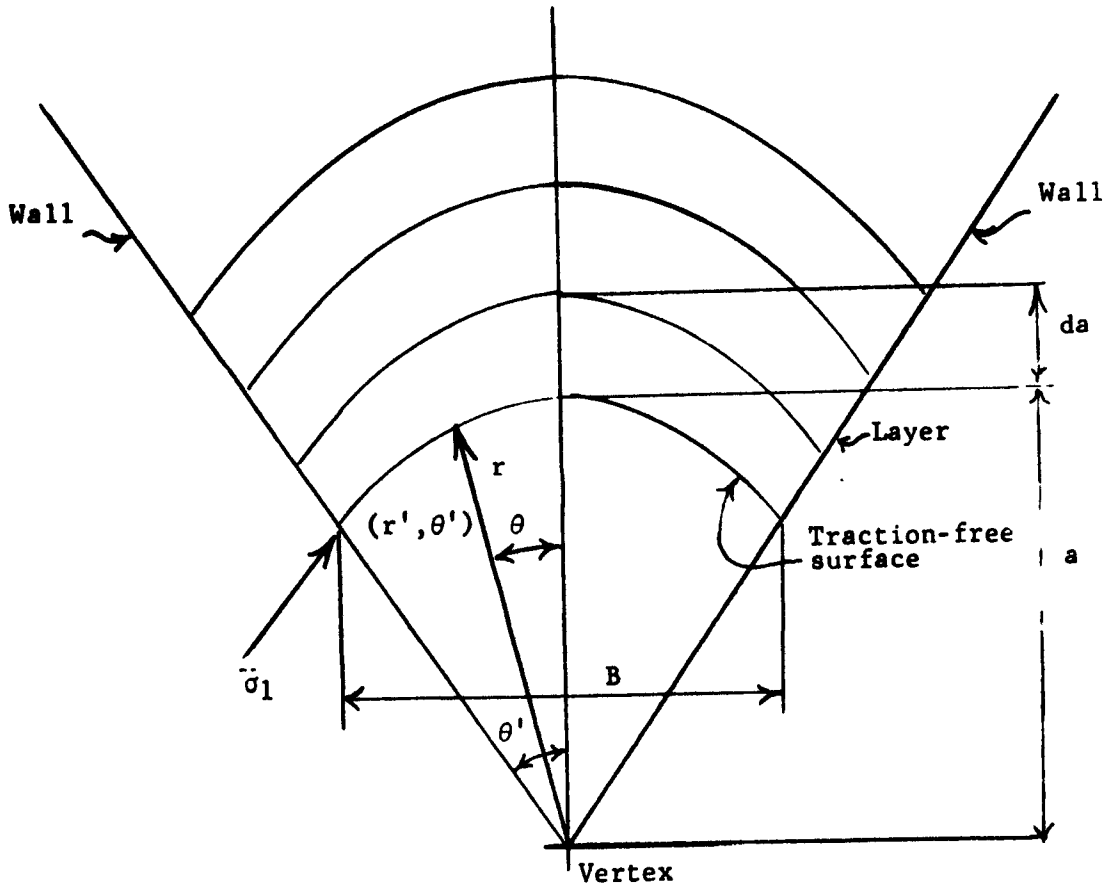

Fig. A-6

A dome across a channel

The no-doming flow-factors are plotted for mass-flow hoppers in Figures 45 to 57, in θ', ϕ' coordinates. The contours show values of constant flow-factor. In symmetric channels the analysis has been carried out for $\delta = 30°$, $40°$, $50°$, $60°$ and $70°$. In asymmetric plane flow channels with one vertical wall the analysis has been made for $\delta = 50°$ and $\phi^{v} = 20°$, $30°$ and $40°$.

In funnel-flow bins, the solid forms its own channel within itself. The angle of friction at the walls should therefore equal the angle of internal friction ϕ of the solid. However, the walls become polished as the flowing solid slides on them and the angle of friction at the walls is less than the angle of internal friction. As was mentioned earlier, the angle of internal friction also varies within a rather wide range and, hence, it is difficult to determine its actual value at the walls. In view of these uncertainties it seems reasonable to assume that the angle of friction at the walls ϕ' in funnel flow is somewhat less than ϕ and estimate it at

$$\tan \phi' = \sin \delta \qquad \text{(A-43)}$$

This implies that $\psi' = 3\pi/4$ at the walls, Eq. (A-20). Such an assumption makes the slope angle θ' a function of δ and of the flow-factor ff.

Contours of the no-doming flow-factor for funnel-flow are plotted in Fig. A-7. The significance of this chart is different from those for mass flow. In funnel-flow, the slope of the channel is not defined: the channel forms within the solid itself. The chart shows that, for any given value of δ, the flow factor increases (flowability

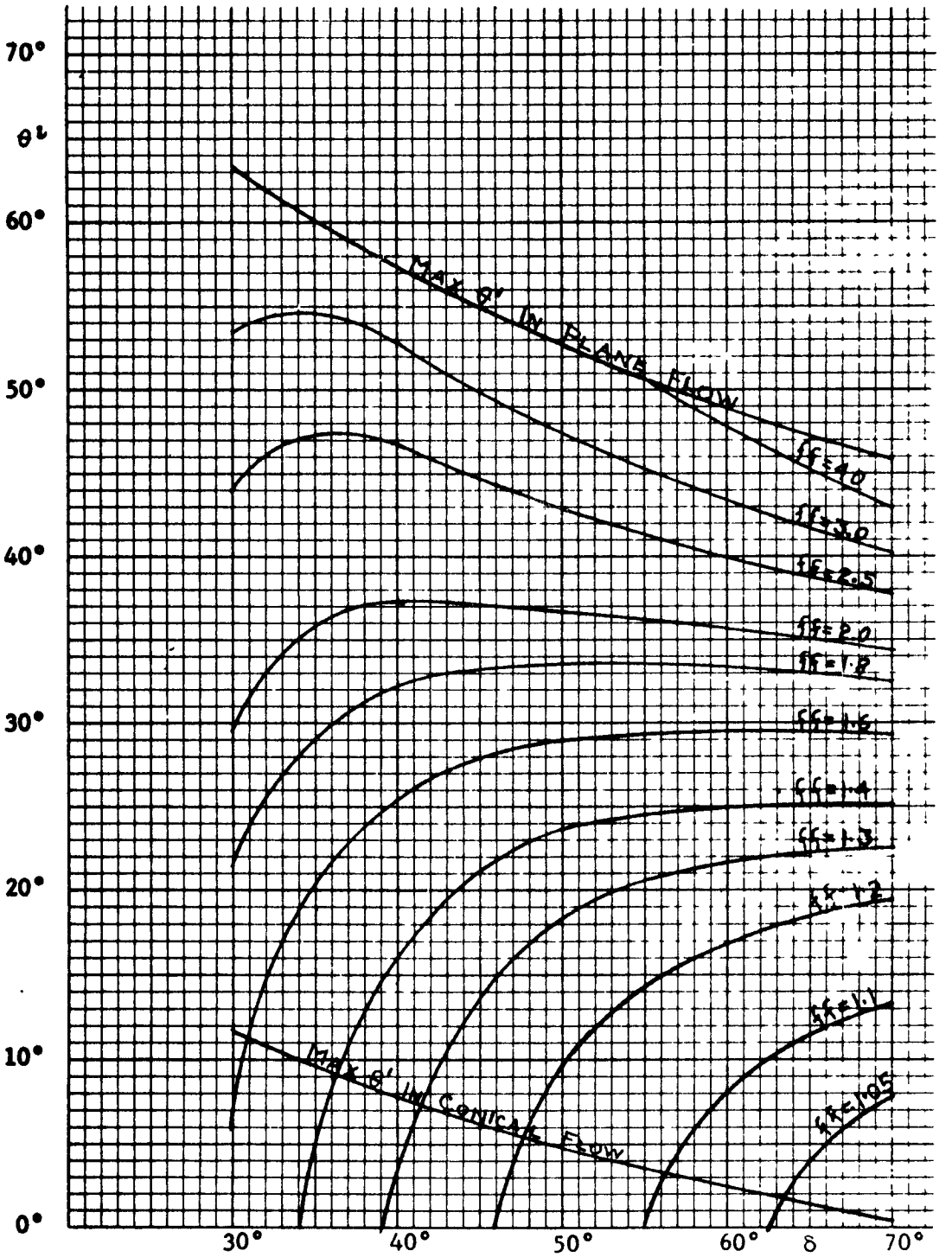

Fig. A-7

ff contours for doming in funnel flow

of the channel decreases) with an increase of the slope angle θ'. The chart also gives the bounds for the angle θ' in conical and in plane-flow. The former lies quite low, hence, a conical channel in funnel-flow is very steep, often vertical. A plane-flow slope can form only at the side of a long rectangular outlet; upward from the outlet the channel approaches a circular, horizontal cross-section and the channel becomes conical, as illustrated in Fig. 30(a). In the design of rectangular outlets, it is recommended that an ff = 1.7 be used. This permits an angle θ' approximately equal to 30° at the sides of the rectangle for most values of δ, and, hence, a widening of the channel from a slot to a circular channel circumscribing the outlet.

Piping

Consolidating pressure in a pipe, σ_1. A stress field which is independent of the vertical coordinate is assumed here and the angle of friction at the walls is assumed to satisfy Eq. (A-43). The equilibrium of an arch across a pipe of diameter D is shown in Fig. A-8: the weight of the arch causes a shearing stress at the walls

$$\tau' = \gamma D/4. \qquad \text{(A-44)}$$

It then follows from the relations of the Mohr stress circle, Fig. A-2, that the major consolidating pressure at the walls of the pipe is

$$\sigma_1 = \frac{\gamma D}{4} \frac{1 + \sin \delta}{\sin \delta} \qquad \text{(A-45)}$$

Critical pressure in a pipe, $\bar{\sigma}_1$. The conditions leading to the failure of a solid around a vertical, circular hole were analyzed in references [39] and [41]. The unconfined yield pressure f_c and the angle of friction ϕ_t were assumed constant throughout the failing region. The stress field was assumed axi-symmetric with a traction-free inner boundary of constant diameter D. The critical major pressure at the surface was computed at

$$\bar{\sigma}_1 = \gamma D/G(\phi_t), \tag{A-46}$$

where function $G(\phi_t)$ is as plotted in Fig. 36.

Replacing $\bar{\sigma}_1$ by the corresponding force $\bar{V}_1 = A\bar{\sigma}_1$, Eq. (A-46) yields the following expression for the critical diameter of the pipe

$$D = G(\phi_t)\bar{V}_1/A\gamma. \tag{A-47}$$

This is Eq. (13) in Chapter I.

Pressure on a wall, σ'

The pressure σ' from a flowing solid on a wall has been computed [39] for symmetric channels in mass flow from Eq. (A-12) with the following substitutions: $r = B/2 \sin \theta'$ from Eq. (A-38), $s(m,\delta,\theta',\phi')$ from Eq. (A-22), and ψ' from Eq. (A-20). This leads to the expression

$$\sigma'/\gamma B = s(m,\delta,\theta',\phi') \frac{1 - \sin \delta \cos 2\,\psi'(\delta,\phi')}{2 \sin \theta'} \qquad \text{(A-49)}$$

Contours of constant values of $\sigma'/\gamma B$ are plotted in Figures 58 to 67 in θ',ϕ' coordinates for constant values of $\delta = 30°$, $40°$, $50°$, $60°$ and $70°$, for conical and plane-flow channels.

Resultant vertical force Q across a channel

Force Q is obtained by integrating the vertical pressure

$$\sigma_x = \gamma r s(m,\delta,\theta,\psi)[1 + \sin \delta \cos 2(\psi + \theta)] \qquad \text{(A-50)}$$

over a horizontal cross-section of a channel, Fig. A-9. The relevant relations are

$$\left.\begin{aligned} r &= B \cot \theta'/2 \cos \theta \\ -y &= (B/2) \cot \theta' \tan \theta \\ d(-y) &= (B \cot \theta'/2 \cos^2\theta)d\theta \end{aligned}\right\} \qquad \text{(A-51)}$$

and the total force Q for symmetric channels is

$$Q = 2\pi^m L^{1-m} \int_o^{B/2} \sigma_x y^m dy. \qquad \text{(A-52)}$$

Upon integration

$$Q = q(m,\delta,\theta',\phi')\gamma\, L^{1-m}\, B^{2+m}. \qquad \text{(A-53)}$$

Contours of constant values of q have been computed [39] and are plotted in Figures 80 to 85, for conical and plane, mass-flow channels, and for $\delta = 30°$, $40°$ and $50°$.

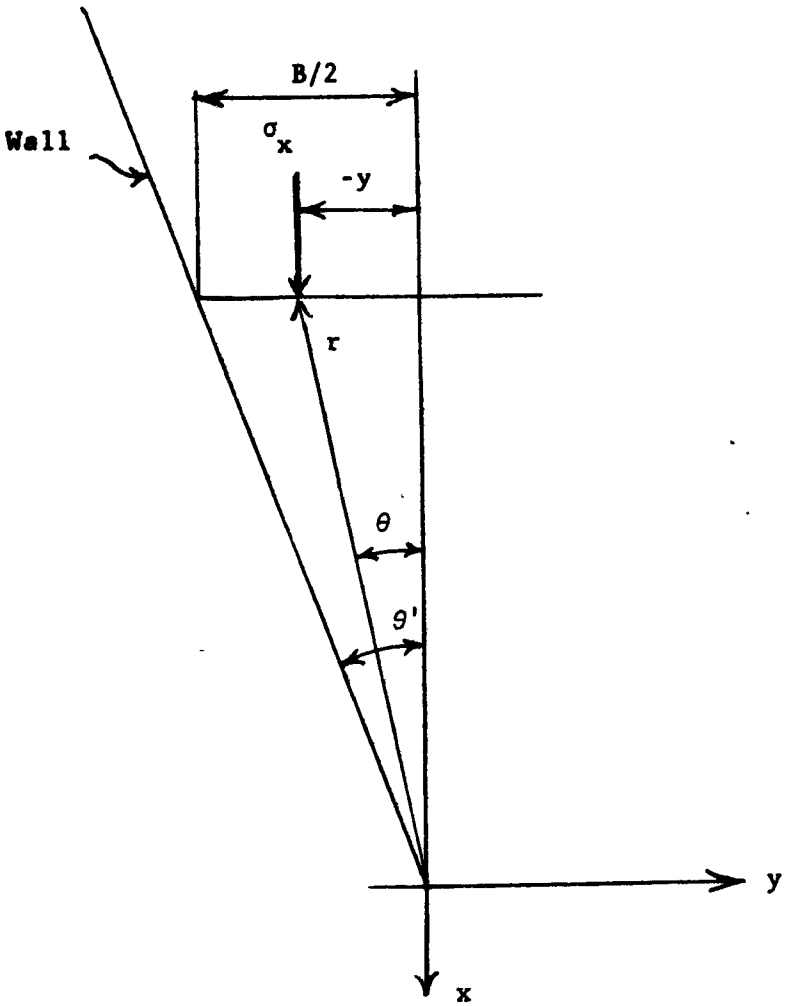

Fig. A-9

Vertical force Q

BIBLIOGRAPHY

1. H. A. Janssen, "Versuche über Getreidedruck in Silozellen", Verein Deutscher Ingenieure, Zeitschrift, V. 39, Aug. 31, 1895, pp. 1045-1049.

2. W. Airy, "The Pressure of Grain", Minutes of Proceedings of the Institution of Civil Engineers, V. 81, Paper No. 3049, 1897.

3. J. A. Jamieson, "Grain Pressures in Deep Bins", Canadian Society of Civil Engineers, Transactions, V. 17, 1903, pp. 554-654.

4. M. S. Ketchum, "The Design of Walls, Bins and Grain Elevators", McGraw-Hill Book Co., New York, 3rd edition, 1919.

5. A. Caquot and J. Kerisel, "Traité de Mecanique des Sols", Gauthier-Villars, Paris, 3rd edition, 1956, Chapter 20.

6. M. and A. Reimbert, "Silos - Traité Theorique et Pratique", Editions Eyrolles, Paris, 1956.

7. W. Nowacki and R. Dabrowski, "Silosy, Metody Obliczeń i Konstrukcja", Budownictwo i Architektura, Warsaw, 1957.

8. S. Sienicki, H. Domaszewski and C. Klos, "Zbiorniki Materjalów Sypkich", Budownictwo i Architektura, Warsaw, 1958.

9. P. Rogers, "Design of Large Coal Bunkers", Transactions, A.S.C.E., V. 117, 1952, pp. 579-595.

10. R. A. Saul, "Measurement of Grain Pressures on Bin Walls and Floors", AGRICULTURAL ENGINEERING, V. 34, Apr. 1953, pp. 231-234.

11. M. North, "Research into the Design of Horizontally Corrugated Grain Silos", Journal, The Institution of Engineers, Australia, Jan.-Feb. 1954.

12. O. F. Theimer, "Zur Berechnung von Mehlsilozellen", DIE BAUTECHNIK, V. 34, Dec. 1957, pp. 458-465.

13. R. L. Brandes, "Design of Deep Bins and Silos", Concrete Engineering Handbook, Section 18, McGraw-Hill Book Co., New York, 1961.

14. A. M. Turitzin, "Dynamic Pressure of Granular Material in Deep Bins", Proceedings ASCE, V. 89, No. ST2, April 1963.

15. J. M. Rausch, "Gravity Flow of Solid Beds in Vertical Towers", Ph.D. Thesis, Princeton University, Princeton, N. J., 1948.

16. F. C. Franklin and L. N. Johanson, "Flow of Granular Material Through Circular Orifices", CHEMICAL ENGINEERING SCIENCE, V. 4, June 1955, pp. 119-129.

17. H. E. Rose and T. Tanaka, "Rate of Discharge of Granular Materials from Bins and Hoppers", ENGINEER, V. 208, Oct. 1959, pp. 456.

18. F. E. Keneman, "Mechanism of Free Discharge of Granular Solids", INZHENERNO-FIZICHESKII ZHURNAL, V. 3, March 1960, pp. 69-73, April 1960, pp. 18-22.

19. W. A. Beverloo, H. A. Leniger and J. van de Velde, The Flow of Granular Solids Through Orifices", CHEMICAL ENGINEERING SCIENCE, V. 15, 1961, pp. 260-269.

20. R. L. Brown, "Minimum Energy Theorem for Flow of Dry Granules Through Apertures", NATURE, V. 191, July 29, 1961, pp. 458-461.

21. H. Wöhlbier and W. Reisner, "Fragen der Bunkerung von mittel und feinkornigem Schüttgut", CHEMIE-INGENIEUR-TECHNIK, V. 34, 1962, pp. 603-609.

22. R. M. LaForge and B. K. Boruff, "Profiling Flow of Particles Through Hopper Openings", INDUSTRIAL AND ENGINEERING CHEMISTRY, Vol. 56, n 2, 1964, pp. 42-46.

23. D. R. Mitchell, "Segregation in the Handling of Coal", AIME Trans. V. 130, 1937, pp. 107-142.

24. H. M. Peacock, "The Design or Adaptation of Storage Bunkers to Prevent Size Segregation of Solids", The Institute of Fuel, Feb. 1938, pp. 230-239.

25. E. F. Wolf and H. L. von Hohenleiten, "Experimental Study of the Flow of Coal in Chutes at Riverside Generating Station", MECHANICAL ENGINEERING, April 1948.

26. J. K. Rudd, "How Does Material Flow From a Bin?", MILLING PRODUCTION, Jan. 1954, pp. 5, 7.

27. J. R. O'Callaghan, "Internal Flow of Beds of Granular Material", Journal of Agric. Res., Wrest Park, Beds, England, V. 4, 1959, pp. 200-217.

28. Y. Lee, "Flow of Coal in Hoppers", COMBUSTION, Jan. 1960.

29. H. Taubmann, "Beitrag zur Speicherung von Schüttgütern", AUFBEREITUNGS-TECHNIK, Nr. 1, 1960, pp. 17-26.

30. W. J. Reynolds and R. S. Carter, "Design of Bunkers for Difficultly Flowing Fuels", COMBUSTION, Sept. 1962, pp. 32-37.

31. F. A. Zenz and D. F. Othmer, "Fluidization and Fluid-Particle Systems", Reinhold Publishing Corp., N.Y., 1960, Chapter 4.

32. F. Silver, "Storage and Handling of Pulverized Materials", MECHANICAL ENGINEERING, Sept. 1951, pp. 730-734.

33. A. W. Jenike, "Flow of Solids in Bulk Handling Systems", and "Flow of Bulk Solids in Bins", Bul. 64 of the Utah Engineering Experiment Station, University of Utah, 1954.

34. _____, "Better Design for Bulk Handling", CHEMICAL ENGINEERING, V. 61, No. 12, Dec. 1954, pp. 175-180.

35. _____, "How Bulk Behaves", FLOW, V. 10, No. 1, Oct. 1954, pp. 74-77, 119-125; No. 2, Nov. 1954, pp. 98-101, 125-131.

36. A. W. Jenike, "How to Keep Solids Flowing in Bins and Hoppers", ENGINEERING AND MINING JOURNAL, V. 156, No. 3a, Mid-March 1955, pp. 83-85, 93.

37. _____ and R. T. Shield, "On the Plastic Flow of Coulomb Solids Beyond Original Failure", J. of Appl. Mech., V. 27, Dec. 1959, pp. 599-602.

38. _____, P. J. Elsey and R. H. Woolley, "Flow Properties of Bulk Solids", Proceedings, A.S.T.M., V. 60, 1960, pp. 1168-1181.

39. _____, "Gravity Flow of Bulk Solids", Bul. 108, Utah Engineering Experiment Station, University of Utah, Salt Lake City, Utah, Oct. 1961.

40. _____, "Gravity Flow of Solids", Trans. of the Institution of Chemical Engineers, V. 40, n 5, 1962, pp. 264-271.

41. _____ and B. C. Yen, "Slope Stability in Axial Symmetry", Proceedings of the Fifth Symposium on Rock Mechanics, University of Minnesota, May 1962, Pergamon Press, 1963, pp. 689-711.

42. _____ and T. Leser, "A Flow-No Flow Criterion in the Gravity Flow of Powders in Converging Channels", Fourth International Congress on Rheology, Brown University, Aug. 1963.

43. _____, "Steady Gravity Flow of Frictional-Cohesive Solids in Converging Channels", J. of Appl. Mech., V. 31, Series E, n 1, 1964, pp. 5-11.

44. J. R. Johanson, "Stress and Velocity Fields in the Gravity Flow of Bulk Solids", J. of Appl. Mech., Series E, V. 86, Sept. 1964.

45. A. W. Jenike, "Gravity Flow of Frictional-Cohesive Solids - Convergence to Radial Stress Fields" to be published as a Brief Note in J. of Appl. Mech. in 1965.

46. D. C. Drucker, "A More Fundamental Approach to Plastic Stress-Strain Relations", Proc. First U. S. Nat. Congress of Appl. Mechanics, ASME, 1951, pp. 487-491.

47. A. Haar and Th. von Karman, "Zur Theorie der Spannungszustaende in plastischen und sandartigen Medien", Nachr. Ges. Wiss. Göttingen, Math.-Phys. Kl., 1909, p. 204.

48. R. A. Wilson, "Belt Feeders", MECHANICAL ENGINEERING, V. 79, 1957, pp. 1042-1043.

49. W. H. Denton, "The Packing and Flow of Spheres", Atomic Energy Research Establishment, E/R 1035, Ministry of Supply, Harwell. Berks, England, 1953.

50. A. W. Jenike, P. J. Elsey and R. H. Wooley, "Flow of Bulk Solids, Progress Report", Bul. 96, Utah Engineering Experiment Station, University of Utah, Salt Lake City, Utah, Dec. 1958.

51. R. W. Olson, "Dust Explosions: Prevent or Supress Explosion Losses in Bulk Materials", MECHANICAL ENGINEERING, V. 83, 1961, pp. 59-61.

52. O. Richmond, "Gravity Hopper Design", MECHANICAL ENGINEERING, Vol. 85, Jan. 1963, pp. 46-49.

53. G. C. Gardner, "The Best Hopper Profile for Cohesive Material", Chemical Engineering Science, Vol. 18, 1963, pp. 35-39.

54. D. M. Walker, "A Theory of Gravity Flow of Cohesive Powders", Central Electricity Generating Board, South Western Region, England, Research and Development Report No. 22, May 1964.

55. J. R. Johanson and H. Colijn, "New Design Criteria for Hoppers and Bins", IRON AND STEEL ENGINEER, V. XLI, Oct. 1964, pp. 85-104.